



VOL. **628** NO. **1** JANUARY 1, 1993

JOURNAL OF

CHROMATOGRAPHY

INCLUDING ELECTROPHORESIS AND OTHER SEPARATION METHODS



EDITORS

U. A. Th. Brinkman (Amsterdam)
R. W. Giese (Boston, MA)
J. K. Haken (Kensington, N.S.W.)
K. Macek (Prague)
L. R. Snyder (Orinda, CA)

EDITORS, SYMPOSIUM VOLUMES,
E. Heftmann (Orinda, CA), Z. Deyl (Prague)

EDITORIAL BOARD

D. W. Armstrong (Rolla, MO)
W. A. Aue (Halifax)
P. Boček (Brno)
A. A. Boulton (Saskatoon)
P. W. Carr (Minneapolis, MN)
N. H. C. Cooke (San Ramon, CA)
V. A. Davankov (Moscow)
Z. Deyl (Prague)
S. Dilli (Kensington, N.S.W.)
H. Engelhardt (Saarbrücken)
F. Erni (Basle)
M. B. Evans (Hatfield)
J. L. Glajch (N. Billerica, MA)
G. A. Guiochon (Knoxville, TN)
P. R. Haddad (Kensington, N.S.W.)
I. M. Hais (Hradec Králové)
W. S. Hancock (San Francisco, CA)
S. Hjertén (Uppsala)
Cs. Horváth (New Haven, CT)
J. F. K. Huber (Vienna)
K.-P. Hupe (Waldbronn)
T. W. Hutchens (Houston, TX)
J. Janák (Brno)
P. Jandera (Pardubice)
B. L. Karger (Boston, MA)
J. J. Kirkland (Wilmington, DE)
E. sz Kováts (Lausanne)
A. J. P. Martin (Cambridge)
L. W. McLaughlin (Chestnut Hill, MA)
E. D. Morgan (Keele)
J. D. Pearson (Kalamazoo, MI)
H. Poppe (Amsterdam)
F. E. Regnier (West Lafayette, IN)
P. G. Righetti (Milan)
P. Schoenmakers (Eindhoven)
R. Schwarzenbach (Dübendorf)
R. E. Shoup (West Lafayette, IN)
A. M. Siouffi (Marseille)
D. J. Strydom (Boston, MA)
N. Tanaka (Kyoto)
S. Terabe (Hyogo)
K. K. Unger (Mainz)
R. Verpoorte (Leiden)
Gy. Vigh (College Station, TX)
J. T. Watson (East Lansing, MI)
B. D. Westerlund (Uppsala)

EDITORS, BIBLIOGRAPHY SECTION

Z. Deyl (Prague), J. Janák (Brno), V. Schwarz (Prague)

ELSEVIER

JOURNAL OF CHROMATOGRAPHY

INCLUDING ELECTROPHORESIS AND OTHER SEPARATION METHODS

Scope. The *Journal of Chromatography* publishes papers on all aspects of **chromatography, electrophoresis** and related methods. Contributions consist mainly of research papers dealing with chromatographic theory, instrumental developments and their applications. The section *Biomedical Applications*, which is under separate editorship, deals with the following aspects: developments in and applications of chromatographic and electrophoretic techniques related to clinical diagnosis or alterations during medical treatment; screening and profiling of body fluids or tissues related to the analysis of active substances and to metabolic disorders; drug level monitoring and pharmacokinetic studies; clinical toxicology; forensic medicine; veterinary medicine; occupational medicine; results from basic medical research with direct consequences in clinical practice. In *Symposium volumes*, which are under separate editorship, proceedings of symposia on chromatography, electrophoresis and related methods are published.

Submission of Papers. The preferred medium of submission is on disk with accompanying manuscript (see *Electronic manuscripts* in the Instructions to Authors, which can be obtained from the publisher, Elsevier Science Publishers B.V., P.O. Box 330, 1000 AH Amsterdam, Netherlands). Manuscripts (in English; *four* copies are required) should be submitted to: Editorial Office of *Journal of Chromatography*, P.O. Box 681, 1000 AR Amsterdam, Netherlands, Telefax (+31-20) 5862 304, or to: The Editor of *Journal of Chromatography, Biomedical Applications*, P.O. Box 681, 1000 AR Amsterdam, Netherlands. Review articles are invited or proposed in writing to the Editors who welcome suggestions for subjects. An outline of the proposed review should first be forwarded to the Editors for preliminary discussion prior to preparation. Submission of an article is understood to imply that the article is original and unpublished and is not being considered for publication elsewhere. For copyright regulations, see below.

Publication. The *Journal of Chromatography* (incl. *Biomedical Applications*) has 40 volumes in 1993. The subscription prices for 1993 are:

J. Chromatogr. (incl. *Cum. Indexes, Vols. 601-650*) + *Biomed. Appl.* (Vols. 612-651):

Dfl. 8520.00 plus Dfl. 1320.00 (p.p.h.) (total ca. US\$ 5927.75)

J. Chromatogr. (incl. *Cum. Indexes, Vols. 601-650*) only (Vols. 623-651):

Dfl. 7047.00 plus Dfl. 957.00 (p.p.h.) (total ca. US\$ 4821.75)

Biomed. Appl. only (Vols. 612-622):

Dfl. 2783.00 plus Dfl. 363.00 (p.p.h.) (total ca. US\$ 1895.25).

Subscription Orders. The Dutch guilder price is definitive. The US\$ price is subject to exchange-rate fluctuations and is given as a guide. Subscriptions are accepted on a prepaid basis only, unless different terms have been previously agreed upon. Subscription orders can be entered only by calendar year (Jan.-Dec.) and should be sent to Elsevier Science Publishers, Journal Department, P.O. Box 211, 1000 AE Amsterdam, Netherlands, Tel. (+31-20) 5803 642, Telefax (+31-20) 5803 598, or to your usual subscription agent. Postage and handling charges include surface delivery except to the following countries where air delivery via SAL (Surface Air Lift) mail is ensured: Argentina, Australia, Brazil, Canada, China, Hong Kong, India, Israel, Japan*, Malaysia, Mexico, New Zealand, Pakistan, Singapore, South Africa, South Korea, Taiwan, Thailand, USA. *For Japan air delivery (SAL) requires 25% additional charge of the normal postage and handling charge. For all other countries airmail rates are available upon request. Claims for missing issues must be made within three months of our publication (mailing) date, otherwise such claims cannot be honoured free of charge. Back volumes of the *Journal of Chromatography* (Vols. 1-611) are available at Dfl. 230.00 (plus postage). Customers in the USA and Canada wishing information on this and other Elsevier journals, please contact Journal Information Center, Elsevier Science Publishing Co. Inc., 655 Avenue of the Americas, New York, NY 10010, USA, Tel. (+1-212) 633 3750, Telefax (+1-212) 633 3764.

Abstracts/Contents Lists published in Analytical Abstracts, Biochemical Abstracts, Biological Abstracts, Chemical Abstracts, Chemical Titles, Chromatography Abstracts, Clinical Chemistry Lookout, Current Awareness in Biological Sciences (CABS), Current Contents/Life Sciences, Current Contents/Physical, Chemical & Earth Sciences, Deep-Sea Research/Part B: Oceanographic Literature Review, Excerpta Medica, Index Medicus, Mass Spectrometry Bulletin, PASCAL-CNRS, Pharmaceutical Abstracts, Referativnyi Zhurnal, Research Alert, Science Citation Index and Trends in Biotechnology.

US Mailing Notice. *Journal of Chromatography* (ISSN 0021-9673) is published weekly (total 58 issues) by Elsevier Science Publishers (Sara Burgerhartstraat 25, P.O. Box 211, 1000 AE Amsterdam, Netherlands). Annual subscription price in the USA US\$ 5927.75 (subject to change), including air speed delivery. Application to mail at second class postage rate is pending at Jamaica, NY 11431. **USA POSTMASTERS:** Send address changes to *Journal of Chromatography*, Publications Expediting, Inc., 200 Meacham Avenue, Elmont, NY 11003. Airfreight and mailing in the USA by Publication Expediting.

See inside back cover for Publication Schedule, Information for Authors and information on Advertisements.

© 1993 ELSEVIER SCIENCE PUBLISHERS B.V. All rights reserved.

0021-9673/93/\$06.00

No part of this publication may be reproduced, stored in a retrieval system or transmitted in any form or by any means, electronic, mechanical, photocopying, recording or otherwise, without the prior written permission of the publisher, Elsevier Science Publishers B.V., Copyright and Permissions Department, P.O. Box 521, 1000 AM Amsterdam, Netherlands.

Upon acceptance of an article by the journal, the author(s) will be asked to transfer copyright of the article to the publisher. The transfer will ensure the widest possible dissemination of information.

Special regulations for readers in the USA. This journal has been registered with the Copyright Clearance Center, Inc. Consent is given for copying of articles for personal or internal use, or for the personal use of specific clients. This consent is given on the condition that the copier pays through the Center the per-copy fee stated in the code on the first page of each article for copying beyond that permitted by Sections 107 or 108 of the US Copyright Law. The appropriate fee should be forwarded with a copy of the first page of the article to the Copyright Clearance Center, Inc., 27 Congress Street, Salem, MA 01970, USA. If no code appears in an article, the author has not given broad consent to copy and permission to copy must be obtained directly from the author. All articles published prior to 1980 may be copied for a per-copy fee of US\$ 2.25, also payable through the Center. This consent does not extend to other kinds of copying, such as for general distribution, resale, advertising and promotion purposes, or for creating new collective works. Special written permission must be obtained from the publisher for such copying.

No responsibility is assumed by the Publisher for any injury and/or damage to persons or property as a matter of products liability, negligence or otherwise, or from any use or operation of any methods, products, instructions or ideas contained in the materials herein. Because of rapid advances in the medical sciences, the Publisher recommends that independent verification of diagnoses and drug dosages should be made.

Although all advertising material is expected to conform to ethical (medical) standards, inclusion in this publication does not constitute a guarantee or endorsement of the quality or value of such product or of the claims made of it by its manufacturer.

This issue is printed on acid-free paper.

CONTENTS

(Abstracts/Contents Lists published in Analytical Abstracts, Biochemical Abstracts, Biological Abstracts, Chemical Abstracts, Chemical Titles, Chromatography Abstracts, Current Awareness in Biological Sciences (CABS), Current Contents/Life Sciences, Current Contents/Physical, Chemical & Earth Sciences, Deep-Sea Research/Part B: Oceanographic Literature Review, Excerpta Medica, Index Medicus, Mass Spectrometry Bulletin, PASCAL-CNRS, Referativnyi Zhurnal, Research Alert and Science Citation Index)

PUBLISHER'S NOTE	1
REGULAR PAPERS	
<i>Column Liquid Chromatography</i>	
Influence of shape parameters on the separation of tetrachlorodibenzo- <i>p</i> -dioxin isomers on reversed-phase columns by U. Pyell, P. Garrigues and M. T. Rayez (Talence, France) (Received September 8th, 1992)	3
Preparation and chromatographic evaluation of 3,5-dimethylphenyl carbamoylated β -cyclodextrin stationary phases for normal-phase high-performance liquid chromatographic separation of enantiomers by T. Hargitai, Y. Kaida and Y. Okamoto (Nagoya, Japan) (Received September 1st, 1992)	11
Separation of C ₆₀ and C ₇₀ on polystyrene gel with toluene as mobile phase by A. Gügel and K. Müllen (Mainz, Germany) (Received September 30th, 1992)	23
Normal-phase high-performance liquid chromatography with a fluorimetric postcolumn detection system for lipid hydroperoxides by K. Akasaka, H. Ohroi and H. Meguro (Sendai, Japan) (Received September 7th, 1992)	31
Analysis of alkylpyrrole autoxidation products by high-performance liquid chromatography with thermospray mass spectrometry and UV photodiode-array detection by M. Zhu, D. C. Spink, S. Bank, X. Chen and A. P. DeCaprio (Albany, NY, USA) (Received September 3rd, 1992)	37
Column liquid chromatography of cefadroxil on poly(styrene-divinylbenzene) by C. Hendrix, C. Wijssen, L. M. Yun, E. Roets and J. Hoogmartens (Leuven, Belgium) (Received June 30th, 1992)	49
<i>Gas Chromatography</i>	
Application of a new numerical method for characterizing heterogeneous solids by using gas-solid chromatographic data by M. Heuchel, M. Jaroniec and R. K. Gilpin (Kent, OH, USA) (Received June 17th, 1992)	59
Calculation of retention indices by molecular topology. III. Chlorinated dibenzodioxins by S. Sekušak and A. Sabljic (Zagreb, Croatia) (Received August 28th, 1992)	69
Determination of C ₆ -C ₁₀ aromatic hydrocarbons in water by purge-and-trap capillary gas chromatography by R. P. Eganhouse (Boston, MA and Long Beach, CA, USA), T. F. Dorsey (Boston, MA and Los Angeles, CA, USA), C. S. Phinney (Boston, MA, USA) and A. M. Westcott (Long Beach, CA, USA) (Received August 14th, 1992)	81
Determination of bacterial muramic acid by gas chromatography-mass spectrometry with negative-ion detection by I. Elmroth (Lund, Sweden), A. Fox (Columbia, SC, USA) and L. Larsson (Lund, Sweden) (Received July 21st, 1992)	93
<i>Planar Chromatography</i>	
Thin-layer chromatography of the positional isomers of some 1,2,3,4-tetrahydro-2-naphthol and 3-amino-1,2,3,4-tetrahydro-2-naphthol derivatives by K. Drandarov and I. M. Hais (Hradec Králové, Czechoslovakia) (Received September 7th, 1992)	103
<i>Electrophoresis</i>	
Structural characterization of polypeptides and proteins by combination of capillary electrophoresis and ²⁵² Cf plasma desorption mass spectrometry by W. Weinmann, K. Baumeister, I. Kaufmann and M. Przybylski (Konstanz, Germany) (Received September 1st, 1992)	111

(Continued overleaf)

Contents (continued)

SHORT COMMUNICATIONS

Column Liquid Chromatography

- Determination of kinetin in callus of *Panax ginseng* by liquid chromatography
by K. Takagi, M. Toyoda and Y. Saito (Tokyo, Japan), K. Mizuno and M. Shimizu (Kanagawa, Japan) and S. Satoh
(Osaka, Japan) (Received October 19th, 1992) 122
- Optimization of the separation of technical aldicarb by semi-preparative reversed-phase high-performance liquid chromatography
by Q.-S. Wang, R.-Y. Gao and B.-W. Yan (Tianjin, China) (Received September 22nd, 1992) 127
- High-performance liquid chromatography of inorganic mercury and organomercury with 2-mercaptobenzothiazole
by Y.-C. Wang and C.-W. Whang (Taichung, Taiwan) (Received September 28th, 1992) 133

Gas Chromatography

- Two-solute method for indicating polarity changes of conventional and novel gas chromatographic stationary phases with
temperature increase
by T. J. Betts (Perth, Australia) (Received October 22nd, 1992) 138
- Gas chromatographic method for the determination of chlorobenzophenone isomers
by A. S. Tambe, T. Daniel, S. Biswas and N. R. Ayyangar (Pune, India) (Received October 1st, 1992) 143

Planar Chromatography

- Thin-layer chromatography on silica gel of a homologous series of bis(alkylxanthato)nickel(II) complexes
by Ž. Lj. Tešić, T. J. Janjić and M. B. Čelap (Belgrade, Yugoslavia) (Received September 30th, 1992) 148

Electrophoresis

- Borate complexation of flavonoid-O-glycosides in capillary electrophoresis. I. Separation of flavonoid-7-O-glycosides differing in
their flavonoid aglycone
by Ph. Morin, F. Villard and M. Dreux (Orléans, France) (Received September 1st, 1992) 153
- Borate complexation of flavonoid-O-glycosides in capillary electrophoresis. II. Separation of flavonoid-3-O-glycosides differing in
their sugar moiety
by Ph. Morin, F. Villard and M. Dreux (Orléans, France) and P. André (St Jean-de-Braye, France) (Received September
16th, 1992) 161

BOOK REVIEW

- Analysis of substances in the gaseous phase (Comprehensive Analytical Chemistry, Vol. XXVIII) (Edited by E. Smolková-
Keulemansová and L. Feltl), reviewed by V. G. Berezkin (Moscow, Russian Federation) 170

JOURNAL OF CHROMATOGRAPHY

VOL. 628 (1993)

JOURNAL of CHROMATOGRAPHY

INCLUDING ELECTROPHORESIS AND OTHER SEPARATION METHODS

EDITORS

U. A. Th. BRINKMAN (Amsterdam), R. W. GIESE (Boston, MA), J. K. HAKEN (Kensington, N.S.W.), K. MACEK (Prague),
L. R. SNYDER (Orinda, CA)

EDITORS, SYMPOSIUM VOLUMES

E. HEFTMANN (Orinda, CA), Z. DEYL (Prague)

EDITORIAL BOARD

D. W. Armstrong (Rolla, MO), W. A. Aue (Halifax), P. Boček (Brno), A. A. Boulton (Saskatoon), P. W. Carr (Minneapolis, MN),
N. H. C. Cooke (San Ramon, CA), V. A. Davankov (Moscow), Z. Deyl (Prague), S. Dilli (Kensington, N.S.W.), H. Engelhardt
(Saarbrücken), F. Erni (Basle), M. B. Evans (Hatfield), J. L. Glajch (N. Billerica, MA), G. A. Guiochon (Knoxville, TN), P. R.
Haddad (Hobart, Tasmania), I. M. Hais (Hradec Králové), W. S. Hancock (San Francisco, CA), S. Hjertén (Uppsala), S. Honda
(Higashi-Osaka), Cs. Horváth (New Haven, CT), J. F. K. Huber (Vienna), K.-P. Hupe (Waldbronn), T. W. Hutchens (Houston,
TX), J. Janák (Brno), P. Jandera (Pardubice), B. L. Karger (Boston, MA), J. J. Kirkland (Newport, DE), E. sz. Kováts (Lausanne),
A. J. P. Martin (Cambridge), L. W. McLaughlin (Chestnut Hill, MA), E. D. Morgan (Keele), J. D. Pearson (Kalamazoo, MI), H.
Poppe (Amsterdam), F. E. Regnier (West Lafayette, IN), P. G. Righetti (Milan), P. Schoenmakers (Eindhoven), R. Schwarzenbach
(Dübendorf), R. E. Shoup (West Lafayette, IN), R. P. Singhal (Wichita, KS), A. M. Siouffi (Marseille), D. J. Strydom
(Boston, MA), N. Tanaka (Kyoto), S. Terabe (Hyogo), K. K. Unger (Mainz), R. Verpoorte (Leiden), Gy. Vigh (College Station,
TX), J. T. Watson (East Lansing, MI), B. D. Westerlund (Uppsala)

EDITORS, BIBLIOGRAPHY SECTION

Z. Deyl (Prague), J. Janák (Brno), V. Schwarz (Prague)



ELSEVIER

AMSTERDAM — LONDON — NEW YORK — TOKYO

J. Chromatogr., Vol. 628 (1993)

© 1993 ELSEVIER SCIENCE PUBLISHERS B.V. All rights reserved.

0021-9673/93/006.00

No part of this publication may be reproduced, stored in a retrieval system or transmitted in any form or by any means, electronic, mechanical, photocopying, recording or otherwise, without the prior written permission of the publisher, Elsevier Science Publishers B.V., Copyright and Permissions Department, P.O. Box 521, 1000 AM Amsterdam, Netherlands.

Upon acceptance of an article by the journal, the author(s) will be asked to transfer copyright of the article to the publisher. The transfer will ensure the widest possible dissemination of information.

Special regulations for readers in the USA. This journal has been registered with the Copyright Clearance Center, Inc. Consent is given for copying of articles for personal or internal use, or for the personal use of specific clients. This consent is given on the condition that the copier pays through the Center the per-copy fee stated in the code on the first page of each article for copying beyond that permitted by Sections 107 or 108 of the US Copyright Law. The appropriate fee should be forwarded with a copy of the first page of the article to the Copyright Clearance Center, Inc., 27 Congress Street, Salem, MA 01970, USA. If no code appears in an article, the author has not given broad consent to copy and permission to copy must be obtained directly from the author. All articles published prior to 1980 may be copied for a per-copy fee of US\$ 2.25, also payable through the Center. This consent does not extend to other kinds of copying, such as for general distribution, resale, advertising and promotion purposes, or for creating new collective works. Special written permission must be obtained from the publisher for such copying.

No responsibility is assumed by the Publisher for any injury and/or damage to persons or property as a matter of products liability, negligence or otherwise, or from any use or operation of any methods, products, instructions or ideas contained in the materials herein. Because of rapid advances in the medical sciences, the Publisher recommends that independent verification of diagnoses and drug dosages should be made.

Although all advertising material is expected to conform to ethical (medical) standards, inclusion in this publication does not constitute a guarantee or endorsement of the quality or value of such product or of the claims made of it by its manufacturer.

This issue is printed on acid-free paper.

Printed in the Netherlands

Publisher's note

Since the beginning of 1992, the *Journal of Chromatography* has encouraged submission of manuscripts on disk. The rationale is that electronic submission of manuscripts enables faster publication of articles and avoids the introduction of errors by the typesetter. Fig. 1 shows the response of authors to date. The vertical axis represents the percentage of accepted articles on disk received by the editorial office and the horizontal axis shows the month. (The articles in Symposium issues are not included yet in these results.) As can be seen, 50% submissions on disk has been attained, and it is expected that within a year a plateau of about 65% will have been reached. Thanks to the very positive response of our authors this development is taking place much faster than was originally anticipated.

The procedure regarding submission of manuscripts on disk is as follows. The editorial office receiving the manuscript (in paper format) forwards the paper to one of the editors who sends it on to referees for review. The editorial office, the editors and the referees work only with the paper manuscript, so there is no need for authors to send disks at this stage. Only once the editorial office has informed the authors that their paper can be accepted by the editor—usually after one or more revision steps—the authors are requested to send a disk along with the (revised) manuscript. It is essential that the printed version (hardcopy) of the (revised) manuscript exactly matches the contents of the disk. The disk **and** the (revised) printed manuscript will then be processed by the desk editors and the typesetter for preparing proofs. This speeds up the

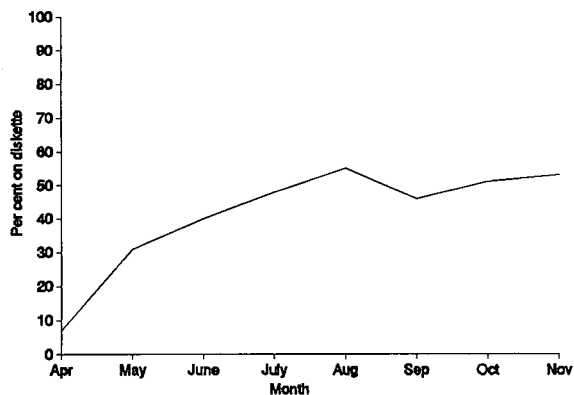


Fig. 1. Percentage of articles accepted for publication in 1992, which were received on disk.

process and minimizes typesetter's errors in the proofs.

In summary, the procedure for submission of manuscripts on disk is:

- First submission: send manuscript in paper format only.
- Submission of revised article: send **disk** (properly labelled) containing manuscript files **and exactly matching printout**.

Full details on disk submission can be found in the Instructions for Authors.

We would like to take this opportunity to thank all those scientists who are participating in this development, which will facilitate the scientific publishing process.

Influence of shape parameters on the separation of tetrachlorodibenzo-*p*-dioxin isomers on reversed-phase columns

U. Pyell and P. Garrigues

URA 348, CNRS, University of Bordeaux I, F-33405 Talence Cedex (France)

M. T. Rayez

URA 503, CNRS, University of Bordeaux I, F-33405 Talence Cedex (France)

(First received June 10th, 1992; revised manuscript received September 8th, 1992)

ABSTRACT

The retention orders of tetrachlorodibenzo-*p*-dioxin (TCDD) isomers on a monomeric and a polymeric ODS column were determined by RP-HPLC. It is demonstrated that the drastic alteration of the retention order with variation of the stationary phase can be explained by a variable influence of steric effects on the retention. The length-to-breadth ratios of TCDDs were calculated and correlated with retention data. The polymeric ODS phase proved to be superior to the monomeric phase with respect to selectivity. The enhanced selectivity is attributed to an enhancement of the shape selectivity of the stationary phase. The retention order is also strongly dependent on the mobile phase.

INTRODUCTION

In recent years, high-performance liquid chromatography (HPLC) has been used by several groups in clean-up procedures for the determination of polychlorodibenzofurans (PCDFs) and polychlorodibenzo-*p*-dioxins (PCDDs) in different matrices. Both normal- and reversed-phase (RP) columns and combinations of the two modes have been used [1–7]. RP-HPLC has also been employed for the separation of individual isomers of reference compounds [8].

In this work, we studied systematically the separation of thirteen commercially available tetrachlorodibenzo-*p*-dioxin (TCDD) isomers on octadecyl-silica gel (ODS) columns of different surface coverages.

Wise and May [9] reported the dependence of selectivity on the surface coverage with octadecyl groups for polycyclic aromatic hydrocarbons (PAHs) separated on ODS columns from various suppliers. Wise *et al.* [10] demonstrated the relationship between the retention on polymeric ODS phases and the shape parameters of PAHs, especially the length-to-breadth ratio (L/B).

The aim of this work was to examine whether the same relationship can be used to explain the different retention orders of TCDD isomers on a polymeric ODS phase compared with monomeric ODS phases with lower surface coverages.

EXPERIMENTAL

Chemicals

All solvents were of HPLC grade (Rathburn, Walkerburn, UK). Eleven of the isomers were obtained from Cambridge Isotope Labs. (Woburn,

Correspondence to: P. Garrigues, URA 348, CNRS, University of Bordeaux I, F-33405 Talence Cedex, France.

MA, USA) as solutions in nonane (50 ± 5 ppm). 1478-, 1236-, 1239-, 1267-, 1378-, 1289- and 2378-TCDD were received as individual isomers; 1237/1238- and 1368/1379-TCDD were received as mixtures of two isomers. The concentrations of the two isomers in the delivered standard mixtures differed considerably. By comparison of the intensity ratios and the retention orders on a PONA gas chromatographic capillary column (50 m \times 0.2 mm I.D.; 5.5 μ m) (Hewlett-Packard, Palo Alto, CA, USA) we succeeded in assigning the peaks of the 1368–1379-TCDD mixture unambiguously (conditions: HP 5970B mass-selective detector with HP 5890A gas chromatograph; injection mode, splitless; temperature programme, 130°C (0.5 min), 130–230°C at 30°C/min, 230–315°C at 1°C/min; carrier gas, helium). 1237-TCDD and 1238-TCDD were assigned according to their shape parameters. 1234-TCDD and 1278-TCDD were received as crystals from Cambridge Isotope Labs. In Fig. 1a the numbering of dioxin substituents is presented according to IUPAC nomenclature.

Apparatus

An HP 1050 liquid chromatograph with a quaternary gradient pump and autoinjector was used in

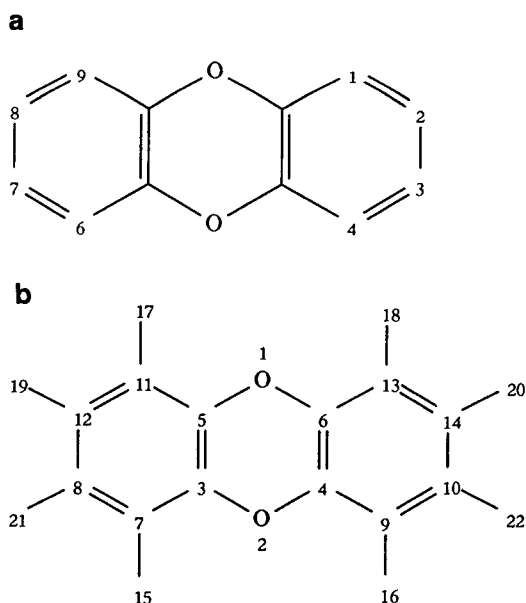


Fig. 1. (a) Numbering of dioxin substituents. (b) Numbering employed for quantum mechanical calculations.

conjunction with a LDC Spectromonitor III spectrophotometric detector. The temperature of the column was controlled by a laboratory-made copper jacket and a water-bath. A PC-based laboratory data system (Hewlett-Packard, Vectra Series) was used to record, store process and plot the data.

Columns

The relative retention indices for one of the monomeric columns (ODS1) were taken from O'Keefe *et al.* [5], who employed two series-connected 250 mm \times 6.2 mm I.D. Zorbax ODS (DuPont Instruments Division, Wilmington, DE, USA) columns. With a given absolute retention time for 2378-TCDD of 15.5 min and a calculated dead time of 6.4 min, we evaluated the capacity factors of the analytes.

We employed a second monomeric column (ODS2): Spherisorb ODS-2, particle diameter 5 μ m (250 mm \times 4.6 mm I.D.). As a polymeric column (ODS3) we used a 250 mm \times 4.6 mm I.D. Vydac 201TP (Separations Group, Hesperia, CA, USA) column (particle diameter 5 μ m).

Chromatographic conditions

All retention data were obtained under isocratic and isothermal (25°C) conditions. The eluents were premixed [ODS2, acetonitrile–water (88:12, v/v) or methanol; ODS3, acetonitrile–water (80:20, v/v)]. The flow-rate was 1 ml/min in all instances. The UV detector was operated at 235 nm with a response time of 1 s. Retention times were measured with solutions of the TCDD isomers and the standards benz[*a*]anthracene and benzo[*b*]chrysene in 2-propanol.

The standard solutions in nonane were diluted with 2-propanol. For mixtures the nonane was evaporated before dissolving the standard in 2-propanol in order to avoid peak broadening or distortion due to the solvent effects of the sample solution. The injection volume was generally 10 μ l, containing 2–6 ng of each isomer. For a mixture of all TCDD isomers the injection volume was 7 μ l, containing 2–5 ng of each isomer.

The measurements with ODS1 were carried out with methanol at 2 ml/min (40°C). Details are given in ref. 5.

Calculation of length-to-breadth ratios

The geometry of the molecules was optimized by the semi-empirical method Austin Model 1 (AM1) with the software package AMPAC, run on an IBM 3090 computer in the CIRCE at Orsay (France). AM1 is a method that is well adapted to large organic molecules [11]. Initial input geometries were created in the form of a *Z*-matrix, involving internal coordinates in which each atom is related to previously specified atoms by a bond length, an angle and a dihedral angle. Each initial geometry was subsequently fully optimized by AM1.

The numbering scheme employed for the input of internal coordinates is given in Fig. 1b. Optimization was started with the following bond lengths: O–O, 0.296 nm; C–O, 0.137 nm; C–C, 0.140 nm; C–H, 0.110 nm; and C–Cl, 0.170 nm. The dihedral angles were taken into the optimization. The starting values were 0° or 180°, respectively, in all instances. The starting values for the bond angles corresponded to an idealized benzene ring.

The cartesian coordinates of the optimized molecule structure were employed to evaluate the length-to-breadth ratio (*L/B*) with in-house software on a desk-top microcomputer (Tandy 3000 NL). The programme calculates the rectangle enclosing the analyte with maximized *L/B*, according to the method of Wise *et al.* [10], with respect to the Van der Waals radii of the outer atoms of the molecule. The Van der Waals radii were taken from ref. 12.

Retention indices

The retention indices were calculated according to Popl *et al.* [13] using the following equation:

$$\log I_R = \log I_n + \frac{\log R - \log R_n}{\log R_{(n+1)} - \log R_n} \quad (1)$$

where *R* represents the corrected retention time of the solute (retention time minus the void volume multiplied by the flow-rate) and *n* and *n* + 1 represent standards with lower or higher retention times, respectively. The standards were assigned the following values ($\log I_n$): benzene 1, naphthalene 2, phenanthrene 3, benz[*a*]anthracene 4 and benzo[*b*]chrysene 5. The void volume was approximated by the retention volume of the non-retained solute acetone (solution in acetonitrile).

RESULTS AND DISCUSSION

Characterization of bonded phases

The two ODS columns examined were characterized according to the method of Sander and Wise [14] by a test mixture of benzo[*a*]pyrene (BaP), phenanthro[3,4-*c*]phenanthrene and tetrabenzonaphthalene (TBN). Following their classification scheme, the Vydac 201TP is polymeric like ($\alpha_{\text{TBN/BaP}} = 0.49$) and the Spherisorb ODS-2 monomeric like ($\alpha_{\text{TBN/BaP}} = 1.83$). $\alpha_{\text{TBN/BaP}}$ is defined as $k'_{\text{TBN}}/k'_{\text{BaP}}$. By Sander and Wise Zorbax ODS was classified as a monomeric-like material.

Retention of TCDDs on OD-silica gels

In Table I the recalculated capacity factors *k'* obtained by O'Keefe *et al.* [5], the capacity factors for the monomeric and the polymeric ODS columns employed in our studies, the relative retention indices (RRI) (retention time relative to the absolute retention time of 2378-TCDD) for all three partition systems and the retention indices ($\log I_R$) for ODS2 and ODS3 are given. The retention times of TCDD isomers on the ODS2 column were measured with pure methanol and with acetonitrile–water (88:12) as mobile phases.

The comparison of the capacity factors shows clearly that the ODS3 column is more selective than the other two ODS columns. Only one co-elution was observed with the ODS3 column (1368- and 1378-TCDD), the capacity factors ranging between 2.83 and 8.48. The ODS2 phase, however, with acetonitrile–water as mobile phase, exhibited several co-elutions and the capacity factors were in the range 3.31–5.06. The selectivity of the ODS2 column is also strongly dependent on the mobile phase. Replacement of acetonitrile–water with pure methanol leads to a drastic alteration of the retention order. The selectivity of the ODS1 column can be compared with that of the ODS2 column. The slight differences in retention order can be attributed to minor variations in the nature of the stationary phase.

Comparison of the relative retention indices defined by O'Keefe *et al.* [5] shows another characteristic difference between the three ODS phases. With methanol as mobile phase 2378-TCDD is eluted from ODS1 and ODS2 as one of the analytes which elute at an average position. With acetonitrile–water

TABLE I

CAPACITY FACTORS (k'), RELATIVE RETENTION INDICES (RRI) AND RETENTION INDICES ($\log I_R$) OF TCDD COMPOUNDS FOR THREE ODS COLUMNS

TCDD isomer	H_f (kcal/mol)	L/B	ODS1 ^a		ODS2 ^b			ODS2 ^c			ODS3 ^d		
			k'^e	RRI ^{e,f}	k'	RRI ^f	$\log I_R$	k'	RRI ^f	$\log I_R$	k'	RRI ^f	$\log I_R$
1234	-12.24	1.35	1.74	1.132	2.31	1.087	4.855	4.08	0.839	4.970	3.34	0.458	4.298
1236	-14.31	1.49	1.46/1.49 ^g	1.016/1.027 ^g	1.98	0.976	4.687	4.03	0.830	4.953	3.13	0.435	4.270
1237	-16.71	1.63	1.44	1.077	1.98	0.976	4.687	4.46	0.902	>5	4.38	0.567	4.431
1238	-16.69	1.59	1.44	1.077	1.98	0.976	4.687	4.46	0.902	>5	3.95	0.522	4.381
1239	-14.13	1.47	1.46/1.49 ^g	1.016/1.027 ^g	1.93	0.961	4.659	3.86	0.802	4.900	3.88	0.514	4.371
1246	-13.01	1.35	1.38	0.983	— ^h	—	—	—	—	—	—	—	—
1247	-15.45	1.47	1.45	1.013	—	—	—	—	—	—	—	—	—
1248	-15.48	1.40	1.45	1.013	—	—	—	—	—	—	—	—	—
1249	-12.99	1.29	1.38	0.983	—	—	—	—	—	—	—	—	—
1267	-14.79	1.68	1.07	0.853	1.50	0.819	4.391	3.39	0.725	4.741	2.71	0.391	4.203
1268	-15.74	1.55	1.31/1.41 ^g	0.953/0.997 ^g	—	—	—	—	—	—	—	—	—
1269	-13.37	1.35	1.02	0.833	—	—	—	—	—	—	—	—	—
1278	-17.12	1.66	1.32	0.956	1.75	0.903	4.5534	4.09	0.839	4.971	3.62	0.487	4.336
1279	-15.57	1.59	1.31/1.41 ^g	0.953/0.997 ^g	—	—	—	—	—	—	—	—	—
1289	-14.56	1.60	1.07	0.853	1.53	0.829	4.410	3.31	0.713	4.713	2.99	0.420	4.251
1368	-16.70	1.48	1.66	1.100	2.24	1.064	4.821	4.86	0.967	>5	3.79	0.505	4.364
1369	-14.35	1.28	1.30/1.33 ^g	0.950/0.963 ^g	—	—	—	—	—	—	—	—	—
1378	-18.10	1.59	1.59	1.068	2.10	1.039	4.784	4.90	0.974	>5	4.77	0.608	4.470
1379	-16.57	1.59	1.66	1.100	2.17	1.039	4.784	4.86	0.967	>5	4.67	0.607	4.472
1469	-12.01	1.17	1.02	0.833	—	—	—	—	—	—	—	—	—
1478	-15.83	1.34	1.30/1.33 ^g	0.950/0.963 ^g	1.75	0.903	4.557	3.92	0.812	4.920	2.83	0.404	4.221
2378	-19.54	1.84	1.42	1.000	2.05	1.000	4.724	5.06	1.000	>5	8.48	1.000	4.743

^a Stationary phase, Zorbax ODS; column dimensions, 500 mm × 6.2 mm I.D.; mobile phase, methanol.^b Stationary phase, Spherisorb ODS-2; column dimensions, 250 mm × 4.6 mm I.D.; mobile phase, methanol.^c Stationary phase, Spherisorb ODS-2; column dimensions, 250 mm × 4.6 mm I.D.; mobile phase, acetonitrile–water (88:12, v/v).^d Stationary phase, Vydac 201TP; column dimensions, 250 mm × 4.6 mm I.D.; mobile phase, acetonitrile–water (88:12, v/v).^e Data from ref. 5.^f Retention time relative to absolute retention time of 2378-TCDD (30.3 min).^g Alignment is not unambiguous.^h — = Not determined.

2378-TCDD is eluted the last from ODS2 and on ODS3 it is well resolved from all the studied TCDD isomers. Possibly the selectivity of ODS3 for TCDDs makes this partition system well suited to separate 2378-TCDD, the most toxic TCDD isomer, from a large excess of the other TCDD isomers prior to analysis by GC–MS or another appropriate method. In Fig. 2 the chromatogram of the thirteen TCDD isomers on ODS3 is shown. 2378-TCDD is perfectly baseline resolved from all the other TCDD isomers within 35 min.

Further, a shift concerning the range of $\log I_R$ is observed on comparing ODS2 to ODS3. For ODS1 no data are available that allow the evaluation of

$\log I_R$. With acetonitrile–water as mobile phase, six of the examined isomers elute from ODS2 after benzo[*b*]chrysene, whereas from ODS3 all isomers elute between benz[*a*]anthracene and benzo[*b*]chrysene. This observation is in agreement with the results of other workers [10], who found that ODS columns from various manufacturers not only provide different efficiencies for PAHs but also different selectivities and retention characteristics. They also observed a dependence of $\log I_R$ of PAHs on the surface coverage with ODS groups and on $\alpha_{\text{TBN/BaP}}$. The dependence of $\log I_R$ on the mobile phase was not reported, however.

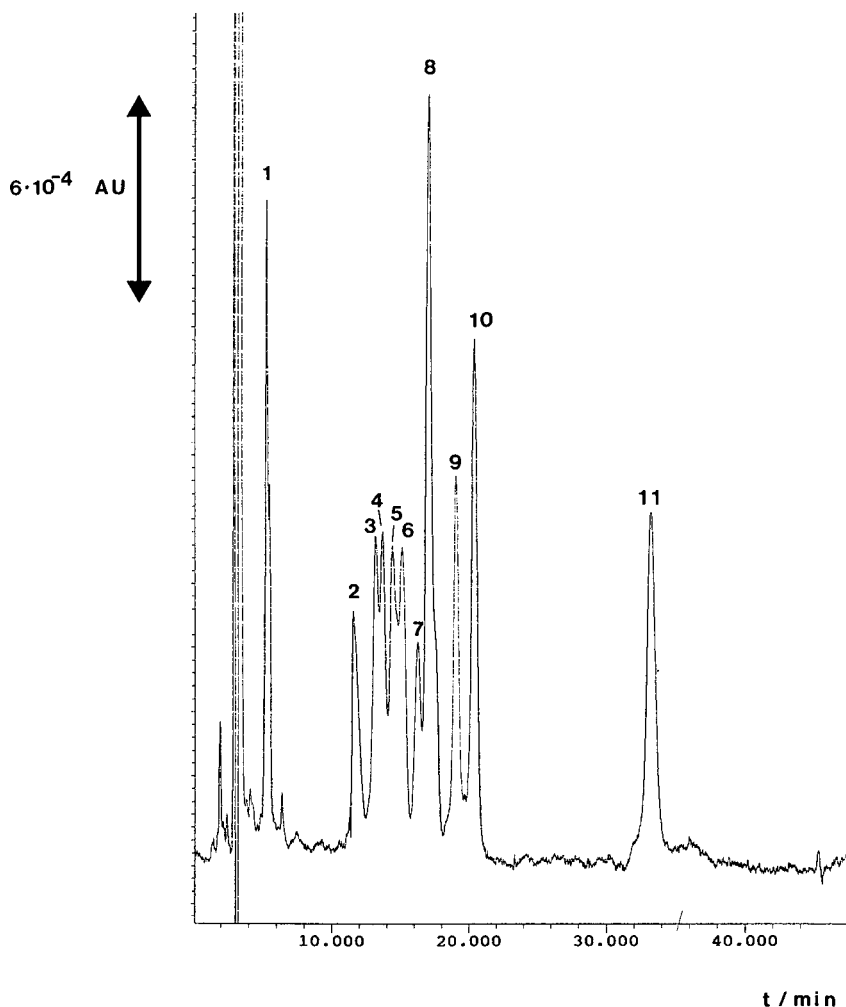


Fig. 2. Separation of TCDD isomers on ODS3. Stationary phase, Vydac 201TP; mobile phase, acetonitrile–water (80:20, v/v); flow-rate, 1 ml/min; detector wavelength, 235 nm; temperature, 25°C. Peaks: 1 = solvent; 2 = nonane; 3 = 1267-TCDD; 4 = 1478-TCDD; 5 = 1289-TCDD; 6 = 1236-TCDD/1234-TCDD; 7 = 1278-TCDD; 8 = 1368-TCDD/1239-TCDD/1238-TCDD; 9 = 1237-TCDD; 10 = 1379-TCDD/1378-TCDD; 11 = 2378-TCDD.

Calculation of geometric parameters

Wise and co-workers [10] found a relationship between shape parameters, particularly the calculated length-to-breadth ratio (L/B), of PAHs and alkylated derivatives and their retention indices on polymeric ODS phases. The parameter L/B was introduced by Radecki *et al.* [15] in quantitative structure–retention relationship studies to explain the retention order of PAH isomers separated on nematic liquid crystal GC phases and by Lamparc-

zyk *et al.* [16] to describe the bioactivity of PAHs. Wise *et al.* [17] found an analogy between the retention order of PAH isomers separated on liquid crystal phases of the smectic type by GC and their retention order on polymeric-type ODS phases employed in RP-HPLC.

The PCDDs constitute a class of compounds with a rigid fused-ring structure, similar to the class of PAHs. It is not yet clear whether all the TCDD isomers exhibit in solution a folded or a near-planar

structure. In the following text a folded structure of TCDDs is defined as a structure with a distortion angle $\beta > 10^\circ$; β is given by the angle between the planes defined by the two benzene rings.

2378-TCDD has a near-planar structure in the crystal lattice [18]. Graininger *et al.* [19] calculated the ether linkage (COC) bond angles for the 22 TCDD isomers from infrared data (studies in the gas phase). The average bond angles range from near planar (115.1°) for 2378-TCDD to approximately tetrahedral for isomers with aromatic rings of low electron-withdrawing capacity. However, it must be stated that dibenzo-*p*-dioxin, with aromatic rings of low electron-withdrawing capacity, also exhibits a near-planar structure in the crystal lattice [20].

We found by quantum mechanical calculation that the energetic difference between a folded and a near-planar structure (closed-shell molecules) for TCDDs is extremely small. The heat of formation (H_f) calculated by AMPAC was -14.20 kcal/mol for 1238-TCDD with a distortion angle β of 14.5° and -14.13 kcal/mol for a planar structure (1 kcal = 4.184 kJ). With 1247-TCDD we obtained $H_f = -15.45$ kcal/mol for the planar and $H_f = -15.52$ kcal/mol for the folded ($\beta = 14.2^\circ$) structure. With 1478-TCDD the energetic difference was even less: $H_f = -15.88$ kcal/mol ($\beta = 14.9^\circ$), $H_f = -15.83$ kcal/mol ($\beta = 0.0^\circ$).

Therefore, we assumed that a near-planar structure can be readily achieved by all the TCDD isomers and might be the preferred structure when the analyte is sorbed on ODS-silica gel. The near-planar structures were employed for the calculation of the optimized L/B values.

The calculated ratios and the data obtained for H_f (near-planar structures) are listed in Table I. The thermodynamic stability follows the general trend that isomers with substituents in lateral positions are more stable than isomers with substituents in an α -position to one of the oxygen atoms. 2378-TCDD with substituents only in lateral positions is thermodynamically the most stable TCDD isomer ($H_f = -19.54$ kcal/mol), and 1469-TCDD with substituents only in α -positions is the least stable isomer ($H_f = -12.01$ kcal/mol). The differences in the H_f values are significant, in order to reflect the stability of these isomers in the environment, and might be useful to explain substitution patterns of TCDD isomers in natural samples.

The values for L/B range from 1.17 to 1.84. The TCDDs clearly differ in their geometric parameters. It can be deduced that 2378-TCDD can be easily separated from the other isomers if the retention mechanism is purely shape controlled.

Correlation of capacity factors with length-to-breadth ratios

A direct correlation of L/B with the retention indices ($\log I_R$) of the TCDD isomers on the polymeric phase (ODS3), in analogy with the work of Wise *et al.* [10], gave only unsatisfactory results ($R = 0.60$). This means that L/B is a parameter that does not independently predict the retention index of TCDDs on polymeric ODS phases. In contrast to the PAHs, the TCDDs have large dipole moments ($\mu = 0.02$ – 2.80 D), owing to the presence of chlorine atoms [21], whereas the dipole moments of PAHs are of the order of $\mu = 0.01$ D, and there is little variation among the values [22]. However, the overall dipole moment is not a parameter that can be used to describe all polar features of a molecule in quantitative structure–retention relationship (QSRR) studies of separations by RP-HPLC [23]. In spite of the limited validity of the overall dipole moment as a descriptor of the polarity of a molecule, it can be deduced that differences in polarity are much smaller with PAHs than with TCDDs.

For a classical RP-HPLC system a submolecular polarity parameter (maximum excess charge difference) was used together with other parameters as a significant descriptor of retention data [24]. Sarna *et al.* [25] pointed out that elution from an RP column with an aqueous mobile phase reflects the hydrophobicity of a compound, in addition to its organic phase–water partition coefficient. They determined octanol–water partition coefficients for a series of PCDDs and PCDFs experimentally by RP-HPLC.

We assume that for the separation of TCDDs by RP-HPLC, differences in the polarity of the solutes cannot be neglected in QSRR studies. The influence of polarity can be superimposed by steric effects (quantitatively expressed by the shape parameter L/B), and this shape parameter gains more influence with increasing surface coverage with ODS groups making the organic layer thicker and denser. Obviously, the mobile phase also influences to a great extent the shape selectivity of the stationary phase.

In order to verify our assumptions, we correlated

TABLE II

RESULTS OF THE REGRESSION ANALYSIS

a, b, c = Regression coefficients; r = partial correlation coefficient; P = probability; R = multiple correlation coefficient.

Correlation	a	b	c	F	P (%)	R	$r(\log k'_2)$	$r(L/B)$
$\text{Log } k'_2 = \log k' \text{ (ODS2)}^a$	-0.872	1.371	0.800	18.51	0.05	0.887	0.817	0.865
$\text{Log } k'_2 = \log k' \text{ (ODS2)}^b$	-0.987	1.538	0.727	21.63	0.03	0.901	0.840	0.865
$\text{Log } k'_2 = \log k' \text{ (ODS1)}$	-1.015	1.495	0.428	21.41	0.03	0.900	0.839	0.714

^a Mobile phase: methanol.

^b Mobile phase: acetonitrile–water (88:12, v/v).

the logarithms of the capacity factors ($\log k'_1$) of ODS3 with those of the columns with less surface coverage with ODS groups ($\log k'_2$) according to the equation

$$\log k'_1 = a + b \log k'_2 + cL/B \quad (2)$$

The variable $\log k'_2$ serves as a polarity descriptor. The results of the three equations are presented in Table II. In all instances the variables $\log k'_2$ and L/B are significant descriptors of $\log k'_1$. The partial correlation coefficients show that the shape parameter L/B contributes strongly to the predictive ability of the three equations.

Fig. 3 shows the plots of experimentally deter-

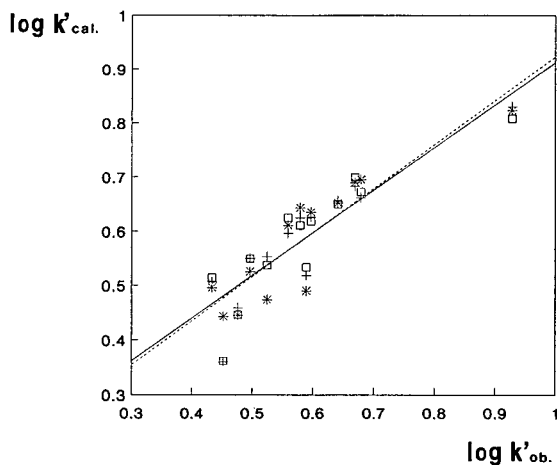


Fig. 3. Plot of logarithms of calculated capacity factors ($\log k'_{\text{cal.}}$) vs. logarithms of observed capacity factors ($\log k'_{\text{ob.}}$) on ODS3. \square = [$k'_2 = k'$ (ODS1)]; $+$ = [$k'_2 = k'$ (ODS2), mobile phase = methanol]; $*$ = [$k'_2 = k'$ (ODS2), mobile phase = acetonitrile–water (80:20, v/v)].

mined $\log k'$ (on ODS3) vs. predicted $\log k'$. The plots show no clustering and uniform error variances.

CONCLUSIONS

The results of the correlation analysis suggest that the observed differences in the selectivity of ODS columns can be attributed to an increasing influence of steric effects on the retention of analytes with increasing surface coverage of the stationary phase. Also, the mobile phase influences to a great extent the selectivity of ODS phases. The exhibited differences in selectivity with variations of the mobile phase can also be attributed to a variable influence of steric effects on the retention.

L/B can be used as a shape parameter to examine the influence of the geometry of the analytes. The relatively low multiple correlations show that L/B does not totally express the variance of steric parameters. It must be kept in mind that L/B is a two-dimensional parameter. If molecules deviate from a planar structure, this will strongly influence the retention behaviour.

Wise and May [9] have shown that polymeric ODS phases are superior to monomeric ODS phases with respect to the selectivity in the separation of PAHs. We found the same superiority in the separation of TCDDs. 1237–1238-TCDD and 1368–1379-TCDD, which co-elute on the monomeric phases, can be baseline separated on the polymeric ODS3 column.

This enhanced selectivity can be understood as an enhancement of the shape selectivity of the stationary phase, due to an organic layer with higher

density compared with the organic layers of monomeric ODS phases. The influence of the mobile phase is not fully understood, however.

ACKNOWLEDGEMENTS

This work was supported by a grant from the Wissenschaftsausschuss der NATO via Deutscher Akademischer Austauschdienst. Groupe BSN and Ministère de la Santé (France) are also acknowledged for financial support.

REFERENCES

- 1 L. L. Lamparski, T. J. Nestruck and R. H. Stehl, *Anal. Chem.*, 51 (1979) 1453.
- 2 L. L. Lamparski and T. J. Nestruck, *Anal. Chem.*, 52 (1980) 2045.
- 3 M. L. Langhorst and L. A. Shadoff, *Anal. Chem.*, 52 (1980) 2037.
- 4 J. J. Ryan and J. C. Pilon, *J. Chromatogr.*, 197 (1980) 171.
- 5 P. W. O'Keefe, R. Smith, C. Meyer, D. Hilker, K. Aldous and B. Jelus-Tyror, *J. Chromatogr.*, 242 (1982) 305.
- 6 J. S. Jasinski, *J. Chromatogr.*, 478 (1989) 348.
- 7 T. S. Thompson, D. H. Schellenberg, K. P. Naikwadi and F. W. Karasek, *Chemosphere*, 19 (1989) 45.
- 8 M. Swerev and K. Ballschmitter, *Chemosphere*, 15 (1986) 1123.
- 9 S. A. Wise and W. E. May, *Anal. Chem.*, 55 (1983) 1479.
- 10 S. A. Wise, W. J. Bonnett, F. R. Guenther and W. E. May, *J. Chromatogr. Sci.*, 19 (1981) 457.
- 11 M. J. S. Dewar, E. G. Zoebisch, E. F. Healy and J. J. P. Stewart, *J. Am. Chem. Soc.*, 107 (1985) 3902.
- 12 R. C. Weast (Editor), *CRC Handbook of Chemistry and Physics*, CRC Press, Boca Raton, FL, 61th ed., 1980.
- 13 M. Popl, V. Dolansky and J. Mostecky, *J. Chromatogr.*, 117 (1976) 117.
- 14 L. C. Sander and S. A. Wise, *LC · GC Int.*, 3 (1989) 24.
- 15 A. Radecki, H. Lamparczyk and R. Kaliszan, *Chromatographia*, 12 (1979) 595.
- 16 H. Lamparczyk, A. Radecki and R. Kaliszan, *Biochem. Pharmacol.*, 30 (1981) 2337.
- 17 S. A. Wise, L. C. Sander, H. C. K. Chang, K. E. Markides and M. L. Lee, *Chromatographia*, 25 (1988) 473.
- 18 F. P. Boer, F. P. Van Remoovtere, P. P. North and M. A. Newman, *Acta Crystallogr., Sect. B*, 28 (1972) 1023.
- 19 J. Graininger, V. V. Reddy and D. G. Patterson, *Appl. Spectrosc.*, 42 (1988) 643.
- 20 M. Senma, Z. Tarra, T. Taya and K. Osak, *Cryst. Struct. Commun.*, 2 (1973) 11.
- 21 U. Pyell, P. Garrigues, G. Félix, M. T. Rayez, A. Thienpont and P. Dentraygues, *J. Chromatogr.*, submitted for publication.
- 22 V. S. Ong and R. A. Hites, *Anal. Chem.*, 63 (1991) 2829.
- 23 R. Kaliszan, *Anal. Chem.*, 64 (1992) 619A.
- 24 R. Kaliszan, K. Ośmiatowski, S. A. Tomellini, S.-H. Hsu, S. D. Fazio and R. A. Hartwick, *J. Chromatogr.*, 352 (1986) 141.
- 25 L. P. Sarna, P. E. Hodge and G. R. B. Webster, *Chemosphere*, 13 (1984) 975.

Preparation and chromatographic evaluation of 3,5-dimethylphenyl carbamoylated β -cyclodextrin stationary phases for normal-phase high-performance liquid chromatographic separation of enantiomers

Tihamér Hargitai[☆], Yuriko Kaida and Yoshio Okamoto

Department of Applied Chemistry, Faculty of Engineering, Nagoya University, Chikusa-ku, 464-01 Nagoya (Japan)

(First received March 23rd, 1992; revised manuscript received September 1st, 1992)

ABSTRACT

Thirteen chiral stationary phases (CSPs) were prepared from β -cyclodextrin (β -CD) and their chiral recognition abilities were evaluated under normal-phase conditions by high-performance liquid chromatography. All materials were prepared by three different methods and contained 3,5-dimethylphenylcarbamate residues. The influence of different spacers, the amount of immobilized carbamoylated β -CD and the degree of substitution on β -CD on the enantioselectivity of the CSPs was considered. The results suggest that the enantioselectivity of the materials is favoured by high degrees of substitution of carbamate groups on β -CD and large amounts of chemically bonded carbamoylated β -CD. The highest selectivities were obtained on CSPs where complete carbamoylated β -CD was immobilized on the silica surface.

INTRODUCTION

β -Cyclodextrin (β -CD) is a cyclic natural oligomer containing seven glucose units connected via α -(1,4)-linkages. Schematically, the shape of β -CD can be presented as a truncated cone with seven primary hydroxy groups attached to the smaller opening of the cone while the remaining fourteen secondary hydroxy groups are located on the larger opening of the cone. Both unfunctionalized and functionalized β -CDs, chemically bonded to silica, have been reported to separate a variety of analytes by HPLC under reversed-phase conditions [1,2]. The separation mechanism has often been claimed

to depend on the formation of inclusion complexes where the guest molecule enters the relative hydrophobic interior of the cone from the larger side of the opening of the cone. This has traditionally resulted in β -CD being chemically bonded to support particles via the primary hydroxy groups situated on the smaller opening of the cone.

Recently, the normal-phase separation of enantiomers on a chiral stationary phase (CSP)-containing partly naphthylethylcarbamate-substituted β -CD has been reported [3,4]. As the maximum degree of substitution per β -CD is about 7 [4], both carbamate groups and remaining unreacted hydroxy groups can interact with the enantiomeric analytes and thus contribute more or less to the separation mechanism. The separation mechanism on this CSP has been considered to act more like the Pirkle-type chiral stationary phases [3].

Enantiomeric separations on 3,5-dimethylphenylcarbamate-functionalized polysaccharides have been reported to be successful [5]. In fact, 343

Correspondence to: Y. Okamoto, Department of Applied Chemistry, Faculty of Engineering, Nagoya University, Chikusa-ku, 464-01 Nagoya, Japan.

[☆] Present address: Department of Chemical Engineering 2, Chemical Centre, University of Lund, P.O. Box 124, S-221 00 Lund, Sweden.

(80%) of 483 racemic compounds could be resolved on at least one of the CSPs containing tris (3,5-dimethylphenylcarbamate)-functionalized cellulose or amylose [6]. The complete substitution of hydroxy groups with 3,5-dimethylphenyl isocyanate on α , β - or γ -cyclodextrin has recently been reported [7]. The carbamoylated cyclodextrins were adsorbed on silica particles and chiral separations were obtained using the normal-phase chromatographic mode. The practical use of the prepared CSPs is limited, however, as highly non-polar solvents must be used as eluents.

In this paper we report the use of CSPs containing 3,5-dimethylphenylcarbamate-functionalized β -CD, chemically bonded to silica, thus avoiding the limited practical use of the above-mentioned adsorbed carbamoylated CD materials. Thirteen CSPs were prepared by using different preparation methods and different spacers. Enantioselectivity of the CSPs was chromatographically evaluated under normal-phase conditions with a variety of racemic solutes. The influence of the degree of substitution on the β -CD and the amount of immobilized carbamoylated β -CD on the enantioselectivity is discussed briefly.

EXPERIMENTAL

Chemicals

The racemic solutes were obtained from different sources. β -Cyclodextrin (β -CD) of guaranteed reagent grade was purchased from Nacalai Tesque (Kyoto, Japan). Triphenylmethyl chloride (trityl chloride) and the spacers 4,4'-diphenylmethane diisocyanate (A), hexamethylene diisocyanate (B) and suberoyl chloride (C) were of guaranteed reagent grade from Tokyo Kasei (Tokyo, Japan) and dodecanedioyl dichloride (D) (98%) was obtained from Aldrich (Milwaukee, WI, USA). 3,5-Dimethylphenyl isocyanate was synthesized from 3,5-dimethylaniline by a conventional method. The silylating reagent 3-aminopropyltriethoxysilane (99%) was obtained from Janssen Chimica (Geel, Belgium) and the silylating agent 3-isocyanatopropyltriethoxysilane (spacer F) from Lancaster Synthesis (Moresambé, UK). Develosil, a totally porous spherical silica gel with a mean particle size of 5 μm , a mean pore diameter of 100 Å and a specific surface area of 345 m^2/g , was purchased from Nomura Chemical

(Nagoya, Japan). Daisogel, a totally porous spherical silica gel with a mean particle size of 5 μm , a mean pore diameter of 120 Å and a specific surface area of 309 m^2/g , was a gift from Daiso (Osaka, Japan). All solvents used in the preparation of the CSPs were of at least analytical-reagent grade and carefully dried before use. Solvents used in the chromatographic experiments were of HPLC grade.

Preparation of chiral stationary phases

Method 1. β -CD (0.5 g) was added to either pure pyridine (12 ml) or tetrahydrofuran (THF)–pyridine (10 + 2 ml), depending on whether isocyanate (pyridine) or acid chloride (THF–pyridine) functionalized spacers (A, B, C or D) were used in the derivatization procedure. About 90 mol% of the available hydroxy groups on the β -CD were reacted with 3,5-dimethylphenyl isocyanate (1.1–1.3 g) for 3 h at 90°C under a nitrogen atmosphere. The disappearance of the isocyanate groups, $-\text{N}=\text{C}=\text{O}$ (2200–2300 cm^{-1}) and appearance of carbonyl groups (1700 cm^{-1}) was monitored by FT-IR spectrometry. A twofold excess of the spacer (A, B, C or D), based on moles of unreacted hydroxy groups on β -CD, was added to the reaction mixture and the reaction was continued for 3 h at 90°C. After evaporation of the solvents under reduced pressure, the modified β -CD was washed with 3 \times 10 ml of hexane and then dissolved in THF–pyridine (10 \times 2 ml). The β -CD solution was injected on to previously vacuum-dried (180°C, 4 h) amino-functionalized silica gel (3.0 g) and reacted at 90°C overnight. The CSPs obtained were filtered and washed carefully with an excess of THF, N,N-dimethylacetamide (DMA), pyridine, methanol, water, THF, and hexane and finally dried under vacuum at 60°C for about 5 h. The carbon contents of phase I materials are approximately comparable to the immobilized carbamoylated β -CD contents determined by the mass difference of the dried particles before and after functionalization.

Method 2. To a suspension containing previously vacuum-dried amino-functionalized silica gel (3.0 g, 180°C, 4 h) and THF–pyridine (10 + 1 ml) was added 0.03 mmol of a spacer (A, B, C or D) per gram of silica. The amount of spacer added corresponds to the same amount of immobilized carbamoylated β -CD prepared by method 1 if every spacer only binds to one β -CD molecule. After

completion of reaction with the spacer (3 h, 90°C, nitrogen atmosphere), a small excess of β -CD (about 1.3 mol excess based on moles of spacer) was added to the reaction solution together with DMA-pyridine (10 + 1 ml) and reacted for 3 h at 90°C. A twofold excess of 3,5-dimethylphenyl isocyanate (based on moles of unreacted hydroxy groups on β -CD) was finally added to the reaction mixture and reacted overnight at 90°C. The CSPs obtained were filtered and washed as described in method 1. The amount of immobilized β -CD was measured as the mass difference of the dried particles before and after functionalization.

Method 3. Pure spacer F, or a previously prepared spacer solution of E (see below), was dropwise added to a pyridine solution (10 ml) of β -CD (0.5 g) and reacted at 90°C for 1 h under a nitrogen atmosphere. A twofold excess of 3,5-dimethylphenyl isocyanate (2.8 g) (based on moles of unreacted hydroxy groups) was then added to the reaction solution and reacted for about 4 h at 90°C. The reaction solution was finally added to previously vacuum-dried silica gel (3.0 g, 180°C, 4 h) and reacted overnight at 90°C. The CSPs obtained were filtered and washed as described in method 1. The materials obtained were end-capped with trimethylchlorosilane (2 ml) in benzene-pyridine (30 + 1 ml). The end-capped materials were filtered and washed as described in method 1. The amount of immobilized β -CD was measured as the mass difference of the dried particles before and after functionalization with β -CD, *i.e.*, before end-capping of the material.

The spacer solution of E was prepared the following way: a solution of spacer B in pyridine (3 ml) was prepared so that the final amount of prepared spacer E would correspond to two spacers per β -CD molecule (about 10 mol% of available hydroxy groups on β -CD). A small excess of 3-aminopropyltriethoxysilane (1.1 mol excess based on moles of added spacer B) was added dropwise to the solution for 5 min at 50°C and allowed to react for 1 h at 50°C.

Preparation of NMR samples

The completely carbamoylated β -CD sample was prepared by adding an excess of 3,5-dimethylphenyl isocyanate (2.5 g) to a pyridine solution (10 ml) of β -CD (0.5 g). After 4 h of reaction at 90°C, the carbamoylated β -CD was precipitated in methanol-

water (4:1, v/v), filtered and vacuum dried at 110°C for 4 h. Elemental analysis data supported the formation of almost completely carbamoylated β -CD (found, C 65.45, H 6.11, N 6.80; calculated, C 65.66, H 6.18, N, 6.96%) [7]. The partly carbamoylated β -CD sample was prepared as described above with the difference that only 20 mol% of available hydroxy groups on β -CD were reacted with 3,5-dimethylphenyl isocyanate. The position C-2- and C-3-carbamoylated β -CD sample was prepared by adding an excess of trityl chloride (1.3 g) to a pyridine solution (14 ml) of β -CD (0.5 g) [8]. After reaction overnight at 90°C, an excess of 3,5-dimethylphenyl isocyanate (1.9 g) was added to the solution and allowed to react for 5 h at 90°C. The product was precipitated in methanol-water (4:1, v/v), filtered and vacuum dried at 80°C for 4 h. The trityl groups on position C-6 were removed by treatment with concentrated hydrochloric acid-methanol solution for 1 h at room temperature. The methanol-soluble products were precipitated in pure water, filtered and finally vacuum dried at 110°C overnight.

Preparation of amino-functionalized silica gel

Vacuum-dried silica gel (20 g, 180°C, 4 h) was suspended in a mixture of 250 ml of dry benzene and 3 ml of dry pyridine under a nitrogen atmosphere. 3-Aminopropyltriethoxysilane (5 ml) was added to the suspension and the reaction mixture was refluxed for about 15 h. The amino functionalized silica gel obtained was washed thoroughly with an excess of THF, methanol, acetone and hexane and finally dried under vacuum at 60°C for about 5 h. The amount of bonded 3-aminopropyltriethoxysilyl groups was determined by elemental analysis: for develosil, C 4–5, N 1.2%; for Daisogel, C 3.2, N 1.0%.

Treatment of amino-functionalized silica gel with isocyanate

3,5-Dimethylphenyl isocyanate (0.65 g) was added to a suspension of previously vacuum-dried amino-functionalized silica gel (3.0 g, 160°C, 2 h) in pyridine (10 ml). The reaction mixture was refluxed overnight and the partly isocyanate-treated silica gel obtained was filtered and washed as described for the preparation of amino-functionalized silica gel.

Apparatus and chromatography

The specific surface area of amino-functionalized silica gel was measured with a Micromeritics (Norcross, GA, USA) Flowsorb II 2300 Flowsorber. ^1H NMR spectra were obtained on a Varian VXR-500 NMR spectrometer operating at 500 MHz, using pyridine- d_5 as the solvent and tetramethylsilane (TMS) as the internal standard. All ^1H NMR spectra were recorded at 80°C . The sample tube size was 5 mm and the sample concentrations were *ca.* 10 mg/ml. Assignment of the three peaks of methyl groups was made on the basis of known results [8].

The carbamoylated β -CD bonded to silica gels was packed into 250×4.6 mm I.D. stainless-steel columns by conventional high-pressure slurry-packing procedures. The chromatographic experiments were performed using a Jasco BIP-I HPLC pump, a Jasco 875 UV detector (254 nm), a Jasco DIP-181C polarimeter (Hg lamp, no filter, 5×0.3 cm I.D.) and a Jasco RC-228 recorder at room temperature. About 1–5 μl of a solution of a racemate was injected into the chromatographic system (20- μl loop) with a Rheodyne Model 7125 injector. *n*-Hexane–2-propanol (90:10, v/v) was usually used as the eluent at a flow-rate of 0.5 ml/min. The dead time (t_0) was determined with 1,3,5-tri-*tert.*-butylbenzene.

RESULTS AND DISCUSSION

Characterization of prepared materials

The chiral stationary phases consisting of 3,5-dimethylphenylcarbamoylated β -cyclodextrin bonded to silica particles were prepared by different methods. The materials obtained were divided into two groups of CSPs, phase I and phase II materials. In phase I materials, probably a large fraction of the immobilized β -CD molecules are bonded to the silica surface by the larger opening of the truncated cone of β -CD. In phase II materials, probably the smaller opening of the cone is bonded to the silica surface (Fig. 1). The CSPs are named according to the orientation of the immobilized β -CD molecule, using the roman numerals I or II, and according to the spacer used. Six different difunctional spacers, A, B, C, D, E and F, shown in Fig. 2, were used to immobilize β -CD. However, depending on the preparation method used, materials IIB and IIE contain identical linkages between the silica surface

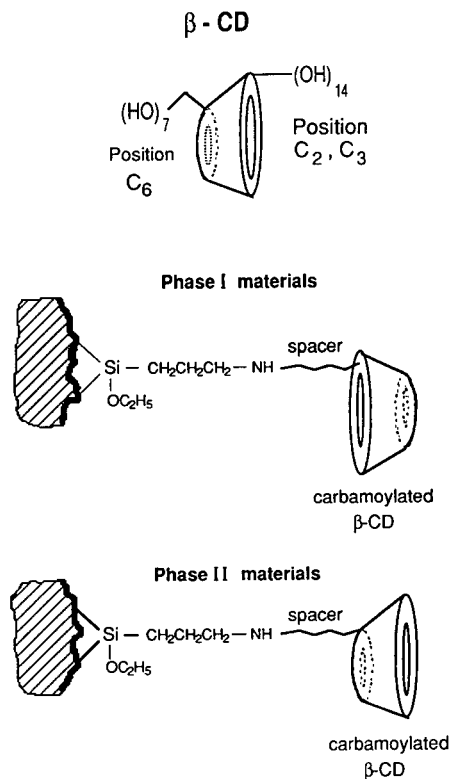


Fig. 1. Schematic model of β -cyclodextrin and phase I and phase II chiral stationary phases.

and the carbamoylated β -CD and are therefore comparable. The number of spacers per β -CD, in Tables I and II, were calculated on the assumption that all added spacers during the preparation of the CSPs were used as spacers. The carbon contents of phase I materials are approximately comparable to the immobilized carbamoylated β -CD contents determined by gravimetric analysis (Table I).

The different phase I and II materials were prepared by utilizing the commonly accepted fact that the seven primary hydroxy groups, located on the smaller opening of the truncated cone (position C-6), have higher reactivities than the fourteen secondary hydroxy groups (positions C-2 and C-3) (Fig. 1) [1]. The higher reactivity of the primary hydroxy groups was confirmed by NMR analysis on three different carbamoylated β -CD samples. Three peaks were detected for the three different positioned carbamoylated groups (Fig. 3a). The posi-

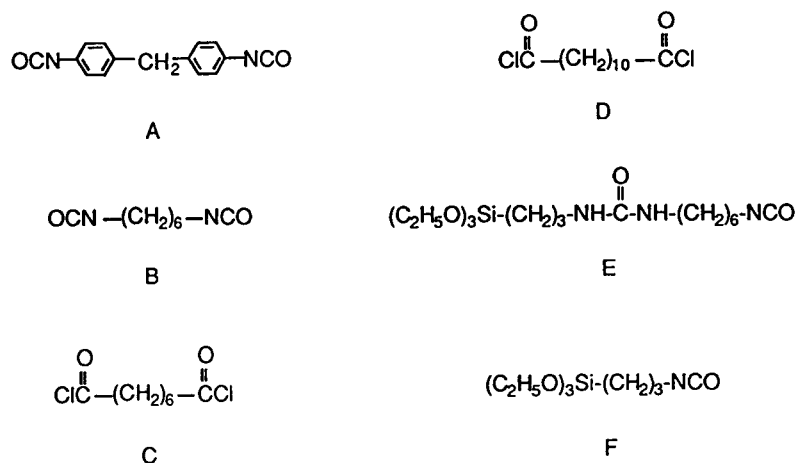


Fig. 2. Difunctional spacers used for immobilization of β -cyclodextrin on silica particles.

tions of the primary *versus* the secondary carbamoylated groups were distinguished by using triphenylmethyl chloride (trityl chloride) as a selective protecting reagent for the primary hydroxy groups [8], thus obtaining predominately position C-2- and C-3-carbamoylated β -CD (Fig. 3b). The higher reactivity of primary hydroxy groups was confirmed by analysis on a partly carbamoylated β -CD sample where about four (20%) of the total available twenty-one hydroxy groups on β -CD were carbamoylated (see *Preparation of NMR samples*). The resulting NMR spectra show only one peak at the position

for primary hydroxy carbamoylated groups (Fig. 3c).

Phase I materials were prepared by carbamoylation of about 85–95 mol% of the available hydroxy groups on β -CD (18–20 OH per β -CDs) with 3,5-dimethylphenyl isocyanate, according to preparation method 1. The remaining unreacted secondary hydroxy groups were reacted with a difunctional spacer and the spacer-functionalized β -CD obtained were immobilized on amino-functionalized silica particles. The degree of carbamoylation on β -CD was confirmed by elemental analysis of nitro-

TABLE I
CHARACTERIZATION OF PHASE I MATERIALS PREPARED BY METHOD 1

Parameter	Chiral stationary phase						
	IA1	IA2	IB1	IB2	IC1	IC2	ID1
Material	IA1	IA2	IB1	IB2	IC1	IC2	ID1
Spacer	A	A	B	B	C	C	D
No. of spacers per β -CD ^a	3–4	1	3	2	3	1–2	1
β -CD (mass %) ^b	6	11	14	17	10	13	12
C_{tot} (%) ^c	5.5	9.3	10.1	11.9	7.0	10.9	9.5
β -CD (mass %) ^d	8	14	16	19	11	17	14
β -CD ($\mu\text{mol}/\text{m}^2$) ^e	0.05	0.10	0.13	0.16	0.09	0.12	0.11

^a Molar ratios of spacer to β -CD used.

^b Based on gravimetric analysis on silica-bonded carbamoylated β -CD.

^c Due to functionalized phase, including spacer and carbamoylated CD but excluding carbon content on the silica surface.

^d Based on C elemental analysis.

^e Surface concentration of carbamoylated β -CD based on gravimetric results for mass% immobilized β -CD.

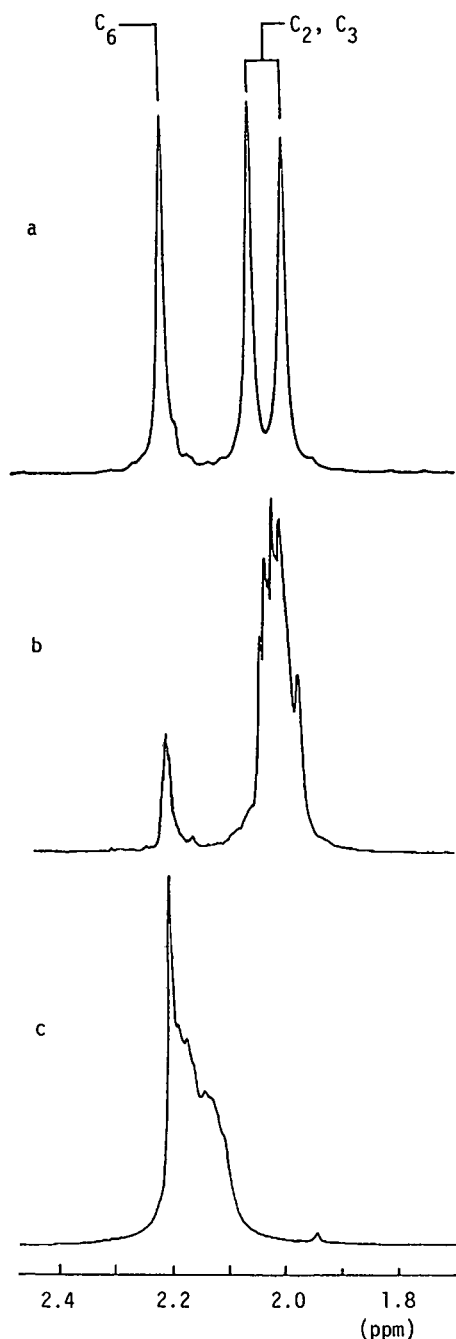


Fig. 3. ^1H NMR spectra of the CH_3 protons of 3,5-dimethylphenylcarbamate of β -cyclodextrines: (a) 100 mol% carbamoylated; (b) C-2-, C-3-carbamoylated; (c) 20 mol% carbamoylated. Pyridine- d_5 , 80°C, 500 MH.

gen for a 95% carbamoylated β -CD, the calculated and found nitrogen contents being 6.87 and 6.88%, respectively. The surface concentration of silica-bonded carbamoylated β -CD for phase I materials is about $0.12 \mu\text{mol}/\text{m}^2$ calculated from gravimetric results (Table I). This is comparable to reported results [9] of 0.12 and $0.19 \mu\text{mol}/\text{m}^2$ of hydroxypropyl-functionalized β -CD, depending on the specific surface area of the bare silica, 170 and $100 \text{ m}^2/\text{g}$, respectively. As the surface area of the amino-functionalized silica gel used in this work is $290 \text{ m}^2/\text{g}$ (bare silica $345 \text{ m}^2/\text{g}$), high absolute amounts of bonded carbamoylated β -CD are prepared by method 1 (Table I).

Phase II materials were prepared by two different methods. In preparation method 2, spacers were first bonded to amino-functionalized silica particles, then unmodified β -CD was immobilized by reaction between the spacers and the primary hydroxy groups on the β -CD. The remaining hydroxy groups on the immobilized β -CD were finally carbamoylated with an excess of the derivatizing agent. In method 3, a small amount of spacer (about two spacers per β -CD) was first reacted with the primary hydroxy groups on β -CD followed by carbamoylation of the remaining unreacted hydroxy groups. The functionalized β -CD obtained was then immobilized on unmodified silica particles and the materials obtained were finally end-capped with trimethylchlorosilane.

Preparation of phase II materials results in small amounts of immobilized carbamoylated β -CD compared with phase I materials (Table II). The gravimetrically determined values of the amount of immobilized carbamoylated β -CD, prepared according to method 2, are influenced by the formation of urea groups as a fraction of the added amount of 3,5-dimethylphenyl isocyanate reacts with amino groups on the silica surface. In an experiment in which amino-functionalized silica particles were reacted with a twofold molar excess of 3,5-dimethylphenyl isocyanate, based on moles of amino groups, about 0.03 g of urea groups per gram of silica particles was formed. The amount of immobilized carbamoylated β -CD of CSPs prepared by method 2 is probably smaller because not all of the available hydroxy groups were carbamoylated, even though a twofold excess of the derivatizing agent was used. Similar results of low degrees of

TABLE II
CHARACTERIZATION OF PHASE II MATERIALS PREPARED BY METHODS 2 AND 3

Parameter	Method 2			Method 3		
	IIA	IIB	IIC	IID	IIE	IIF
Material	A	B	C	D	E	F
Spacer	A	B	C	D	E	F
No. of spacers per β -CD ^a	1	1	1	1	2	2
β -CD (mass%) ^b	7–9	7–9	6–8	5–7	6	3

^a Molar ratio of spacer to β -CD used.

^b Based on gravimetric analysis of silica-bonded carbamoylated β -CD.

substitution on immobilization of unfunctionalized β -CD have been reported [3,10]. A simple calculation, assuming that the same number of unfunctionalized β -CD molecules as carbamoylated β -CD molecules by preparation method 1 were immobilized by preparation method 2, indicates that only about ten of the available twenty-one hydroxy groups of β -CD are carbamoylated. This is comparable to values of seven and ten reported for the degree of substitution of β -CD bonded to silica with naphthylethyl isocyanate and 2,6-dimethylphenyl isocyanate, respectively [3]. By using preparation method 3, completely carbamoylated β -CD (calculated and found nitrogen contents 7.4 and 7.6%, respectively) was immobilized on the silica particles. The small amount (3%, w/w) of immobilized β -CD on material IIF can be ascribed to steric difficulties with the relative short spacer arm of spacer F reacting with the silica surface. A satisfactory explanation for the small amount of immobilized β -CD on material IIE cannot be given.

Different batches of amino-functionalized silica gels were prepared. The surface concentration of bonded amino-groups, which was calculated on results obtained from C and N elemental analysis, was $2.7 \mu\text{mol}/\text{m}^2$. The average number of reacted ethoxy groups per 3-aminopropyltriethoxysilane was calculated to be 1.9 which corresponds to 3.0 hydroxy groups/ nm^2 having reacted on the silica surface. These results can be compared with reported values of chemically reactive hydroxy groups on silica surfaces, based on reactions of monosilanes, of 2.3 [11] and 2.7 [12] hydroxy groups/ nm^2 .

Most columns exhibited a theoretical plate num-

ber of 3000 per column with benzene as solute. No improvements in the theoretical plate number by varying the packing procedure were observed.

Chromatographic evaluation

The chromatographic results for the optical resolution of fourteen racemic solutes (Fig. 4) are presented in Tables III, IV and V. Thirteen CSPs were prepared and chromatographically evaluated, seven phase I materials and six phase II materials. Also, different spacers were used for the immobilization of β -CD, the amount of carbamoylated β -CD bonded to silica and the number of spacers bonded to each carbamoylated β -CD being varied. As a general conclusion, phase I materials show superior enantioselectivity to phase II materials. On phase I materials, eleven of thirteen racemates were separated whereas on phase II materials only five of fourteen racemates were separated.

Phase I materials. For most racemates an increase in selectivity was observed as the amount of immobilized carbamoylated β -CD increased. For racemate 5, however, a higher selectivity was observed on the materials containing smaller amounts of carbamoylated β -CD (materials IB and IC, Table III). A reverse elution order was also observed for racemate 5 depending on whether large or small amounts of β -CD were immobilized. An increased amount of bonded carbamoylated β -CD resulted in higher capacity factors. A few exceptions from these observations are for racemates 7 and 11 eluted on materials IA and IB, for which the capacity factors decrease with increasing amount of bonded carbamoylated β -CD (Table III). This can be ex-

TABLE III
 NORMAL-PHASE HPLC SEPARATION DATA FOR PHASE I MATERIALS

Separation data for a variety of racemic solutes (Fig. 4). k'_1 = Capacity factor with optical rotation (in parentheses) of the first-eluted enantiomer. Separation factor $\alpha = k'_2/k'_1$. Mobile phase, *n*-hexane–2-propanol (90:10, v/v); flow-rate, 0.5 ml/min.

Solute No.	IA1		IA2		IB1		IB2		IC1		IC2		ID	
	k'_1	α	k'_1	α	k'_1	α	k'_1	α	k'_1	α	k'_1	α	k'_1	α
1	3.32(–)	ca. 1	3.60(–)	ca. 1	3.93(–)	ca. 1	4.82(+)	ca. 1	1.46(–)	ca. 1	1.60(–)	ca. 1	1.85(–)	ca. 1
2	0.50(+)	ca. 1	0.72(+)	ca. 1	0.53(+)	ca. 1	0.63(+)	ca. 1	0.40(+)	ca. 1	0.85(–)	ca. 1	0.53(–)	ca. 1
3	1.45(+)	1.25	2.31(+)	1.44	2.56(+)	1.23	2.94(+)	1.45	2.54(+)	1.14	3.17(+)	1.42	1.57(+)	1.54
4	2.27	1.0	4.83	1.0	3.47	1.0	2.76	1.0	2.62	1.0	4.4	1.0	1.67	1.0
5	0.99	1.0	0.99(–)	1.16	0.84(+)	1.14	1.33(–)	ca. 1	0.60(+)	ca. 1	1.10(–)	1.09	0.90(–)	ca. 1
6	0.99(–)	ca. 1	1.35(–)	1.10	1.12(–)	ca. 1	1.68(–)	ca. 1	0.92(–)	ca. 1	1.42(–)	1.09	1.01(–)	ca. 1
7	($k'_1 > 26$)	–	8.56(–)	ca. 1	8.84	ca. 1	4.13(+)	ca. 1	5.06	ca. 1	5.39(–)	1.05	2.52(–)	ca. 1
8	0.99	1.0	3.98(+)	1.03	3.0(+)	ca. 1	1.65	ca. 1	2.49(+)	ca. 1	3.96(+)	1.03	2.27(+)	ca. 1
9	1.42(+)	1.39	2.24(+)	1.98	1.46(+)	1.07	2.22(+)	1.27	1.05(+)	1.13	2.19(+)	1.69	1.28(+)	1.73
10	1.27(–)	1.07	1.95(–)	1.12	1.33	1.0	1.45	1.0	0.97	1.0	1.79(–)	1.09	0.97(–)	ca. 1
11	($k'_1 > 19$)	–	($k'_1 > 23$)	–	($k'_1 > 19$)	–	11.8(+)	–	10.1	1.07	10.1	1.0	12.7(+)	1.04
12	4.36(+)	ca. 1	6.57(–)	1.08	3.92	1.0	7.30(–)	1.03	3.19(+)	ca. 1	6.79(–)	1.13	4.50(–)	1.08
14 ^a	–	–	8.84(–)	1.40	7.26(–)	1.04	12.4(–)	1.27	4.38(–)	1.08	9.95(–)	1.35	6.36(–)	1.23

^a Mobile phase = *n*-hexane–2-propanol (70:30, v/v).

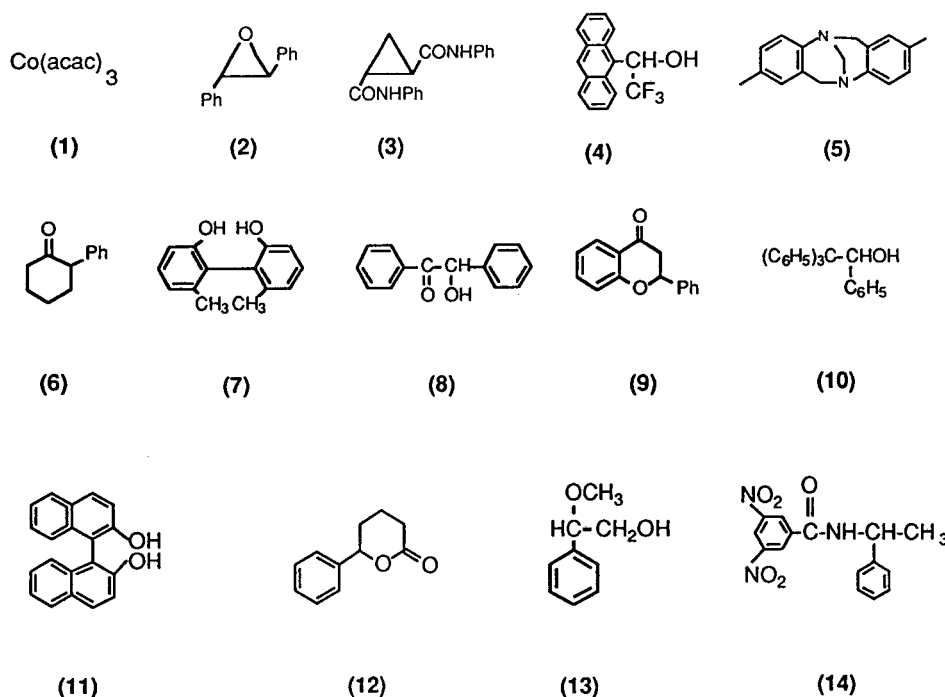


Fig. 4. Structures of racemic solutes.

plained by the strong interaction of the racemates with amino groups on the silica surface. As the amount of bonded carbamoylated β -CD increases, the effect of the strong interaction between racemates **7** and **11** and the amino groups decreases.

The four spacers A, B, C and D (Fig. 3) can be divided into two reactive functional groups, isocyanate and acyl chloride groups. The spacers bonds to β -CD through carbamate or ester bonds and to the amino groups on the silica surface by either urea or amide bonds. No significant difference in enantioselectivity, depending on the type of spacer used, could be observed between the different materials even though a reversed elution order could be detected for racemate **2** depending on the functionality of the spacers used (Table III). On the other hand, a greater influence on the enantioselectivity of the materials could be observed between the two isocyanate spacers and the two acid chloride spacers. Higher enantioselectivity was usually observed for the shorter acid chloride spacer C than the longer acid chloride spacer D. Similarly, higher enantioselectivity was usually observed for the aromatic, more rigid, space A than spacer B.

The influence of the number of bonded spacers per β -CD on the enantioselectivity is difficult to establish as the amounts of immobilized carbamoylated β -CD on the materials IA, IB and IC are different.

Phase II materials. As mentioned before, phase II materials usually have lower enantioselectivity than phase I materials. The four phase II materials, prepared according to method 2, have very similar enantioselectivities and capacity factors (Table IV); hence no significant effect of the spacers can be observed for these materials.

The two phase III materials prepared according to method 3 show an improved enantioselectivity compared with the other phase II materials in spite of the small amounts of immobilized carbamoylated β -CD (Table V). This probably depends on the higher degree of substitution of carbamate groups on β -CD achieved by method 3. The enantioselectivities of the two materials are comparable except for racemate **11**, which on material IIF exhibited the highest selectivity among all the materials prepared.

Influence of functionality of silica surface. Most of

TABLE IV

NORMAL-PHASE HPLC SEPARATION DATA FOR PHASE II MATERIALS PREPARED BY METHOD 2

Separation data for a variety of racemic solutes (Fig. 4) obtained on phase II materials prepared by method 2. k'_1 = Capacity factor with optical rotation (in parentheses) of the first-eluted enantiomer. Separation factor $\alpha = k'_2/k'_1$. Mobile phase, *n*-hexane–2-propanol (90:10, v/v); flow-rate, 0.5 ml/min.

Solute No.	IIA		IIB		IIC		IID	
	k'_1	α	k'_1	α	k'_1	α	k'_1	α
1	5.59(+)	ca. 1	8.76(+)	ca. 1	3.82(+)	ca. 1	4.89(+)	ca. 1
2	0.28(+)	ca. 1	0.31(+)	ca. 1	0.29(+)	ca. 1	0.29(+)	ca. 1
3	0.69(+)	1.20	0.64(+)	1.17	0.86(+)	1.23	0.67(+)	1.31
4	1.08	1.0	1.17	1.0	1.59	1.0	1.29	1.0
5	0.57	1.0	0.62(–)	ca. 1	0.55(–)	ca. 1	0.60(–)	ca. 1
6	0.71(–)	ca. 1	0.72(–)	ca. 1	0.74(–)	ca. 1	0.70(–)	ca. 1
7	0.94	1.0	1.10	1.0	1.54	1.0	1.17(+)	ca. 1
8	1.41	1.0	1.45(+)	1.05	1.50(+)	1.07	1.37(+)	1.07
9	0.71(+)	ca. 1	0.79(+)	ca. 1	0.75(+)	1.13	0.74(+)	1.04
10	0.56	1.0	0.60	1.0	0.66	1.0	0.58	1.0
11	1.99(+)	1.05	2.40(+)	ca. 1	3.15(+)	ca. 1	2.38(+)	1.06
12	2.39(+)	ca. 1	2.86(+)	ca. 1	2.78(+)	ca. 1	3.03(+)	ca. 1
14 ^a	–	–	4.40(–)	1.09	4.35(–)	1.12	–	–

^a Mobile phase = *n*-hexane–2-propanol (70:30, v/v).

TABLE V

NORMAL-PHASE HPLC SEPARATION DATA FOR PHASE II MATERIALS PREPARED BY METHOD 3

Separation data for a variety of racemic solutes (Fig. 4). k'_1 = Capacity factor with optical rotation (in parentheses) of the first-eluted enantiomer. Separation factor $\alpha = k'_2/k'_1$. Mobile phase, *n*-hexane–2-propanol (90:10, v/v); flow-rate, 1.0 ml/min.

Solute No.	IIE ^a		IIE ^b		IIF	
	k'_1	α	k'_1	α	k'_1	α
1	2.23	1.0	0.82	1.0	0.41	ca. 1
2	0.20(+)	ca. 1	0.15(+)	ca. 1	0.15(+)	ca. 1
3	0.53(+)	1.36	0.38(+)	1.43	0.28(+)	1.47
4	0.62	1.0	0.46	1.0	0.29	1.0
5	1.63(–)	ca. 1	0.25(–)	ca. 1	0.38(–)	ca. 1
6	0.50(–)	ca. 1	0.56	1.0	0.41(–)	ca. 1
7	0.63(–)	1.09	0.50(–)	ca. 1	0.35(–)	ca. 1
8	0.88(+)	ca. 1	0.50	1.0	0.44(+)	ca. 1
9	0.46(+)	1.47	0.34(+)	1.82	0.35(+)	1.60
10	0.37	1.0	0.31	1.0	0.23	1.0
11	1.00(+)	1.06	0.69(+)	1.09	0.47(+)	1.25
12	2.03	1.0	0.79(–)	ca. 1	0.88(–)	ca. 1
13	1.00(+)	ca. 1	0.32(+)	ca. 1	0.29	1.0
14	6.20(–)	1.29	1.40(–) ^c	1.23	0.82(–)	1.36

^a Before end-capping with trimethylchlorosilane.

^b After end-capping with trimethylchlorosilane.

^c Mobile phase = *n*-hexane–2-propanol (70:30, v/v).

the racemates show significantly lower capacity factors (k') on phase II than phase I materials. This can be explained by the functionality of the silica surface and to some extent also by the smaller amounts of immobilized carbamoylated β -CD on the phase II materials. During the preparation of phase II materials by method 2, some of the available amino groups are partly converted into urea residues, which should influence the surface functionality on the silica gel. The effect of a partly urea-functionalized silica surface on the capacity factors of the racemates was compared with capacity factors obtained on the pure amino-functionalized silica gel. About 30 mol% of the available amino groups on the silica surface reacted with 3,5-dimethylphenyl isocyanate. The results in Table VI confirm that the functionality of the silica surface influences the capacity factors of the racemates, especially for materials with a small amount of bonded carbamoylated β -CD. Some racemates, **7** and **11**, interact very strongly with amino groups on the silica surface, and racemate **1** interacts strongly with the partly isocyanate-reacted silica surface. These results explain the higher capacity factors for racemate **1** on phase IIA, B, C and D materials compared with phase I materials and the lower capacity factors for racemates **7** and **11** on phase IIA, B, C and D materials compared with those on phase I materials (Tables III and IV).

The capacity factors for the racemates are lower on the trimethylsilane end-capped materials IIE and IIF than on the other materials. The influence of end-capping on material IIE is presented in Table V. The capacity factors for the racemates decrease after the end-capping reaction. The selectivities for racemates **7** and **9** are affected by the end-capping reaction. The separation factor (α) for racemate **9** increases whereas α decreases for racemate **7** after the end-capping reaction.

Chiral separation mechanism. There are many reasons for believing that the enantiomeric separation mechanism is not due to the formation of inclusion complexes in the relatively hydrophobic interior of the truncated cone on completely carbamoylated β -CD. As the normal-phase chromatographic mode was used to evaluate the materials, probably the interior is occupied with the non-polar eluent (hexane) [13]. Each glucose unit contains five chiral centres. Two of these chiral centres are on the

TABLE VI

NORMAL-PHASE HPLC SEPARATION DATA FOR FUNCTIONALIZED SILICA PARTICLES

Separation data for a variety of racemic solutes (Fig. 4) obtained on amino-functionalized and partly isocyanate-treated amino-functionalized silica gel. k' = Capacity factor. Mobile phase, *n*-hexane–2-propanol (90:10, v/v); flow-rate, 0.5 ml/min.

Solute No.	k'	
	Amino-silica	Isocyanate-treated silica
1	0.58	10.99
2	0.12	0.12
3	0.72	0.25
4	2.01	0.47
5	0.28	0.71
6	0.34	0.41
7	Not eluted	0.42
8	0.30	0.27
9	0.23	0.33
10	0.59	0.23
11	Not eluted	0.79
12	1.21	1.78

C-2 and C-3 atoms. The carbamate groups on C-2 are located at the entrance of the cone and point in a clockwise direction whereas those on C-3 are located on the outside of the cyclodextrin molecule and point in a counter-clockwise direction [14]. Hence the number and orientation of carbamate groups on β -CD have a large effect on the enantioselectivity of the materials.

Comparison with other CSPs functionalized with 3,5-dimethylphenylcarbamate groups. Recently CSPs have been prepared by complete carbamoylation of α , β - or γ -CD with 3,5-dimethylphenyl isocyanate, followed by adsorption of the carbamoylated cyclodextrins on amino-functionalized silica gel [7]. The CSPs prepared were chromatographically evaluated with racemates **1**, **2**, **4**, **5** and **6**. The only racemates that were better or comparably separated on the materials presented in this paper are **5** and **6**; the latter racemate was not separated at all on the adsorbed β -CD CSP. The three other racemates (**1**, **2** and **4**) were all separated on the adsorbed β -CD CSP; in fact, **1** and **4** were the only racemates that could not be separated on the materials presented in this paper.

Racemates **1–10** have been separated on CSPs

containing the tris(3,5-dimethylphenylcarbamate) of cellulose or amylose [5]. Of the ten racemates, only racemate **9** has a higher separation factor (α) on the phase I materials presented in this paper.

CONCLUSIONS

Many factors influence the separation mechanism on the materials considered here. The influences of the degree of substitution of carbamate groups on β -CD and the amount of immobilized carbamoylated β -CD seem to be the most important factors for the enantioselectivity. Other factors such as the functionality and chain length of the spacer arm, the orientation of immobilized β -CD and the functionality of the silica surface all contribute to the total interaction possibilities and thus also influence the separation mechanism. More work remains to be done before more convincing explanations can be presented for the separation mechanism. The inclusion complexation mechanism, however, does not appear to play an important role in the separation mechanism.

ACKNOWLEDGEMENTS

T. H. was financially supported by a scholarship from the Swedisch National Board for Technical Development. This work was supported by the Grant-in-Aid Scientific Research (No. 02555184) from the Ministry of Education, Science and Culture of Japan.

REFERENCES

- 1 T. Ward and D. W. Armstrong, in M. Zieff and L. J. Crane (Editors), *Chromatographic Chiral Separations (Chromatographic Science Series, Vol. 40)*, Marcel Dekker, New York, 1989, Ch. 5.
- 2 D. W. Armstrong, C.-D. Chang and S. H. Lee, *J. Chromatogr.*, 539 (1991) 83.
- 3 A. M. Stalcup, S.-C. Chang and D. W. Armstrong, *J. Chromatogr.*, 540 (1991) 113.
- 4 D. W. Armstrong, A. M. Stalcup, M. L. Hilton, J. D. Duncan, J. R. Faulkner, Jr., and S.-C. Chang, *Anal. Chem.*, 62 (1990) 1610.
- 5 Y. Okamoto and Y. Kaida, *J. High Resolut. Chromatogr.*, 13 (1990) 708.
- 6 Y. Okamoto, Y. Kaida, R. Aburatani and K. Hatada, in S. Ahuja, *Chiral Separations by Liquid Chromatography (ACS Symposium Series, No. 471)*, American Chemical Society, Washington, DC, 1991, Ch. 5.
- 7 R. Aburatani, Y. Okamoto and K. Hatada, *Bull. Chem. Soc. Jpn.*, 63 (1990) 3606.
- 8 F. Cramer, G. Mackensen and Sensesse, *Chem. Ber.*, 102 (1969) 494.
- 9 A. M. Stalcup, S.-C. Chang, D. W. Armstrong and J. Pitha, *J. Chromatogr.*, 513 (1990) 181.
- 10 M. Tanaka, Y. Kawaguchi, T. Niinae and T. Shono, *J. Chromatogr.*, 314 (1984) 193.
- 11 G. E. Berendsen and L. de Galan, *J. Liq. Chromatogr.*, 1 (1978) 403.
- 12 K.K. Unger, N. Becker and P. Roumeliotis, *J. Chromatogr.*, 125 (1976) 115.
- 13 A. M. Stalcup, H. L. Jin, D. W. Armstrong, P. Mazur, F. Derguini and K. Nakanishi, *J. Chromatogr.*, 499 (1990) 627.
- 14 A. M. Alak, *Dissertation*, Texas Tech University, August, 1986; University Microfilms International, Ann Arbor, MI.

Separation of C₆₀ and C₇₀ on polystyrene gel with toluene as mobile phase

Andreas Gugel and Klaus Müllen

Max-Planck-Institut für Polymerforschung, Ackermannweg 10, W-6500 Mainz (Germany)

(First received September 8th, 1992; revised manuscript received September 30th, 1992)

ABSTRACT

The separation of C₆₀ and C₇₀ on polystyrene gel using toluene as mobile phase is described. A fully automated system was designed that permits the separation of 5–10 g of C₆₀–C₇₀ mixture within 24 h on a column of only 20 mm I.D. The purity of the isolated C₆₀ is greater than that achieved by standard procedures (separation on alumina) and the recovery is nearly 100%.

INTRODUCTION

Alkali-metal-doped C₆₀ is a molecular superconductor with by far the highest onset temperature of superconductivity, T_c [1], C₆₀-based material (charge-transfer complex) has the highest critical temperature, T_c , of any molecular organic ferromagnet [2,3] and buckminsterfullerene and its derivatives possess remarkable non-linear optical properties [4]. Owing to these outstanding properties and the resulting extensive research activity [5], there is an increasing need for an efficient separation of fullerenes. The isolation of pure C₆₀ is tedious and has proved to be the major constraint on the pace at which research can proceed.

In the last 2 years, several attempts at the separation of fullerenes have been published, *e.g.*, on C₁₈ reversed-phase [6], silica gel [7], alumina [8], graphite [9] and a π -acidic Pirkle phase [10]. Attempts to achieve the separation on a 10- μ m nitrophenyl phase (60 \times 25 mm I.D. column) with pure toluene as the mobile phase were unsuccessful because all fullerenes were eluted together. Mixtures

of hexane and toluene as mobile phases gave good separations but were not superior to the other reported methods.

All the methods described so far suffer from severe disadvantages: either the fullerenes are only slightly to moderately soluble in the mobile phase, which severely limits the amount of purifiable material, or the separation requires higher temperatures and is therefore not transferable to columns with larger inner diameter. Pure toluene, in which the fullerenes are more soluble (the solubility at room temperature is *ca.* 6 mg of fullerene mixture in 1 ml of toluene compared with about 0.4 mg/ml in hexane or 0.8 mg/ml in chloroform) is due to its greater elution power, generally not applicable to the above separation procedures. Thus, chromatography on alumina using pure toluene or even hexane with only 10% toluene leads to virtually no retention of the fullerenes. In summary, all the chromatographic methods applied so far are not suitable for the purification of larger amounts of C₆₀, because either the solvent consumption is very large (solvent mixtures are even not suitable for continuous recovery) or the efficiency, expressed in grams of raw material separated per day, is very low.

Owing to the size differences of C₆₀ and C₇₀ (7 Å spheres *versus* 7 \times 7 \times 9 Å ellipsoids) (Fig. 1), it

Correspondence to: Professor Dr. K. Müllen, Max-Planck-Institut für Polymerforschung, Ackermannweg 10, W-6500 Mainz, Germany.

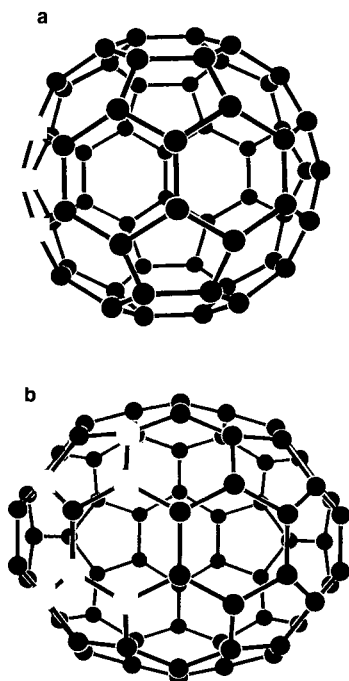


Fig. 1. (a) Structure of C_{60} ; (b) structure of C_{70} .

seemed appropriate to try to separate C_{60} and C_{70} by size-exclusion chromatography (SEC) on polystyrene gel [11,12]. In addition to the ability of SEC to separate compounds with a size difference of about 10%, this method possesses the following additional advantages over conventional chromatographic methods [13,14]: (1) compounds are eluted isocratically with a pure solvent so that equilibration after each run is not necessary, saving much time and solvent, and further the isocratic elution allows for immediate recycling of the mobile phase by distillation, permitting the design of a fully automated system; (2) the reproducibility of retention times is excellent, which makes unattended use of the apparatus possible; and (3) the lifetime of SEC columns is generally greater than that of conventional chromatographic columns.

EXPERIMENTAL

Equipment

For SEC, the pumps, manometer module, detector, printer and additional accessories were obtained from Abimed Analysen-Technik (Langen-

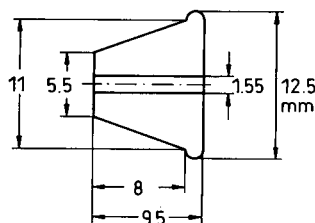


Fig. 2. Septum for leak-free connection of capillaries to the distillation flask.

feld, Germany), the motor valve and controller from Latek Labortechnik (Eppelheim, Germany), 500 Å columns from Polymer Standards Service (Mainz, Germany) and 50 Å columns from Showa Denko (Shodex, Japan). For HPLC, the column and stationary phase were obtained from Merck (Darmstadt, Germany), the elution pump from Spectra-Physics (Darmstadt, Germany) and the detector from Waters (Milford, MA, USA).

An M 305 master pump and an M 306 slave pump, both with 25 SC piston pump heads, an M 803 C manometer module with integrated pulse damper, a holochrome UV detector with a 0.3- μ l flow-through type cell (light path 0.1 mm) an HMV-6 motor valve (six-way valve) with a PT 810 S-controller and a BD-40 printer were used.

Two 600 \times 20 mm I.D. main columns (10 μ m, 500 Å) in series with a 60 \times 20 mm I.D. guard column (10 μ m, 500 Å) were used (two columns in series improve the resolution, allowing the amount of material that can be purified in a single injection to be increased or the purity of the fractions to be increased [11]; 10- μ m material was used because of the improved life time and flow compatibility compared with 5- μ m material). Capillaries were in front of the T connection (I.D. 1 mm) and behind the T connection (I.D. 0.5 mm to avoid a dead volume). Slip-on filters (10- μ m frit) were located in front of the pump heads and in-line membrane filters (0.5- μ m frit) behind the pump heads. For the distillation apparatus, all glassware was made of brown glass to avoid exposure of the fullerenes and the solvent to daylight [15–17]. The septa of the distillation flasks were conical and made of PTFE (Fig. 2). By tightening the G1 14 screw-caps the capillaries were clamped and sealed. The distillation head was heated by a heating tape to ensure rapid distillation of the solvent. The complete apparatus

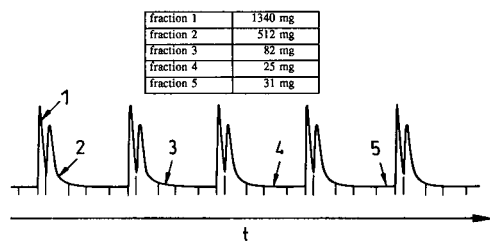


Fig. 3. Elution diagram showing the automatic separation of fullerene raw material obtained by Soxhlet extraction of carbon soot with hexane. The mass balance for the separation of about 2000 mg raw material is also shown. Injection frequency, 8 min; detection, UV at 350 nm; other conditions as in Fig. 4.

must be a closed system because the fullerenes are oxidized in refluxing, oxygen-containing toluene [15–17].

Procedure

Carbon soot, produced by evaporation of graphite rods in an arc reactor under a helium atmosphere [18,19], was Soxhlet extracted with hexane [20] for 48 h. After evaporation of the solvent, the residue was dissolved in toluene with the aid of ultrasound, filtered through a 0.25- μm PTFE membrane filter, injected by the M 306 pump into the elution stream at 8-min intervals and eluted with pure toluene. Hence there were always about three substance bands simultaneously on the column. Switching of the elute subsequently from one distillation flask to the other was achieved with the six-way valve (remote controlled by the time-programmable controller) (Fig. 3). The purity of fraction 1 (C_{60} fraction) was always $>99.8\%$ (determined by HPLC).

The conditions for HPLC were as follows: column and stationary phase, RP-18 (5 μm) cartridge (12.5 cm \times 8 mm I.D.); mobile phase, 2-propanol-toluene (60:40) at a flow-rate of 1 ml/min (Spectra-Physics gradient pump); injection, 10 μl of toluene eluate; detection, UV at 590 nm (Waters Model 281). At 590 nm the ratio of the molar absorptivities of C_{60} and C_{70} has been given as 1:1.2 [21]. However, the calculation of this C_{60} : C_{70} ratio of the used fullerene raw material using the published [21] molar absorptivity ratio gave 0.75, which is obviously not correct; therefore, the C_{60} / C_{70} ratios in Fig. 7b should be corrected to higher values:

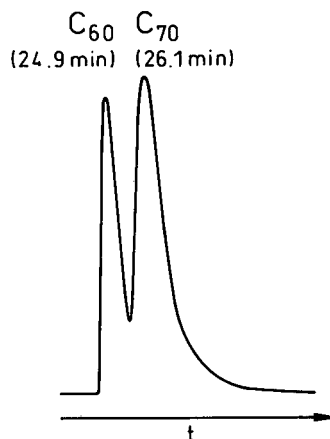


Fig. 4. Separation of fullerene raw material obtained by Soxhlet extraction of carbon soot with toluene. Two columns (600 \times 20 mm I.D.) in series + 60 \times 20 mm I.D. guard column; stationary phase, PSS-Gel (10 μm , 500 \AA); mobile phase, toluene at 15 ml/min; injection, 7.5 ml of a saturated solution of fullerene raw material in toluene (ca. 80% C_{60} , 18% C_{70} and 2% higher fullerenes); detection, UV at 380 nm.

RESULTS AND DISCUSSION

It appears that neither the mobile phase nor the pore diameter of the polystyrene gel influences the separation. Both chloroform and toluene mobile phases on 50 or 500 \AA pore diameter polystyrene gel gave nearly identical chromatograms (see Fig. 4 for elution with toluene). The smaller C_{60} is eluted before C_{70} , followed by the higher fullerenes (C_{76} , C_{78} , C_{82} , C_{84}). All of them have an elution volume comparable to the column volume (column volume = 395.6 ml; elution volume of C_{60} \approx 370 ml).

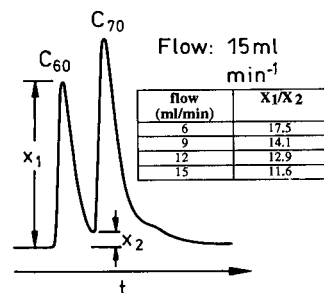


Fig. 5. Influence of the toluene mobile phase flow-rate on resolution. Injection volume, 1.5 ml; other conditions as in Fig. 4.

TABLE I
INFLUENCE OF INJECTION VOLUME ON RESOLUTION

Conditions as in Fig. 4.

Injection volume (ml)	X_1/X_2^a	Injection volume (ml)	X_1/X_2^a
1.5	11.6	7.5	3.9
3.0	10.0	9.0	2.9
4.5	7.7	10.5	2.2
6.0	5.6	12.0	1.7

^a See Fig. 5.

Hence it is obvious that the compounds are not separated by a true size-selective filtration. The greater contact area of C_{70} vs. C_{60} assuming that the adsorption face of the solute is the maximum available may explain the different elution behaviours of C_{60} and C_{70} on polystyrene gel.

Toluene was used for further separations owing to the higher solubility of the fullerenes. Optimum conditions for the separation were found by first increasing the mobile phase flow-rate at constant injection volumes (1.5 ml of saturated fullerene so-

lution) (Fig. 5) and then increasing the amount of sample injected at a flow-rate that still gave a nearly baseline separation of C_{60} and C_{70} at an injection volume of 1.5 ml (Table I and Fig. 6). Up to a mobile phase flow-rate of 15 ml/min and an injection volume of 12 ml no distortion of the C_{60} peak shape was observed, suggesting that the stationary phase has not been overloaded. Nevertheless, we observe that with increasing injection volume the C_{70} peak becomes more and more symmetrical, which may be attributed to the complete occupation of "active centres" by C_{60} at larger injection volumes, resulting in the "normal" elution of C_{70} . Further, we observe that C_{70} and the higher fullerenes (C_{76} , C_{78} , C_{82} and C_{84}) elute together at an injection volume of 7.5 ml. The optimum separation conditions were determined to be a flow-rate of 15 ml/min mobile phase and an injection volume of 7.5 ml. The best fraction cut points (Fig. 7a) were found by analysis of certain subfractions by HPLC on a reversed-phase column (Fig. 7b). The vertical dashed line in Fig. 7a indicates the change from the violet colour of C_{60} to the red-brown colour of C_{70} in the elute. The injection interval was determined by switching the detector to higher sensitivity (Fig. 8). Fullerene raw material, which was obtained by Soxhlet extraction of soot with toluene, showed marked tailing, resulting in the elution of fullerenes over 9 min,

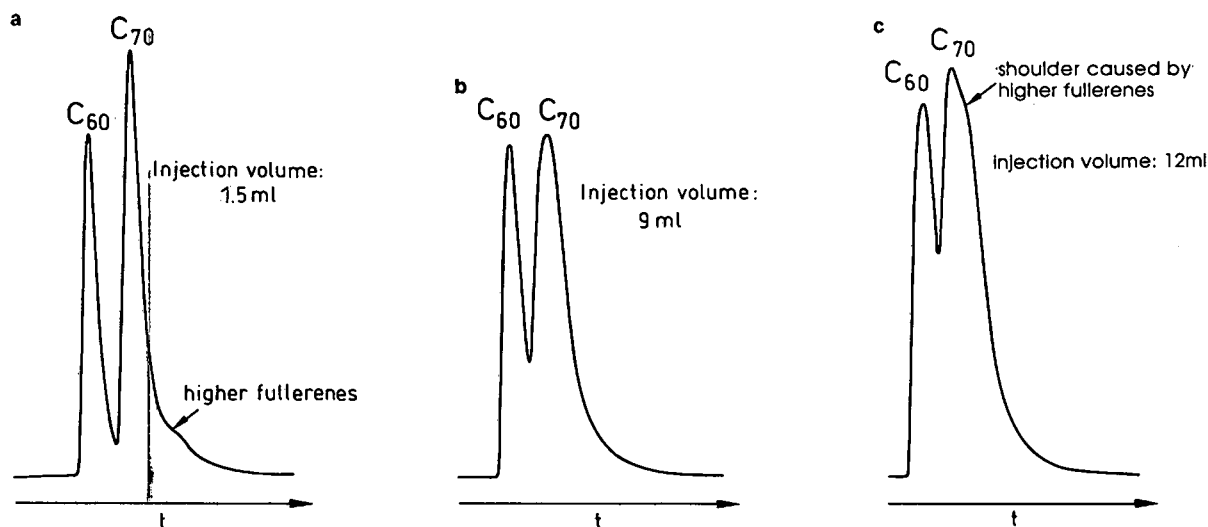


Fig. 6. Effect of injection volume: (a) 1.5; (b) 9; (c) 12 ml. Conditions as in Fig. 4.

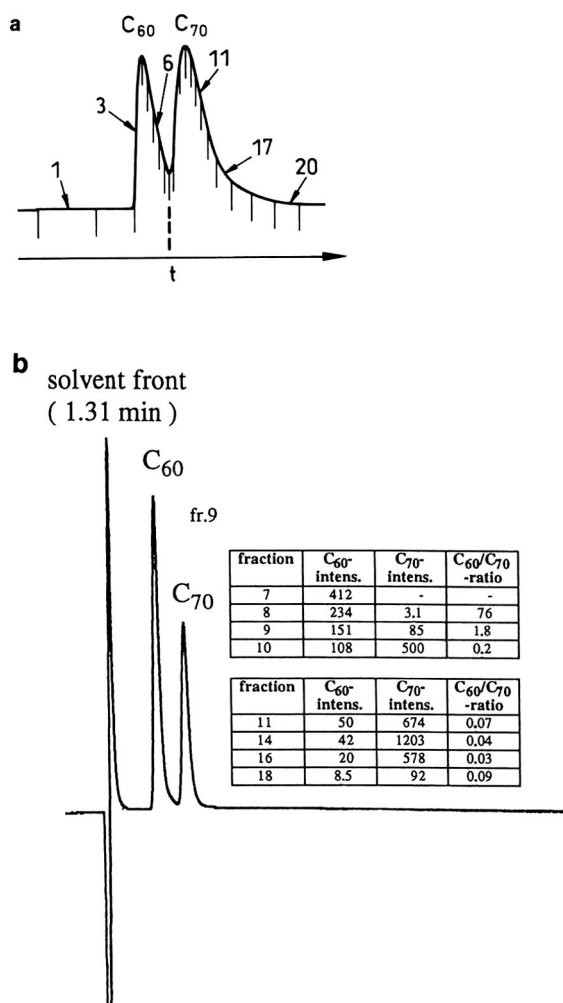


Fig. 7. (a) Separation of fullerene raw material obtained by Soxhlet extraction of carbon soot with toluene, with cut points for fractions 1–20. Conditions as in Fig. 4. (b) HPLC of fraction 9 and C₆₀/C₇₀ content of certain fractions determined by HPLC.

whereas the material obtained by Soxhlet extraction with hexane showed minor tailing, allowing the injection frequency to be increased to 8 min (Soxhlet extraction with hexane yields predominantly C₆₀ and C₇₀ and only traces of higher fullerenes, whereas Soxhlet extraction with toluene yields more of the higher fullerenes) [20].

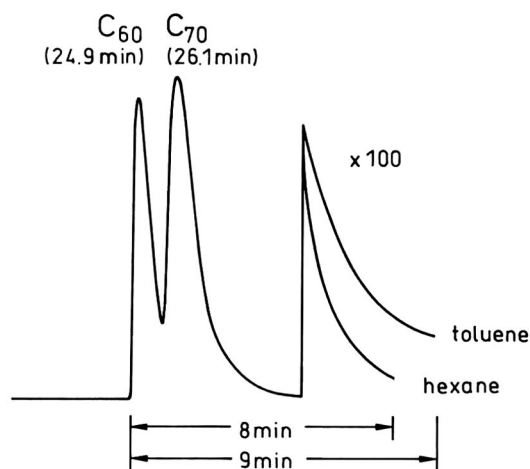


Fig. 8. Chromatogram of fullerene raw material obtained by Soxhlet extraction of carbon soot with toluene and hexane. Conditions as in Fig. 4.

CONCLUSIONS

The major advantage of the described procedure is the use of pure toluene as eluent. In addition to the improved efficiency compared with literature methods, this solvent allows an automatic apparatus to be set up, which redistills the elute continuously (Figs. 9 and 10). Using this technique it is possible to separate 5–10 g of fullerene raw material per day without any solvent consumption. Moreover, the method can be easily scaled up by using columns of larger inner diameter. Two points are worth mentioning. Owing to the exceptionally long retention time of C₆₀ and the other fullerenes (“normal” compounds are eluted much earlier) the method is suitable for the detection of very small amounts of fullerenes in complex matrices (*e.g.*, engine exhaust deposits or reaction mixtures). The interruption of buckminsterfullerene’s conjugation by functionalization leads to dramatically reduced retention times, permitting the separation of fullerenes from their reaction products: Diels–Alder addition products of C₇₀ with diphenylisobenzofuran are easily separated from the educts, which also applies to fragmentation and other addition products of C₆₀ and C₇₀. Additional work using other stationary phases (polystyrene gel for reversed-phase

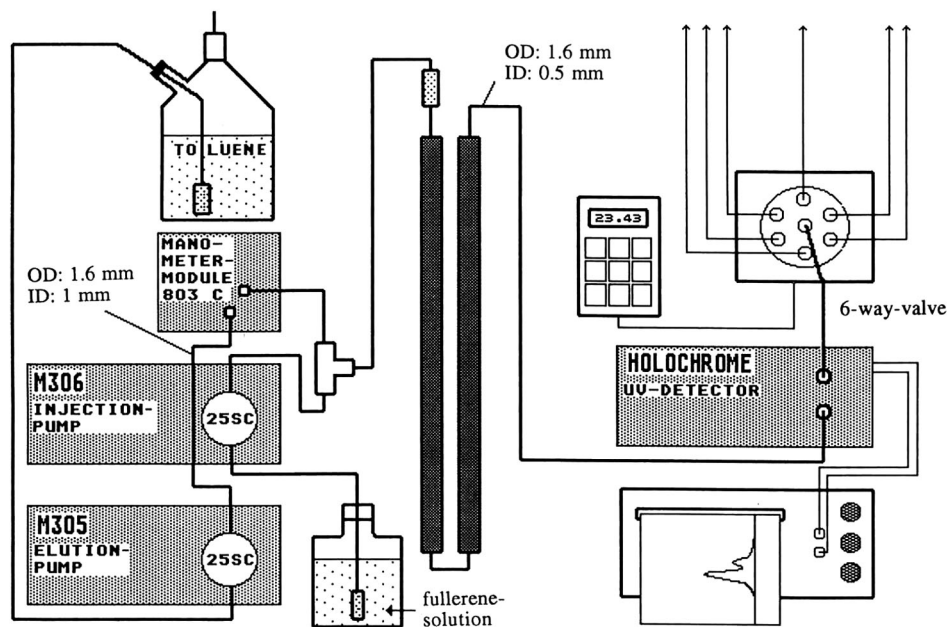


Fig. 9. Apparatus for automated separation of fullerene raw material.

chromatography, C_{18} -modified polystyrene gel, π -basic stationary phases which possibly separate the fullerenes by intermediary formation of charge-transfer complexes) and other solvents is in progress. Because the column is probably only volume overloaded at large injection volumes, replacement of toluene with a better solvent for fullerenes will dramatically enhance the productivity. Work is in

progress using *m*-xylene as solvent (the solubility amounts is *ca.* 8 mg of fullerene raw material in 1 ml of *m*-xylene) and working at higher temperatures with alkylated and halogenated aromatics and tetrachloroethane, which are excellent solvents for fullerenes under these conditions.

ACKNOWLEDGEMENTS

We thank Professor Dr. R. Schlögl (University, Frankfurt a. M., Germany) for supplying the fullerene raw material. We also thank Mr. Andreas Kühn (Max-Planck-Institut für Polymerforschung) for HPLC analyses, Mr. J. Quack (Max-Planck-Institut für Polymerforschung) for the distillation apparatus and Mr. W. Laufersweiler (Max-Planck-Institut für Polymerforschung) for designing and making the PTFE seals.

REFERENCES

- 1 See, e.g., R. C. Haddon, *Acc. Chem. Res.*, 25 (1992) 127–134.
- 2 P. M. Allemand, K. C. Khemani, A. Koch, F. Wudl, K. Holczer, S. Donovan, G. Grüner and J. D. Thompson, *Science*, 253 (1991) 301–303.

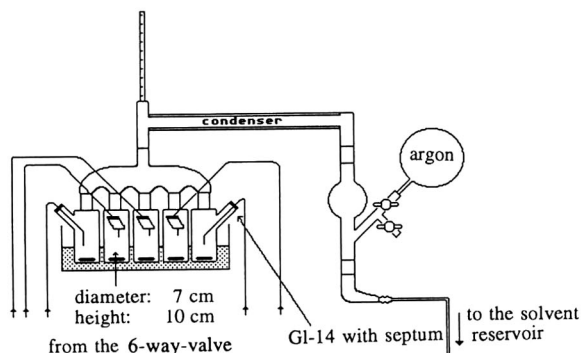


Fig. 10. Distillation apparatus for continuous recovery of the mobile phase.

- 3 P. W. Stephens, D. Cox, J. W. Lauher, L. Mihaly, J. B. Wiley, P. Allemand, A. Hirsch, K. Holczer, Q. Li, J. D. Thompson and F. Wudl, *Nature*, 355 (1992) 331–332.
- 4 See, e.g., Y. Wang and L. Cheng, *J. Phys. Chem.*, 96 (1992) 1530–1532.
- 5 T. Braun, *Angew. Chem.*, 104 (1992) 602–603.
- 6 R. C. Haddon, L. F. Schneemayer, J. V. Waszcak, S. H. Glarum, R. Tycko, G. Dabbagh, A. R. Kortan, A. J. Muller, A. M. Mujsce, M. J. Rosseinsky, S. M. Zahurak, A. V. Makhija, F. A. Thiel, K. Raghavachari, E. Cockayne and V. Elser, *Nature*, 350 (1991) 46–47.
- 7 H. Ajje, M. M. Alvarez, S. J. Anz, R. D. Beck, F. Diederich, K. Fostiropoulos, D. R. Huffman, W. Krätschmer, Y. Rubin, K. E. Schriver, D. Sensharma and R. L. Whetten, *J. Phys. Chem.*, 94 (1990) 8630–8633.
- 8 J. M. Hawkins, T. A. Lewis, S. D. Loren, A. Meyer, J. R. Heath, Y. Shibato and R. J. Saykally, *J. Org. Chem.*, 55 (1990) 6250–6252.
- 9 A. M. Vassallo, A. J. Palmisano, L. S. K. Pang and M. A. Wilson, *J. Chem. Soc., Chem. Commun.*, (1992) 60–61.
- 10 W. H. Pirkle and C. J. Welch, *J. Org. Chem.*, 56 (1991) 6973–6974.
- 11 A. Gügel, M. Becker, D. Hammel, L. Mindach, J. Räder, T. Simon, M. Wagner and K. Müllen, *Angew. Chem.*, 104 (1992) 666–667.
- 12 M. S. Meier and J. P. Selegue, *J. Org. Chem.*, 57 (1992) 1924–1926.
- 13 B. J. Hunt and S. R. Holding, *Size Exclusion Chromatography*, Chapman and Hall, New York, 1989.
- 14 W. W. Yau, J. J. Kirkland and D. D. Bily, *Modern Size Exclusion Liquid Chromatography*, Wiley, New York, 1979.
- 15 A. M. Vassallo, L. S. K. Pang, P. A. Cole-Clarke and M. A. J. Wilson, *J. Am. Chem. Soc.*, 113 (1991) 7820.
- 16 J. M. Wood, B. Kahr, S. H. Hoke, L. Dejarne, R. G. Cooks and D. J. Ben-Amotz, *J. Am. Chem. Soc.*, 113 (1991) 5907.
- 17 R. Taylor, J. P. Parsons, A. G. Avent, S. P. Rannard, T. J. Dennis, J. P. Hare, H. W. Kroto and D. R. M. Walton, *Nature*, 351 (1991) 277.
- 18 W. Krätschmer, L. D. Lamb, K. Fostiropoulos and R. D. Huffman, *Nature*, 347 (1990) 354.
- 19 R. Taylor, J. P. Hare, A. K. Abdul-Sada and H. W. Kroto, *J. Chem. Soc., Chem. Commun.*, (1990) 1423.
- 20 D. H. Parker, P. Wurz, K. Chatterjee, K. R. Lykke, J. E. Hunt, M. J. Pellin, J. C. Hemminger, D. M. Gruen and L. M. Stock, *J. Am. Chem. Soc.*, 113 (1991) 7499–7503.
- 21 P. M. Allemand, A. Koch, F. Wudl, Y. Rubin, F. Diederich, M. M. Alvarez, S. J. Anz and R. L. Whetten, *J. Am. Chem. Soc.*, 113 (1991) 1050–1051.

Normal-phase high-performance liquid chromatography with a fluorimetric postcolumn detection system for lipid hydroperoxides

Kazuaki Akasaka, Hiroshi Ohruai and Hiroshi Meguro

Department of Applied Biological Chemistry, Faculty of Agriculture, Tohoku University, Tsutsumidori-Amamiyamachi 1-1, Aoba, Sendai 981 (Japan)

(First received July 7th, 1992; revised manuscript received September 7th, 1992)

ABSTRACT

Hydroperoxides (HPO) of triacylglycerols (TG) and cholesterol esters (ChE) were selectively determined at picomole levels with a fluorescence detector by postcolumn reaction with diphenyl-1-pyrenylphosphine. Hydroperoxides were separated on a normal-phase silica gel column with gradient elution with *n*-hexane-1-butanol. With this system, TG-HPO and ChE-HPO were separated according to their class and determined in the range 5–1000 pmol. Detection limits of hydroperoxides of cholesterol linolate and trilinolein were about 2 pmol (signal-to-noise ratio = 3) and the relative standard deviations of their peak areas were 3.4% (39.1 pmol, *n* = 7) and 1.8% (32.4 pmol, *n* = 7), respectively.

INTRODUCTION

Lipid peroxidation has attracted much attention as one of the factors that cause some diseases and ageing [1–4]. However, it has been difficult to determine lipid peroxides in biological materials because of their trace concentrations, instability and diversity. In the initial stage of lipid peroxidation, hydroperoxides are produced both enzymatically and non-enzymatically, and they decompose or polymerize gradually to various secondary products.

Lipid hydroperoxides have been determined according to their class of molecular levels by both normal- and reversed-phase high-performance liquid chromatography (HPLC) [5–9]. UV detection at 235 nm, depending on their conjugated diene systems, or refractive index detection were used. However, these methods suffer problems such as se-

lectivity, sensitivity or interferences from co-existing compounds.

Recently, chemiluminescence has been proposed for the highly sensitive and selective postcolumn detection of lipid hydroperoxides using isoluminol [10] or luminol [11]. Electrochemical detection has also been used for this purpose [12]. With chemiluminescence methods, hydroperoxides of cholesterol esters (ChE) and triacylglycerols (TG) were separated on a reversed-phase ODS column and gave multiple peaks based on their fatty acid compositions. However, some hydroperoxides of ChE and TG might not be separated from each other.

Hydroperoxides of ChE and TG were expected to separate into their class levels by normal-phase HPLC with gradient elution, as non-oxidized lipids were separated [13]. However, the system is not suitable for either chemiluminescence or electrochemical detection because of the incapability of detection with non-polar organic solvents such as *n*-hexane, which is popular solvent for normal-phase HPLC.

Correspondence to: H. Meguro, Department of Applied Biological Chemistry, Faculty of Agriculture, Tohoku University, Tsutsumidori-Amamiyamachi 1-1, Aoba, Sendai 981, Japan.

We have previously reported an aryl phosphine, diphenyl-1-pyrenylphosphine (DPPP), as a fluorescence reagent for lipid hydroperoxides [14,15]. This reagent was successfully applied to the highly sensitive and selective determination of lipid hydroperoxides by methods HPLC postcolumn [16–18]. The reaction proceeded in organic solvents such as methanol, 1-butanol, acetone, benzene and *n*-hexane. This allowed us to use a normal-phase column eluted with *n*-hexane. In this paper, we describe the HPLC determination of hydroperoxides of TG and ChE separated by a gradient elution with *n*-hexane–1-butanol on a silica gel column with postcolumn fluorimetric detection with DPPP.

EXPERIMENTAL

Chemicals

DPPP was synthesized according to the method described previously [14]. Trilinolein (TLo), triolein (TOl), cholesteryl linoleate (ChLo), cholesteryl oleate (ChOl), and cholesteryl arachidonate (ChAr) were purchased from Sigma (St. Louis, MO, USA). Methylene blue and triphenylphosphine were obtained from Wako (Osaka, Japan). Methanol and 1-butanol were of HPLC grade from Wako and used as received. *n*-Hexane was used after distillation. *tert*-Butylhydroxytoluene (BHT) was purchased from Tokyo Kasei Kogyo (Tokyo, Japan). Vegetable oils were obtained from Nacalai Tesque (Kyoto, Japan). The solvents for dissolving the samples contained BHT (0.5 g/l) as an antioxidant.

Preparation of hydroperoxides

TLo, ChLo, ChAr and vegetable oils were autoxidized at room temperature or 40°C in the dark for 12–72 h. TOl and ChOl were photooxidized in the presence of 0.1–0.3 mM of methylene blue in ethanol. TOl-HPO was also prepared by autoxidation at 40°C for 1 week. They were used after purification as their monohydroperoxides by silica gel column chromatography. Their hydroperoxide contents were determined by fluorimetry [19]. They were stored in a refrigerator at –25°C as a chloroform–*n*-hexane (1:1) solution.

Separation and detection of hydroperoxides

The HPLC separation was performed on a Develosil 60-3 (3 μm) column (100 mm × 4.6 mm I.D.)

(Nomura Chemical, Aichi, Japan). The chromatographic mobile phase were solvent A = *n*-hexane and solvent B = *n*-hexane–1-butanol (20:1, v/v), with a linear solvent gradient from 8% to 90% B between 2 and 24 min. The flow-rate of the mobile phases was 0.6 ml/min.

The HPLC eluate was monitored by UV absorbance measurement at 235 nm prior to the postcolumn reaction with DPPP, but this was not essential for this system. The eluent was mixed with DPPP reagent [3 mg in 400 ml of methanol–1-butanol (1:1, v/v)] which was kept in an ice-bath in the dark to prevent drifting of the baseline. The flow-rate of the reagent was 0.3 ml/min and the mixture was passed through a 20 m × 0.5 mm I.D. reaction coil (stainless steel) at 80°C followed by a 0.5 m × 0.5 mm I.D. coil in a 20°C water-jacket. Detection was performed by monitoring the fluorescence intensity at 380 nm with excitation at 352 nm. The DPPP reagent was degassed by sonication under reduced pressure before use. The mobile phase solutions were also degassed and stood for 12–24 h.

Equipment

The HPLC pump used was a CCPM multipump (Tosoh, Tokyo, Japan) in the high-pressure gradient mode. The pump for the reagent solution was an LC-3A (Simadzu, Tokyo, Japan). The reaction oven was an RE-8000 reactor. The detectors used were a UV-8000 spectrophotometer and an FS-8000 spectrofluorimeter (Tosoh). An SC-8010 data processor (Tosoh) was used.

RESULTS AND DISCUSSION

The properties of DPPP and the mechanism of its reaction with hydroperoxides have been described previously [14,15].

The effect of reaction temperature on the peak height of ChLo-HPO was examined between 40 and 80°C. The peak became higher with increasing reaction temperature as shown in Fig. 1. This means that hydroperoxides were not decomposed to unreactive compounds under these conditions. No increase in the baseline noise level was observed with increase in temperature. The flow-rate of the reagent solution had no effect on the peak height in the range 0.2–0.4 ml/min, but at 0.6 ml/min the peak became smaller (about 70%) owing to short-

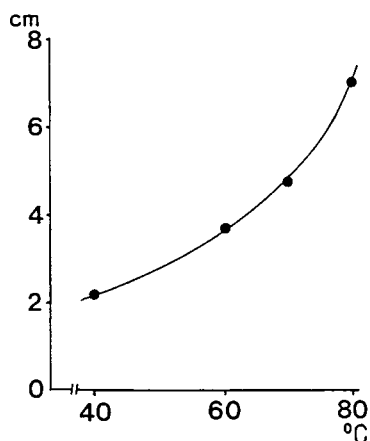


Fig. 1. Effect of reaction temperature on the peak height of ChLo-HPO. The separation column was Develosil 60-3 (100 mm \times 4.6 mm I.D.) eluted isocratically with hexane-1-butanol (100:1, v/v) at 0.6 ml/min.

ening of the reaction time at higher flow-rate. The flow-rate of reagent solution adopted in subsequent work was 0.3 ml/min. After the reaction, the mixture was cooled to room temperature by passing it through a 0.5-m coil in a water-jacket to prevent foaming in the fluorimeter cell. This coil also prevented the methanol and *n*-hexane from boiling in the reaction coil by increasing the pressure.

The effects of the solvent of the reagent solution on the peak height of ChLo-HPO were examined. *n*-Hexane alone was not suitable because of the instability of the baseline. *n*-Hexane-1-butanol (1:1, v/v) solution gave the highest peak. 1-Butanol and 1-butanol-methanol (1:1, v/v) gave 85% and 92% peak heights, respectively, of that of the *n*-hexane-1-butanol. This might be attributed to the viscosity of the reaction solution. Although 1-butanol-methanol gave a smaller peak than *n*-hexane-1-butanol, it was selected as the solvent in this method because the baseline became unstable with *n*-hexane-1-butanol with prolonged operation.

The most significant characteristic of the method is that gradient elution with mobile phase from *n*-hexane to *n*-hexane-1-butanol (5:1, v/v) is usable without any effect on the peak area of ChLo-HPO. The mobile phase solutions were degassed by sonication under reduced pressure. It was recommended that they be used after standing for 12–24 h to

minimize baseline drift and to improve the reproducibilities of the peak areas.

Fig. 2 shows the chromatograms obtained with gradient elution. ChLo-HPO and TLo-HPO were separated from each other. The baseline drift was negligibly small for determination in this range. Table I shows the retention times and relative peak areas of ChE-HPOs and TG-HPOs detected by fluorimetry. ChLo-HPO, ChAr-HPO and ChOl-HPO gave three or two peaks. This might be attributed to the separation of the structural isomers. With the exception of the last peak of ChAr-HPO, which was eluted at 13.75 min, ChE-HPOs and TG-HPOs were eluted between 8.5 and 12.5 min and between 13.8 and 14.5 min, respectively, independent of their structural differences. Although there was only one exception tested, this allowed us to assign generally the peaks eluted between 8 and 13 min as ChE-HPO and those between 13.8 and 14.5 min as TG-HPO. Although unoxidized ChE and TG gave no peaks in this system, they eluted at 7.5 min.

The peak areas of ChOl-HPO and TOl-HPO were smaller than those of other HPOs. This could be attributed to the lower reactivities of the HPO of oleic acid derivatives with DPPP [19] or less probably to the much lower reactivity of the ChOl-HPOs with a sterically hindered hydroperoxy group on the cholesterol moiety. These HPOs could not be detected by the UV method because they do not contain a conjugated diene system. This means that the present method is much superior to the UV method in selectivity for hydroperoxides.

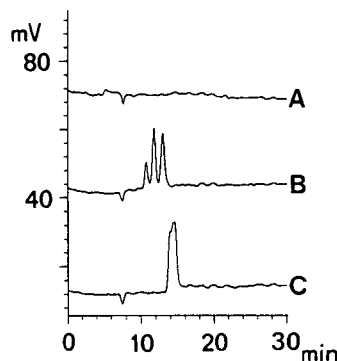


Fig. 2. HPLC of ChLo-HPO and TLo-HPO. (A) No injection (baseline); (B) ChLo-HPO (39.2 pmol); (C) TLo-HPO (42.5 pmol).

TABLE I
RETENTION TIMES AND RELATIVE PEAK AREAS OF LIPID HYDROPEROXIDES

Hydroperoxide	Oxidation method ^a	Retention time (min)	Relative peak area
ChOl-HPO	P	8.50, 12.30	0.57
ChLo-HPO	A	10.37, 11.50, 12.37	1.00
ChAr-HPO	A	9.24, 12.33, 13.75	1.06
TOl-HPO	A	13.87, 14.23	0.79
	P	13.83	0.73
TLo-HPO	A	14.23	1.11
TLn-HPO	A	14.25	0.92
Olive oil-HPO	A	13.83	0.98
Soybean oil-HPO	A	13.80	1.07
Linseed oil-HPO	A	14.07	1.04

^a Hydroperoxides were prepared by (A) autoxidation and (P) photooxidation with methylene blue.

The HPOs of polyunsaturated fatty acid derivatives gave almost the same peak area (R.S.D. = 6.4%, $n = 7$). The polyunsaturated fatty acid parts are much more sensitive to peroxidation than the monoenoic acid and cholesterol parts, and therefore it may be expected that most of the HPOs in foods and biological materials were those of polyunsaturated fatty acid derivatives.

With the proposed method, the calibration graphs for ChLo-HPO and TLo-HPO showed good linearity in the range 5–1000 pmol (ChLo-HPO, $y = 13.09x + 44.4$, $r = 0.9999$; TLo-HPO, $y = 13.66x - 12.4$, $r = 0.9997$; x = concentration of hydroperoxide; y = peak area). From two calibration graphs, the ChE-HPO/TG-HPO peak-area ratios were 1.04 ($x = 50$ pmol) and 0.966 ($x = 500$ pmol). This allowed us to use the calibration graph of either ChLo-HPO or TLo-HPO for the determination of HPOs in these ranges. The R.S.D.s of their peak areas were 3.4% (ChLo-HPO, 39.1 pmol, $n = 7$) and 1.8% (TLo-HPO, 32.4 pmol, $n = 7$). At lower concentrations, ChE-HPO gave larger errors than TG-HPO because ChE-HPO separated into a few peaks and the concentration was calculated from their total peak areas. Although the peak area of ChE-HPO was larger than that of TG-HPO at lower concentrations, for both the detection limits were about 2 pmol (signal-to-noise ratio = 3). This was also attributed to the peak separation of ChE-HPO.

Lipid hydroperoxides with a wider range of po-

larities can also be determined by this method. Fig. 3 shows the HPLC of hydroperoxides produced by autoxidation of trilinolein at 40°C in air. At the beginning, only TLo-HPO (monohydroperoxides) was detected at 14 min and it increased gradually. After incubation for 48 h, very small peaks other than TLo-HPO were also detected at about 18 min. The peaks were considered as bishydroperoxides because of their polarities and reaction times. The more polar hydroperoxides, at 20–28 min, were detected after autoxidation for 120 h. Some of them

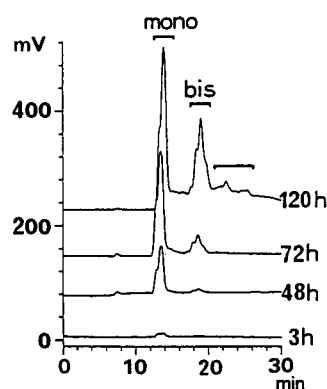


Fig. 3. Development of hydroperoxides of TLo by autoxidation at 40°C. TLo was sampled after autoxidation for 3 h (POV = 7.1), 48 h (POV = 91.4), 72 h (POV = 440) and 120 h (POV = 1470), and aliquots (5.4, 4.8, 3.0 and 2.8 μ g, respectively) were injected on to the HPLC column as *n*-hexane solutions. POV = Peroxide values determined by our previous method.

gave no peaks with UV monitoring at 235 nm. They were probably decomposed products of trilinolein mono- and bishydroperoxides because they had no conjugated diene system and the products of the later stages of oxidation.

CONCLUSIONS

ChE-HPO, TG-HPO and hydroperoxides with higher polarity were separated by gradient elution with a normal-phase column. The postcolumn detection system with DPPP was successfully combined with this separation system, and the combination made it possible to determine lipid hydroperoxides with high sensitivity and selectivity. The present system should be useful for studying lipid peroxidation in complex systems such as foods and biological materials. The 1-butanol content of the mobile phase could be raised at least to 16.7% without influencing the postcolumn reaction. This suggests the possibility of the determination lipid hydroperoxides with a wider range of polarities using this system.

ACKNOWLEDGEMENT

This work was supported in part by a grant from the Biomedica Project of the Ministry of Agriculture, Forestry and Fisheries of Japan.

REFERENCES

- 1 J. Glavind, S. Hartmann, J. Clemmesen, K. E. Jessen and H. Dam, *Acta Pathol. Microbiol. Scand.*, 30 (1952) 1.
- 2 T. Yoshikawa, K. Yamaguchi, M. Kondo, N. Mizukawa, T. Ohta and K. Hirakawa, *Arch. Gerontol. Geriatr.*, 1 (1982) 209.
- 3 T. Nakayama, M. Kodama and C. Nagata, *Agric. Biol. Chem.*, 48 (1984) 571.
- 4 D. Hartman, in W. A. Pryor (Editor), *Free Radicals in Biology*, Vol. V, Academic Press, New York, 1982, pp. 255–275.
- 5 H. W. S. Chan, G. Levett and J. A. Matthew, *Chem. Phys. Lipids*, 24 (1979) 245.
- 6 D. K. Park, J. Terao and S. Matsusita, *Agric. Biol. Chem.*, 45 (1981) 2448.
- 7 J. Terao, I. Asano and S. Matsusita, *Lipids*, 20 (1985) 312.
- 8 C. G. Crawford, R. D. Plattner, D. J. Sessa and J. J. Rackis, *Lipids*, 15 (1984) 325.
- 9 S. Hara, K. Nemoto, H. Yamaya and Y. Totani, *J. Jpn. Oil Chem. Soc.*, 37 (1988) 541.
- 10 Y. Yamamoto, M. H. Brodsky, J. C. Baker and B. N. Ames, *Anal. Biochem.*, 160 (1987) 7.
- 11 T. Miyazawa, K. Yasuda and K. Fujimoto, *Anal. Lett.*, 21 (1988) 1033.
- 12 K. Yamada, J. Terao and S. Matsushita, *Lipids*, 22 (1987) 125.
- 13 S. Hara, T. Ono, K. Uchikoshi and Y. Totani, *J. Jpn. Oil Chem. Soc.*, 39 (1990) 629.
- 14 K. Akasaka, T. Suzuki, H. Ohruai and H. Meguro, *Anal. Lett.*, 20 (1987) 731.
- 15 K. Akasaka, T. Suzuki, H. Ohruai and H. Meguro, *Anal. Lett.*, 20 (1987) 797.
- 16 H. Meguro, K. Akasaka and H. Ohruai, *Methods Enzymol.*, 186 (1990) 157.
- 17 K. Akasaka, H. Ohruai and H. Meguro, *Anal. Lett.*, 21 (1988) 965.
- 18 K. Akasaka, S. Ijichi, K. Watanabe, H. Ohruai and H. Meguro, *J. Chromatogr.*, 596 (1992) 197.
- 19 K. Akasaka, I. Sasaki, H. Ohruai and H. Meguro, *Biosci. Biotechnol. Biochem.*, 56 (1992) 605.

Analysis of alkylpyrrole autoxidation products by high-performance liquid chromatography with thermospray mass spectrometry and UV photodiode-array detection[☆]

Mingshe Zhu and David C. Spink

Department of Environmental Health and Toxicology, The University at Albany, State University of New York; and Wadsworth Center for Laboratories and Research, New York State Department of Health, Albany, P.O. Box 509, NY 12201-0509 (USA)

Shelton Bank and Xi Chen

Department of Chemistry, The University at Albany, State University of New York, Albany, NY 12222 (USA)

Anthony P. DeCaprio

Department of Environmental Health and Toxicology, The University at Albany, State University of New York; and Wadsworth Center for Laboratories and Research, New York State Department of Health, P.O. Box 509, Albany, NY 12201-0509 (USA)

(First received June 19th, 1992; revised manuscript received September 3rd, 1992)

ABSTRACT

A method employing high-performance liquid chromatography with thermospray mass spectrometry (TSP-MS) and photodiode-array detection was developed and applied to the analysis of autoxidation products of 2,5-dimethyl-N-alkylpyrroles in aqueous solution under air or ¹⁸O₂. Numerous oxidation products were separated, characterized and categorized, primarily as (1) non-polar oligomers without incorporated oxygen, and (2) polar, oxygen-containing monomers. Kinetic studies showed that oligomerization was the dominant autoxidation pathway, with production of unstable dimers and trimers and, ultimately, a high-molecular-mass sediment. TSP-MS together with UV and proton nuclear magnetic resonance spectral data revealed that both the dimer and trimer contained a novel methylene bridge. These results suggest that this method is suitable for the analysis of alkylpyrrole autoxidation products that may be relevant to hexane neuropathy and products that are responsible for the instability of fuels in storage.

INTRODUCTION

Autoxidation of alkyl-substituted pyrroles is a phenomenon with important toxicological and chemical implications. For example, 2,5-hexane-

dione (2,5-HD), the ultimate neurotoxic γ -diketone metabolite of *n*-hexane, reacts with amino groups in neurofilament proteins to yield 2,5-dimethylpyrrole protein adducts [1]. These adducts undergo autoxidation, resulting in protein cross-linking *in vitro* [2,3] and *in vivo* [1,4]. Several groups have confirmed pyrrole formation as a necessary step in the pathogenesis of hexane neuropathy [5–7], although it is not clear whether autoxidative protein cross-linking is also required. One study indirectly showed that intermolecular cross-linking of protein required pyrrole adducts on both proteins, suggest-

Correspondence to: D. C. Spink, Wadsworth Center for Laboratories and Research, New York State Department of Health, P.O. Box 509, Albany, NY 12201-0509 (USA).

^{*} Portions of this work were presented at the 40th ASMS Conference on Mass Spectrometry and Allied Topics, Washington, DC, May 31–June 5, 1992.

ing pyrrole-to-pyrrole bridging [8]. These reactions were accelerated by free radical initiators and thus were suggested to be free radical-mediated. In contrast, a recent investigation suggested that protein cross-linking was the consequence of the attack of a nucleophile such as a thiol or an amine of one protein on an electrophilic, oxidized pyrrole adduct of a second protein [9].

Alkylpyrrole autoxidation has also been associated with problems of storage instability of fossil and synthetic fuels. The presence of trace amounts of alkylpyrroles in these fuels under air atmosphere resulted in formation of a highly colored sediment [10–12]. 2,5-Dimethylpyrrole (DMP) was much more reactive than unsubstituted pyrrole and was used as a model compound in these experiments. Although several groups have presented evidence for the presence of different functional groups in the sediment produced in DMP oxidation [13,14] and have proposed reaction mechanisms [11,15], no intermediates or products of autoxidation have been identified.

It is well known that alkylpyrroles in aqueous or organic solutions are quickly oxidized by molecular oxygen to form insoluble, amorphous, and dark-colored polymers referred to as “pyrrole black” [16–18]. However, little structural information about these products is available. Alkylpyrrole oxidation products, particularly oligomers, are very difficult to analyze because they are extremely insoluble in water and in most organic solvents, and the intermediates in their formation appear to be very unstable.

Most previous attempts to analyze alkylpyrrole oxidation products have employed open column liquid chromatography and traditional chemical separation procedures such as extraction and distillation to isolate the oxidation products, followed by nuclear magnetic resonance (NMR) and infrared spectrometric analyses [17–19]. The instability of the autoxidation products during these manipulations renders several of these techniques inappropriate for their analysis. In addition, attempts to separate and analyze products of DMP autoxidation in dodecane and hexane by capillary gas chromatography (GC) have been unsuccessful [20], possibly because of the lack of volatility or the thermolabile nature of the products.

Reversed-phase high-performance liquid chro-

matography (HPLC) has been used successfully for the separation of several classes of pyrrole-containing compounds, including bile pigments [21] and phenylpyrrole derivatives that are products of tryptophan metabolism [22]. Coupling of HPLC with thermospray mass spectrometry (TSP-MS) [23,24] and with photodiode-array detection (PAD) [25] has proven useful for identification of unknown xenobiotic metabolites. This paper reports a method employing HPLC with TSP-MS and PAD for the separation and characterization of alkylpyrrole autoxidation products. In addition, we describe the structure of novel alkylpyrrole oligomers produced from 2,5-dimethyl-N-alkylpyrrole autoxidation.

EXPERIMENTAL

Materials

Ethanolamine and acetonitrile were obtained from Fisher Scientific (Fair Lawn, NJ, USA), and 5-amino-1-pentanol was obtained from Aldrich (Milwaukee, WI, USA). 2,5-Hexanedione was obtained from Eastman Kodak (Rochester, NY, USA). An equimolar mixture of $^{16}\text{O}_2$ and $^{18}\text{O}_2$, and $[^2\text{H}]\text{CHCl}_3$ were from Cambridge Isotope Labs. (Woburn, MA, USA). Water was purified by the Milli-Q system (Millipore, Bedford, MA, USA).

Synthetic procedures

Synthesis of 1-(2-hydroxyethyl)-2,5-dimethylpyrrole (HEDMP) was by Paal–Knorr condensation [26]. A mixture of ethanolamine (1 ml) and 2,5-HD (1 ml) was heated at 50°C under argon atmosphere for 1 h, followed by evaporation in vacuum (5 mmHg; 1 mmHg = 133.322 Pa) at 70°C for 2 h. A single component for the product was detected by HPLC and GC–MS, and its structure was confirmed as HEDMP by GC–MS (m/z 139, 108, 94), proton magnetic resonance (^1H NMR) spectroscopy (2.25 ppm, s, 6 H; 3.70 ppm, t, $^3J = 6$ Hz, 2 H; 3.88 ppm, t, $^3J = 6$ Hz, 2 H; 5.78 ppm, s, 2 H.) and UV spectroscopy ($\lambda_{\text{max}} = 230$ nm). 1-(2-Hydroxypentyl)-2,5-dimethylpyrrole (HPDMP) was prepared by the same method as HEDMP. The structure of HPDMP was confirmed by its TSP mass spectrum ($[\text{M} + \text{H}]^+$ at m/z 182), and UV absorption spectrum ($\lambda_{\text{max}} = 226$ nm). The product showed a single peak by HPLC. Pyrroles were maintained under argon to avoid reactions prior to the oxidation experiments.

Autoxidation of alkylpyrroles

Solutions of 1% (v/v) HEDMP in 0.2 M sodium phosphate buffer (pH 7.4) or 5% (v/v) phosphate buffer–methanol (90:5) were incubated at 37°C, in the dark, under air or $^{18}\text{O}_2$. Oxidation of HPDMP (5%, v/v) in phosphate buffer–methanol (1:1) was carried out under the same conditions. Each sample was filtered through a 0.2- μm nylon filter before analysis by HPLC.

HPLC–TSP–MS

The HPLC system (Waters, Milford, MA, USA) consisted of two Model 510 pumps, a Model 680 gradient controller, a Model 740 data module, a Model 490 multiwavelength detector and a Nova-Pak (Waters) C_{18} column (15 \times 0.39 cm, 4- μm particle size). The TSP–MS system consisted of a Hewlett–Packard (Palo Alto, CA, USA) 5970 quadrupole mass analyzer and a Vestec (Houston, TX, USA) Model 101 thermospray interface. The data system consisted of a Hewlett–Packard series 200 computer with MS ChemStation software.

Chromatography was performed with gradients of acetonitrile concentration that were formed by pumping varying amounts of eluent A (0.1 M ammonium acetate in water) and eluent B (acetonitrile–water, 1:1, v/v, containing 0.1 M ammonium acetate) to give a total flow-rate of 1.2 ml/min. For the analysis of HEDMP oxidation samples the gradient was as follows: from 2% B to 20% B over 10 min, a hold for 15 min, to 70% B over 20 min, a hold for 5 min, to 100% B over 5 min, a hold for 5 min, to 2% B over 5 min. For the analysis of HPDMP oxidation samples the following gradient was used: from 20% to 40% B over 5 min, to 100% B over 20 min, a hold for 15 min, to 20% B over 5 min. The UV detector monitored two wavelengths, 225 and 320 nm, in the maxplot mode, which records the greater of the two absorbance values.

TSP–MS was performed with a source block temperature of 300–305°C, without the use of filament or discharge ionization. The vaporizer temperatures were chosen to be 10°C below the total vaporization point of the initial mobile phase. The vaporizer setting was sufficiently low to prevent fluctuations in ionization as the mobile phase composition changed later in the gradient.

HPLC–PAD detection

The Waters HPLC–PAD system consisted of two 6000A solvent delivery pumps, a WISP 710B sample processor, a Model 720 controller, and a Model 990 photodiode-array detector. The columns, mobile phases, and gradients used for the separation of pyrrole oxidation products were same as those used in the HPLC–TSP–MS analyses, except that the flow-rate was 1.4 ml/min. UV absorbance spectra were recorded over the range of 200 to 400 nm with a 2-s scanning interval.

GC–MS

The GC–MS system (Hewlett–Packard) consisted of a Model 5890 GC, a Model 5970 quadrupole mass analyzer and a Model 9000 computer with MS ChemStation software. A fused-silica capillary column (HP-1, 12 m \times 0.2 mm, Hewlett–Packard) was used with helium as the carrier gas at a head pressure of 30 kPa.

^1H NMR spectroscopy

The HPLC peak corresponding to HEDMP dimer was collected and immediately subjected to nitrogen sparging. The eluted sample was then lyophilized and redissolved in 0.5 ml [^2H]CHCl₃ and placed in a 5-mm NMR tube maintained at room temperature. ^1H NMR spectra were acquired on a Varian XL-300 multinuclear spectrometer operating at 299.94 MHz using a 4000 Hz sweep width and 16 000 data points. The pulse width was set as 5.0 μs to provide a 30° flip angle. The recycle time was 2.0 s. A desirable signal-to-noise ratio was obtained after 1000 transients were acquired. Chemical shifts were referenced to tetramethylsilane (TMS).

Methods for kinetic and stability studies

Freshly synthesized HEDMP was added to phosphate buffer to give a 1% (v/v) solution and allowed to autoxidize at 37°C in the dark under air atmosphere. Aliquots of this solution were analyzed by HPLC after 3, 18, 72 and 122 h of oxidation. In order to test the stability of autoxidation products in aqueous solution, major products of HEDMP autoxidation (5%, v/v, 5-day sample) were isolated by HPLC and lyophilization. These were redissolved in phosphate buffer (1:5 dilution compared with original oxidation solution) and reincubated

under the same autoxidation conditions. Concentrations of the major components at different periods of incubation were determined by HPLC.

RESULTS AND DISCUSSION

HPLC separation of pyrrole autoxidation products

The spontaneous autoxidation of HEDMP in aqueous solution yielded a complex mixture of products which are illustrated in a three-dimensional HPLC–PAD plot (Fig. 1). Peak A5, corresponding to HEDMP, exhibited a UV absorbance maximum at 230 nm. Other peaks represented autoxidation products, some of which (peaks A1 and A2) showed absorbance maxima in the range of 310 to 340 nm. Based on these UV spectral data, 225 and 320 nm were chosen as HPLC multiple detection wavelengths in order to simultaneously detect parent pyrroles and their major oxidation products. Fig. 2a shows a dual-wavelength HPLC chromatogram of HEDMP after incubation in phosphate buffer (5%, v/v) under air atmosphere for 174 h. Autoxidation products of HEDMP were also detected by on-line TSP-MS. Fig. 2b shows the total ion current (TIC) chromatogram recorded during the same sample analysis (10-fold greater sample injection) as in Fig. 2a. Both detection methods showed a similar pattern of oxidation products. The

lower relative response in the TIC chromatogram to components eluting later in the gradient (*e.g.*, peak A7) reflects the suppressive influence of acetonitrile on the ionization.

Reversed-phase HPLC of HPDMP autoxidation products in aqueous solution and of a CHCl_3 extract of “pyrrole black” are presented in Fig. 3, in which peak B3 represents HPDMP. HPLC elution profiles of both HEDMP (Fig. 2) and HPDMP (Fig. 3) oxidation samples showed similar patterns for major autoxidation products. Several polar products (peak A1, A2 and A3 in Fig. 2a and peak B1 and B2 in Fig. 3) eluted at low concentrations of acetonitrile, and two non-polar products (peaks A6 and A7 in Fig. 2a and peaks B4 and B5 in Fig. 3) were found to be concentrated in the CHCl_3 extract.

A single analysis by HPLC on C_{18} columns enabled the separation of numerous components, including polar, oxygen-containing monomers and unstable oligomers (see below). In contrast, GC-MS was found to be inappropriate for the analysis of the pyrrole derivatives in these complex mixtures (data not shown). The advantages of this HPLC method include the lack of a requirement for chemical derivatization or other sample pretreatment, and increased sensitivity and rapidity of analysis as compared with previously used open column chro-

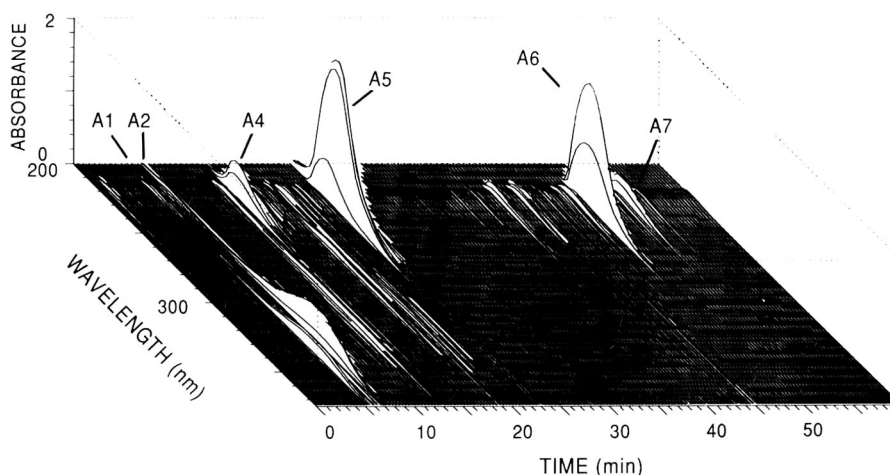


Fig. 1. Three-dimensional HPLC–PAD chromatogram from the analysis of an HEDMP autoxidation sample. HEDMP was incubated in phosphate buffer (5%, v/v) under air for 89 h (see under Experimental). Peak A5 corresponds to HEDMP; other peaks represent autoxidation products.

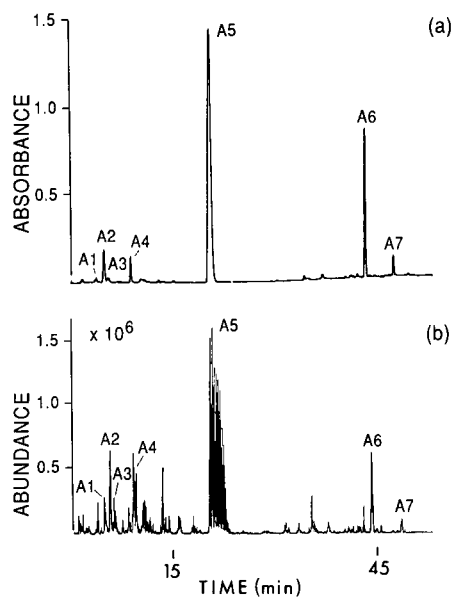


Fig. 2. HPLC separation of HEDMP autoxidation products. HEDMP was incubated in phosphate buffer (5%, v/v) under air for 174 h. (a) Maxplot chromatogram (dual-wavelength detection; 225 and 320 nm). (b) Total ion current chromatogram from HPLC-TSP-MS analysis of the same sample. Peak designations refer to data in Table I.

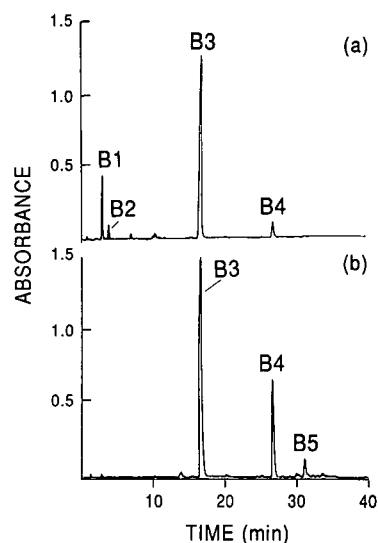


Fig. 3. HPLC separation of HPDMP autoxidation products. HPDMP was incubated under air for 76 h (see under Experimental). (a) Maxplot chromatogram (225, 320 nm) of HPDMP oxidation solution. (b) Maxplot chromatogram of CHCl₃ extract from autoxidation sediment. Peak B3 represents HPDMP, while other peaks correspond to its oxidation products.

matographic techniques. In addition, the HPLC technique has the capability of quantitative determination, providing a useful tool for kinetic studies of alkylpyrrole autoxidation.

Characterization of autoxidation products by TSP-MS and PAD

Thermospray mass spectra of both parent pyrroles exhibited single peaks representing protonated molecules without fragmentation (Figs. 4a and 5a). TSP mass spectra of major products of both HEDMP and HPDMP autoxidations are summarized in Table I. To investigate the incorporation of oxygen into alkylpyrrole autoxidation products, HEDMP was oxidized under an equimolar mixture of ¹⁶O₂ and ¹⁸O₂. TSP mass spectra of these autoxidation products were recorded and are summarized in Table I. In addition, PAD was employed

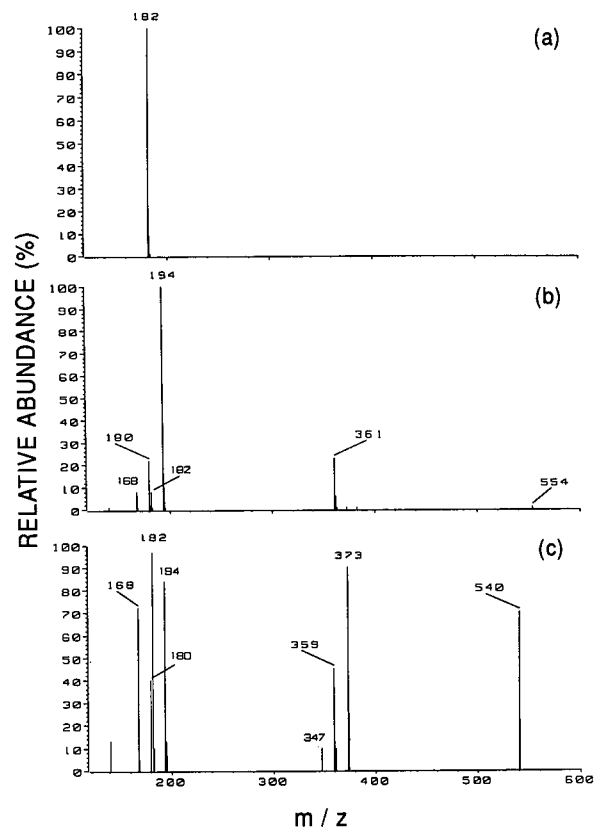


Fig. 4. Representative TSP mass spectra of HPDMP and its oligomers. (a) HPDMP; (b) HPDMP dimer; (c) HPDMP trimer. Molecular ions, major fragments and HPLC retention times are listed in Table I.

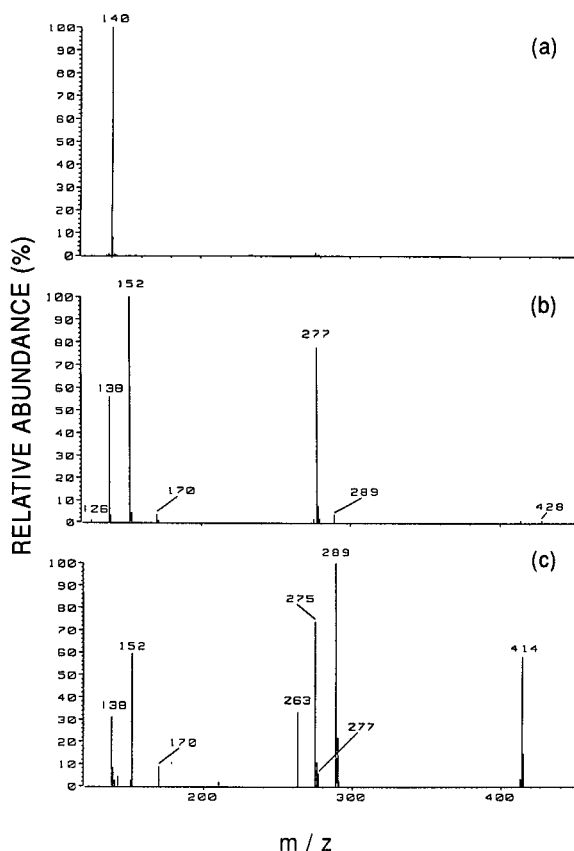


Fig. 5. Representative TSP mass spectra of HEDMP and its oligomers. (a) HEDMP; (b) HEDMP dimer; (c) HEDMP trimer. Molecular ions, major fragments and HPLC retention times are listed in Table I.

to provide structural information (Table I), since the substitution of carbonyl or other groups containing double bonds at the pyrrole methyl carbon, and/or the coupling of a pyrrole ring directly to that of the second pyrrole would be expected to extend the conjugation of the system, resulting in absorbance at longer wavelengths [27,28].

As can be seen in the UV chromatogram, one major group of autoxidation products consisted of non-polar alkyppyrrrole species (peaks A6 and A7 in Fig. 2 and peaks B4 and B5 in Fig. 3). TSP mass spectra of the two non-polar oxidation derivatives of HEDMP are shown in Fig. 4b and 4c. On the basis of intense ions corresponding to $[M + H]^+$,

peaks B4 and B5 were assigned to the dimer and trimer of HEDMP, respectively. Similarly, two non-polar products of HEDMP autoxidation were determined to be the dimer (Fig. 5b) and trimer of HEDMP (Fig. 5c).

Another major category of autoxidation products was polar oxygen-containing alkyppyrrrole monomers. Two components eluting from the HEDMP autoxidation solution (peaks A1 and A2 in Fig. 2a) exhibited the same molecular ion $[M + H]^+$ at m/z 172, corresponding to the mass of the protonated alkyppyrrrole plus 32 (Table I). The data suggested incorporation of two oxygen atoms, possibly due to sequential oxidation of the pyrrole methyl group to an aldehyde and then to a carboxylic acid. In addition, a common fragment ion (m/z 154) of both components may have resulted from the loss of water from the $[M + H]^+$ ion. TSP-MS of these two products (Table I) following autoxidation under a 1:1 mixture of $^{16}\text{O}_2$ and $^{18}\text{O}_2$ showed similar intensities of peaks at m/z 172 and 174 and ions assigned to $[M + H - \text{H}_2\text{O}]^+$ at m/z 154 and 156, but no isotopic peak at m/z 176. These data indicated that during the oxidation process only one oxygen atom was incorporated into alkyppyrrrole from molecular oxygen, which remained in the alkyppyrrrole fragment after the loss of water during thermospray ionization. The second oxygen atom was probably incorporated from the aqueous solvent.

The values of λ_{max} of these derivatives, 338 nm for peak A1 and 328 nm for peak A2, were consistent with extended conjugation of the pyrrole ring with functional groups that contain a double bond, possibly resulting from oxidation of the pyrrole methyl groups to aldehydes. For HEDMP autoxidation, similar monomeric autoxidation products (peaks B1 and B2) were present in UV chromatograms; these exhibited the same pattern of $[M + H]^+$ ions and value of λ_{max} (Table I). The component corresponding to peak A3 (Table I) was another monomeric HEDMP derivative that exhibited a $[M + H]^+$ ion consistent with incorporation of only one oxygen atom.

In addition to the two categories of major products, there were a number of minor autoxidation products from both alkyppyrrroles (Figs. 2 and 3). These minor pyrrole derivatives exhibited moderate polarity and were observed only after prolonged in-

TABLE I
CHARACTERIZATION OF MAJOR PRODUCTS OF HEDMP AND HPDMP AUTOXIDATION

Peak ^a	Retention time (min)	TSP-mass spectra <i>m/z</i> (relative intensity)	λ_{\max}
A1	4.8	172 ^b (100), 154 (9) [174 (76), 172 (100), 156 (28), 154(35)] ^c	338
A2	5.6	172 ^b (100), 154 (32) [174 (100), 172 (92), 156 (54), 154(81)] ^c	328
A3	6.1	156 ^b (100), 154 (66) [158 (42), 156 (100), 154 (38)] ^c	317
A4	8.9	170 ^b (55), 152 (100)	224
A5	19.9	140 ^b (100)	230
A6	42.9	428 ^d (0.3), 289 ^d (0.8), 277 ^b (66), 152 (100), 140 (4), 138 (94), 126 (4)	229
A7	47.3	565 ^d (0.1), 428 ^d (2), 414 ^b (24), 289 (67), 277 (9), 275 (79), 263 (17), 152 (100), 140 (15), 138 (89)	226
B1	2.9	214 ^b (100), 196 (22)	337
B2	4.2	214 ^b (21), 198 (100), 196 (42)	318
B3	18.1	182 ^b (100)	226
B4	29.1	554 ^d (0.8), 373 ^d (0.5), 361 ^b (24), 194 (100), 182 (8), 180 (22), 168 (8)	225
B5	33.9	540 ^b (18), 373 (100), 359 (18), 347 (6), 194 (59), 182 (61), 180 (28), 168 (50)	223

^a Peaks A1–A7 are from the analysis of HEDMP autoxidation, peaks B1–B5 are from the analysis of HPDMP oxidation.

^b Assigned to $[M + H]^+$;

^c Oxidation under $^{16}\text{O}_2/^{18}\text{O}_2$;

^d Assigned to adduct ion.

cubation time. Based on their respective $[M + H]^+$ ions, most of them were assigned as various oxygen-containing dimers. For example, in HEDMP oxidation samples, a peak at retention time 14 min exhibited an apparent $[M + H]^+$ at m/z 293, consistent with a dimer with one oxygen atom incorporated, while another peak (retention time 30.6 min) showed an apparent $[M + H]^+$ ion at m/z 311, corresponding to a dimer with two oxygens incorporated (Fig. 2).

Identification of the alkylpyrrole dimer

An important goal of this study was to characterize the type of linkage in 2,5-dimethyl-N-alkylpyrrole dimers and larger polymers, since it may constitute the protein cross-link in 2,5-HD-treated protein. The dimer molecular mass indicated by TSP-MS suggested oxidation, or a net loss of 2 H, in its formation. In addition, the identical UV spectra of alkylpyrrole monomer and dimer (Table I) indicated a lack of conjugation between the pyrrole

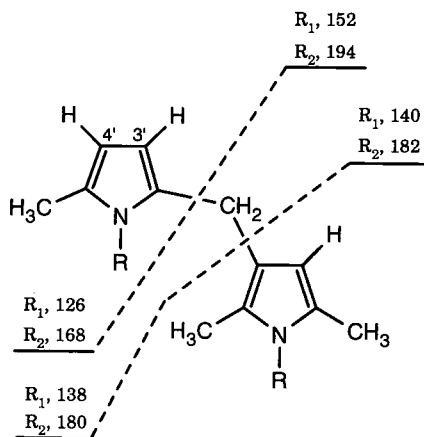


Fig. 6. Proposed general structure of 2,5-dimethyl-N-alkylpyrrole dimer and its thermospray mass spectral fragmentation pattern. R_1 is $-(CH_2)_2OH$ and R_2 is $-(CH_2)_5OH$.

rings of the dimer. These results argued against a direct ring-to-ring dimeric bridging structure [28], and were instead consistent with involvement of either the methyl or N-alkyl groups in pyrrole dimeric bridging. Since the only structural difference between the two pyrrole monomers examined in this study was in the N-alkyl group, the mass spectra would have exhibited some differences if the N-alkyl group was involved in cross-linking. This possibility was excluded by the identical fragmentation patterns of both HEDMP and HPDMP dimers.

Fig. 6 shows the proposed structure and TSP-MS fragmentations of the 2,5-dimethyl-N-alkylpyrrole dimers, which contain methylene bridges from C-2 of one pyrrole ring to C-3 of another pyrrole ring. During thermospray ionization, the N-alkylpyrrole moieties remained intact, while the methylene bridges were less stable. The TSP mass spectra of the dimers (Fig. 4b and Fig. 5b) showed peaks which were interpreted as being formed by cleavage of either of the C-C bonds of the methylene bridge (Fig. 6). Despite the fact that both fragments would be derived from substituted pyrroles and thus would be expected to have high proton affinities, in each case ions from the fragment retaining the methylene carbon, e.g. the ions with m/z 152 and 138 in the mass spectrum of the HEDMP dimer, showed much higher intensities than those derived from the other pyrrole ring, e.g. the ions with m/z

126 and 140. This might be explained by protonation of the dimer followed by a cleavage mechanism [29] in which the ions at m/z 138 and 152 arise from formation of alkyl-substituted 1- and 2-azafulvenium ions carrying the positive charge, and the second pyrrole is eliminated as a neutral fragment that would require subsequent protonation for MS detection.

In addition, there were several adduct ions with higher values of m/z than those of the corresponding $[M + H]^+$ ions in the mass spectra of both the HEDMP and the HPDMP dimers (Figs. 4b and 5b). The formation of these ions also followed a pattern. For example, the ion at m/z 428 in the mass spectrum of HEDMP dimer could be interpreted as an adduct of the dimer with a major fragment ion (m/z 152). This TSP mass fragmentation pattern may be characteristic of the unique bridge structure of 2,5-dimethyl-N-alkylpyrrole dimers and higher oligomers.

In the 1H NMR spectrum of the HEDMP dimer (Fig. 7), three singlets were observed at 2.16, 2.18 and 2.24 ppm, respectively, which arise from three isolated methyl groups on the pyrrole ring (protons labeled e in the structure illustrated in Fig. 7). Four triplets, at 3.55, 3.74, 3.86 and 3.89 ppm, were as-

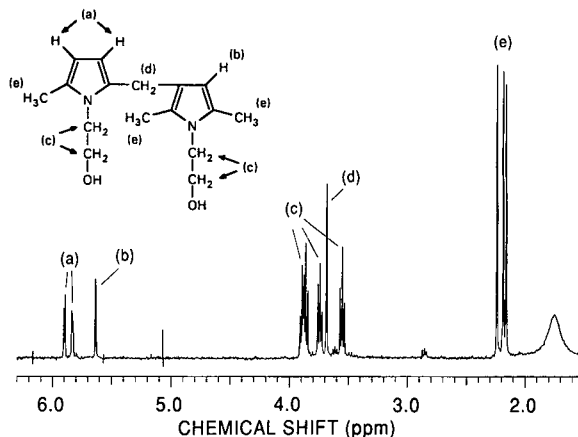


Fig. 7. The 1H NMR spectrum of the HEDMP dimer. Chemical shifts were referenced to TMS. The numbers of protons within specified chemical shift ranges are: 2.1 to 2.3 ppm, 9; 3.5 to 3.6 ppm, 2; 3.6 to 3.8 ppm, 4; 3.8 to 4.0 ppm, 4; 5.6 to 5.7 ppm, 1; 5.8 to 6.0 ppm, 2. The letters assigned to groups of peaks on the spectrum correspond to the letters denoting the different groups of protons in the proposed structure.

signed to the four methylenes in the two 2-hydroxyethyl groups (protons labeled c, $^3J = 5.0$ Hz). A singlet at 3.68 ppm was assigned to the isolated methylene connecting the two pyrrole rings (protons labeled d). In the aromatic region, a singlet at 5.63 ppm was assigned to the isolated proton on one of the pyrrole rings (proton b), and the two doublets at 5.83 and 5.89 ppm were ascribed to the two vicinal protons on the second pyrrole ring (protons a, $^3J = 3.5$ Hz). There were three non-equivalent methyl groups in the HEDMP dimer, as demonstrated by its ^1H NMR spectrum, implying that the dimerization was not symmetrical. Asymmetry of the dimer is also supported by the appearance of two pairs of triplets which arise from two chemically non-equivalent ethylene groups in the N-alkyl sidechains. The appearance of the aromatic proton signals indicate that one proton is isolated on one of the pyrrole rings and that the other two are adjacent on the second pyrrole ring. All these observations confirm the proposed methylene bridge structure of the HEDMP dimer as shown in Figs. 6 and 7.

UV spectral data also indicated that 2,5-dimethyl-N-alkylpyrrole trimers were formed without conjugation between the pyrrole rings. Furthermore, a similar TSP-MS fragmentation pattern of the trimer as with the dimer suggested an identical methylene bridging structure (Table I). This trimer is proposed to be formed by substitution at the C-4' position of the dimer by a methyl carbon of a third pyrrole monomer (Fig. 6). Since there are two methylene-bridge linkages in this trimer, cleavage of the C–C bonds on either side of the methylene bridges could yield a total of eight fragment ions in the mass spectra of both HPDMP and HEDMP trimers. Most of these ions were observed (Figs. 4c, 5c and Table I). An isomer of the proposed trimer having the same linkage structure but a different substitution position (*i.e.* at C-3' of the dimer; Fig. 6) is also possible. However, the structure of the trimer with C-4' substitution is considered the most likely because it would have less steric hindrance.

Kinetic studies

The time course of HEDMP autoxidation is illustrated in Fig. 8. At 3 h (Fig. 8a), only the peak corresponding to the HEDMP dimer (peak A6) was present, indicating that this derivative was produced in the initial stage of autoxidation. After 18

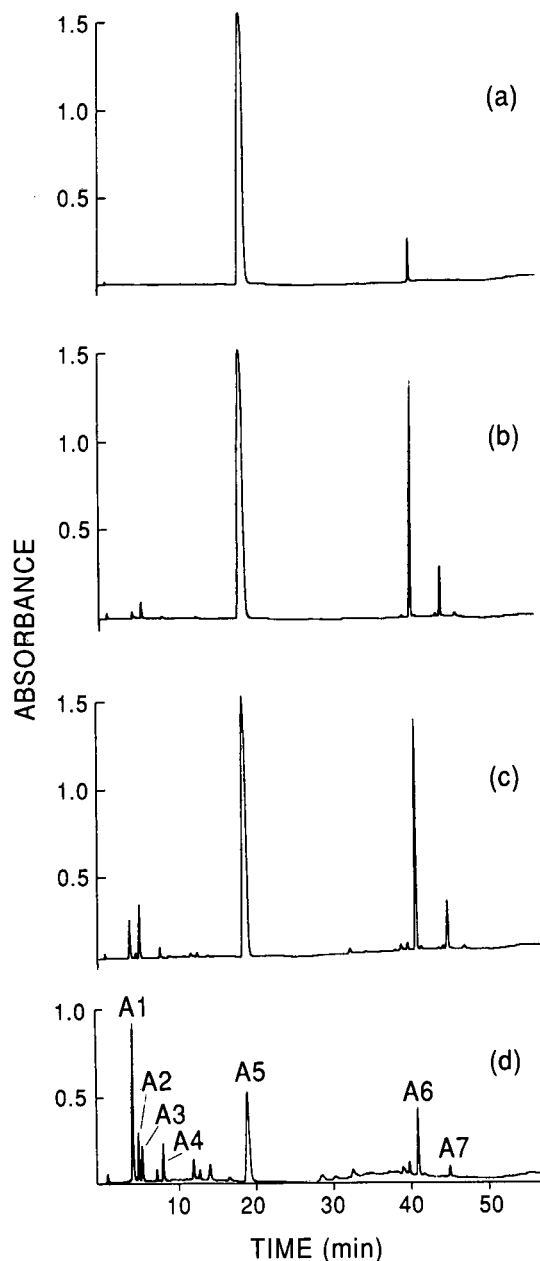


Fig. 8. Time course of HEDMP autoxidation. HEDMP was oxidized in phosphate buffer (1%, v/v) under air for various times. (a), (b), (c), (d) Analysis of samples after 3, 18, 44 and 128 h incubation, respectively. The oxidation products were analyzed by HPLC with dual-wavelength detection (maxplot; 225 and 320 nm).

h, the solution was slightly yellow, and HPLC at this time (Fig. 8b) revealed primarily dimer and

trimer (peak A7), suggesting that the HEDMP dimer may further react with HEDMP monomer to form the trimer. In addition, two polar, oxygen-containing products (peaks A1 and A3) were present at much lower concentrations at this time. The concentrations of the dimer and the trimer in reaction solutions reached a maximum after 44 h of oxidation (Fig. 8c) and then slowly decreased. In contrast, the levels of oxygen-containing polar monomeric products increased proportionally with incubation time. The only exception was peak A3, corresponding to a monomer with one oxygen incorporated, which decreased in intensity during the middle period of autoxidation.

In the later stages of autoxidation (122 h), a "pyrrole black" sediment was present. HPLC at 122 h (Fig. 8d) revealed a decrease in the concentrations of the HEDMP monomer, dimer and trimer, while polar monomeric components were now the major products, in particular peak A1. Results of other studies with isolated component A2 suggest that A1 may have been generated from A2 during prolonged incubation. Additionally, HPLC analysis at 122 h showed a number of new peaks, possibly representing additional autoxidation products, such as oxygen-containing dimers (e.g. $[M + H]^+$ at m/z 309) or degradation products of the polymers.

Fig. 9 shows the stability of HEDMP dimer, trimer, and polar monomeric derivatives, recovered by HPLC and then reincubated in aqueous solution. Both oligomers were unstable, with $t_{1/2}$ of approximately 10–12 h. This indicated that these oligomers may quickly undergo further reactions to form polymers or other unknown insoluble products. Additionally, the decrease in the relative concentration of the HEDMP dimer with time followed apparent first-order kinetics. The instability of the dimer and trimer in aqueous solution accounts for the decrease in the concentrations of these derivatives in the later stages of autoxidation (Fig. 8). In contrast, the intensities of peak A4 and the total of peaks A1 and A2 were relatively constant in aqueous solution (Fig. 9). Studies of the time course of autoxidation and stabilities of the major products in aqueous solution revealed that the formation of pyrrole dimer was the predominant reaction at physiological pH. However, there were additional pathways yielding oxygen-containing monomers or other derivatives which occurred at a slower rate.

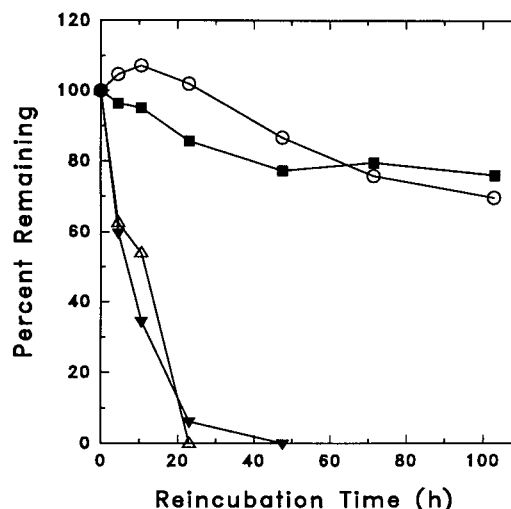


Fig. 9. Stability of major HEDMP autoxidation products in aqueous solution. Isolated HEDMP oxidation products (collected from HPLC eluent) were reincubated in phosphate buffer (ca. 1%, v/v). Relative levels of these components were measured as peak areas by HPLC maxplot with dual-wavelength detection after various reincubation times, as compared with zero time areas. Retention times, UV absorption data, and molecular mass information of individual components corresponding to each peak are listed in Table I. ■ = Peak A1 plus peak A2; ○ = peak A4; ▼ = peak A6; △ = peak A7.

CONCLUSIONS

The application of HPLC coupled with TSP-MS and PAD allowed the simultaneous separation and characterization of autoxidation products of 2,5-dimethyl-N-alkylpyrroles, including polar, oxygen-containing monomers and high-molecular-mass oligomers. The proposed methylene bridge structure formed upon dimerization of these pyrroles, which has not been previously reported, was confirmed by ^1H NMR spectroscopy. The techniques reported here should be useful in future mechanistic studies of pyrrole chemistry as it relates to hexane neurotoxicity and the stability of petroleum-based fuels.

ACKNOWLEDGEMENTS

This work was supported in part by a research grant (ES-05172) from the US National Institute for Environmental Health Sciences. In addition,

support from the National Science Foundation for the purchase of the NMR instrumentation used in this research is gratefully acknowledged.

REFERENCES

- 1 A. P. DeCaprio and E. A. O'Neill, *Toxicol. Appl. Pharmacol.*, 78 (1985) 235.
- 2 A. P. DeCaprio, E. J. Olajos, and P. Weber, *Toxicol. Appl. Pharmacol.*, 65 (1982) 440.
- 3 D. G. Graham, D. C. Anthony, K. Boekelheide, N. A. Maschmann, R. G. Richard, J. W. Wolfram and B. R. Shaw, *Toxicol. Appl. Pharmacol.*, 64 (1982) 415.
- 4 D. M. Lapidula, R. D. Irwin, E. Suwita and M. B. Abou-Donia, *J. Neurochem.*, 46 (1986) 1843.
- 5 L. M. Sayre, C. M. Shearson, T. Wongmongkolrit, R. Medori and P. Gambetti, *Toxicol. Appl. Pharmacol.*, 84 (1986) 36.
- 6 M. B. Genter, G. Szakal-Quin, C. W. Anderson, D. C. Anthony and D. G. Graham, *Toxicol. Appl. Pharmacol.*, 87 (1987) 351.
- 7 A. P. DeCaprio, R. G. Briggs, S. J. Jackowski and J. C. S. Kim, *Toxicol. Appl. Pharmacol.*, 92 (1988) 75.
- 8 A. P. DeCaprio, *Mol. Pharmacol.*, 30 (1986) 452.
- 9 D. C. Anthony, V. Amarnath and D. G. Graham, *Toxicologist*, 10 (1990) 183.
- 10 A. A. Oswald and F. Noel, *J. Chem. Eng. Data*, 6 (1961) 294.
- 11 J. Li and N. C. Li, *Fuel*, 64 (1985) 1041.
- 12 J. W. Frankenfeld and W. F. Taylor, *Ind. Eng. Chem. Prod. Res. Dev.*, 22 (1983) 615.
- 13 J. W. Frankenfeld and W. F. Taylor, *Ind. Eng. Chem. Prod. Res. Dev.*, 22 (1983) 608.
- 14 M. C. Loeffler and N. C. Li, *Fuel*, 64 (1985) 1047.
- 15 J. V. Cooney and R. N. Hazlett, *Heterocycles*, 22 (1984) 1513.
- 16 A. Gossauer and P. Nesvadba, in R. A. Jones (Editor), *Pyrroles, Part I, Synthesis and Physical and Chemical Aspects of the Pyrrole Ring*, Wiley, New York, 1990, p. 499.
- 17 E. Höft, A. R. Katritzky and M. R. Nesbit, *Tetrahedron Lett.*, 32 (1967) 3041.
- 18 E. B. Smith and H. B. Jensen, *J. Org. Chem.*, 32 (1967) 3330.
- 19 G. B. Quistad and D. A. Lightner, *Tetrahedron Lett.*, 46 (1971) 4417.
- 20 B. D. Beaver, J. V. Cooney and J. M. Watkins, Jr., *J. Heterocyclic Chem.*, 23 (1986) 1095.
- 21 G. B. Odell, W. S. Mogilevsky and G. R. Gourley, *J. Chromatogr.*, 529 (1990) 287.
- 22 N. E. Mahoney and J. N. Roitman, *J. Chromatogr.*, 508 (1990) 247.
- 23 J. K. Baker, R. H. Yarber, C. D. Hufford, I. Lee, H. N. El Sohly and J. D. McChesney, *Biomed. Environ. Mass Spectrom.*, 18 (1988) 337.
- 24 I. G. Beattie and T. J. A. Blake, *Biomed. Environ. Mass Spectrom.*, 18 (1989) 872.
- 25 R. L. Jansing, E. S. Chao and L. S. Kaminsky, *Mol. Pharmacol.*, 41 (1992) 209.
- 26 C. Paal, *Chem. Ber.*, 17 (1884) 2756.
- 27 A. I. Scott, *Interpretation of Ultraviolet Spectra of Natural Products*, Pergamon Press, New York, 1964, p.165.
- 28 L. Chierici and G. P. Gardini, *Tetrahedron*, 22 (1966) 53.
- 29 D. J. Chadwick, in R. A. Jones (Editor), *Pyrroles, Part I, Synthesis and Physical and Chemical Aspects of Pyrrole Ring*, Wiley, New York, 1990, p. 65.

Column liquid chromatography of cefadroxil on poly(styrene–divinylbenzene)

C. Hendrix, C. Wijsen, Li Ming Yun, E. Roets and J. Hoogmartens

Laboratorium voor Farmaceutische Chemie, Instituut voor Farmaceutische Wetenschappen, Katholieke Universiteit Leuven, Van Evenstraat 4, B-3000 Leuven (Belgium)

(Received June 30th, 1992)

ABSTRACT

Isocratic column liquid chromatography on a poly(styrene–divinylbenzene) stationary phase (PLRP-S, 25 cm × 0.46 cm I.D.) at 50°C allowed the separation of cefadroxil from related substances. The mobile phase was acetonitrile–0.02 M sodium 1-octanesulphonate–0.2 M phosphoric acid–water (10.5:20:5:up to 100, v/v). The flow-rate was 1.0 ml/min and UV detection was performed at 254 nm. Official standards were compared and a number of commercial bulk samples and specialities were analysed.

INTRODUCTION

Cefadroxil is a semi-synthetic β -lactam antibiotic from the group of the cephalosporins. Although column liquid chromatography (LC) of cefadroxil has been discussed in several papers, the separation of cefadroxil from its potential impurities has not been reported. Some papers have described the determination of cefadroxil in biological samples [1–4], and mainly considered to the separation of the antibiotic from the biological matrix. The separation of cefadroxil from a mixture of cephalosporins has also been reported [5,6]. Tsuji *et al.* [7] studied the degradation kinetics of cefadroxil by means of LC techniques. LC has also been used for pharmacokinetic studies of cefadroxil [8]. The separation of cefadroxil from excipients of pharmaceuticals has also been reported [9]. The European Pharmacopoeia (Ph. Eur.) proposed an LC method for the assay of cefadroxil [10]. Nearly the same LC method is prescribed by the United States Pharma-

copeia XXII (USP) for the assay of cefadroxil [11]. This method was examined in our laboratory and it was found that it did not allow the complete separation of cefadroxil from its potential impurities; these results will be reported later. The Ph. Eur. and the USP prescribe the use of reversed-phase materials based on silica, for which the poor reproducibility of the selectivity towards cephalosporins has been reported earlier [5].

In this paper, an isocratic method using poly(styrene–divinylbenzene) (PS–DVB) as the stationary phase is described. It permits the complete separation of cefadroxil from known related substances and performs equally well on different available brands of PS–DVB. The method has been used to compare official standards and to analyse a number of commercial samples of different origin.

EXPERIMENTAL

Reference substances and samples

The United States Pharmacopoeia Reference Standard (USP-RS; Lot H; 929 $\mu\text{g}/\text{mg}$) and the European Pharmacopoeia Chemical Reference Standard (Ph. Eur.-CRS; 94.2%) were used.

Bulk samples were obtained from Italy, India and

Correspondence to: J. Hoogmartens, Laboratorium voor Farmaceutische Chemie, Instituut voor Farmaceutische Wetenschappen, Katholieke Universiteit Leuven, Van Evenstraat 4, B-3000 Leuven, Belgium.

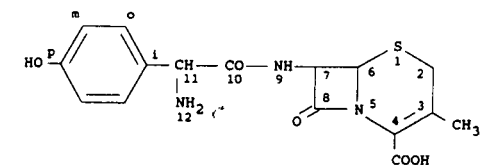
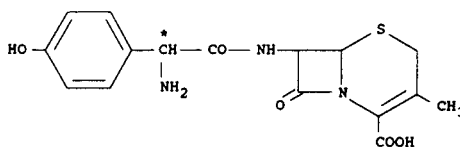
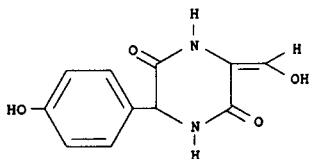
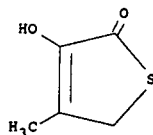
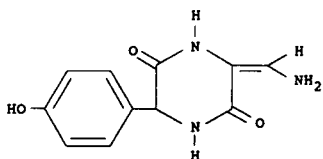
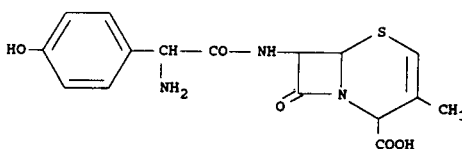
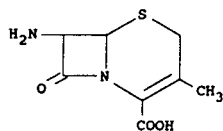
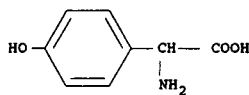
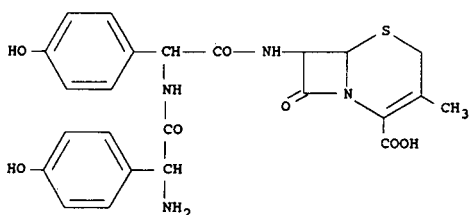
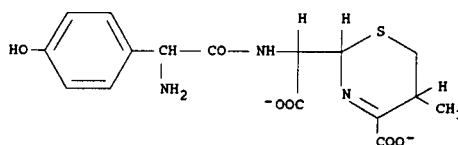
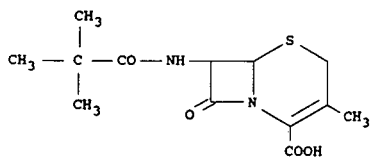
**I D-Cefadroxil****II L-Cefadroxil ******III 3-Hydroxymethylene-6-(4-hydroxyphenyl)-piperazine-2,5-dione *****IV 3-Hydroxy-4-methyl-2(5H)-thiophenone *****V 3-Aminomethylene-6-(4-hydroxyphenyl)-piperazine-2,5-dione *****VI Δ²-Cefadroxil ******VII 7-Aminodesacetoxycephalosporanic acid (7-ADCA) *******VIII 4-Hydroxyphenylglycine *******IX 4-Hydroxyphenylglycylcefadroxil ******X Cefadroxil Δ⁴-cephalosporoates *****XI Pivalamide of 7-ADCA ****

Fig. 1. Structures of cefadroxil and related substances. * Degradation product. ** Side-product of the synthesis. *** Starting product of the synthesis.

Belgium. Dosage forms containing cefadroxil (Duracef, Moxacef, Bristol) were obtained commercially in Belgium.

Related substances

Related substances present as impurities in cefadroxil can originate from the semi-synthesis and from degradation. Fig. 1 shows the structures of D-cefadroxil and its potential impurities. Compounds VII and VIII, which are the basic constituents of the cefadroxil molecule, are commercially available (VII, Gist-Brocades, Delft, Netherlands; VIII, Janssen Chimica, Beerse, Belgium). Compounds II, VI, IX and XI can arise from the semi-synthesis of cefadroxil. Compounds II, VI and IX were prepared in the laboratory and XI was provided by a manufacturer. The other related substances are decomposition products formed in acidic (III, IV), neutral (III, V) and alkaline (X) media. Compounds III, IV, V and X were prepared in the laboratory. The preparation of these products will be described elsewhere. Compound X was never isolated but was prepared *in situ* by dissolving cefadroxil in 0.1 M NaOH (1 mg/ml) and storing the solution at room temperature for 10 min.

Solvents and reagents

Acetonitrile (99%) (Janssen Chimica) and methanol (Roland, Brussels, Belgium) were distilled before use. 2-Methyl-2-propanol (99.5%) (Janssen Chimica) was used as received. Phosphoric acid (85%) and potassium dihydrogen phosphate (analytical-reagent grade) were purchased from Merck (Darmstadt, Germany) and sodium 1-octanesulphonate (NaOS) from Janssen Chimica. Water was distilled twice.

LC apparatus and operating conditions

Isocratic elution (1 ml min^{-1}) was used throughout. The equipment consisted of an L-6200 pump (Merck-Hitachi, Darmstadt, Germany), a CV-6-UHPa-N60 20- μl loop injector (Valco, Houston, TX, USA), a 25 cm \times 0.46 cm I.D. column, packed with 8- μm PLRP-S 100 Å (Polymer Labs., Church Stretton, Shropshire, UK), a Model D 254-nm fixed-wavelength UV monitor (LDC/Milton Roy, Riviera Beach, FL, USA) and a Model 3396 A integrator (Hewlett-Packard, Avondale, PA, USA). The column temperature was maintained at 50°C by

means of a water-bath heated by a Julabo EM thermostat (Julabo Labortechnik, Seelbach, Germany). The selectivity of the method was also tested on other PS-DVB stationary phases [PRP-1 (10 μm) and PRP-1 (7–9 μm); Hamilton, Reno, NV, USA]. For the examination of peak homogeneity the UV detector was replaced with a Model 990 photodiode-array detector (Waters Assoc., Milford, MA, USA). A Marathon autosampler with sample cooling (Spark Holland, Emmen, Netherlands) equipped with a fixed 20- μl loop and a Julabo C and F10 cryomat was used for quantitative analysis.

Mobile phase

The mobile phase finally used was prepared by mixing 500 ml of water, 105 ml of acetonitrile, 200 ml of 0.02 M NaOS and 50 ml of 0.2 M phosphoric acid. The mixture was diluted to 1000 ml with water and degassed by ultrasonication before use.

Sample preparation

Samples for quantitative analysis were prepared by weighing an amount corresponding to 30 mg of cefadroxil into a 20-ml volumetric flask. Mobile phase containing 30% of 0.02 M NaOS solution was used as the solvent. For the specialities a mixture of sample powder and solvent was ultrasonicated and centrifuged and the supernatant was analysed. The reference substances were dissolved the same way as the samples.

RESULTS AND DISCUSSION

Development of the chromatographic method

PS-DVB was used as the stationary phase because of its good stability, even at extreme pH conditions and high temperatures [12]. The stationary phase was heated at 60°C to enhance the mass transfer and to reduce the back-pressure. The influence of the column temperature is discussed below.

The mobile phase, developed earlier for the chromatography of cefalexin [13], was examined for its suitability to separate cefadroxil from its potential impurities. It consisted of acetonitrile–0.02 M NaOS–0.2 M phosphoric acid (pH 1.4)–water (10:5:10:up to 100, v/v). Using this mobile phase, cefadroxil was separated from the related substances, but some substances (II and VI) were eluted as split peaks. The composition of the mobile phase

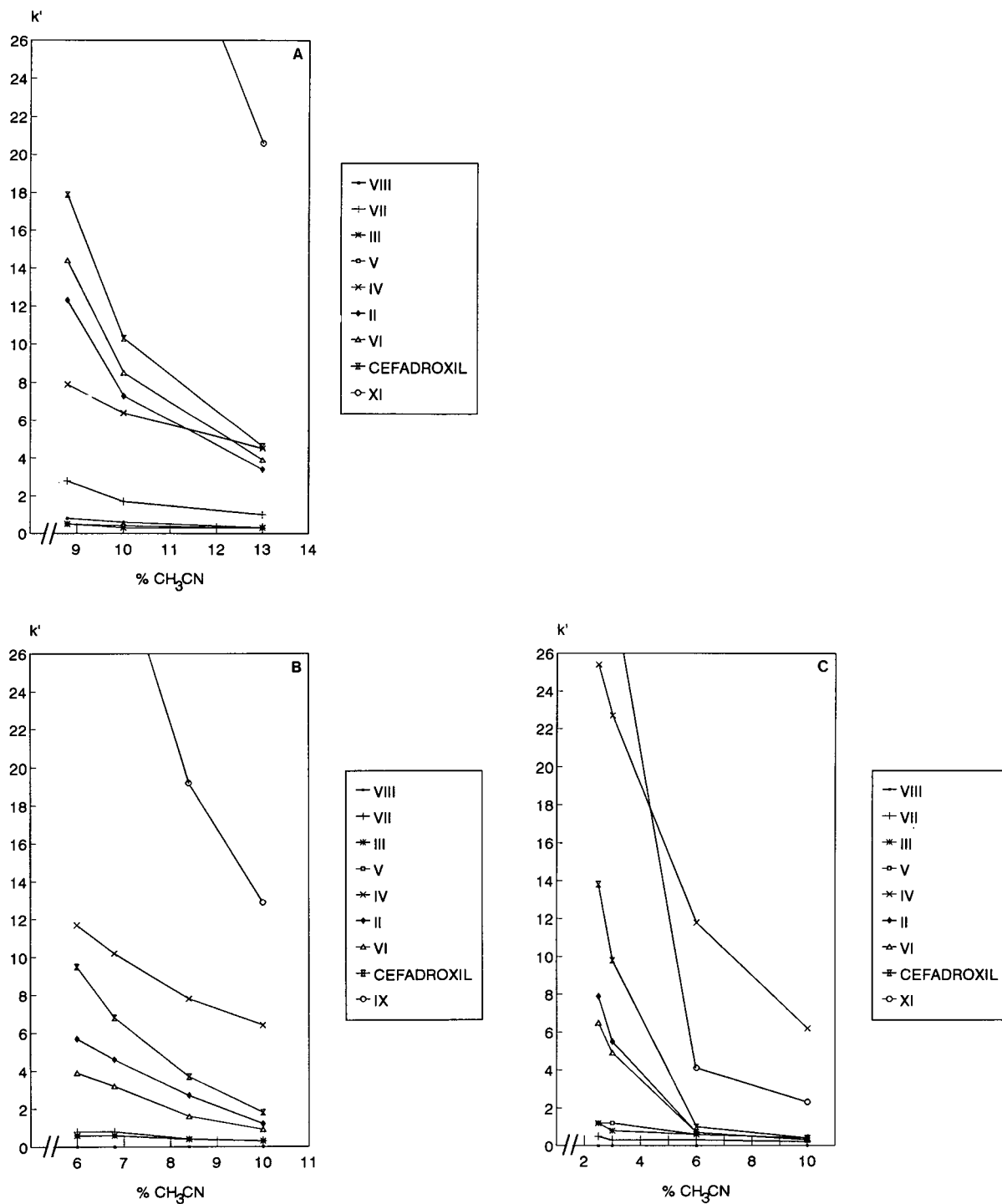


Fig. 2. Influence of the concentration of acetonitrile on the separation of cefadroxil and related substances at (A) pH 1.4, (B) pH 3.0 and (C) pH 4.0. Stationary phase: PLRP-S 100 Å (8 μm). Mobile phase: acetonitrile–0.02 M NaOS–0.2 M H_3PO_4 or 0.2 M phosphate buffer (pH 3.0 or 4.0)–water [x:10:5:up to 100, v/v].

obviously needed some modification. Therefore, the mobile phase was further evaluated by systematic examination of its components.

The solution of phosphoric acid was replaced with 0.2 M phosphate buffers of pH 3.0 or 4.0 in order to examine the influence of the pH on the separation. For each pH, the amount of organic modifier was varied to optimize the separation (Fig. 2). All the products eluted much faster at higher pH, except for III, IV and V, which were not affected by the pH. Compounds III and IV had no positively charged amino group like the other related substances and consequently did not interact with the ion-pairing reagent. Compounds III and V were almost never separated at the investigated pH values. Compound V was probably hydrolysed by acidic mobile phases and converted into III. This was confirmed by photodiode-array detection. Compound XI was eluted very late compared with the other substances, except at pH 4.0. At pH 1.4

complete separation between cefadroxil and related substances was achieved when less than 12% of acetonitrile was used. A pH of 1.4 gave an average plate number of 3000/m. At pH 3.0 the order of elution was changed, IV being eluted after cefadroxil. Using about 7% of acetonitrile, all the related substances were separated from cefadroxil. The efficiency was distinctly lower, however, than at pH 1.4 (1600 plates/m). At pH 4.0 a very low efficiency was obtained (400 plates/m). Only very slow elution with 3% or less of acetonitrile present allowed the complete separation of cefadroxil. In conclusion, phosphoric acid was chosen to adjust the pH of the mobile phase. At this pH the retention time of IX was at least four times that of cefadroxil, and because its separation caused no problem, IX was omitted from subsequent experiments.

Mobile phases with other organic modifiers were also examined. 2-Methyl-2-propanol had already been demonstrated to be very suitable for the LC of tetracycline [14] or erythromycin [15] on PSDVB. Fig. 3 shows the capacity factors obtained with different concentrations of 2-methyl-2-propanol. None of the investigated mobile phases was able to separate cefadroxil and its Δ^2 -isomer VI, although the efficiency (3500 plates/m) was better than with acetonitrile. In Fig. 4 the elution pattern obtained with different concentrations of methanol as organic modifier is shown. Also owing to the low efficiency (1700 plates/m), cefadroxil was not separated from IV and VI. As a result, acetonitrile was preferred as the organic modifier.

The concentration of 0.2 M phosphoric acid did not affect the selectivity in the range examined (2.5–7.5%, v/v). Therefore, the initial concentration of 5% was maintained.

The influence of the ion-pairing reagent NaOS is shown in Fig. 5. With 5% of the 0.02 M NaOS solution most substances were eluted too fast and the elution order had changed, the non-protonated IV now being eluted between cefadroxil and VI. Doubling the original concentration of 0.02 M NaOS to 20% gave a remarkable improvement. The peaks corresponding to II and VI were symmetrical and the separation between II and IV had improved. In further experiments, 20% of 0.02 M NaOS solution in the mobile phase was adopted.

The mobile phase finally selected for further use throughout the study was acetonitrile–0.02 M

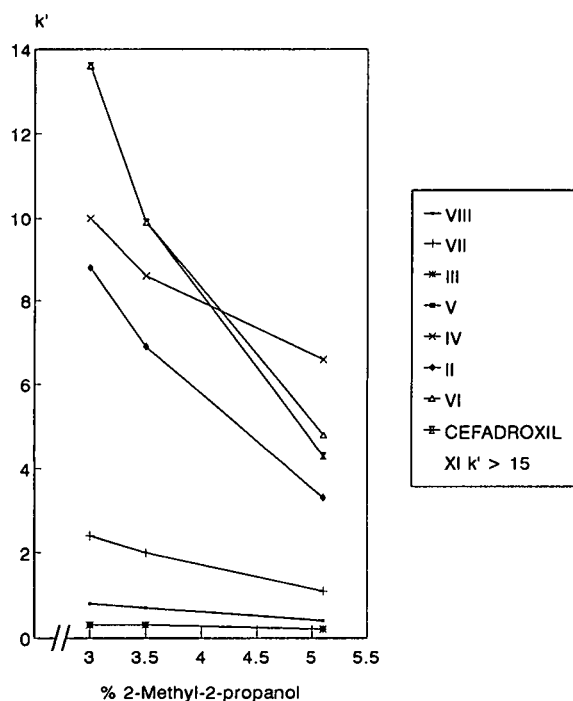


Fig. 3. Influence of the concentration of 2-methyl-2-propanol as organic modifier on the separation of cefadroxil and related substances. Stationary phase: PLRP-S 100 Å (8 μ m). Mobile phase: 2-methyl-2-propanol–0.02 M NaOS–0.2 M H₃PO₄–water [x:10:5:(85–x), w/v/v/v].

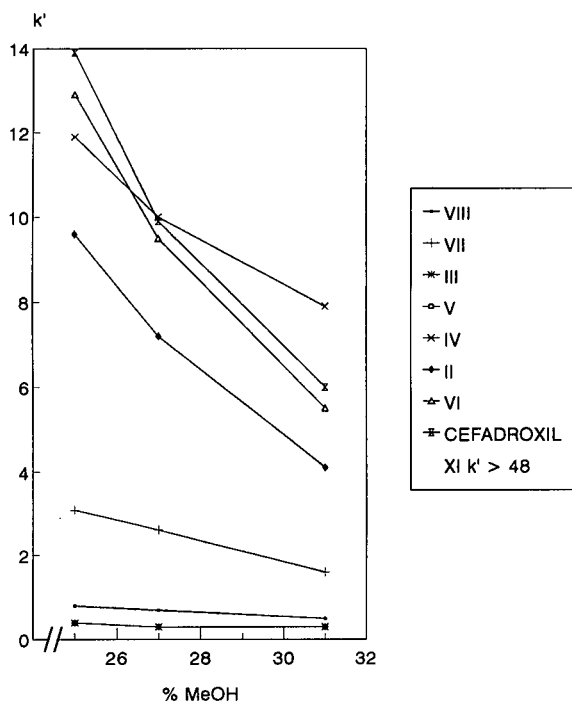


Fig. 4. Influence of the concentration of methanol as organic modifier on the separation of cefadroxil and related substances. Stationary phase: PLRP-S 100 Å (8 μ m). Mobile phase: methanol–0.02 M NaOS–0.2 M H₃PO₄–water [x:10:5:up to 100, v/v].

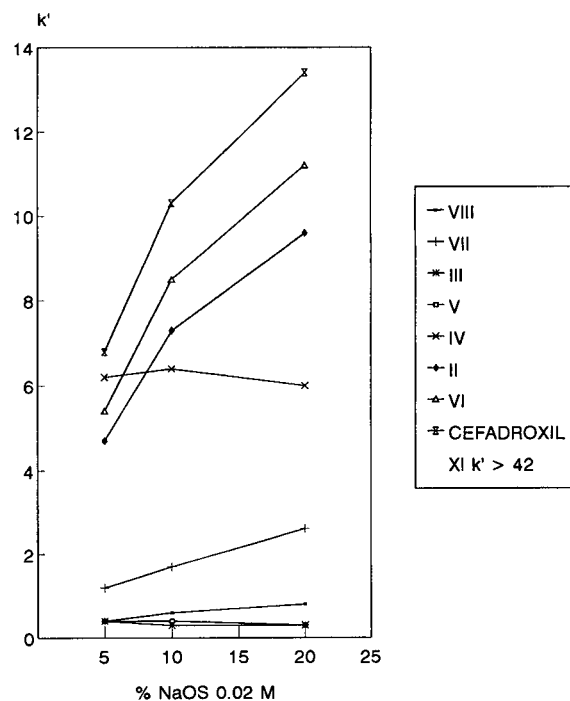


Fig. 5. Influence of the concentration of NaOS in the mobile phase on the separation of cefadroxil and related substances. Stationary phase: PLRP-S 100 Å (8 μ m). Mobile phase: acetonitrile–0.02 M NaOS–0.2 M H₃PO₄–water [10:x:5:up to 100, v/v].

NaOS–0.2 M phosphoric acid–water (10.5:20:5 up to 100, v/v).

The selectivity of the method was further validated by examination of the peak homogeneity of the cefadroxil peak after decomposition of a sample in alkaline or acidic medium. For this purpose, the chromatograms were recorded by means of photodiode-array detection. A solution of cefadroxil in 0.1 M NaOH (1 mg/ml) was stored at room temperature for 10 min, neutralized and analysed. The cefadroxil content had already decreased by 50%. After examination of the UV spectra of the left-hand slope, the maximum and the right-hand slope of the cefadroxil peak, it was found to be homogeneous. A solution of cefadroxil in 0.1 M HCl (1 mg/ml) stored at 60°C for 5 h was examined in the same way. The cefadroxil content was reduced by about 5% but the peak was homogeneous.

The reproducibility of the selectivity on other PS–DVB stationary phases was checked using the same mobile phase. The content of acetonitrile was

adapted for each column to obtain comparable retention times. The characteristics of the columns are listed in Table I. The separation pattern, shown in Fig. 6, is the same for each column. This reproducible selectivity is an advantage with regard to the use of reversed-phase stationary phases based on silica and ensures an improvement of the between-laboratory precision.

The influence of the column temperature on the separation was investigated at 50, 60 and 70°C. The products were eluted faster at higher temperature, but the selectivity was similar at all three temperatures. The stability of a solution of cefadroxil in the mobile phase stored at these three temperatures was also examined. The solutions stored at 60 or 70°C showed decomposition after 45 minutes (0.3% and 3.7%, respectively), whereas at 50°C no decomposition was observed. In order to guarantee stability of the samples during analysis, the column temperature was decreased to 50°C.

Analysis of a solution of cefadroxil in water gave

TABLE I

CHARACTERISTICS OF THE PS-DVB COLUMNS USED, WITH THE RESPECTIVE CONCENTRATIONS OF ACETONITRILE IN THE MOBILE PHASE

Column	Age (years)	Stationary phase (250 × 4.6 mm I.D.)	Batch	Acetonitrile (%)
A	5	PLRP-S 100 Å (8 μm)	(10-12-85)B	11.0
B	5	PLRP-S 100 Å (8 μm)	(10-12-85)B	11.0
C	2	PLRP-S 100 Å (8 μm)	35	10.5
D	1	PLRP-S 100 Å (8 μm)	35	11.0
E	1	PLRP-S 100 Å (8 μm)	35	11.5
F	New	PLRP-S 100 Å (8 μm)	8M-RPS-1-64	10.5
G	6	PRP-1 (10 μm)	79400	11.5
H	New	PRP-1 (7-9 μm)	457	11.0

several disturbing system peaks. Using the mobile phase as the solvent, some system peaks disappeared. After systematic variation of the composition of this solvent, a mobile phase containing 30% of 0.02 M NaOS was chosen as the solvent for the samples. Unfortunately, one small system peak was still present.

Fig. 7 shows a typical chromatogram of cefadroxil obtained using the selected chromatographic conditions. The positions of the related substances are indicated.

Finally, a resolution test for this LC method was developed. The products that eluted closest to cefadroxil were **IV**, **II** and **VI**. As these related substances were not commercially available, a solution of 5 mg of cefadroxil and 40 mg of amoxicillin trihydrate in 50 ml of water was used to calculate the resolution. Amoxicillin was chosen because its structure is closely related to that of cefadroxil. As its specific absorption is much lower than that of cefadroxil, the concentration was adjusted in order to obtain peaks of equal height. A mixture of ce-

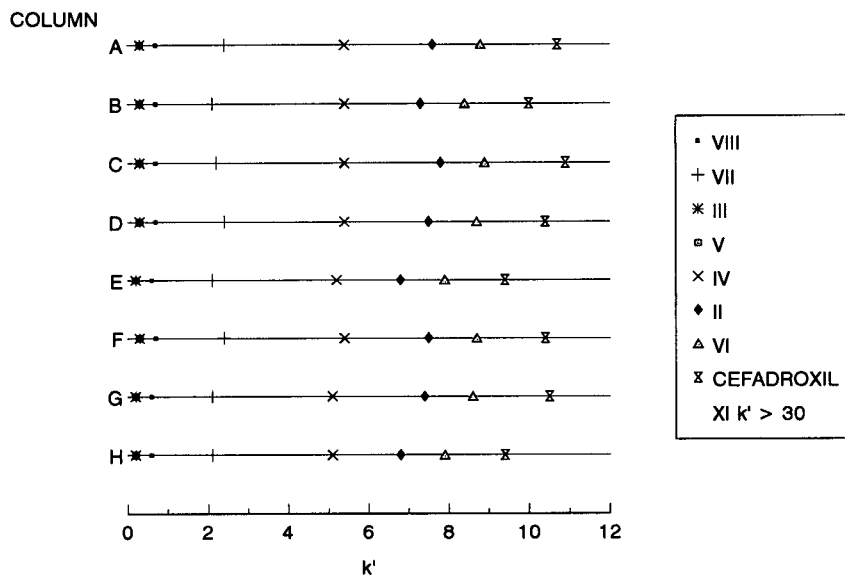


Fig. 6. Capacity factors of cefadroxil and related substances on different PS-DVB columns (see Table I for characteristics). Mobile phase: acetonitrile-0.02 M NaOS-0.2 M H₃PO₄-water [x:20:5:up to 100, v/v]; for x, see Table I.

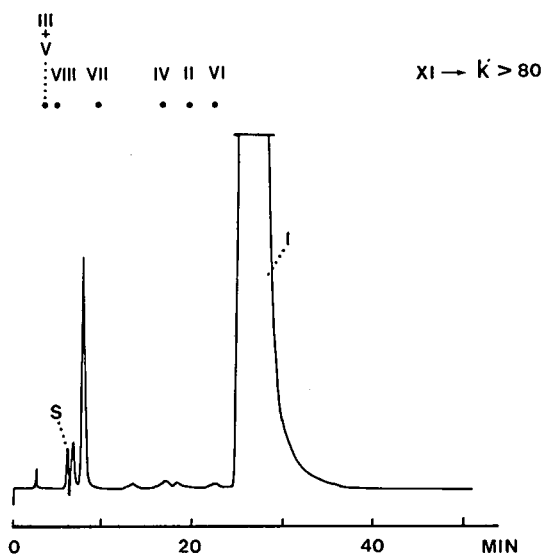


Fig. 7. Typical chromatogram of cefadroxil (30 μg). The positions of the related substances are indicated. Stationary phase: PLRP-S 100 \AA (8 μm), 50°C. Mobile phase: acetonitrile–0.02 M NaOS–0.2 M H_3PO_4 –water (10.5:20:5:up to 100, v/v). S = System peak.

fadroxil and small amounts of IV, II and VI was analysed for visual evaluation of the separation. These solutions were repeatedly analysed on the columns listed in Table I, while the amount of organic modifier was increased. It was concluded that a resolution of 4.0, calculated for the peaks of ce-

fadroxil and amoxicillin, guaranteed sufficient separation of cefadroxil from IV, II and VI.

Quantitative aspects of the LC method

The loadability was not only limited by the capacity of the column or the composition of the mobile phase, but also by the equipment used. Analysis of more than 100 μg of cefadroxil gave a chromatogram with an incompletely integrated cefadroxil peak. It was decided to use a 30- μg amount for quantitative analysis of cefadroxil samples. For this amount the limit of detection (LOD) ($S/N = 3$) was 0.04%, expressed as cefadroxil. The limit of quantification (LOQ) was 0.08% [$n = 8$, relative standard deviation (R.S.D.) = 16%]. The repeatability was checked by analysing six times the same solution of cefadroxil (30 μg) (R.S.D. = 0.04%, calculated on the area of the cefadroxil peak) and by analysing subsequently six freshly prepared solutions of cefadroxil (30 μg) (R.S.D. = 0.3%, calculated on the area of the cefadroxil peak). At about 6°C, solutions of cefadroxil in the mobile phase remained stable for at least 24 h. Linearity tests were performed ($y = \text{peak area}/1000$, $x = \text{amount injected in } \mu\text{g}$): $y = 9969x - 2709$, standard error of estimate $S_{y,x} = 609$, correlation coefficient $r = 0.999$ ($n = 9$), range of x covered in the experiments = 24–36 μg .

TABLE II

COMPOSITION OF CEFADROXIL STANDARDS

Values in % (w/w); R.S.D. values (%) are given in parentheses.

Parameter	Ph. Eur.-CRS (94.2%)	USP-RS (929 $\mu\text{g}/\text{mg}$)
Number of analyses	9	9
Number of solutions analysed	3	3
Cefadroxil	94.24 ^a (0.8)	93.92 (0.4)
Impurities	0.31 ^a	0.48 (9.5)
Residual solvents	0.29 ^a	<0.1 ^b , ND ^c
Water	5.16 ^a	5.21 ^b , ND ^c
Total	100.0	99.6

^a Following ref. 16.

^b Following ref. 17.

^c ND = Not determined owing to limited amount of sample.

TABLE III
COMPOSITION OF BULK SAMPLES OF CEFADROXIL

Values in % (w/w); R.S.D. (%) is given in parentheses. Water was determined by Karl Fischer titration. *N* = Number of analyses.

Origin	Sample No.	LC: Cefadroxil (<i>n</i> = 5) (A)	LC: Impurities (<i>n</i> = 5) (B)	Water (<i>n</i> = 4) (C)	Total (A + B + C)	Total (C + D)	Non-aqueous titration (<i>n</i> = 4) (D)
A	1	94.01 (0.4)	0.30 (10.0)	5.52 (2.3)	99.83	100.03	94.51 (0.1)
A	2	92.47 (0.3)	1.06 (11.2)	5.50 (2.3)	99.03	100.10	94.60 (0.2)
B	3	93.98 (0.6)	0.59 (12.6)	5.65 (2.0)	100.22	101.06	95.41 (0.4)
C	4	93.72 (0.2)	0.58 (7.8)	5.68 (2.4)	99.98	100.46	94.78 (0.3)
C	5	94.21 (0.5)	0.44 (11.0)	5.16 (1.5)	99.81	100.45	95.29 (0.0)

Comparison of cefadroxil standards

The USP-RS and the Ph. Eur.-CRS were compared by means of the proposed LC method. The cefadroxil content of the USP-RS was calculated by comparison with the Ph. Eur.-CRS, which has an assigned cefadroxil content of 94.2% on "as is" [16]. Samples of 30 μg of each standard were analysed. Because the standards contained only small amounts of impurities, the total content of impurities was calculated by comparison with the peak area obtained for 0.3 μg of cefadroxil Ph. Eur.-CRS (1% of the main peak). The results are given in Table II. The R.S.D. values, given in parentheses, are within acceptable limits. The LC result for the USP-RS seems to be higher than the declared content. The latter, however, is expressed in μg of activity per mg and not in μg of mass per mg. The sum of cefadroxil, impurities, residual solvents and water

for the USP-RS is close to 100%. Owing to the limited amount of this standard available, the contents of water and residual solvents were not determined.

Analysis of commercial samples

A number of bulk samples of cefadroxil were analysed against the Ph. Eur.-CRS and the results are given in Table III. The R.S.D. on the cefadroxil content did not exceed 1.0%. The total mass was well explained by addition of the content of cefadroxil, impurities and water, except for sample 2, which has the lowest content of cefadroxil. This may be because some of the decomposition products have a lower UV absorbance than cefadroxil at 254 nm.

For comparison, the base content of the bulk samples was determined by non-aqueous titration. Cefadroxil (250 mg) was dissolved in 40 ml of acetic

TABLE IV
CEFADROXIL CONTENT OF PHARMACEUTICALS AS A PERCENTAGE OF LABEL CLAIM

Sample No.	Form	Mean content (% w/w) (<i>n</i> = 4)	R.S.D. (%)
1	Capsules	106.78	0.9
2		104.92	0.4
3	Powder for suspension	111.18	0.8
4		120.90	1.0
5		101.57	0.8
6		111.08	1.3

acid and titrated with 0.1 M perchloric acid using potentiometric end-point detection. Each sample was titrated four times. The results are given in Table III. The total figures are higher for the titration results, which might be due to the presence of impurities carrying a basic function. The content of residual organic solvents was not determined. All the samples complied with Ph. Eur. requirements for content (95.0% on an anhydrous basis) and water (3.0–6.0%).

A few pharmaceutical preparations of the same origin were analysed following the same method. The content was expressed as a percentage of the label claim. The results are given in Table IV.

CONCLUSIONS

The results show that the described LC method is suitable for purity control and assay of bulk samples and of preparations of cefadroxil. Important advantages of the method are its reproducible selectivity and the applicability on PS–DVB stationary phases of different origins and ages.

ACKNOWLEDGEMENTS

The National Fund for Scientific Research (Belgium) is acknowledged for financial support. The gift of samples by the Belgian Ministry of Health and by different manufacturers is gratefully acknowledged. The authors thank A. Decoux and I. Quintens for editorial assistance.

REFERENCES

- 1 M. C. Nahata and D. S. Jackson, *J. Liq. Chromatogr.*, 13 (1990) 1651.
- 2 M. D. Blanchin, H. Fabre and B. Mandrou, *J. Liq. Chromatogr.*, 11 (1988) 2993.
- 3 J. A. McAteer, M. F. Hiltke, B. M. Silber and R. D. Faulkner, *Clin. Chem.*, 33 (1987) 1788.
- 4 S. Ting, *J. Assoc. Off. Anal. Chem.*, 71 (1988) 1123.
- 5 I. Wouters, S. Hendrickx, E. Roets, J. Hoogmartens and H. Vanderhaeghe, *J. Chromatogr.*, 291 (1984) 59.
- 6 R. W. Slingsby and M. Rey, *J. Liq. Chromatogr.*, 13 (1990) 107.
- 7 A. Tsuji, E. Nakashima, Y. Deguchi, K. Nishide, T. Shimizu, S. Horiuchi, K. Ishikawa and T. Yamana, *J. Pharm. Sci.*, 70 (1981) 1120.
- 8 P. G. Welling, A. Selen, J. G. Pearson, F. Kwok, M. C. Rogge, A. Ifan, D. Marrero, W. A. Graig and C. A. Johnson, *Biopharm. Drug Dispos.*, 6 (1985) 147.
- 9 J. Parasrampur and V. Das Gupta, *Drug Dev. Ind. Pharm.*, 16 (1990) 1435.
- 10 "Cefadroxilum", *Pharmeuropa*, 2 (1990) 184.
- 11 *United States Pharmacopeia XXII*, United States Pharmacopoeial Convention, Rockville, MD, 1989.
- 12 J. V. Dawkins, L. L. Llyod, and F. F. Warner, *J. Chromatogr.*, 352 (1986) 157.
- 13 C. Hendrix, J. Thomas, L. M. Yun, E. Roets and J. Hoogmartens, *J. Liq. Chromatogr.*, in press.
- 14 N. H. Khan, P. Wera, E. Roets and J. Hoogmartens, *J. Liq. Chromatogr.*, 13 (1990) 1351.
- 15 J. Paesen, E. Roets and J. Hoogmartens, *Chromatographia*, 32 (1991) 162.
- 16 *European Pharmacopoeia*, Technical Secretariat, Council of Europe, Strasbourg.
- 17 W. W. Wright, *United States Pharmacopeia*, Rockville, MD, personal communication.

Application of a new numerical method for characterizing heterogeneous solids by using gas–solid chromatographic data

M. Heuchel[☆], M. Jaroniec and R. K. Gilpin*

Department of Chemistry, Kent State University, Kent, OH 44242 (USA)

(Received June 17th, 1992)

ABSTRACT

A new numerical method for calculating the adsorption energy distribution function from retention volume data obtained by gas–solid adsorption chromatography is introduced. The method, which considers the ill-posed character of the problem, is applicable to all physico-chemical models that describe the local adsorption on one kind of sites. Using Langmuir and Jovanovic local isotherms the distribution functions are determined for *n*-hexane and 1-hexene on a glass and for cyclohexane and cyclohexene on two silica gels with different pore sizes.

INTRODUCTION

In recent years the problem of finding the distribution of adsorption energies for heterogeneous adsorbents has been considered in detail (see refs. 1 and 2 and references cited therein). The application of gas chromatography (GC) has received a great deal of attention because the technique is an effective method of obtaining information about the interaction of gases with solid surfaces and can be used to collect both temperature- and pressure-dependent data [3]. Although both types of data have been used for evaluating energetic heterogeneity of adsorbents [1,4], pressure-dependent GC measurements appear especially appropriate for calculating the energy distributions of different solids [3,5].

There are two possible ways of using GC for calculating the distribution of adsorption energies.

One of these involves the initial calculation of the adsorption isotherm from retention measurements and then using an analytical or numerical algorithm for evaluating the energy distribution function from the isotherm. Recently, Guiochon and co-workers [6–8] have employed this approach to obtain the energy distributions for different alumina samples. Also, Roles and Guiochon [9–11] have reexamined the procedure of calculating adsorption isotherms and have discussed the precision and accuracy of this procedure. The above approach also has been used by Jagiello and co-workers [12–14] for studying energetic heterogeneity of modified silicas.

The other way of using GC measurements for calculating the energy distribution functions is based on theoretical equations, which relate directly retention volume measurement to the energy distribution. This later approach has a long history. In 1974 Rudzinski *et al.* [15] showed that the energy distribution function could be expressed as a series, which contained derivatives of the retention volume with respect to equilibrium pressure. According to this formulation, a crude approximation of the energy distribution is expressed by the retention volume,

Correspondence to: R. K. Gilpin, Department of Chemistry, Kent State University, Kent, OH 44242, USA.

* Permanent address: Department of Chemistry, Leipzig University, O-7010 Leipzig, Germany.

whereas a better approximation of this distribution is obtained from the first derivative of the retention volume with respect to pressure. Rudzinski *et al.* [15] and later Boudreau and Cooper [16] used the latter more refined approach for calculating the energy distribution function of different solids. In 1976 Suprynowicz *et al.* [17] proposed an integral equation for expressing the overall retention volume in terms of the energy distribution function, which characterizes energetic heterogeneity of solid surfaces. These authors [17] and others [18] used this integral representation to propose simple analytical equations for calculating the energy distribution functions of different modified silicas. These works are discussed in recent monographs by Paryjczak [3] and Jaroniec and Madey [1]. Recently, this integral equation was solved analytically for a γ -type distribution in order to model the pressure dependence [5] and temperature dependence [4] of retention volume on energetically heterogeneous surfaces.

The integral representation of the overall retention volume on energetically heterogeneous surfaces gives a direct relationship between GC measurements and the energy distribution function. Therefore, numerical inversion of this integral with respect to the energy distribution function seems to be a promising approach for evaluating the energetic heterogeneity of different solids on the basis of GC measurements, which has not been discussed in the literature.

The aim of the current work has been to develop a numerical method for inverting the integral equation of the retention volume with respect to the energy distribution. In addition, problems associated with the calculation of the above distribution from GC data (*e.g.*, ill-posed nature of this numerical problem) have been considered. A regularization method [19] has been used for inverting the retention integral equation.

THEORY

One of the fundamental measurable quantity in chromatography is the net specific retention volume, V_N , which is defined as follows:

$$V_N = (V_R - V_M)/w \quad (1)$$

In the above V_R is the corrected retention volume, V_M is the void volume, and w is the adsorbent's mass.

For a heterogeneous surface consisting of L different types of adsorption sites ($l = 1, 2, \dots, L$) the total specific retention volume, $V_{N,t}$, can be represented as a sum

$$V_{N,t} = \sum_{l=1}^L V_{N,l} \quad (2)$$

where $V_{N,l}$ denotes the specific net retention volume of the l th type of adsorption sites. If n_l^0 is the total number of adsorption sites of the l th type, then a new retention volume $V_{N,l}^*$ can be introduced, and the total net specific retention volume rewritten in the following form

$$V_{N,t} = \sum_{l=1}^L n_l^0 V_{N,l}^* = n^0 \sum_{l=1}^L f_l V_{N,l}^* \quad (3)$$

where

$$V_{N,l}^* = V_{N,l}/n_l^0 \quad (4)$$

and

$$f_l = n_l^0/n^0, \quad n^0 = \sum_{l=1}^L n_l^0 \quad (5)$$

In the above n^0 denotes the total number of all adsorption sites and f_l is the fraction of adsorption sites of the l th type. If the total number of types of adsorption sites is large (*i.e.*, $L \rightarrow \infty$) then the summation in eqn. 3 can be replaced by an integration

$$V_{N,t}(p) = n^0 \int_{\varepsilon_m}^{\infty} V_{N,l}^*(p, \varepsilon) F(\varepsilon) d\varepsilon \quad (6)$$

where p is the equilibrium pressure, ε is the adsorption energy, ε_m is the minimum adsorption energy, and $F(\varepsilon)$ is the distribution function of ε normalized to unity:

$$\int_{\varepsilon_m}^{\infty} F(\varepsilon) d\varepsilon = 1 \quad (7)$$

In order to solve the integral eqn. 6 with respect to the energy distribution function $F(\varepsilon)$ it is necessary to assume a model for the local retention, $V_{N,l}^*$. Since adsorption determines retention in gas–solid chromatography, an expression for $V_{N,l}^*$ can be obtained by using the relationship between retention volume and the amount adsorbed, n_l . For an ideal gas the relationship between the total net specific retention volume, $V_{N,t}$, and n_t is given by:

$$V_{N,t}(p) = jRT(\partial n_t / \partial p)_T \quad (8)$$

In the above T is the absolute temperature, R is the universal gas constant and j is the compressibility correction factor [20]. Eqn. 8 is valid for an adsorbate which fulfils the ideal gas law. Since chromatographic measurements are usually carried out for very small amounts of the adsorbate at relatively high temperatures, the mobile phase can be considered as an ideal phase.

For a heterogeneous surface, the total amount adsorbed n_t , is a simple sum of the amounts adsorbed on the l th type of adsorption sites, n_l . If θ_l denotes the relative coverage of adsorption sites of the l th type, then the specific retention volume, $V_{N,i}^*$, defined by eqn. 3 is related to θ_l as follows:

$$V_{N,i}^*(p) = V_{N,i}/n_l^0 = jRT(\partial\theta_l/\partial p)_T \text{ where } \theta_l = n_l/n_l^0 \quad (9)$$

Substitution of eqn. 9 into eqn. 6 gives the relationship between the total net specific retention volume, $V_{N,i}$, and the relative surface coverage $\theta(p, \varepsilon)$:

$$V_{N,i}(p) = jRTn^0 \int_{\varepsilon_m}^{\infty} [\partial\theta(p, \varepsilon)/\partial p]_T F(\varepsilon) d\varepsilon \quad (10)$$

According to eqn. 10 in order to determine $F(\varepsilon)$ it is necessary to know the isotherm $\theta = \theta(p, \varepsilon)_T$, which describes the adsorption of gas molecules on sites with adsorption energy ε . Since the GC sample's concentration is very small, the local adsorption $\theta(p, \varepsilon)$ can be modelled as a monolayer adsorption without lateral interactions. In the current paper, two well known models have been considered: the Langmuir and Jovanovic models.

The Langmuir model describes the case when adsorbed molecules form a localized monolayer without lateral interactions. For this model thermodynamics gives the following expression for the relative surface coverage θ

$$\theta(p, \varepsilon) = \frac{Kp}{1 + Kp} \quad (11)$$

where K is so-called Langmuir constant given by

$$K = K^0(T) \exp(\varepsilon/RT) \quad (12)$$

In the above $K^0(T)$ is the pre-exponential factor, which is the ratio of the partition function of an isolated molecule in the gas and adsorbed phases and thus, it reflects changes in the rotational, vibrational and translational degrees of freedom during the adsorption of an isolated molecule.

Detailed expressions for K^0 are given in a monograph by Clark [21]. In the current calculations a low-temperature approximation for K^0 was used, which according to Ross and Olivier [22] leads to the following equation:

$$K^0 = kT \left(\frac{2\pi m_a kT}{h^2} \right)^{3/2} \quad (13)$$

where m_a is the molecule mass, k is the Boltzmann constant and h is the Planck's constant.

The second local isotherm, proposed by Jovanovic [23], has the following form:

$$\Theta(p, \varepsilon) = 1 - \exp(-Kp) \quad (14)$$

where K is again the Langmuir constant given by eqn. 12. It has been shown elsewhere [1] that at moderate pressure eqn. 14 reduces to the Langmuir eqn. 11. Eqn. 14 has been used in earlier work to describe the local retention, $V_{N,i}^*$ [5].

NUMERICAL PROCEDURE FOR DETERMINING THE ENERGY DISTRIBUTION FUNCTION FROM RETENTION DATA

General considerations

From a mathematical point of view, eqn. 10 is a linear Fredholm integral equation of the first kind, which can be written in a more general form as follows:

$$g(y) = \int_a^b K(x, y) f(x) dx \quad (15)$$

The integral kernel $K(x, y)$ corresponds to the first derivative of the local adsorption isotherm with respect to the pressure $[\partial\theta(p, \varepsilon)/\partial p]_T$ where $\theta(p, \varepsilon)$ represents the physico-chemical model of adsorption on sites with the adsorption energy ε . The function $g(y)$ in eqn. 15 is a known function representing the experimentally measured retention volumes $V_{N,i}(p)$.

Expressions like eqn. 15 also have been derived for the adsorption of gases on energetically heterogeneous surfaces [2, 24, 25] and in microporous heterogeneous solids [1], overall thermodesorption rates [26], gas–solid virial coefficients [27], and liquid–solid adsorption excess quantities [28]. In the last 15 years numerous attempts have been made to calculate $f(x) \equiv F(\varepsilon)$ from experimental data, especially in the field of gas adsorption where the earliest

method, known as the “condensation approximation” (CA-method), was introduced by Roginskij in 1944 [29]. Distribution functions determined by this method are often used in other iterative procedures as a first approximation [1]. Some authors have assumed a-priori the shape of $F(\varepsilon)$, e.g., Gaussian or γ -distribution [1,5], and used these functions to integrate eqn. 10 analytically for local isotherms like the Jovanovic equation. The resulting expressions for the overall retention volume contain free parameters, which can be determined by a numerical least square fit using the experimental $V_{N,t}(p)$ data.

In spite of their elegance, every analytical representation has two main disadvantages: (i) the correct shape of the distribution function is unknown, and (ii) a variety of different analytical distribution functions often can be used to describe experimental data, which usually are measured in a limited region with a insufficient accuracy.

The second case is known as the so-called numerical ill-posedness of the integral eqn. 15, which arises from small changes in $V_{N,t}(p)$, caused by experimental errors, that can influence significantly $F(\varepsilon)$. Likewise, errors generated in numerical calculations or errors arising from the quadrature of the integral eqn. 10 can lead to a similar situation. Thus, the ill-posedness of eqn. 15 is mainly a mathematical numerical problem. Additionally, since the integral kernel contains a theoretical adsorption isotherm, which has only a hypothetical character, the assumed local adsorption model may not accurately represent the experimental observations.

Recommendations for handling numerical instable problems have been made by Tichonov and Arsenin [30,31], who introduced the regularization method. Subsequently, this method was first applied to gas adsorption by House [32] and Merz [33]. A short summary of the developments in regularization methods can be found elsewhere [19]. In the field of gas–solid adsorption chromatography only Roles and Guiochon [6] have mentioned the ill-posed nature of the determination of $F(\varepsilon)$, but their approach assumes the shape of the distribution function and is not a numerical regularization method, which seems to be a better approach to deal with ill-posed problems.

In the current work eqn. 10 will be solved by a regularization method based on the singular value decomposition developed by Von Szombathely [34],

which already has been used successfully to calculate gas adsorption isotherms on energetically heterogeneous surfaces [19].

REGULARIZATION METHOD

Each regularization requires discretization of the integral equation by a quadrature. The integral equation has to be transformed to a system of linear equations

$$g(y) = \int_a^b K(x,y)f(x)dx \Leftrightarrow \mathbf{g} = \mathbf{A}\mathbf{f} \quad (16)$$

where $\mathbf{g} = (g_i)_{1 \dots m}$ is a vector of m experimental data points, $g_i = g(y_i)$. The vector $\mathbf{f} = (f_i)_{1 \dots n}$ represents the unknown function, $f(x)$, with n interpolation nodes in the integration range $[a,b]$. The (m,n) matrix \mathbf{A} contains the product of the kernel-values, $K(x_j, y_i)$, and the corresponding quadrature weights. Such a linear system of equations is commonly solved by minimizing the residual, i.e., the sum of least squares:

$$\text{Min} (\|\mathbf{A}\mathbf{f} - \mathbf{g}\|^2) \quad (17)$$

The idea of regularization is to replace an ill-posed problem by a well-behaved one which smoothes the resulting function and changes the original condition given by eqn. 17 only insignificantly. This can be done by addition of a second minimizing term to eqn. 17 which stabilizes the numerical solution:

$$\text{Min} (\|\mathbf{A}\mathbf{f} - \mathbf{g}\|^2 + \gamma \|\mathbf{W}(\mathbf{f})\|^2) \quad (18)$$

The regularization parameter γ is a measure for the weighting of both terms in eqn. 18. The second term in eqn. 18 is defined as the norm of the function f

$$\|\mathbf{W}(\mathbf{f})\|^2 \approx \int_a^b f^2(t)dt \quad (19)$$

where t is the integration variable.

It was shown [19] that this choice additionally minimizes the residual and suppresses oscillations in the numerical solution. In principle the regularization method still can be improved through inclusion of additional restrictions on the solution, e.g., restriction of the solution to non-negative values (NNLS) [19].

The regularization parameter γ is usually chosen on the basis of a lot of numerical experience. A

detailed description of strategies for finding the optimal γ -value in the case of gas adsorption is given in [19]. Usually, to start a high regularization parameter, e.g., $\gamma = 1$, is assumed, which results in a strongly smoothed distribution function with a residual $\|\mathbf{Af} - \mathbf{g}\|^2$ generally higher than the one calculated from experimental errors. Subsequently γ is reduced until experimental accuracy is reached.

In the current work calculations were carried out using the program INTEG developed by Von Szombathely [19]. This regularization program uses singular value decomposition (SVD) of matrix \mathbf{A} , which represents the discretized operator \mathbf{A} in eqn. 16. The above algebraic technique leads to minimization of numerical errors, fast optimization of the result by choosing different regularization parameters, and allows very often a judgment about the validity of the physico-chemical model of adsorption leading to the operator in eqn. 16.

EXPERIMENTAL

n-Hexane and 1-hexene on a porous glass at 374.2 K

The details of the GC measurements have been given previously [17]. A controlled porosity glass (i.e., 7% Na₂O, 23% B₂O₃ and 70% SiO₂) was prepared from sodium borosilicate glass, and had a BET specific surface area of 50.5 m² g⁻¹ and a particle size distribution between 0.2–0.3 mm. Porosimetric analysis for a similar porous glass [35] gave no indications of the presence of micropores in these types of adsorbents and allowed determination of the pore radius associated with the maximum of the pore size distribution equal to 13.5 nm.

Adsorbates, *n*-hexane and 1-hexene, were of GC purity. The GC measurements were carried out on a Chromatron (GCHF 18.3) gas chromatograph with a thermal conductivity detector. The experimental dependence of the specific retention volume, $V_{N,i}$ on the adsorbate pressure p for *n*-hexane and 1-hexene were measured by the peak maxima elution method [3]. These measurement conditions were chosen in order to minimize dynamic effects.

Cyclohexane and cyclohexene on wide- and narrow-pore silica gel at 400 K

These experimental data are published in ref. 36. The wide-pore silica gel (the particle fraction of 0.20–0.39 mm) and the narrow-pore silica gel (the

particle fraction of 0.15–0.20 mm) had BET specific surface areas as measured by nitrogen adsorption of 35 m² g⁻¹ and 180 m² g⁻¹, respectively. Analysis of the pore-size distribution leads to the average pore radii of 2 nm for the narrow-pore silica gel and 14 nm for the wide-pore silica. The bulk density measured with helium were 2.1 g cm⁻³ for the wide-pore silica and 2.5 g cm⁻³ for the narrow-pore silica gel. The solutes cyclohexane and cyclohexene were purified by using a 5 Å molecular sieve. The measurements of the $V_{N,i}(p)$ data were carried out with the chromatograph described above.

RESULTS AND DISCUSSION

The adsorption energy distribution functions were calculated using all of the data points shown in Fig. 1. Summarized in Table I are the number of data points, the lowest (p_{\min}) and highest (p_{\max}) pressures and the standard deviation of the fit between actual data and calculated data using the energy distribution obtained by solving eqn. 10 with INTEG and by assuming the Jovanovic equation for the local adsorption.

The numerical determination of $F(\epsilon)$ with INTEG has the general advantage that there is no limitation concerning the chosen local isotherm and thus, very complicated (non-analytical) local isotherms can in principle be used. As mentioned earlier, in GC the sample concentrations are small and the retention can be represented by equations associated with simple adsorption models as those proposed by Langmuir and Jovanovic. To illustrate how the particular model influences $F(\epsilon)$, Fig. 2 shows the distribution functions of the adsorption energy $F(\epsilon)$ for *n*-hexane on the porous glass calculated by assuming the Langmuir model (eqn. 11) and the Jovanovic model (eqn. 14). For the same regularization parameter $\gamma = 0.1$ the general shape and the location of the peak maxima are in close agreement for both models. However, since the Jovanovic local isotherm seems to have better smoothing properties, as can be seen in the energy range about 25 kJ/mol, this model was chosen to carry out all additional calculations. Further, the choice of the Jovanovic equation to represent the local isotherm is consistent with approaches often used in the theory of GC [5].

The distribution function $F(\epsilon)$ also is influenced by the pre-exponential factor K^0 . The determination

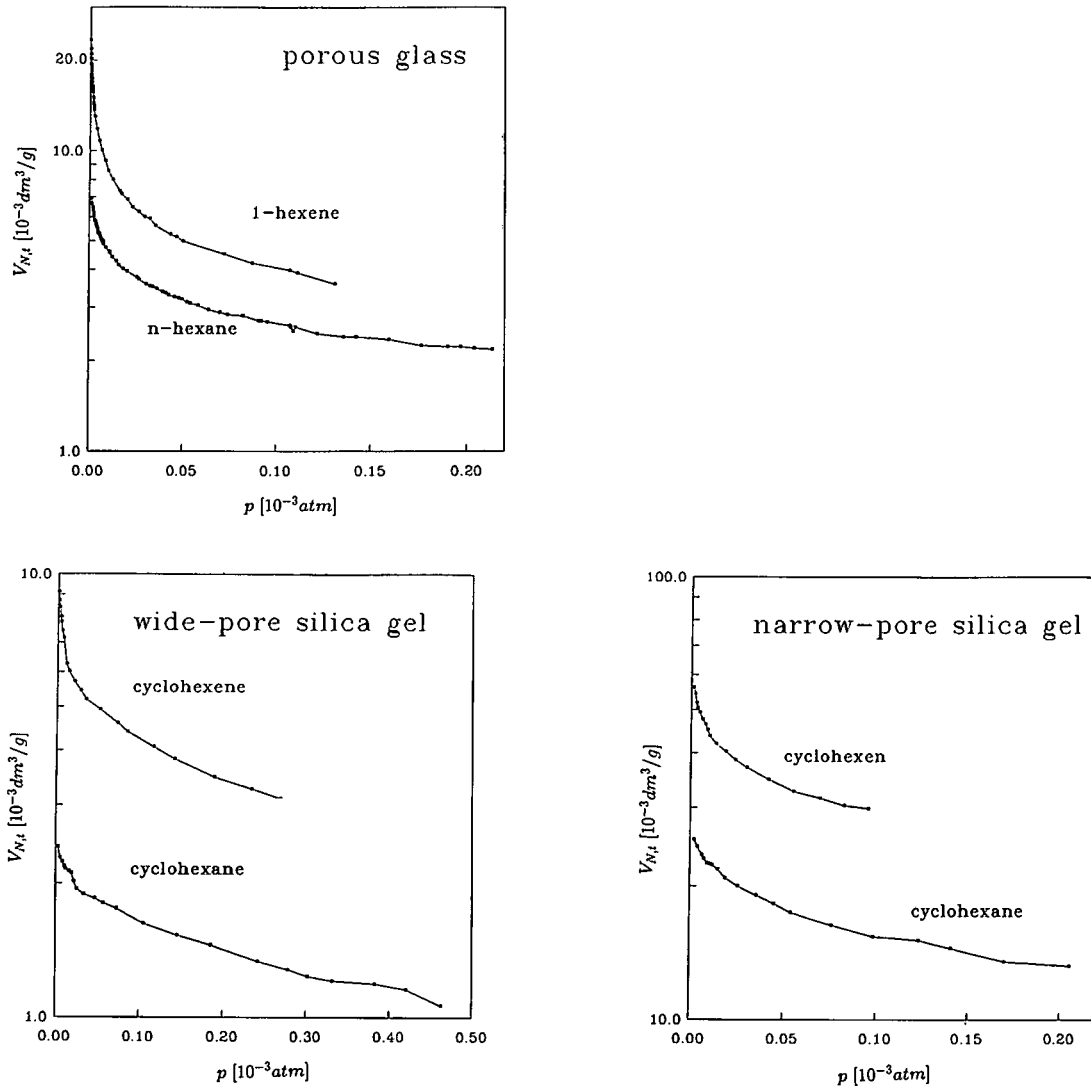


Fig. 1. $\ln V_{N,t}$ vs. p representation for the experimental systems studied.

of K^0 has received considerable attention in the literature [1,2,21]. The calculation of K^0 on the basis of pure statistical thermodynamics requires the approximation of the partition functions for molecules in the mobile and stationary phases. Especially for organic vapors typically used in GC experiments, the theoretical calculation of the partition function is often complicated. Simpler methods for determining K^0 refer only to simple gases and low temperatures. An alternative way of calculating K^0

values is from measurements of solute retention at different temperatures [35].

The influence of the pre-exponential factor K^0 on the distribution function $F(\epsilon)$ calculated from chromatographic data using INTEG is shown in Fig. 3. The solid line represents the distribution function for *n*-hexane on porous glass using K^0 calculated according to eqn. 13. The dotted and dashed lines show $F(\epsilon)$ calculated for values of K^0 differing by one order of magnitude from that obtained by

TABLE I
INFORMATION ABOUT EXPERIMENTAL SYSTEMS

Experimental system	T (K)	p_{\min} (atm · 10 ³)	p_{\max} (atm · 10 ³)	Number of points used	Standard deviation (eqn. 10)
<i>n</i> -Hexane/glass	374	0.92	213.3	67	±0.02
1-Hexene/glass	374	0.14	131.3	45	±0.14
Cyclohexane/wide-pore silica	400	2.77	462.3	23	±0.02
Cyclohexane/narrow-pore silica	400	1.82	205.3	19	±0.10
Cyclohexene/wide-pore silica	400	0.91	268.2	20	±0.04
Cyclohexene/narrow-pore silica	400	0.91	95.3	18	±0.20

means of eqn. 13. All functions are very similar in shape but they are shifted 2 kJ/mol on the energy axis. The same tendency also was observed by calculating $F(\epsilon)$ from adsorption isotherms for different values of K^0 . Since obviously the pre-exponential factor did not change the shape of $F(\epsilon)$, eqn. 13 was used to evaluate K^0 .

The energy distributions for both *n*-hexane and 1-hexene on porous glass show only one peak. It follows from Fig. 4 that the specific interaction of 1-hexene with the surface of the adsorbent is greater than *n*-hexane. The maximum of the adsorption

energy distribution is approximately 32 kJ/mol for 1-hexene which is nearly 10 kJ/mol higher than the maximum of $F(\epsilon)$ for *n*-hexane. Jaroniec *et al.* [5] derived an analytical equation for $V_{N,t}$ assuming the Jovanovic local isotherm and a γ -type distribution for $F(\epsilon)$. The authors applied this equation to the same experimental data and obtained exponential type distribution functions with peak maxima at 23 kJ/mol and 33 kJ/mol, respectively, for *n*-hexane and 1-hexene. These values and the difference in the adsorption energies are in very good agreement with current pure “numerical” results using the regular-

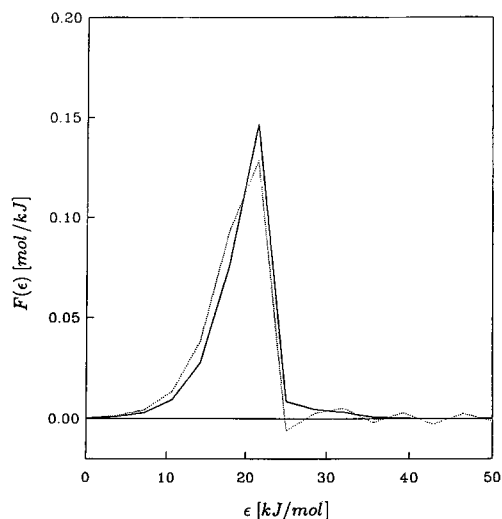


Fig. 2. Comparison of the distribution functions of the adsorption energy $F(\epsilon)$ for *n*-hexane on porous glass calculated with INTEG using the Jovanovic (solid line) and Langmuir (dotted line) local isotherm models.

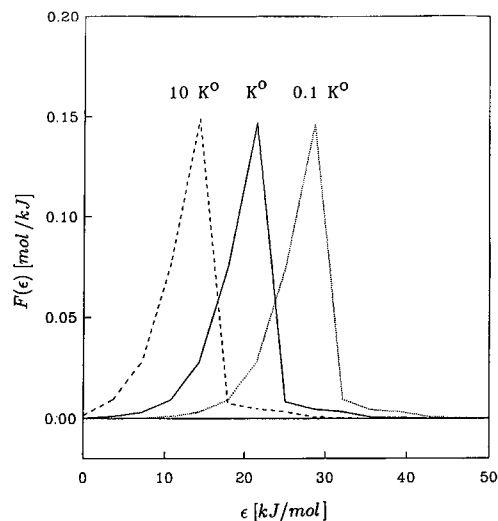


Fig. 3. Dependence of the numerically calculated distribution function on the value of the pre-exponential factor K^0 in the Jovanovic local isotherm for *n*-hexane on porous glass.

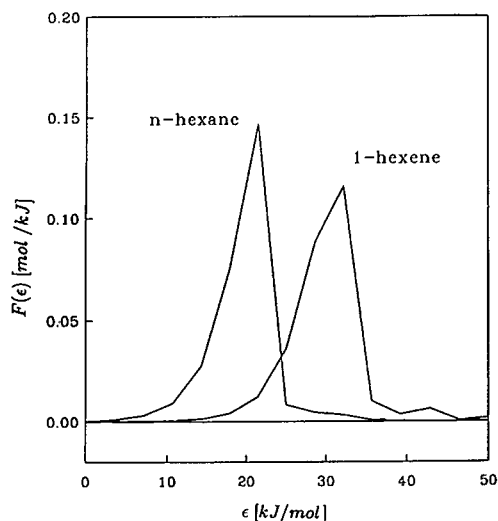


Fig. 4. Distribution functions of the adsorption energy $F(\epsilon)$ for *n*-hexane and 1-hexene on controlled porous glass. The calculations were carried out with INTEG using the Jovanovic local isotherm model and a constant regularization parameter $\gamma = 0.01$.

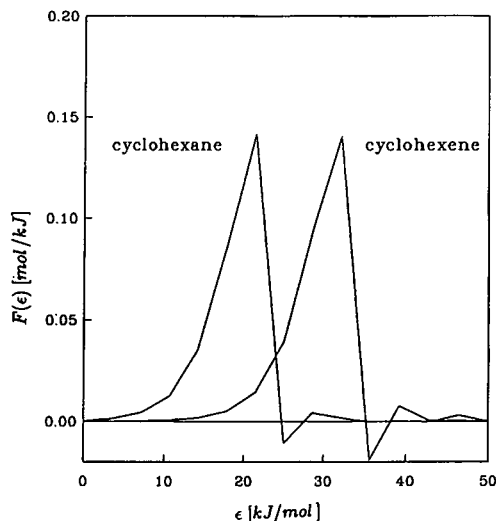


Fig. 6. Distribution functions of the adsorption energy $F(\epsilon)$ for cyclohexane and cyclohexene on narrow-pore silica gel calculated with INTEG (for details see Fig. 4).

ization method. However, the present method gives a better representation of the lower-energy part of the $F(\epsilon)$ -function, which was not predicted by the analytical method.

Figs. 5 and 6 show the calculated distribution functions for cyclohexane and cyclohexene on wide-

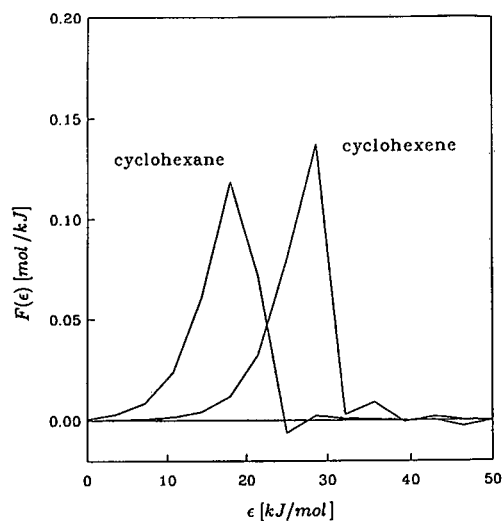


Fig. 5. Distribution functions of the adsorption energy $F(\epsilon)$ for cyclohexane and cyclohexene on wide-pore silica gel calculated with INTEG (for details see Fig. 4).

and narrow-pore silica gels. For both adsorbents cyclohexene was more strongly adsorbed than cyclohexane. For cyclohexane and cyclohexene on wide-pore silica gel the adsorption energies associated with the maxima in the distribution $F(\epsilon)$ were 18 and 28 kJ/mol, respectively. However, for the narrow-pore adsorbent these values were slightly higher, 21 and 32 kJ/mol. These results are consistent with greater interactions (*i.e.*, about 10–11 kJ/mol in the adsorption energy) which arises from the double bond in cyclohexene. Similarly, this trend is in good agreement with the double bond contribution of 1-hexene in comparison to *n*-hexane on porous glass. Further the current result indicates the observed π -electrons effects are similar between the silica gels and the porous glass.

The influence of the pore-size on the adsorption behavior can be seen by a comparison of the distribution functions for cyclohexane on the wide- and narrow-pore silicas shown in Fig. 7. For the narrow-pore silica gel the distribution function $F(\epsilon)$ is slightly sharper and the maximum of the distribution is shifted approximately 3 kJ/mol to higher values of ϵ (4 kJ/mol for cyclohexane). The 3–4 kJ/mol increase in ϵ can be attributed to either the presence of fine pores in the narrow-pore silica gel, or a difference in surface composition. Although

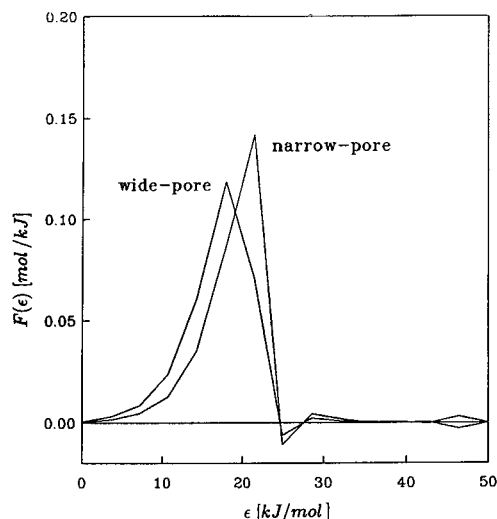


Fig. 7. Comparison of the distribution functions $F(\epsilon)$ for cyclohexane on wide- and narrow-pore silica gel (for details see Fig. 4).

neither of these can be ruled out, it seems more possible that pore structure may play a larger role.

CONCLUSIONS

The numerical regularization method INTEG is a useful procedure for determining the distribution function of the adsorption energy from gas chromatographic measurements. A comparison of the shapes of $F(\epsilon)$ curves calculated for different systems provides information about the interaction of solute molecules with solid surfaces. Studies of relative changes in the $F(\epsilon)$ functions should be useful for analyzing surface treatments of adsorbents and chromatographic packings, e.g., activation and chemical modification of adsorbents and stationary phases for GC.

ACKNOWLEDGEMENT

This work was supported by US Army Research Office Grant DAAL03-90-G-0061.

REFERENCES

- M. Jaroniec and R. Madey, *Physical Adsorption on Heterogeneous Solids*, Elsevier, Amsterdam, 1988.
- W. Rudzinski and D. H. Everett, *Adsorption of Gases on Heterogeneous Surfaces*, Academic Press, New York, 1991.
- T. Paryjczak, *Gas Chromatography in Adsorption and Catalysis*, Ellis Horwood, Chichester, 1986.
- R. K. Gilpin, M. Jaroniec and M. B. Martin-Hopkins, *J. Chromatogr.*, 513 (1990) 1.
- M. Jaroniec, X. Lu and R. Madey, *J. Phys. Chem.*, 94 (1990) 5917.
- J. Roles and G. Guiochon, *J. Phys. Chem.*, 95 (1991) 4098.
- J. Roles, K. McNerney and G. Guiochon, *Anal. Chem.*, 64 (1992) 25.
- J. Roles and G. Guiochon, *Anal. Chem.*, 64 (1992) 32.
- J. Roles and G. Guiochon, *J. Chromatogr.*, 591 (1992) 233.
- J. Roles and G. Guiochon, *J. Chromatogr.*, 591 (1992) 245.
- J. Roles and G. Guiochon, *J. Chromatogr.*, 591 (1992) 267.
- J. Jagiello, G. Ligner and E. Papirer, *J. Colloid Interface Sci.*, 137 (1990) 128.
- E. Papirer, S. Li, H. Balard and J. Jagiello, *Carbon*, 8 (1991) 1135.
- I. Tjiburg, J. Jagiello, A. Vidal and E. Papirer, *Langmuir*, 7 (1991) 2243.
- W. Rudzinski, A. Waksmundzki, R. Lebeda and Z. Suprynowicz, *J. Chromatogr.*, 92 (1974) 25.
- S. P. Boudreau and W. T. Cooper, *Anal. Chem.*, 59 (1987) 353.
- Z. Suprynowicz, M. Jaroniec and J. Gawdzik, *Chromatographia*, 9 (1976) 161.
- R. Lebeda and S. Sokolowski, *J. Colloid Interface Sci.*, 61 (1977) 365.
- M. von Szombathely, P. Bräuer and M. Jaroniec, *J. Comp. Chem.*, 13 (1992) 17.
- J. R. Conder and J. H. Prunell, *Trans. Faraday Soc.*, 64 (1968) 3100.
- A. Clark, *The Theory of Adsorption and Catalysis*, Academic Press, New York, 1970.
- S. Ross and J. P. Olivier, *On Physical Adsorption*, Interscience, New York, 1964.
- D. S. Jovanovic, *Kolloid Z. Polym.*, 235 (1969) 1203.
- A. W. Adamson, *Physical Chemistry of Surfaces*, Wiley, New York, 1990.
- A. W. Adamson and I. Ling, *Adv. Chem. Ser.*, 33 (1961) 51.
- J. A. Britten, B. J. Travis and L. F. Brown, *AIChE Symp. Ser.*, 79 (1983) 7.
- A. Waksmundzki, S. Sokolowski and W. Rudzinski, *Z. Phys. Chem.*, 257 (1976) 833.
- A. Drabrowski, M. Jaroniec and J. Oscik, *Surface Colloid Sci.*, 14 (1987) 83.
- S. S. Roginskij, *Dokl. Akad. Nauk SSSR*, 61 (1944) 194.
- A. N. Tichonow, *Dokl. Akad. Nauk SSSR*, 39 (1943) 195.
- A. N. Tichonow and V. Ja. Arsenin, *Metody resenija nekorrektnych zadacz*, Nauka, Moskov, 1979.
- W. A. House, *J. Colloid Interface Sci.*, 67 (1978) 166.
- P. H. Merz, *J. Comput. Phys.*, 38 (1980) 64.
- M. von Szombathely, *Ph. D. Thesis*, Leipzig University, Leipzig, 1988.
- J. Gawdzik, Z. Suprynowicz and M. Jaroniec, *J. Chromatogr.*, 121 (1976) 185.
- A. Waksmundzki, W. Rudzinski, Z. Suprynowicz, R. Lebeda and M. Lason, *J. Chromatogr.*, 92 (1974) 9.

Calculation of retention indices by molecular topology

III[☆]. Chlorinated dibenzodioxins

Sanja Sekušak and Aleksandar Sabljčić

Institute Ruđer Bošković, Bijenička 54, P.O. Box 1016, 41001 Zagreb (Croatia)

(First received May 14th, 1992; revised manuscript received August 28th, 1992)

ABSTRACT

A model is developed, based entirely on chemical structure, for the accurate prediction of the retention of chlorinated dibenzodioxins (PCDDs) on a non-polar stationary phase (DB-5) and for reproducing their experimental elution sequence. The first-order molecular connectivity index ($^1\chi$) and six other topological properties, the specific mono-, di- and trichloro substitution patterns, were used as structural descriptors. Thus, one can predict the retention index for any given PCDD having only a knowledge of its chlorine substitution pattern. The agreement between observed and calculated retention indices (the average residual of 1.8 units) indicates that this model works fairly well to describe the retention indices of all analysed PCDDs (37 tetra- to octachlorinated congeners). The developed model was successfully validated by extrapolation on a small set of retention indices determined for di- and trichlorinated PCDD congeners and by interpolation on a set of sixteen retention indices determined for tetra- to octachlorinated PCDDs on a low-polarity HP-5 capillary column. The regression analysis shows that the PCDD retention indices are primarily influenced by their bulk properties, *i.e.*, the size of these molecules. This property, described best by the $^1\chi$ index, accounts for more than 97% of the variation in the retention index data. The other factors that control the magnitude of the retention indices are various chlorine substitution patterns, having either a positive or a negative effect on the magnitude of the retention indices. Finally, a mechanism for the interaction of PCDDs with the non-polar stationary phase is also discussed.

INTRODUCTION

Polychlorinated dibenzodioxins (PCDDs) are xenobiotic contaminants of great concern [1]. Owing to their persistence in the environment, they can be transported over long distances and they are widespread contaminants in the atmospheric and aquatic ecosystems. Residues of polychlorinated dibenzodioxins are found in most organisms sampled in natural aquatic and terrestrial environments. In addition, high toxicity has been associated with many of the individual congeners in these series. As a result, many countries monitor chlorinated dibenzodioxins in the environment. Despite considerable ef-

forts during the last decade, analytical standards are still needed for many of the 75 dioxin congeners. Isomer-specific measurement information is necessary because of the major toxicological differences between individual congeners. Hence it would be very helpful to have a structural model that can predict the retention indices of any particular isomer. Such a method would be useful for identifying chlorinated dioxins found during environmental monitoring efforts.

Many investigators have noted [2] a very good correlation between the experimental retention indices and structural characteristics of molecules by either the application of DARC topological system [3–6] or topological indices such as molecular connectivity indices [2,7–13] and Wiener numbers [2,12,14–16]. Previously, we have demonstrated that the molecular connectivity model [17,18] suc-

Correspondence to: A. Sabljčić, Institute Ruđer Bošković, Bijenička 54, P.O. Box 1016, 41001 Zagreb, Croatia.

* For Part II, see ref. 20.

cessfully predicts gas chromatographic (GC) retention indices (I) and elution sequences of series of chlorinated alkanes [19] and chlorinated benzenes [20] on non-polar and polar stationary phases. As a continuation of our research on harmful organochlorine compounds in the environment [21–24], this paper reports on the ability of a molecular connectivity model to describe, in quantitative terms, the GC retention behaviour of PCDDs on a non-polar DB-5 capillary column. The ring structure of polychlorinated dibenzodioxins and the numbering scheme for available chlorination positions are shown in Fig. 1.

In this study, models based on the molecular characteristics of PCDDs will be developed for calculating GC retention indices and for predicting elution sequences of PCDDs. The molecular connectivity indices, which are calculated exclusively on the basis of information such as the number and type of atoms and bonds and the number of all electrons and valence electrons in each non-hydrogen atom, will be used as molecular descriptors. Such data are readily available for all chemicals, synthesized or hypothetical, from their structural formulae and from the Periodic Table. In addition, if necessary, other simple topological properties, such as the presence or absence of particular structural features, may also be tested as potential molecular descriptors. As in our earlier studies [19,20], two criteria will be used to test the quality of fit between observed and calculated retention indices: (i) a very high correlation coefficient and (ii) the correctly predicted elution sequence.

METHOD OF CALCULATION

Several extensive reviews of the theory and method of calculation of molecular connectivity indices have been published [17,18,25–27]. Therefore, only a description of the calculation of the first-order molecular connectivity index used in this study is

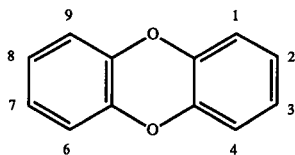


Fig. 1. Structural formula of substituted dibenzodioxins.

given here. Information used in the calculation of molecular connectivity indices is the number and type of atoms and bonds in a molecule and the numbers of all electrons and valence electrons in each non-hydrogen atom. These data are readily available for all chemicals, synthesized or hypothetical, from their structural formulae and the Periodic Table. All molecular connectivity indices are calculated for the non-hydrogen part of the molecule. In the non-valence approximation each non-hydrogen atom is described by its atomic δ value, which is equal to the number of adjacent non-hydrogen atoms. The first-order molecular connectivity index (${}^1\chi$) is calculated from the atomic δ values by the equation:

$${}^1\chi = \sum (\delta_i \delta_j)^{-0.5} \quad (1)$$

where i and j correspond to the pairs of adjacent non-hydrogen atoms and the summation is over all bonds between non-hydrogen atoms. The ${}^1\chi$ index has been used extensively in various quantitative structure–property relationship (QSPR) and quantitative structure–activity relationship (QSAR) studies [17,18,25–27]. It has been found in several studies [21,22,28] that this index correlates extremely well with the molecular surface for various classes of chemicals and consequently correlates well with most of molecular surface-dependent properties and processes.

Other structural descriptors, *i.e.*, the presence of a specific substitution pattern, used in this study are the following: the number of *meta* chlorine substituents (Cl_M), the number of pairs of *ortho/meta* chlorine substituents (Cl_{OM}), the number of pairs of chlorine substituents in positions 1 and 3 or analogous relative positions (Cl_{13}), the number of pairs of chlorine substituents in positions 1 and 4 or analogous relative positions (Cl_{14}), the number of sequences of three consecutive chlorine substituents (Cl_{SEQ3}) and the simultaneous presence of chlorine substituents in positions 1 and 9 or 4 and 6 (Cl_{OCI}). All possible combinations of substituents for those structural descriptors are listed below:

Cl_M : substituents on positions 2, 3, 7 and 8;

Cl_{OM} : pairs of substituents on positions 1–2, 3–4, 6–7 and 8–9;

Cl_{13} : pairs of substituents on positions 1–3, 2–4, 6–8 and 7–9;

Cl_{14} : pairs of substituents on positions 1–4 and 6–9;

Cl_{SEQ3}: sequences of substituents on positions 1–2–3, 2–3–4, 6–7–8 and 7–8–9;

CIOCI: pairs of substituents on positions 1–9 and 4–6.

The numbering scheme for chlorine substituents is presented in Fig. 1. The *ortho* and *meta* positions of chlorine substituents are defined relative to the ring oxygen atoms. All variables, except the CIOCI variable, have an identical and linear weights system. Thus, for each occurrence of a specific substitution pattern the corresponding variable increases by 1. For the CIOCI variable, the presence of one pair of substituents has a weight of 1 and the presence of two pairs of substituents has a weight of 1.5. The non-linear weights for the CIOCI variable are based on earlier experimental findings [29].

The molecular connectivity indices used in this study were calculated with the GRAPH III computer program for microcomputers on an Apple Macintosh SE/30 personal computer. [The GRAPH III program is now fully operational and it is distributed by MacAda, Apple Center Ljubljana, Parmova 41, 61000 Ljubljana, Slovenia. Tables of molecular connectivity indices (up to 6th order), other structural variables and retention indices (measured and/or predicted) for 75 chlorinated dibenzodioxins may be obtained on diskette (Macintosh or IBM PC format) at a small cost from the corresponding author.] The GRAPH III computer program can calculate molecular connectivity indices up to the tenth order for the molecules with 36 non-hydrogen atoms or less. Regression analysis was carried out using a statistical analysis system (SYSTAT, version 5.0) on an Apple Macintosh SE/30 personal computer. To test the quality of the generated regression equation, the following statistical parameters were used: the correlation coefficient (r), the standard error of estimate (s), a test of the null hypothesis (F -test) and the amount of explained variance (EV).

The I values used in this study were taken from a study by Donnelly *et al.* [29]. A Hewlett-Packard Model 5880A gas chromatograph equipped with a flame ionization detector was used with a 60 m × 0.252 mm I.D. (0.25 μm film thickness) DB-5 fused-silica capillary column (J & W Scientific, Rancho Cordova, CA, USA) to determine the retention indices of available PCDDs. The gas chromatograph was programmed from 170 to 340°C at 2°C/min

with an initial hold of 1 min. Helium was used as the carrier gas with a flow-rate at 340°C of 20.2 cm/s. C₂₀–C₄₄ *n*-alkanes were used to measure retention indices.

RESULTS

A list of 37 polychlorinated dibenzodioxins (PCDDs) with four to eight chlorine substituents is shown in Table I together with their I values, the first-order molecular connectivity indices and other structural descriptors.

By modelling the retention behaviour of chlorinated alkanes [19] and chlorinated benzenes [20], we found that the combination of global and local structural descriptors is needed to describe their elution sequences correctly. It was reasonable to assume that a similar combination of structural properties will also be important for chromatographic behaviour of PCDD congeners. Therefore, we concentrated our initial search for structural descriptors on molecular connectivity indices and other parameters that describe primarily the size of molecules. The single-variable linear models were calculated for the simple and valence zero- and first-order molecular connectivity indices, molecular mass of the PCDDs, the number of non-hydrogen atoms and bonds, plus the sums of ${}^0\chi$ and ${}^0\chi^v$ or ${}^1\chi$ and ${}^1\chi^v$ indices. The first-order molecular connectivity index (${}^1\chi$) was found the most successful (correlation coefficient 0.988). The same index was also found to be the most successful in describing the chromatographic behaviour of chlorinated benzenes on a non-polar stationary phase [20]. However, as all other global structural descriptors also exhibit very high correlations with the PCDD retention indices, we decided to continue the modelling process with the ${}^1\chi$ index, as the most promising global descriptor, and to re-evaluate the successful model with other global structural descriptors listed above. Most of the calculated connectivity indices were unavailable for statistical evaluation in the multivariable models with the ${}^1\chi$ index because they intercorrelate strongly. Therefore, additional structural variables, describing the presence of specific substitution patterns such as the number of *ortho* and *meta* chlorine substituents, the number and types of pairs of chlorine substituents and the presence of longer sequences of adjacent chlorine sub-

TABLE I

MEASURED RETENTION INDICES (*I*) FOR 37 CHLORINATED DIBENZODIOXIN DERIVATIVES (PCDDs)

The values of the structural descriptors ($^1\chi$, Cl_M , Cl_{OM} , Cl_{13} , Cl_{14} , Cl_{SEQ3} , ClOCl) used in the modelling procedure are also listed.

Compound	<i>I</i>	$^1\chi$	Cl_M	Cl_{OM}	Cl_{13}	Cl_{14}	Cl_{SEQ3}	ClOCl
1234-PCDD	2379	8.592	2	2	2	1	2	0
1236-PCDD	2378	8.575	2	1	1	0	1	0
1237-PCDD	2382	8.559	3	1	1	0	1	0
1238-PCDD	2382	8.559	3	1	1	0	1	0
1239-PCDD	2392	8.575	2	1	1	0	1	1
1246-PCDD	2346	8.575	1	1	1	1	0	1
1247-PCDD	2340	8.559	2	1	1	1	0	0
1248-PCDD	2340	8.559	2	1	1	1	0	0
1249-PCDD	2346	8.575	1	1	1	1	0	1
1267-PCDD	2408	8.575	2	2	0	0	0	0
1268-PCDD	2349	8.559	2	1	1	0	0	0
1269-PCDD	2378	8.575	1	1	0	1	0	1
1278-PCDD	2400	8.559	3	1	0	0	0	0
1279-PCDD	2364	8.559	2	1	1	0	0	1
1289-PCDD	2428	8.575	2	2	0	0	0	1
1368-PCDD	2290	8.542	2	0	2	0	0	0
1369-PCDD	2315	8.559	1	0	1	1	0	1
1378-PCDD	2340	8.542	3	0	1	0	0	0
1379-PCDD	2304	8.542	2	0	2	0	0	1
1469-PCDD	2341	8.575	0	0	0	2	0	1.5
1478-PCDD	2353	8.559	2	0	0	1	0	0
2378-PCDD	2386	8.542	4	0	0	0	0	0
12347-PCDD	2573	8.986	3	2	2	1	2	0
12367-PCDD	2604	8.986	3	2	1	0	1	0
12378-PCDD	2587	8.969	4	1	1	0	1	0
12389-PCDD	2623	8.986	3	2	1	0	1	1
12468-PCDD	2501	8.969	2	1	2	1	0	1
12479-PCDD	2501	8.969	2	1	2	1	0	1
123467-PCDD	2812	9.414	3	3	2	1	2	1
123468-PCDD	2742	9.397	3	2	3	1	2	1
123478-PCDD	2781	9.397	4	2	2	1	2	0
123678-PCDD	2788	9.397	4	2	2	0	2	0
124679-PCDD	2713	9.397	2	2	2	2	0	1.5
124689-PCDD	2713	9.397	2	2	2	2	0	1.5
1234678-PCDD	2994	9.824	4	3	3	1	3	1
1234679-PCDD	2949	9.824	3	3	3	2	2	1.5
12346789-PCDD	3196	10.252	4	4	4	2	4	1.5

stituents, were tested in multivariate regression analysis. The simultaneous presence of two chlorine substituents in either positions 1 and 9 or positions 4 and 6 (Fig. 1) was also found [29] to have a large influence on the resulting *I* values of PCDD congeners. Therefore, a structural descriptor describing this particular substitution patterns was also tested in multivariate regression analysis. All these specific structural descriptors are shown in Fig. 2 for octachlorodibenzodioxin.

To generate the experimental elution sequence for all 37 PCDD congeners, seven-variable regression equation was necessary. The following structural descriptors have been found to be important in a multiple linear regression with the $^1\chi$ index: the number of *meta* chlorine substituents (Cl_M), the number of pairs of *ortho/meta* chlorine substituents (Cl_{OM}), the number of pairs of chlorine substituents in positions 1 and 3 or analogous relative positions (Cl_{13}), the number of pairs of chlorine substituents

in positions 1 and 4 or analogous relative positions (Cl_{14}), the number of sequences of three consecutive chlorine substituents (Cl_{SEQ3}), and the simultaneous presence of chlorine substituents in positions 1 and 9 or positions 4 and 6 (Cl_{IOCl}). All variables are statistically significant above the 99.95% level (Student's *t*-test).

$$I = -1580.2 + 457.5^1\chi + 14.8Cl_M + 19.9Cl_{OM} - 35.4Cl_{13} - 12.9Cl_{14} + 22.1Cl_{SEQ3} + 15.3Cl_{IOCl} \quad (2)$$

$N = 37, r = 1.000, s = 3.2, F^{7,29} = 26\ 016, EV = 100\%$

The statistical parameters show that eqn. 2 is statistically significant above the 99.9% level and it accounts for all of the variation in the *I* data. It is also very accurate in calculating *I* data of PCDDs and the average residual of calculated values was only 2.4 units. This topological model was also effective in predicting the correct elution sequence for all 37 PCDD congeners. However, the residual analysis shows that 1,2,3,8,9-PCDD, 1,2,3,4,6,7-PCDD and octachlorodibenzodioxin are outliers which exert an undue influence on the regression

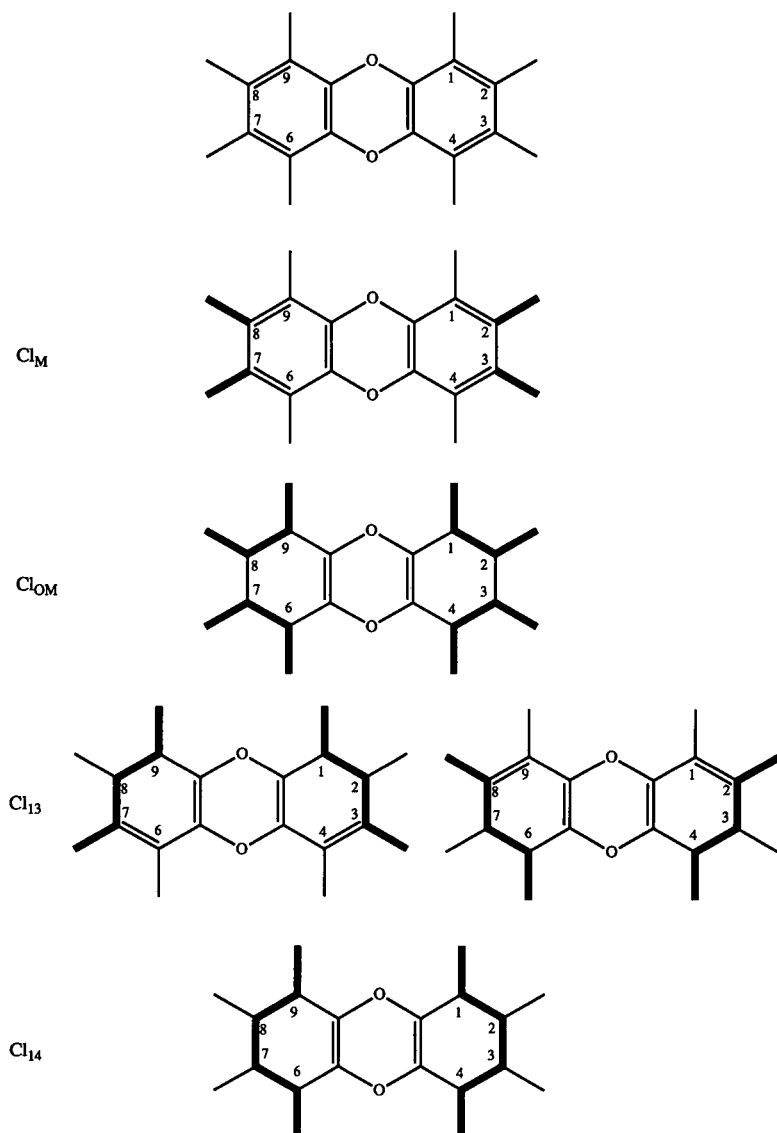


Fig. 2.

(Continued on p. 74)

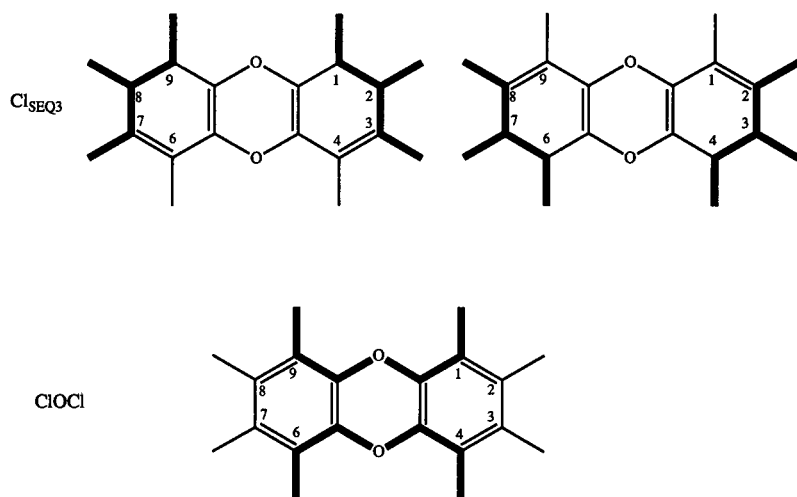


Fig. 2. Structural formulae of octachlorodibenzodioxin with outlined specific substitution patterns, used in this study as local structural descriptors: the four *meta* chlorine substituents (Cl_M), the four pairs of *ortho* and *meta* chlorine substituents (Cl_{OM}), the four pairs of chlorine substituents in positions 1 and 3 or analogous relative positions (Cl_{13}), the two pairs of chlorine substituents in positions 1 and 4 or analogous relative positions (Cl_{14}), the four sequences of three consecutive chlorine substituents (Cl_{SEQ3}), and the simultaneous presence of chlorine substituents in positions 1 and 9 or 4 and 6 ($ClOCl$).

model since their I values are all underestimated by 3.6–6.2 units. Eliminating them from the regression analysis resulted in an improved correlation and also in a statistically more reasonable and meaningful quantitative model described by eqn. 3 and its statistical parameters:

$$I = -1586.4 + 458.4^1\chi + 14.3Cl_M + 19.1Cl_{OM} - 34.9Cl_{13} - 12.5Cl_{14} + 21.3Cl_{SEQ3} + 13.5ClOCl$$

$$N = 34, r = 1.000, s = 2.4, F^{7,26} = 29\,350, \quad (3)$$

$$EV = 100\%$$

Eqn. 3 is also very accurate in calculating I data of PCDDs and in predicting their correct elution sequence. The average residual of calculated values is now only 1.8 units. The high accuracy of the molecular connectivity model in predicting the I values of PCDDs is also shown in Fig. 3, where the observed vs. predicted (eqn. 3) retention indices are plotted.

Because of its high statistical significance and ability to explain all variations in the measured retention indices, the developed model (eqn. 3) was used to estimate the I values for the PCDD congeners with two to six chlorine substituents whose GC retention data have not yet been measured. The results are presented in Table II.

The experimental control of the predicted I values of several selected PCDDs with different degrees of chlorination should afford a constructive challenge to the molecular topology approach and the quantitative model described by eqn. 3.

Finally, an attempt was made to test the other

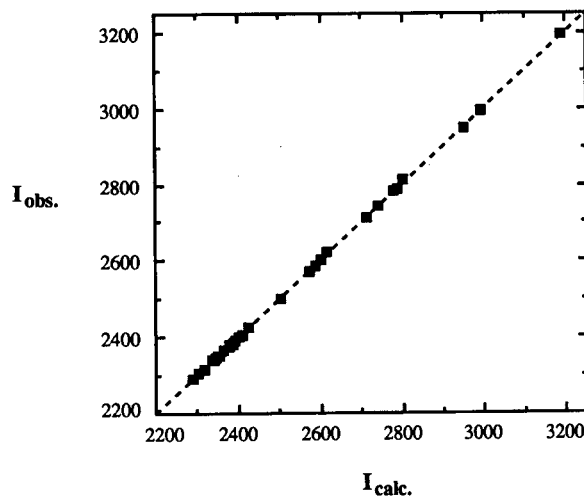


Fig. 3. Plot of calculated vs. observed retention indices of 37 PCDDs shown in Table I. The broken line corresponds to the molecular connectivity model, eqn. 3.

TABLE II

CALCULATED RETENTION INDICES (I) FOR 36 CHLORINATED DIBENZODIOXIN DERIVATIVES (PCDDs) WITH TWO TO SIX CHLORINE SUBSTITUENTS BY THE MOLECULAR TOPOLOGY MODEL, (EQN. 3)The values of the structural descriptors (${}^1\chi$, Cl_M , Cl_{OM} , Cl_{13} , Cl_{14} , Cl_{SEQ3} , $ClOCl$) used in the estimation procedure are also listed.

Compound	I_{CALC}	${}^1\chi$	Cl_M	Cl_{OM}	Cl_{13}	Cl_{14}	Cl_{SEQ3}	$ClOCl$
13-PCDD	1940	7.737	1	0	1	0	0	0
14-PCDD	1956	7.754	0	0	0	1	0	0
16-PCDD	1968	7.754	0	0	0	0	0	0
17-PCDD	1975	7.737	1	0	0	0	0	0
18-PCDD	1975	7.737	1	0	0	0	0	0
27-PCDD	1981.4 ^a	7.720	2	0	0	0	0	0
28-PCDD	1981.4 ^a	7.720	2	0	0	0	0	0
19-PCDD	1982	7.754	0	0	0	0	0	1
23-PCDD	1989 ^a	7.737	2	0	0	0	0	0
12-PCDD	2002	7.754	1	1	0	0	0	0
136-PCDD	2128	8.148	1	0	1	0	0	0
137-PCDD	2135	8.131	2	0	1	0	0	0
138-PCDD	2135	8.131	2	0	1	0	0	0
139-PCDD	2142	8.148	1	0	1	0	0	1
124-PCDD	2143 ^a	8.165	1	1	1	1	0	0
147-PCDD	2151	8.148	1	0	0	1	0	0
146-PCDD	2158	8.165	0	0	0	1	0	1
236-PCDD	2177	8.148	2	0	0	0	0	0
237-PCDD	2184	8.131	3	0	0	0	0	0
126-PCDD	2190	8.165	1	1	0	0	0	0
123-PCDD	2191	8.165	2	1	1	0	1	0
127-PCDD	2197	8.148	2	1	0	0	0	0
128-PCDD	2197	8.148	2	1	0	0	0	0
129-PCDD	2204	8.165	1	1	0	0	0	1
12469-PCDD	2527	8.986	1	1	1	2	0	1.5
12368-PCDD	2539	8.969	3	1	2	0	1	0
12478-PCDD	2540	8.969	3	1	1	1	0	0
12379-PCDD	2552	8.969	3	1	2	0	1	1
12467-PCDD	2566	8.986	2	2	1	1	0	1
12489-PCDD	2566	8.986	2	2	1	1	0	1
12369-PCDD	2568	8.986	2	1	1	1	1	1
12346-PCDD	2581	9.003	2	2	2	1	2	1
123679-PCDD	2755	9.397	3	2	2	1	1	1
123689-PCDD	2755	9.397	3	2	2	1	1	1
123469-PCDD	2764	9.414	2	2	2	2	2	1.5
123789-PCDD	2803	9.397	4	2	2	0	2	1

^a The measured I values [29] for these four PCDDs are as follows: 27-PCDD and 28-PCDD, 1985; 23-PCDD, 1993; and 124-PCDD, 2152.

size descriptors such as the ${}^0\chi$, ${}^0\chi^v$ and ${}^1\chi^v$ indices, the molecular mass of the PCDDs, the number of non-hydrogen atoms and bonds and the sums of ${}^0\chi$ and ${}^0\chi^v$ or ${}^1\chi$ and ${}^1\chi^v$ indices in place of the first-order molecular connectivity index in eqn. 3. However, those models were unsuccessful in reproducing the experimental elution sequence for all 37 PCDD congeners.

DISCUSSION

Model description

QSAR analysis with topological features shows that the retention indices of PCDDs are primarily influenced by their bulk properties, *i.e.*, the size of the molecules. In the model developed this property is described best by the ${}^1\chi$ index, whose numerical

values are directly proportional to the number of bonds in the PCDD congeners, and it accounts for more than 97% of the variation in the I data. However, all parts of a PCDD do not contribute equally to its retention index. The highest contribution stems from the chlorine–carbon bonds, followed by the bonds between unsubstituted carbon atoms, and the lowest from the bonds between substituted carbon atoms. The other factors that control the magnitudes of the retention indices can be collectively termed the chlorine substitution pattern. It is possible to subdivide this general term into three more specific structural features: (1) the absolute position of chlorine atoms on each ring (Cl_M , Cl_{OM}), (2) the relative position of chlorine atoms on each ring (Cl_{13} , Cl_{14} , Cl_{SEQ3}) and (3) the absolute position of chlorine atoms on both aromatic rings ($ClOCl$). Some of these structural features (Cl_M , Cl_{OM} , Cl_{SEQ3} , $ClOCl$) have a positive effect on the magnitude of retention indices whereas the others (Cl_{13} , Cl_{14}) have a negative effect. The regression coefficients in eqn. 3 can be used as quantitative estimates for the effects of those chlorination patterns.

Model validation

There was a possibility of validating our model both by extrapolation and by interpolation. The extrapolation test was performed with a small number of reported [29] retention indices for di- and trisubstituted PCDDs which were not included in the regression analysis. The calculated and observed retention indices for 2,3-, 2,7-, 2,8- and 1,2,4-chlorinated PCDDs are presented in Table II. A comparison of these observed and calculated indices clearly demonstrates that the developed model (eqn. 3) is accurate in predicting I data even in this extrapolation region. The average difference between the predicted and observed retention indices is only 5 units, their elution sequence is predicted correctly and the relative differences in retention indices within dichlorinated PCDDs are reproduced very well. Unfortunately, it must be pointed out that our model underestimated the retention indices for all four test compounds used in this extrapolation procedure.

The interpolation test was performed with recently reported [30] retention indices for sixteen tetra- to octachlorinated PCDDs determined on a low-polarity HP-5 capillary column, which is very similar

to the DB-5 column used in the study by Donnelly et al. [29] (Table I). The calculated and observed [29,30] retention indices for the second set of test compounds are presented in Table III. The retention indices obtained on the HP-5 column [30] are systematically lower than those obtained earlier on the DB-5 column [29]. This is due mainly to the different stationary phases used and to the different operating conditions. However, there is a very high correlation between the two sets of reported retention indices ($r^2 = 1.000$). The set of calculated retention indices (eqn. 3) also correlates to a high degree with the retention indices obtained on the HP-5 column ($r^2 = 1.000$). Further, the developed model (eqn. 3) generates the correct elution sequence for all sixteen PCDD congeners obtained on the HP-5 column and also for the so-called “window” isomers, *i.e.*, the first and last isomer eluting in each isomeric group. Consequently, the reliable retention indices on the HP-5 column can be calculated for the remaining 33 tetra- to hexachlorinated isomers by a simple linear relationship from the retention indices calculated by our model (eqn. 3). Hence it is fair to conclude that the developed model (eqn. 3) was very successful in predicting the retention

TABLE III

COMPARISON OF MODEL (EQN. 3) PREDICTIONS TO MEASURED RETENTION INDICES (I_1 [30] AND I_2 [29]) FOR SIXTEEN TETRA- TO OCTACHLORINATED DIBENZODIOXIN DERIVATIVES (PCDDs)

Compound	I_{calc}	I_{1obs} [30]	I_{2obs} [29]
1368-PCDD	2288	2262.3	2290
2378-PCDD	2387	2353.1	2386
1289-PCDD	2425	2393.8	2428
12468-PCDD	2504	2464.3	2501
12479-PCDD	2504	2464.3	2501
12378-PCDD	2588	2554.8	2587
12389-PCDD	2614	2579.5	2623
124679-PCDD	2714	2668.3	2713
124689-PCDD	2714	2668.3	2713
123478-PCDD	2777	2741.8	2781
123678-PCDD	2790	2746.9	2788
123789-PCDD	2803	2762.0	–
123467-PCDD	2803	2762.0	2812
1234679-PCDD	2950	2893.9	2949
1234678-PCDD	2992	2937.2	2994
12346789-PCDD	3189	3132.6	3196

indices of PCDDs in both the interpolation region and the extrapolation region and that this model can be recommended as a reliable means for calculating retention indices.

The results in Table III indicate that the retention index system introduced by Kováts [31] to minimize the influence of operating conditions on measured retention indices are still influenced to a certain extent by the type of stationary phase and the column temperature or temperature cycle. Thus, strictly, the model developed in this study (eqn. 3) is valid only for retention indices obtained on a DB-5 column and with the temperature cycle used in the study by Donnelly *et al.* [29]. However, it has been demonstrated [31–33] that retention indices are linearly dependent on temperature and that in most instances the temperature coefficients are very small. Further, for stationary phases where the non-specific interaction forces control the retention process, the measured retention indices are linearly dependent and highly correlated [29,30]. This is also demonstrated in our study (see Table III) for two capillary columns, DB-5 and HP-5. Retention indices obtained for chlorinated dibenzodioxins on this two columns correlate above the 99.9% level. Hence it seems that our model can be adapted very rapidly in order to be used for other column types or temperature cycles, provided that two or three reference points are available for its calibration to a particular type of stationary phase and/or temperature cycle.

In the following section, as a part of the validation process, we compare our model with those already published. At present, there are two quantitative models [29,34] that are available for the comparison procedure (an attempt was also made to model the retention indices of PCDDs for tetrachlorinated isomers by solubility parameters [35]). The first model [34] is based on three calculated physical properties as parameters: molecular polarizabilities, ionization potentials and dipole moments. The second model [29] is based on an empirical additive scheme with eleven parameters (ten fragments and one correction factor). For the first model [34] the standard error of the estimate is above 32 units. Hence this model can estimate the retention indices of PCDDs only on a semi-quantitative level, *i.e.*, neither the generation of experimental elution sequences nor reliable isomer-specific estimations are possible with this model.

The second model [29], based on an empirical additive scheme, has an average residual of 3.1 units for the calculated retention indices of 37 tetra- to octachlorinated isomers. This result is comparable to the estimation performance of our model (average residual 2.4 units). However, our model was superior in estimating the retention indices of di- and trichlorinated PCDDs. The average residual for calculated retention indices was only 5 units, while the empirical additive scheme has an average residual of 9 units for this group of PCDD congeners. An additional advantage of the structural model developed in this study is the smaller number of parameters that are needed to attain (a) the same level of precision in estimating retention indices and (b) the experimental elution sequence for PCDD congeners. The introduction of the first-order molecular connectivity index made it possible to reduce the number of necessary structural parameters from eleven to seven and the possibility of a chance correlation.

Mechanism of interaction of PCDDs with non-polar stationary phase

The retention process of PCDDs is primarily influenced by their bulk properties, *i.e.*, the size of these molecules. In the model developed, their size is described best by the $^1\chi$ index. It has been found in several studies [21,22,28] that the $^1\chi$ index correlates extremely well with the molecular surface of various classes of hydrocarbons, halogenated hydrocarbons and similar compounds. Therefore, it was logical to find that this structural descriptor accounts for more than 97% of the variation in the PCDD *I* data, *i.e.*, correlates well with this molecular surface-dependent process.

The six local structural parameters that control the magnitude of retention indices can be classified into two groups: (i) parameters that increase the magnitude of retention indices (Cl_M , Cl_{OM} , Cl_{SEQ3} , $ClOCl$) and (ii) parameters that decrease the magnitude of retention indices (Cl_{13} , Cl_{14}). From the mechanistic point of view, the first group of parameters describes structural features that have attractive interactions with the stationary phase while the second group of parameters describes structural features that either have repulsive interactions with the stationary phase or interfere with a possible favourable interaction.

From our results, it is also possible to speculate about the mechanism of interaction of PCDD congeners and non-polar stationary phases in gas chromatography. It seems that the *meta* chlorine substituents interact more strongly with a stationary phase than the *ortho* substituents. Further, the accumulation or adjacent substitution also has a positive effect on the magnitude of retention indices described by positive contributions of the pairs of *ortho* and *meta* chlorine substituents and the sequences of three consecutive substituents. The positive effect of the simultaneous presence of chlorine substituents in positions 1 and 9 or 4 and 6 can be rationalized as the two chlorines blocking the repulsive interactions of the polar ether oxygens with the non-polar stationary phase, *i.e.*, the shielding effect. Finally, the negative effects of two types of non-neighbouring substitutions (Cl_{13} and Cl_{14}) can be rationalized as the steric hindrance of possible favourable interactions between PCDD congeners and the non-polar stationary phase. However, in a recent study [36] with similar solutes, chlorinated dibenzofurans, it was suggested that the formation of local dipoles has a strong influence on their interaction with a non-polar stationary phase, *i.e.*, local dipoles reduce the positive interaction between the solute molecules and the stationary phase. Hence it is also possible that in chlorinated dibenzodioxins the presence of substitution patterns such as Cl_{13} and Cl_{14} stimulates the formation of local dipoles which interfere with the positive interaction between the solute molecules and a non-polar stationary phase and consequently reduce the magnitude of the retention indices.

CONCLUSIONS

We have demonstrated that a relatively simple model, based on topological properties of molecules, can be used to predict successfully the retention indices of chlorinated dibenzodioxins on a non-polar stationary phase. The agreement between the observed and calculated retention indices, the r^2 value of 1.000 and the standard deviation of 2.4 all indicate that this model works well to describe the retention indices of all the PCDDs analysed. To reproduce the experimental elution sequence of 37 PCDD congeners the seven-variable model was necessary. Those variables account for

(i) the number of chlorine atoms present, *i.e.*, the molecular size of the PCDD congeners, (ii) the position and the relationship of chlorine atoms on each aromatic ring and (iii) the relationship of chlorine atoms on both aromatic rings. Hence one can predict the retention index for any given PCDD having only a knowledge of its chlorine substitution pattern.

The developed mathematical model, which describes the pattern in PCDD retention data from the chlorine substitution patterns, will be of great analytical value. It could be used to verify the observed retention data because of the difficulties associated with preparing and then positively identifying any particular PCDD. In any case, with this model, it is possible to narrow greatly the range to search for and identify a given PCDD. Further, the developed model can predict the retention characteristics of PCDDs which have not yet been synthesized (see Table II).

ACKNOWLEDGEMENT

This work was supported by grant 1-07-159 awarded by the Ministry of Science, Technology and Information of Croatia.

REFERENCES

- 1 B. Birmingham, A. Gilman, R. Clement, C. Tashiro, G. Hunt, L. LaFleur and V. Ozvacic (Guest Editors), *Chlorinated Dioxins and Related Compounds 1989, Parts 1 and 2, Atmosphere*, Vol. 20, Nos. 7–12, 1990.
- 2 R. Kaliszan, *Quantitative Structure Chromatographic Retention Relationships*, Wiley, New York, 1988; and references cited therein.
- 3 J. R. Chrétien and J. E. Dubois, *J. Chromatogr.*, 126 (1976) 171.
- 4 J. R. Chrétien and J. E. Dubois, *Anal. Chem.*, 49 (1977) 747.
- 5 J. E. Dubois, J. R. Chrétien, L. Soják and J. A. Rijks, *J. Chromatogr.*, 194 (1980) 121.
- 6 J. E. Dubois, C. Mercier and A. Panaye, *Acta Pharm. Jugosl.*, 36 (1986) 135.
- 7 R. Kaliszan, *Chromatographia*, 10 (1977) 346.
- 8 M. J. M. Wells, C. R. Clark and R. M. Patterson, *Anal. Chem.*, 58 (1986) 1625.
- 9 N. Funasaki, S. Hada and S. Neya, *J. Chromatogr.*, 361 (1986) 33.
- 10 R. H. Rohrbaugh and P. C. Jurs, *Anal. Chem.*, 59 (1987) 1048.
- 11 D. Noël and P. Vangheluwe, *J. Chromatogr.*, 388 (1987) 75.
- 12 F. Khorasheh, M. R. Gray and M. L. Selucky, *J. Chromatogr.*, 481 (1989) 1.

- 13 V. A. Gerasimenko and V. M. Nabivach, *J. Chromatogr.*, 498 (1990) 357.
- 14 D. Bonchev, O. Mekenyan, G. Protić and N. Trinajstić, *J. Chromatogr.*, 176 (1979) 149.
- 15 N. Adler, D. Babić and N. Trinajstić, *Fresenius' Z. Anal. Chem.*, 322 (1985) 426.
- 16 N. Bošnjak, Z. Mihalić and N. Trinajstić, *J. Chromatogr.*, 540 (1991) 430.
- 17 N. Trinajstić, *Chemical Graph Theory*, CRC Press, Boca Raton, FL, 2nd ed., 1992.
- 18 L. B. Kier and L. H. Hall, *Molecular Connectivity in Structure–Activity Analysis*, Research Studies Press, Chichester, 1986.
- 19 A. Sabljic, *J. Chromatogr.*, 314 (1984) 1.
- 20 A. Sabljic, *J. Chromatogr.*, 319 (1985) 1.
- 21 A. Sabljic, R. Lara and W. Ernest, *Chemosphere*, 19 (1989) 1665.
- 22 A. Sabljic, *Environ. Health Perspect.*, 83 (1989) 179.
- 23 A. Sabljic and H. Güsten, *Chemosphere*, 19 (1989) 1503.
- 24 A. Sabljic, H. Güsten, J. Schönherr and M. Riederer, *Environ. Sci. Technol.*, 24 (1990) 1321.
- 25 A. Sabljic and N. Trinajstić, *Acta Pharm. Jugosl.*, 31 (1981) 189.
- 26 A. T. Balaban, I. Motoc, D. Bonchev and O. Mekenyan, *Top. Curr. Chem.*, 114 (1983) 21.
- 27 A. Sabljic, *Sci. Total Environ.*, 109/110 (1991) 197.
- 28 A. Sabljic, *Environ. Sci. Technol.*, 21 (1987) 358.
- 29 J. R. Donnelly, W. D. Munslow, R. K. Mitchum and G. W. Sovocool, *J. Chromatogr.*, 392 (1987) 51.
- 30 I. O. O. Korhonen and K. M. Mantykoski, *J. Chromatogr.*, 477 (1989) 327.
- 31 E. Kovats, *Helv. Chim. Acta*, 41 (1958) 1915.
- 32 H. van den Dool and P. D. Kratz, *J. Chromatogr.*, 11 (1963) 463.
- 33 G. Guiochon, *Anal. Chem.*, 36 (1964) 661.
- 34 V. S. Ong and R. A. Hites, *Anal. Chem.*, 63 (1991) 2829.
- 35 H. A. J. Govers, R. Luijk and E. H. G. Evers, *Sci. Total Environ.*, 109/110 (1991) 105.
- 36 K. Osmialowski and R. Kaliszan, *Quant. Struc.–Act. Relat.*, 10 (1991) 125.

Determination of C₆–C₁₀ aromatic hydrocarbons in water by purge-and-trap capillary gas chromatography

Robert P. Eganhouse

Environmental Sciences Program, University of Massachusetts, Boston, MA 02125 (USA) and Southern California Coastal Water Research Project, 646 W. Pacific Coast Highway, Long Beach, CA 90806 (USA)

Thomas F. Dorsey

Environmental Sciences Program, University of Massachusetts, Boston, MA 02125 (USA) and Department of Earth and Space Sciences, University of California, Los Angeles, CA 90024 (USA)

Curtis S. Phinney[☆]

Environmental Sciences Program, University of Massachusetts, Boston, MA 02125 (USA)

Alvin M. Westcott

Southern California Coastal Water Research Project, 646 W. Pacific Coast Highway, Long Beach, CA 90806 (USA)

(First received April 22nd, 1992; revised manuscript received August 14th, 1992)

ABSTRACT

A method is described for the determination of the C₆–C₁₀ aromatic hydrocarbons in water based on purge-and-trap capillary gas chromatography with flame ionization and mass spectrometric detection. Retention time data and 70 eV mass spectra were obtained for benzene and all 35 C₇–C₁₀ aromatic hydrocarbons. With optimized chromatographic conditions and mass spectrometric detection, benzene and 33 of the 35 alkylbenzenes can be identified and measured in a 45-min run. Use of a flame ionization detector permits the simultaneous determination of benzene and 26 alkylbenzenes.

INTRODUCTION

In recent years numerous investigators have reported the presence of volatile hydrocarbons in groundwater, rivers, lakes and even coastal and estuarine ecosystems [1–15]. Contamination of aquatic environments results from a variety of causes.

These include: (1) leakage of underground storage tanks, (2) leaching of landfills and other waste disposal sites, (3) discharge of industrial and municipal effluents and (4) occasional oil spills. Among the most toxic and water soluble constituents of crude oil and refined petroleum products are the aromatic hydrocarbons. When oil comes in contact with water the most soluble compounds enter the aqueous phase and are subsequently removed or transformed by a variety of physical and biological processes [16–18]. Because of differences in their physical properties and structures, the aromatic hydrocarbons may be transported and/or removed at

Correspondence to: R. P. Eganhouse, United States Geological Survey, Water Resources Division, Reston, VA 22092, USA (present address).

[☆] Present address: United States Geological Survey, Water Resources Division, Reston, VA 22092, USA.

different rates [3,19]. Consequently, the determination of a wide range of aromatics is of interest not only because these compounds are toxic, but also because they can serve as useful indicators of natural removal processes.

A number of techniques have been used to determine benzene and its alkylated derivatives in water. These include headspace analysis [5], purge-and-trap gas chromatography (GC) [11,20–24], microextraction [25,26] and closed loop stripping analysis [27,28]. Each technique has specific advantages and drawbacks [26,29,30], but purge-and-trap GC and its variants (*e.g.* Bianchi *et al.* [14] and Lucas *et al.* [31]) have enjoyed the widest use. Introduced originally in 1974 by Bellar and Lichtenberg [32] and currently recommended by the US Environmental Protection Agency, the purge-and-trap method is sensitive, precise, relatively simple and suitable for a wide range of volatile contaminants. However, it has rarely been applied to the determination of aromatic hydrocarbons other than benzene, toluene and the C₈ aromatics (BTEX). The principal objective of the present work was to develop a method based on purge-and-trap GC that permitted the measurement of most, if not all, of the C₆–C₁₀ aromatic hydrocarbons in water. Extending the range of analytes to include the C₉ and C₁₀ aromatics has substantially improved our ability to understand processes affecting the fate of petroleum hydrocarbons in groundwater. Because of the large number of isomeric C₉ and C₁₀ aromatics (8 and 22, respectively) and similarities in the physicochemical properties of these isomers, it was possible to establish the importance of biological degradation in hydrocarbon removal [3,19]. Moreover, differences in apparent removal rates of isomeric hydrocarbons strongly suggest that the structures of the hydrocarbons control their rates of removal. Thus, the C₉ and C₁₀ aromatics represent powerful molecular probes of biogeochemical processes affecting the fate of petroleum in aquatic environments. Here we present information on the identification, chromatographic separation and instrumental analysis of these compounds.

EXPERIMENTAL

Materials

Water used for preparation of standard solutions

and for dilution of samples was purified by boiling with concurrent helium sparging. The volatile-free water (VFW) was stored in the erlenmeyer flask in which it was boiled. Purge-and-trap grade methanol (Burdick and Jackson) was used for preparation of standards without further purification.

Alkylbenzenes and alkanes were obtained from the following suppliers: Supelco, Alltech, Aldrich, Wiley Organics and the American Petroleum Institute. In all but one case (1,2-diethylbenzene; purity 95%), quoted purities exceeded 98%. The compounds were stored at –4°C in ampoules or in glass vials sealed with PTFE-lined lids. Prior to use in standard solutions, each compound was tested for purity by high-resolution gas chromatography–flame ionization detection (HRGC–FID).

Six alkylbenzenes were evaluated for suitability as recovery and internal quantitation standards: [²H₆]benzene, [²H₁₀]o-xylene, [²H₁₀]p-xylene, [²H₁₀]ethylbenzene, n-hexylbenzene and n-octylbenzene. [Perdeuterated species were obtained from Cambridge Isotope Laboratories (Woburn, MA, USA).] Comparison of the retention times of volatile hydrocarbons present in 12 oil-contaminated groundwater samples showed that [²H₁₀]o-xylene and [²H₁₀]ethylbenzene eluted in chromatographic regions free of interference. The higher alkylbenzenes we tested proved unsuitable because of their low stripping efficiencies in the purge-and-trap HRGC system under the conditions of analysis we employed. Perdeuterated p-xylene offered no advantage over [²H₁₀]o-xylene or [²H₁₀]ethylbenzene and [²H₆]benzene was not always baseline-resolved from benzene, typically the dominant hydrocarbon in our samples. The C₈ aromatics elute in the middle of the elution range of alkylbenzenes considered here, whereas the other candidate elute either very early or late in the gas chromatogram. For these reasons, we selected [²H₁₀]o-xylene and [²H₁₀]ethylbenzene as recovery and internal (quantitation) standards, respectively.

Standard solutions used for instrument calibration were prepared as follows. A 1-dram (*ca.* 1.5 ml) borosilicate vial fitted with a PTFE mininert valve was positioned in a Dewar containing liquid nitrogen. Amounts of 50 μl of each component were transferred quantitatively into the vial with a 100-μl microsyringe. After this mixture had been prepared at liquid nitrogen temperatures, it was allowed to

warm to room temperature (valve closed). The mixture was then agitated to insure homogeneity, and a measured aliquot was transferred by microsyringe to a volumetric flask containing methanol. This stock solution was serially diluted to provide calibration standard solutions over an appropriate concentration range ($2\text{--}260\text{ ng } \mu\text{l}^{-1}$ component $^{-1}$).

Sample preparation

Samples of contaminated groundwater were collected from water table wells using an all-PTFE bailer. Details of the sampling procedures are given elsewhere [33]. Groundwater was introduced to 40-ml amber glass bottles sealed with PTFE-faced silicone rubber liners. Before the bottle was sealed, each sample was poisoned with HgCl_2 and spiked with $2\text{ }\mu\text{l}$ of the recovery surrogate solution ($[\text{2H}_{10}]o\text{-xylene}$ in methanol). We prepared recovery surrogate solutions at several levels within a concentration range of $8.1\text{--}810\text{ ng } \mu\text{l}^{-1}$. The concentration of $[\text{2H}_{10}]o\text{-xylene}$ used for introduction to a given sample was based on the expected concentration of volatile hydrocarbons in that sample. The bottles were sealed without headspace, taped secure and placed on ice in a cooler until return to the laboratory (where they were stored at 4°C). Similar procedures were used for collection and storage of produced water with the exception that these samples were taken directly from a spigot at the onshore water treatment plant (Carpenteria, CA, USA). Field banks, consisting of VFW spiked with various amounts of $[\text{2H}_{10}]o\text{-xylene}$, were prepared and preserved according to the same protocol.

Just prior to analysis, water samples were permitted to warm to room temperature. When the concentration of volatiles was known to be extremely low ($< ca. 5\text{--}15\text{ }\mu\text{g l}^{-1}$ component $^{-1}$), an aliquot of the sample was poured (to overflowing) directly into a 5-ml gastight Luer-lok syringe fitted with a PTFE mininert valve in the open position. The syringe plunger was quickly inserted in order to seal the sample in the syringe without bubbles or headspace. The sample volume was then adjusted to 5 ml, expelling the excess to waste, and the mininert valve was closed. The internal standard solution ($0.5\text{ }\mu\text{l}$ of $[\text{2H}_{10}]ethylbenzene$ in methanol; $44.5\text{ ng } \mu\text{l}^{-1}$) was taken up in a $1.0\text{-}\mu\text{l}$ syringe. The mininert valve was then removed, the needle of the microsyringe was inserted into the 5-ml syringe, and the in-

ternal quantitation standard was introduced to the sample. The sample was immediately transferred to the purge vessel (see below) via the Luer-lok fitting.

As discussed below, the linear calibration range of the purge-and-trap HRGC-FID system described here is limited (<0.2 to $10\text{ }\mu\text{g l}^{-1}$ in purge vessel). At the same time, the concentrations of aromatic hydrocarbons encountered in oil-contaminated waters often span more than four orders of magnitude [3–4]. Consequently, samples having individual hydrocarbon concentrations greater than *ca.* $10\text{--}15\text{ }\mu\text{g l}^{-1}$ required dilution prior to being introduced into the purge vessel. First, an appropriate aliquot of the sample was measured in the 5-ml syringe and transferred to the purge vessel. Then VFW was loaded into the same syringe without headspace (as described above), and the volume was adjusted such that the total volume of the diluted sample (*i.e.* VFW + sample) equalled 5 ml. The VFW was immediately transferred to the purge vessel. The internal standard solution was introduced to either the VFW or the sample depending on which volume was greater. For extremely contaminated water ($> ca. 300\text{ }\mu\text{g l}^{-1}$ component $^{-1}$), microsyringes were used to transfer small aliquots ($5\text{--}250\text{ }\mu\text{l}$) of the sample to a syringe containing 5 ml VFW. As before, the internal standard solution was spiked into the 5-ml syringe before the diluted sample was introduced to the purge-and-trap concentrator.

Purge-and-trap gas chromatography

Analyses were performed on Tekmar LSC-2 and LSC-2000 purge-and-trap concentrators interfaced to Varian 3300 or 3500 high-resolution gas chromatographs equipped with hydrogen flame ionization detectors. In the case of the LSC-2, the heated transfer line (175°C) from the purge-and-trap device was $1/16$ in. stainless-steel tubing. This was connected (within the GC oven) to a retention gap consisting of an uncoated length of deactivated fused-silica capillary ($0.3\text{ m} \times 0.25\text{ mm I.D.}$) using a stainless-steel union. The uncoated fused-silica capillary was, in turn, connected to a $30\text{ m} \times 0.25\text{ mm I.D.}$ fused-silica capillary column coated with a $1.0\text{-}\mu\text{m}$ film of DB-5 (J&W Scientific) using a stainless-steel zero dead volume union. By contrast, the LSC-2000 interfaces directly to the capillary column via an uncoated length of fused-silica capillary

tubing (0.5 m \times 0.32 mm I.D.) originating at the multiport valve of the purge-and-trap device. Thus, only one zero dead volume union was required.

Although several purge-and-trap protocols were investigated, routine conditions of analysis were as follows: purge gas, nitrogen; purge flow, 40 ml min^{-1} ; purge time, 11 min; dry purge time, 4 min; trap temperature (during purge), 22°C; (during desorption), 175°C; desorption time 4 min. Sample components were transferred from the trap to the column using helium carrier gas at a flow-rate of ca. 1.5 ml min^{-1} (linear velocity at 150°C = ca. 30 cm s^{-1}). The column was maintained at -50°C, the column was programmed to 40°C at 50°C min^{-1} (5-min hold), then to 150°C at 3°C min^{-1} followed by a 25-min isothermal hold. This temperature program was developed after evaluating and optimizing the conditions of separation using complex oil-

contaminated groundwater samples. The chromatographic conditions described here are similar to those reported by Johansen *et al.* [34] who analyzed gasoline samples on a glass capillary column coated with OV-101. Data were acquired and processed on a Nelson 2700 chromatography data system equipped with a Nelson 900 intelligent analog-to-digital interface operating at a sampling rate of 2 points s^{-1} .

The use of a narrow bore capillary column afforded the resolving power needed to separate the complex assemblages of alkylbenzenes we were primarily interested in. However, the low column flow-rates acted to reduce the efficiency of sample transfer from the trap for the most abundant components (principally benzene) in heavily contaminated samples. As described earlier, this affected only those samples having alkylbenzenes at concentra-

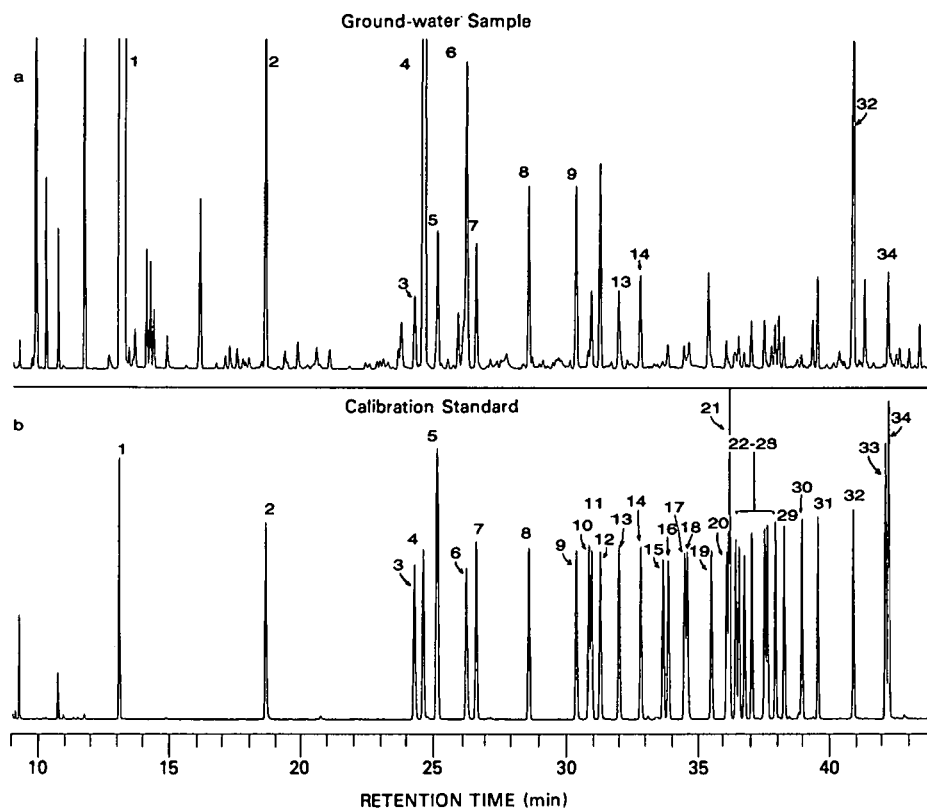


Fig. 1. High resolution gas chromatograms resulting from purge-and-trap HRGC-FID showing (a) volatile hydrocarbons in petroleum-contaminated groundwater, (b) calibration standard used for determination of benzene and C_7 - C_{10} aromatic hydrocarbons. Identities of compounds in numbered peaks are given in Table I.

tions that spanned several orders of magnitude. This limitation was readily overcome by simply diluting the sample.

Gas chromatography–mass spectrometry

For purposes of qualitative analysis, the Tekmar LSC-2 was interfaced to a Finnigan 4510B HRGC–mass spectrometry (MS) apparatus in the same manner as described above. The end of the analytical column was inserted directly into the ion source. The HRGC–MS system was equipped with a Data General Nova 4C computer and SuperIncos data acquisition and processing software. The purge-and-trap concentrator and GC conditions were identical to those described in the preceding section. Mass spectral data were acquired in the full scan, electron impact mode (70 eV) with scanning from 50 to 150 amu at a rate of 1 scan s^{-1} .

RESULTS AND DISCUSSION

Qualitative analysis

Our interest in volatile hydrocarbons originated with a study of groundwater contamination in a remote area of northern Minnesota (USA). At this site, crude oil accidentally released from an underground pipeline in 1979, migrated to the water table. Dissolution of the more soluble components of the oil resulted in volatile dissolved organic carbon concentrations of approximately 20 mg l^{-1} in the groundwater near the oil body [33]. A typical gas chromatogram of the volatile hydrocarbons in groundwater collected at the water table near the oil is shown in Fig. 1a. Preliminary purge-and-trap HRGC–MS analysis of this sample indicated the presence of a large number of aliphatic and aromatic hydrocarbons. The latter included benzene, a complex mixture of C_7 – C_{11} monoaromatics and naphthalene [35]. Our initial efforts were, therefore, aimed at determining the retention characteristics of the alkylbenzenes and optimizing conditions for their purge-and-trap GC analysis.

Previous investigators have established the retention behavior of many of the C_6 – C_{10} aromatic hydrocarbons on a variety of stationary phases under isothermal and programmed temperature conditions (Johansen *et al.* [34]; Kumar *et al.* [36]; and references cited therein). These studies have demonstrated the difficulty of separating all isomeric C_6 –

C_{10} aromatics on a single high resolution capillary column. Kumar *et al.* [36] achieved the baseline separation of many of the alkylbenzenes on a 91-m capillary column coated with Carbowax 1540 using programmed temperature GC. They noted that the two principle problems associated with the GC analysis of the C_6 – C_{10} aromatics are: (1) their separation from low-molecular-weight saturated hydrocarbons and (2) complete resolution of the aromatics from each other. Although non-polar phases provide excellent selectivity for the C_6 – C_{10} aromatics [34,37–39], difficulties in separating them from saturated hydrocarbons can arise when petroleum products are analyzed. This obstacle is mitigated in the case of petroleum-contaminated waters for two reasons: (1) the high solubilities of the aromatic leads to their enrichment in the aqueous phase and (2) the saturated hydrocarbons are more rapidly biodegraded [33]. As illustrated in Fig. 1a, these phenomena result in elution of most of the C_7 – C_{10} aromatics in regions that are effectively free of chromatographic interference from saturated hydrocarbons.

Retention data are provided in Table I for benzene, all 35 C_7 – C_{10} aromatics, specific deuterated analogues (4) and selected alkanes (11) under two different temperature programs. Both of these programs provide good overall separations. For comparison, a typical gas chromatogram obtained using the faster program (RRT2) for a mixture of *most* of these pure compounds is shown in Fig. 1b. Benzene and all but seven of the alkylbenzenes can be (at least partially) resolved within 45 min under these conditions; 20 compounds (including the deuterated substances) are baseline-resolved (Table II).

Because of the incomplete chromatographic resolution of certain alkylbenzenes it was of interest to determine whether MS would permit more accurate qualitative and quantitative analysis of the partially resolved and co-eluting peaks. We, therefore, collected 70-eV electron impact mass spectra for benzene, each of the 35 C_7 – C_{10} aromatics and 3 of the perdeuterated analogues. Only one pair of *co-eluting* alkylbenzenes (*m*-xylene/*p*-xylene) was found to have indistinguishable mass spectra. There are also two pairs of *partially* resolved alkylbenzenes whose mass spectra are virtually identical: (1) 1-methyl-3-ethylbenzene/1-methyl-4-ethylbenzene and (2) 1,4-methyl-2-ethylbenzene/1,3-dimethyl-4-ethylben-

TABLE I
RELATIVE RETENTION TIME DATA FOR VOLATILE ALIPHATIC AND AROMATIC HYDROCARBONS

Compound	RRT1 ^a	RRT2 ^b	Peak ^c
<i>Aliphatic hydrocarbons</i>			
2,3-Dimethylbutane	— ^d	0.3495	—
2-Methylpentane	0.3417	0.3527	—
3-Methylpentane	0.3449	0.3677	—
2,4-Dimethylpentane	0.3999	0.4284	—
2,3-Dimethylpentane	0.4756	0.4870	—
3-Methylhexane	0.4863	0.4977	—
2,2,4-Trimethylpentane	0.5078	0.5193	—
2,5-Dimethylhexane	0.5874	0.5990	—
2,3,4-Trimethylpentane	0.6258	0.6326	—
3-Methylheptane	0.6739	0.6838	—
2,2,5-Trimethylhexane	0.6931	0.7208	—
<i>Aromatic hydrocarbons</i>			
[² H ₆]Benzene	0.4620	— ^d	—
Benzene	0.4655	0.4787	1
Toluene	0.6609	0.6717	2
[² H ₁₀]Ethylbenzene	— ^d	0.8582	3
Ethylbenzene	0.8618	0.8691	4
[² H ₁₀]p-Xylene	0.8574	— ^d	—
m,p-Xylene	0.8797	0.8863	5
[² H ₁₀]o-Xylene	— ^d	0.9227	6
o-Xylene	0.9294	0.9352	7
Isopropylbenzene	1.0000	1.0000	8
n-Propylbenzene	1.0712	1.0595	9
1-Methyl-3-ethylbenzene	1.0906	1.0748	10
1-Methyl-4-ethylbenzene	1.0947	1.0781	11
1,3,5-Trimethylbenzene	1.1083	1.0866	12
1-Methyl-2-ethylbenzene	1.1399	1.1124	13
tert.-Butylbenzene	1.1758	1.1372	—
1,2,4-Trimethylbenzene	1.1776	— ^d	14
Isobutylbenzene	1.2179	1.1642	15
sec.-Butylbenzene	1.2276	1.1698	16
1-Methyl-3-isopropylbenzene	1.2580	1.1862	17
1,2,3-Trimethylbenzene	1.2637	1.1912	18
1-Methyl-4-isopropylbenzene	1.2672	— ^d	—
1-Methyl-2-isopropylbenzene	1.3113	1.2154	19
1,3-Diethylbenzene	1.3438	1.2311	20
1-Methyl-3-propylbenzene	1.3497	1.2340	21
1-Methyl-4-propylbenzene	1.3621	— ^d	—
1,4-Diethylbenzene	1.3649	1.2410	22
n-Butylbenzene	1.3653	— ^d	—
1,3-Dimethyl-5-ethylbenzene	1.3847	1.2510	23
1,2-Diethylbenzene	1.3721	1.2439	24
1-Methyl-2-propylbenzene	1.4031	1.2589	25
1,4-Dimethyl-2-ethylbenzene	1.4356	1.2724	26
1,3-Dimethyl-4-ethylbenzene	1.4422	1.2754	27
1,2-Dimethyl-4-ethylbenzene	1.4641	1.2842	28
1,3-Dimethyl-2-ethylbenzene	1.4877	1.2948	29
1,2-Dimethyl-3-ethylbenzene	1.5395	1.3145	30
1,2,4,5-Tetramethylbenzene	1.5730	— ^d	—
1,2,3,5-Tetramethylbenzene	1.5874	1.3324	31
1,2,3,4-Tetramethylbenzene	1.7094	1.3753	32
[² H ₈]Naphthalene	— ^d	— ^d	33
Naphthalene	— ^d	— ^d	34

^a RRT1 = relative retention times using isopropylbenzene as reference peak. Chromatographic conditions as follows: –50°C → 40°C at 50°C min⁻¹, 5 min isothermal hold, → 90°C at 3°C min⁻¹ → 150°C at 1°C min⁻¹.

^b RRT2 = relative retention times using isopropylbenzene as reference peak. Chromatographic conditions as follows: –50°C → 40°C at 50°C min⁻¹, 5 min isothermal hold, → 150°C at 3°C min⁻¹, 40 min isothermal hold.

^c Peak numbers refer to Fig. 1.

^d Not determined.

TABLE II
IDENTIFICATION OF ALKYL BENZENES BASED ON RETENTION TIMES AND MASS SPECTRAL CHARACTERISTICS

Compound	Resolution ^a	Potential GC–MS quantitation ions ^b	Other significant ions ^c
Benzene	b	78	77(25)
Toluene	b	91	92(62)
[² H ₁₀]Ethylbenzene	b	98	116(31)
Ethylbenzene	b	91	106(34), 77(11)
[² H ₁₀]p-Xylene	b	98	116(52), 114(16)
p-Xylene	c } ^d	91	106(53), 105(25), 77(17)
m-Xylene	c } ^d	91	106(53), 105(25), 77(17)
[² H ₁₀]o-Xylene	b	98	116(49), 114(13)
o-Xylene	b	91	106(50), 105(21), 77(15)
Isopropylbenzene	b	105	120(30), 77(18)
n-Propylbenzene	b	91	120(25)
1-Methyl-3-ethylbenzene	p } ^d	105	120(33), 91(9), 77(10)
1-Methyl-4-ethylbenzene	p } ^d	105	120(31), 91(9), 77(9)
1,3,5-Trimethylbenzene	b	105	120(55), 91(9), 77(12)
1-Methyl-2-ethylbenzene	b	105	120(32), 91(10), 77(10)
tert.-Butylbenzene	c } ^e	<u>119</u> , 134(27)	120(10), 105(1), 91(58)
1,2,4-Trimethylbenzene	c } ^e	<u>105</u> , 120(52)	119(13), 91(8)
Isobutylbenzene	p } ^c	<u>91</u> , <u>92</u> (57)	134(29), 105(1)
sec.-Butylbenzene	p } ^c	105	134(20), 92(2), 91(13), 77(10)
1-Methyl-3-isopropylbenzene	b	<u>119</u>	134(27), 91(21), 77(6)
1,2,3-Trimethylbenzene	p } ^c	<u>105</u> , 120(49)	119(11), 91(8), 77(10)
1-Methyl-4-isopropylbenzene	p } ^c	<u>119</u> , <u>134</u> (27)	105(5), 91(18), 77(6)
1-Methyl-2-isopropylbenzene	b	119	134(29), 91(19)
1,3-Diethylbenzene	p } ^e	<u>119</u> (98)	134(48), 105 , 91(21)
1-Methyl-3-propylbenzene	p } ^e	105	134(26), 119(4), 91(8), 77(9)
1-Methyl-4-propylbenzene	c } ^e	105	134(22), 119(1), 91(6), 92(2)
1,4-Diethylbenzene	c } ^e	<u>119</u> , 105(82)	134(47), 92(2), 91(26)
n-Butylbenzene	c } ^e	<u>91</u> , <u>92</u> (56)	134(29), 119(3), 105(8)
1,2-Diethylbenzene	b	105	134(50), 119(86), 91(28)
1,3-Dimethyl-5-ethylbenzene	b	119	134(33), 91(14), 77(6)
1-Methyl-2-propylbenzene	b	105	134(24), 91(14), 77(6)
1,4-Dimethyl-2-ethylbenzene	p } ^d	119	134(33), 105(15), 91(13)
1,3-Dimethyl-4-ethylbenzene	p } ^d	119	134(28), 105(4), 91(12)
1,2-Dimethyl-4-ethylbenzene	b	119	134(30), 105(8), 91(13)
1,3-Dimethyl-2-ethylbenzene	b	119	134(29), 105(5), 91(12)
1,2-Dimethyl-3-ethylbenzene	b	119	134(32), 105(10), 91(14)
1,2,4,5-Tetramethylbenzene	b	119	134(54), 105(3), 91(13)
1,2,3,5-Tetramethylbenzene	b	119	134(49), 105(3), 91(12)
1,2,3,4-Tetramethylbenzene	b	119	134(47), 105(3), 91(14)

^a Chromatographic resolution based on chromatographic conditions given in Table I (RRT2): b = baseline resolved, c = coelution, p = partial coelution.

^b Masses underlined are specific to the compound present in the coeluting peak. Negligible or no interference from other alkylbenzenes. Base peak is in **bold**.

^c Numbers in parentheses indicate abundance (%) relative to base peak.

^d Mass spectra of coeluting peaks are essentially identical.

^e Mass spectra are readily distinguishable.

zene. All other non-baseline-resolved alkylbenzenes can be readily differentiated by HRGC–MS for purposes of qualitative analysis. In some of these

latter cases, the co-eluting components yield ions that are sufficiently unique to make quantitation by selected ion monitoring possible. In other instances,

the mass spectra differ only in the relative abundances of common ions, and some deconvolution would be necessary. Table II summarizes these findings.

Together these data indicate that purge-and-trap HRGC–MS should permit the qualitative and quantitative analysis of benzene and 33 of the 35 alkylbenzenes of interest here. Assuming there are no interferences from substances other than aromatic hydrocarbons, purge-and-trap HRGC–FID should, in principle, be applicable to the determination of 28 of the 35 C₇–C₁₀ aromatic hydrocarbons. In practice, however, separation of the 1,2,3-trimethylbenzene/1-methyl-4-isopropylbenzene doublet was not sufficient to permit accurate determination of the individual components. Use of more selective stationary phases either in series (*e.g.* Mathews *et al.* [40]) or in parallel could provide further improvements in the separation of the difficult multicomponent peaks.

Quantitative analysis

Based on the retention data described above, we developed a 35-component calibration standard solution (*cf.* Fig. 1b). A multipoint calibration was performed on the LSC-2000/Varian 3500 system using eight serial dilutions of the calibration standard ranging in concentration from 2 to 250 ng μl^{-1} . Purge-and-trap HRGC–FID analyses were carried out on 5-ml aliquots of VFW amended with 0.5 μl

of each dilution of the calibration standard solution (duplicate analyses at each level). Calibration of the system was performed for all targeted compounds because the stripping efficiencies of the C₆–C₁₀ aromatics decrease with decreasing vapor pressure.

Table III lists results developed from linear regression analysis of the data obtained during the multipoint calibration experiment. Results are shown for benzene and six representative alkylbenzenes. The tabulation is for data that span the full concentration range (eight levels) as well as subsets of the complete data set. In the latter cases, levels have been excluded from the regression in a cumulative fashion starting with the highest concentration and progressing to increasingly lower concentrations. This procedure provides an objective means of evaluating the practical linear calibration range using trends in the correlation coefficient and response factors (*i.e.* the slope) for each regression analysis.

All calibration curves for the complete concentration range (All Data) exhibit a convex upward trend. The correlation coefficients and slopes tend to increase (and then plateau) as increasing numbers of levels (at the highest concentrations) are excluded from analysis. For example, higher correlation coefficients and slopes are obtained when all but the three highest levels (All Data-3) are used as compared to the case where all eight levels (All Data) are included in the regressions. The results show

TABLE III
STATISTICAL RESULTS OF MULTIPOINT CALIBRATION

Compound	Dataset ^a									
	All Data		All Data-1		All Data-2		All Data-3		All Data-4	
	<i>r</i> ²	Slope ^b	<i>r</i> ²	Slope	<i>r</i> ²	Slope	<i>r</i> ²	Slope	<i>r</i> ²	Slope
Benzene	0.790	1.98	0.879	3.96	0.964	5.74	0.994	7.86	0.995	7.26
Toluene	0.841	2.53	0.922	4.76	0.925	6.55	0.989	7.79	0.967	7.47
Ethylbenzene	0.889	3.11	0.962	5.48	0.963	6.94	0.996	7.38	0.993	6.63
<i>o</i> -Xylene	0.864	2.80	0.946	5.14	0.997	6.79	0.997	7.36	0.995	6.94
1-Methyl-3-ethylbenzene	0.929	5.51	0.974	8.82	0.996	6.92	0.998	7.51	0.998	6.99
1-Methyl-2-propylbenzene	0.853	2.59	0.941	4.84	0.994	6.47	0.996	7.23	0.987	6.68
1,2,3,4-Tetramethylbenzene	0.854	2.34	0.935	4.33	0.989	5.81	0.994	6.84	0.983	6.04

^a All data = includes all eight levels; All Data-1 = all levels but highest; All Data-2 = all levels but two highest; All Data-3 = all levels but 3 highest; All Data-4 = all levels but 4 highest.

^b Slope = [peak area (cts)/concentration (ng ml⁻¹)] · 10⁻⁵

TABLE IV

LIMITS OF DETECTION (LOD) AND QUANTITATION (LOQ) FOR PURGE-AND-TRAP CAPILLARY GC WITH FID ($\mu\text{g l}^{-1}$)LOD and LOQ determined as mean + 3 S.D. and mean + 10 S.D., respectively based on $n = 5$ (Keith et al. [43]).

Compound	LOD	LOQ
Benzene	0.019	0.043
Toluene	0.043	0.058
Ethylbenzene	0.022	0.037
<i>m,p</i> -Xylene	0.072	0.155
[$^2\text{H}_{10}$] <i>o</i> -Xylene	0.022	0.054
<i>o</i> -Xylene	0.027	0.066
Isopropylbenzene	0.011	0.029
<i>n</i> -Propylbenzene	0.006	0.014
1-Methyl-3-ethylbenzene	0.041	0.109
1-Methyl-4-ethylbenzene	0.015	0.035
1,3,5-Trimethylbenzene	0.023	0.060
1-Methyl-2-ethylbenzene	0.016	0.042
<i>tert.</i> -Butylbenzene + 1,2,4-Trimethylbenzene	0.169	0.442
Isobutylbenzene	0.022	0.060
<i>sec.</i> -Butylbenzene	0.003	0.005
1-Methyl-3-isopropylbenzene	0.016	0.041
1,2,3-Trimethylbenzene + 1-Methyl-4-isopropylbenzene	0.008	0.016
1-Methyl-2-isopropylbenzene	0.003	0.007
1,3-Diethylbenzene	0.020	0.048
1-Methyl-3-propylbenzene	0.020	0.046
1-Methyl-4-propylbenzene + 1,4-Diethylbenzene + <i>n</i> -Butylbenzene	0.020	0.049
1,2-Diethylbenzene	0.035	0.080
1,3-Dimethyl-5-ethylbenzene	0.023	0.058
1-Methyl-2-propylbenzene	0.035	0.092
1,4-Dimethyl-2-ethylbenzene	0.028	0.073
1,3-Dimethyl-4-ethylbenzene	0.020	0.054
1,2-Dimethyl-4-ethylbenzene	0.011	0.026
1,3-Dimethyl-2-ethylbenzene	0.080	0.191
1,2-Dimethyl-3-ethylbenzene	0.120	0.299
1,2,3,5-Tetramethylbenzene	0.027	0.067
1,2,3,4-Tetramethylbenzene	0.025	0.066

that the effective linear calibration range is approximately <0.2 to $10 \mu\text{g l}^{-1}$ (purge vessel concentration). This narrow range does not reflect a limitation of the flame ionization detector, but rather the purge-and-trap GC system as a whole.

We also analyzed VFW repetitively in order to estimate limits of detection and quantitation for all the compounds in our calibration mixture. A summary of these results is given in Table IV. In general, the data show that the C_6 - C_{10} aromatics can be detected at concentrations above approximately 30 ng l^{-1} . These detection limits are similar to, albeit slightly higher than, data reported by Ho [22] obtained with a photoionization detector. On the other

hand, they are significantly lower than those observed by a number of other investigators using variants of the purge-and-trap method [15,23,41,42].

Method performance

In order to develop estimates of method precision, we performed analyses of contaminated groundwater samples collected with a PTFE bailer. Groundwater was sampled from water table wells in the vicinity of a crude oil spill. All wells were located downgradient of the spill area, and no visible free oil phase was present. Data for three representative wells are presented in Table V. Replicates

TABLE V

RESULTS OF ANALYSES OF REPLICATE SAMPLES OF OIL-CONTAMINATED GROUNDWATER AND PRODUCED WATER

Sample	n	Component	Concentration ($\mu\text{g l}^{-1}$)		R.S.D. (%)
			Mean	S.D.	
<i>Groundwater samples^a</i>					
522A	7	Benzene	2080	198	9.5
		Toluene	353	51	14.4
		$\sum\text{C}_8\text{-aromatics}$	1060	71	6.7
		$\sum\text{C}_9\text{-aromatics}$	470	40	8.5
		$\sum\text{C}_{10}\text{-aromatics}$	218	19	8.5
		Bz + $\sum\text{ABs}$	4190	293	7.0
534B	3	Benzene	618	19	3.1
		Toluene	94.2	9.5	10.0
		$\sum\text{C}_8\text{-aromatics}$	313	5.1	1.6
		$\sum\text{C}_9\text{-aromatics}$	235	11.5	4.9
		$\sum\text{C}_{10}\text{-aromatics}$	150	4.9	3.3
		Bz + $\sum\text{ABs}$	1410	21	1.5
530B	5	Benzene	15.2	1.6	10.5
		Toluene	0.48	0.23	47.6
		$\sum\text{C}_8\text{-aromatics}$	0.73	0.04	5.4
		$\sum\text{C}_9\text{-aromatics}$	2.21	0.18	8.3
		$\sum\text{C}_{10}\text{-aromatics}$	61.0	4.08	6.7
		Bz + $\sum\text{ABs}$	79.7	5.79	7.3
<i>Produced water^b</i>					
Wemco #3	4	Benzene	1210	15.6	1.3
		Toluene	1390	22.7	1.6
		$\sum\text{C}_8\text{-aromatics}$	945	30.5	3.2
		$\sum\text{C}_9\text{-aromatics}$	319	18.6	5.8
		$\sum\text{C}_{10}\text{-aromatics}$	361	46.5	12.9
		Bz + $\sum\text{ABs}$	4225	103	2.4

^a Samples collected in 1987 from groundwater contamination site near Bemidji, MN, USA (Eganhouse *et al.* [33]).^b Sample collected in 1988 from onshore treatment plant, Carpinteria, CA, USA.

were taken as separate subsamples ($n = 3\text{--}7$) from a single deployment of the bailer at wells representing varying degrees of contamination (benzene + $\sum\text{C}_7\text{--C}_{10}$ aromatics = 0.08 to 4.2 mg l⁻¹). It is assumed that the water collected within the bailer is homogeneous with respect to dissolved constituents. However, for purposes of comparison, we also performed replicate analyses of a produced water sample collected from an onshore oil production treatment plant. In this case, the *same* sample was repeatedly analyzed ($n = 4$) over a one day period to estimate method precision. Alkylbenzenes were determined by purge-and-trap HRGC-FID according to procedures described in the Experimental section.

The method precision for individual (benzene, toluene) and homologue group analytes ranges from *ca.* 1.3–48% relative standard deviation (R.S.D.), but most values fall below 10%. The high R.S.D. values for toluene in the groundwater sample from well 530B (48%) is attributable to an anomalous result obtained for one of the five replicate subsamples (toluene concentration = 0.88 $\mu\text{g l}^{-1}$). The R.S.D. values for individual alkylbenzenes (data not tabulated here) were generally less than 10% with the lowest values being observed for the more highly contaminated samples. These results are consistent with data developed by other investigators using purge-and-trap HRGC methodology [15,23,41].

TABLE VI

RECOVERY OF [²H₁₀]o-XYLENE FROM CONTAMINATED GROUNDWATER SAMPLES

Spiked concentration ($\mu\text{g l}^{-1}$)	n	Recovery		
		Mean (%)	1 S.D.	R.S.D. (%)
51.4	28	85.4	16.5	19.3
5.14	17	108.8	21.8	20.1
0.51	19	103.8	20.5	19.7

Finally, as part of our field studies near Bemidji in 1987 we measured the recovery of [²H₁₀]o-xylene from 64 field-spiked groundwater samples. These included petroleum-contaminated water samples containing widely varying concentrations of aromatic hydrocarbons and pristine groundwater collected from a control well. Three spiking levels were used within a concentration range of 0.51 to 51.4 $\mu\text{g l}^{-1}$. The results, given in Table VI, show that mean recoveries ranged from ca. 85–109%. The same degree of variation (about 20% R.S.D.) was observed regardless of the spike solution concentration. These recoveries are similar to data reported by other investigators [22,23,41]. However, when compared with results obtained from the analysis of replicate samples of ground water (Table V), the precision associated with recovery of [²H₁₀]o-xylene in the field-spiked samples was significantly poorer. This difference is most likely attributable to errors associated with the field spiking procedures and possible matrix effects. Until improved procedures for spiking field samples are developed, recovery correction of the data would appear to be unwarranted.

CONCLUSIONS

A method for determining C₆–C₁₀ aromatic hydrocarbons in contaminated water samples has been developed based on purge-and-trap GC with FID and MS. When HRGC–MS is used, benzene and 33 of the 35 C₇–C₁₀ aromatics can be identified and measured within a chromatographic run time of approximately 45 min. When FID is employed, benzene and 26 alkylbenzenes can be determined with a detection limit of approximately 30 ng l⁻¹. The precision of the method is generally less than

10%, and recovery of surrogates spiked in contaminated field samples ranges from 85–108%.

ACKNOWLEDGEMENTS

The authors wish to acknowledge the assistance of the following individuals in collecting field samples: M. Hult, B. Miller, G. Justin, M. J. Baedecker, I. M. Cozzarelli and B. A. Bailer. Financial assistance for this work was provided by the US Geological Survey Toxic Substances Hydrology Research Program and the American Petroleum Institute.

REFERENCES

- 1 M. J. Baedecker, I. Cozzarelli and C. Phinney, in *Proc. U.S. Geological Survey Toxic Substances Hydrology Program, Monterey, CA, March 11–15, 1991*, US Geological Survey, Reston, VA, 1991, pp. 287–293.
- 2 J. F. Barker, J. S. Tessmann, P. E. Plotz and M. Reinhard, *J. Contam. Hydrol.*, 1 (1986) 171.
- 3 R. P. Eganhouse, T. F. Dorsey and C. S. Phinney, in *Proc. U.S. Geological Survey Toxic Substances Hydrology Program, Pensacola, FL, March 23–27, 1987; Report 87-109*, US Geological Survey Open-File, VA, 1987, p. C-29.
- 4 G. A. Eiceman, J. T. McConnon, M. Zaman, C. Shuey and D. Earp, *Int. J. Environ. Anal. Chem.*, 24 (1986) 143.
- 5 C. Först, L. Stieglitz, W. Roth and S. Kuhnlich, *Int. J. Environ. Anal. Chem.*, 37 (1989) 287.
- 6 S. Lesage, R. E. Jackson, M. W. Priddle and P. G. Riemann, *Environ. Sci. Technol.*, 24 (1990) 559.
- 7 M. Reinhard, N. L. Goodman and J. F. Barker, *Environ. Sci. Technol.*, 18 (1984) 953.
- 8 D. H. Stuermer, D. J. Ng and C. J. Morris, *Environ. Sci. Technol.*, 16 (1982) 582.
- 9 J. M. Thomas, V. R. Gordy, S. Fiorenza and C. H. Ward, *Water Sci. Technol.*, 22 (1990) 53.
- 10 R. P. Schwarzenbach, W. Giger, E. Hoehn and J. K. Schneider, *Environ. Sci. Technol.*, 17 (1983) 472.
- 11 R. Otson, *Int. J. Environ. Anal. Chem.*, 31 (1987) 41.
- 12 J. B. Ferrario, G. C. Lawler, I. R. DeLeon and J. L. Laseter, *Bull. Environ. Contam. Toxicol.*, 34 (1985) 246.

- 13 D. van de Meent, J. A. den Hollander, W. G. Pool, M. J. Vredenburg, H. A. M. van Oers, E. de Greef and J. A. Luijten, *Water Sci. Technol.*, 18 (1986) 73.
- 14 A. Bianchi, M. S. Varney and J. Phillips, *J. Chromatogr.*, 467 (1989) 111.
- 15 B. J. Harland, F. J. Whitby and M. H. I. Combèr, *Int. J. Environ. Anal. Chem.*, 20 (1985) 295.
- 16 J. F. Barker, G. C. Patrick and D. Major, *Ground Water Monitor. Rev.*, 7 (1987) 64.
- 17 J. A. Swallow and P. M. Gschwend, in *Proc. 3rd National Symposium Aquifer Restoration and Ground-Water Monitoring, Columbus, OH, May 25-27, 1983*, 1983, pp. 327-333.
- 18 W. J. Weber, P. M. McGinley and L. E. Katz, *Water Res.*, 25 (1991) 499.
- 19 I. M. Cozzarelli, R. P. Eganhouse and M. J. Baedeker, *Environ. Geol. Water Sci.*, 16 (1990) 135.
- 20 M. Duffy, J. N. Driscoll, S. Pappas and W. Sanford, *J. Chromatogr.*, 441 (1988) 73.
- 21 W. E. Hammers and H. F. P. M. Bosman, *J. Chromatogr.*, 360 (1986) 425.
- 22 J. S.-H. Ho, *J. Chromatogr. Sci.*, 27 (1989) 91.
- 23 R. Otson and C. Chan, *Int. J. Environ. Anal. Chem.*, 30 (1987) 275.
- 24 J. F. Pankow, *J. High Resolut. Chromatogr. Chromatogr. Commun.*, 9 (1986) 18.9.
- 25 S. Sporstøl, K. Urdal, H. Drangsholt and N. Gjøs, *Int. J. Environ. Anal. Chem.*, 21 (1985) 129.
- 26 D. R. Thielen, G. Olsen, A. Davis, E. Bajor, J. Stefanovski and J. Chodkowski, *J. Chromatogr. Sci.*, 25 (1987) 12.
- 27 J. I. Gómez-Belinchón and J. Albaigés, *Int. J. Environ. Anal. Chem.*, 30 (1987) 183.
- 28 K. Grob, *J. Chromatogr.*, 84 (1973) 255.
- 29 E. Stottmeister, P. Hendel and H. Hermenau, *Chemosphere*, 17 (1988) 801.
- 30 P. L. Wylie, *J. Am. Water Works Assoc.*, 80 (1988) 65.
- 31 S. V. Lucas, H. M. Burkholder and A. Alford-Stevens, *Project Summary: Heated Purge and Trap Method Development and Testing*, US Environmental Protection Agency, Washington, DC, 1988, 5 pp.
- 32 T. Bellar and J. J. Lichtenberg, *J. Am. Water Works Assoc.*, 66 (1974) 739.
- 33 R. P. Eganhouse, M. J. Baedeker, I. M. Cozzarelli, G. R. Aiken, K. A. Thorn and T. F. Dorsey, *Appl. Geochem.*, submitted for publication.
- 34 N. G. Johansen, L. S. Etre and R. L. Miller, *J. Chromatogr.*, 256 (1983) 393.
- 35 R. P. Eganhouse, M. J. Baedeker, C. Phinney and J. Hopple, in *Proc. 2nd Techn. Meeting, Cape Cod, MA, October 21-25 1985; Report 86-481*, US Geological Survey Open-File, Reston, VA, 1988, p. C-27.
- 36 B. Kumar, R. K. Kuchhal, P. Kumar and P. L. Gupta, *J. Chromatogr. Sci.*, 24 (1986) 899.
- 37 E. Matisová, J. Krupčík, P. Cellár and A. Kocan, *J. Chromatogr.*, 346 (1985) 177.
- 38 B. S. Middleditch, *J. Chromatogr.*, 239 (1982) 171.
- 39 L. Soják and J. A. Rijks, *J. Chromatogr.*, 119 (1976) 505.
- 40 R. G. Mathews, J. Torres and R. D. Schwartz, *J. Chromatogr. Sci.*, 20 (1982) 160.
- 41 R. Otson and D. T. Williams, *Anal. Chem.*, 54 (1982) 942.
- 42 J. G. Schnable, B. Dussert, I. H. Suffet and C. D. Hertz, *J. Chromatogr.*, 513 (1990) 47.
- 43 L. H. Keith, W. Crummett, J. Deegan, R. A. Libby, J. K. Taylor and G. Wentler, *Anal. Chem.*, 55 (1983) 2210.

CHROM. 24 599

Determination of bacterial muramic acid by gas chromatography–mass spectrometry with negative-ion detection

Ingrid Elmroth

Department of Technical Analytical Chemistry, Chemical Centre, University of Lund, Box 124, 221 00 Lund (Sweden)

Alvin Fox

Department of Microbiology and Immunology, School of Medicine, University of South Carolina, Columbia, SC 29208 (USA)

Lennart Larsson

Department of Medical Microbiology, University of Lund, Sölvegatan 23, 223 62 Lund (Sweden)

(Received July 21st, 1992)

ABSTRACT

A gas chromatographic–mass spectrometric method for the determination of trace amounts of muramic acid was developed. Muramic acid, a compound unique to bacterial peptidoglycan, not present elsewhere in nature, was measured as its trifluoroacetylated methyl glycoside, and in that form could be determined at low picogram levels (injected amount) when using negative-ion chemical ionization. The method included methanolysis, extraction, evaporation and acetylation. The presence of excess amounts of yeast in the samples did not interfere with the analysis. The method is rapid and simple and is useful for the determination of small amounts of peptidoglycan in complex environments.

INTRODUCTION

The development of chromatographic and mass spectrometric methods for the analysis of bacterial constituents has considerably facilitated the detection and differentiation of small amounts of bacteria in complex samples. Such methods are of importance when early detection of bacteria is vital, as in medical diagnosis and in the food and biotechnology industries [1]. Chemical markers, that is, cellular components specific to the microorganisms, are used as analytes.

Correspondence to: I. Elmroth, Department of Technical Analytical Chemistry, Chemical Centre, University of Lund, Box 124, 221 00 Lund, Sweden.

One of the most selective and sensitive chromatographic detectors is the mass spectrometer. In gas chromatography–mass spectrometry (GC–MS), the ionization techniques commonly used are electron impact (EI) and chemical ionization (CI). Compared with EI, negative-ion chemical ionization (NICI) of halogenated derivatives frequently improves the selectivity as underivatized materials are not detected (as they do not contain halogens). Minimum fragmentation of the analyte occurs with NICI because the ionization is gentler, which in turn often results in reduced background noise. In addition, halogenated derivatives are extremely strong electron-capturing compounds, hence the sensitivity is also greatly enhanced.

The bacterial cell wall skeleton, peptidoglycan,

contains a polysaccharide backbone with the repeating monomers N-acetylglucosamine and N-acetylmuramic acid. As muramic acid (MuAc) is unique to bacteria, it has been used as a chemical marker for detecting both intact bacteria and bacterial debris in, *e.g.*, synovial fluids in animal models of arthritis [2]. In the literature on MuAc analysis, MS methods described include GC–EI–MS of alditol acetate [3], aldononitrile [4,5] and trimethylsilyl (TMS) derivatives [6], and NICI–MS of N-heptafluorobutyryl isobutyl ester derivatives [7]. In addition, an HPLC–MS method for the determination of underivatized MuAc has been reported [8].

In the alditol acetate GC–MS procedure, MuAc is released by hydrolysis and the aldehyde group of the acid is then reduced (to eliminate the anomeric centre) and hydroxyl and amino moieties are subsequently acetylated. The carboxyl group of MuAc forms a lactam [9]; other carboxyl groups, such as those found in amino acids, do not appear to be derivatized. Between the reduction and acetylation steps, the reducing agent (borohydride) is removed (as tetramethylborate gas) by multiple evaporations with methanol–acetic acid, a process that is time consuming. The procedure incorporates prederivatization clean-up steps that remove hydrophobic substances (*e.g.*, fatty acids) before acetylation of hydroxyl or amino groups.

Earlier attempts to develop simpler methods to replace the alditol acetate procedure have not been entirely successful. In the aldononitrile procedure, reaction of the aldehyde moiety with hydroxylamine (to destroy the anomeric centre) replaces reduction with sodium borohydride, and multiple evaporation steps to remove borate are thus eliminated. Unfortunately, with this procedure, extraneous peaks are generated from side-reactions between the hydroxylamine and acetic anhydride [4,5]. The TMS derivative of MuAc is simple to prepare although rather unstable [6]. HPLC–MS analysis, in contrast to other methods, requires a minimum of sample pre-treatment as derivatization is not necessary, but at present this technique does not allow the detection of sub-nanogram injected amounts of MuAc [8].

In this work, a procedure for the trace determination of MuAc was developed in which samples were methanolysed and then subjected to trifluoroacetylation. This procedure was adapted from the technique that Pritchard *et al.* [10] used successfully with

electron-capture detection. Other NICI–MS procedures for MuAc determination have been developed, but not widely used, however [2,7]. In comparison, highly sensitive and useful GC–NICI–MS methods have been developed for certain other chemical markers of microorganisms, *e.g.*, tuberculostearic acid [11], D-alanine [12,13] and 3-hydroxy-fatty acids [14,15].

EXPERIMENTAL

Chemicals

Acetyl chloride (purity >99%) was obtained from Fluka (Buchs, Switzerland), trifluoroacetic anhydride (TFA) (purity >99%) from Janssen Chimica (Beerse, Belgium), muramic acid (purity 99%), L-rhamnose, D-ribose, D-glucose, D-galactose, D-glucosamine and D-galactosamine from Sigma (St. Louis, MO, USA) and N-methyl-D-glucamine (purity 99%) from Aldrich Chemie (Steinheim, Germany). All solvents were of analytical-reagent grade and used without further purification. Prior to use, glassware was washed in 5% Deconex (Borer Chemie, Zuchwil, Switzerland), rinsed several times with hot tap water and then heated at 400°C for 10 h.

Microorganisms

A strain of group G streptococci isolated from a clinical specimen at the Clinical Microbiology Laboratory, Lund Hospital, was sub-cultured overnight on blood agar plates at 37°C and then inoculated in 10 ml of Todd Hewitt Broth (Difco, MI, USA) and grown overnight at 37°C. The bacteria were then washed and centrifuged (10 000 *g*, 15 min) three times and then resuspended in 0.9% sodium chloride. *Saccharomyces cerevisiae*, isolated from bakers' yeast, was cultured in 100 ml of Lactobacillus Carrying Medium [16] at 32°C for 24 h and then washed and centrifuged and resuspended five times, as described above. Following this procedure, the microorganisms were freeze-dried.

Group A streptococcal cell walls (PG-PS) were prepared as described previously [17]. In brief, streptococcal cells were solubilized by extensive sonication and intact cells and high-molecular-mass debris were removed by centrifugation at 10 000 *g*. The cell wall fragments were then treated sequentially with hyaluronidase, ribonuclease and deoxyribonuclease, papain and pepsin; between the enzyme

treatments, buffers were changed by dialysis. Cell walls were then separated from enzymes and degraded cellular constituents by centrifugation at 110 000 g, extracted with chloroform–methanol and freeze-dried.

Gas chromatography–mass spectrometry

The GC–MS analyses were performed on a Hewlett-Packard (Palo Alto, CA, USA) Model 5890 gas chromatograph connected to a VG Trio 1-S mass spectrometer (VG Masslab, Manchester, UK). The mass spectrometer was used in the CI mode with NI detection. A fused-silica capillary column (25 m × 0.25 mm I.D.), containing cross-linked OV-1 as the stationary phase, was interfaced directly to the ion source. Volumes of 1 μ l were injected in the splitless mode (injector temperature 260°C) using a Hewlett-Packard Model 7673 autosampler. Helium, at a column head pressure of 10 psi (1 psi = 6894.76 Pa), served as the carrier gas, and isobutane (ionized at an energy of 70 eV) as the reagent gas. The initial column temperature (70°C) was increased at 8°C/min to 200°C and the temperature of the GC–MS interface was 260°C. The ion source temperature was 110°C; for comparisons, fragmentation patterns of the MuAc derivative were also studied at ion source temperatures of 80, 110, 130 and 150°C. Both scan mode and selected ion monitoring (SIM), measuring the ions m/z 674, 657, 567 and 480, were used in the experiments.

Sample treatment

Samples (1–2 mg) were methanolysed under a nitrogen atmosphere at 85°C for 18 h in 1 ml of 4 M methanolic hydrochloric acid (HCl; prepared by adding acetyl chloride dropwise to methanol while cooling in an ice-bath). After cooling, 1–10 μ g of the internal standard N-methyl-D-glucamine, dissolved in 100 μ l methanol, were added, and the methanolysate was extracted with 2 ml of hexane. After evaporating the methanolic phase to dryness at 40°C under a stream of nitrogen, 50 μ l of TFA and 50 μ l of acetonitrile were added; derivatization was performed at 60°C for 5 min. Subsequently, the derivatized samples were allowed to stand for 5 min at room temperature, whereafter 400 μ l of acetonitrile were added. Sample portions (50–100 μ l) were then transferred to new test-tubes, evaporated to approximately half the volume, diluted with acetonitrile

(0.1–1.0 ml) and finally analysed (1- μ l aliquots) by GC–MS.

Relative yield and chemical stability

To investigate the influence of methanolysis time and concentration of the HCl on the relative yield of MuAc, duplicate bacterial samples were heated in 4 M methanolic HCl for 1, 3, 6, 18, 25, 38 and 48 h. In addition, separate samples were heated for 25 h in 1, 2, 3 and 4 M methanolic HCl and treated as described under *Sample treatment*. The area ratio between the molecular ion peak of MuAc and that of the internal standard was calculated.

Different TFA derivatization conditions were also investigated. Bacteria were first heated in 4 M methanolic HCl at 85°C for 18 h and then subjected to hexane extraction (see *Sample treatment*), whereafter eight 100- μ l aliquots of the methanolic phase were placed in separate tubes. The liquid in the tubes was evaporated and 50 μ l of acetonitrile and the same amount of TFA were added. Derivatization of duplicate samples was performed at 80°C for 10 min, 80°C for 5 min, 60°C for 10 min and 60°C for 5 min. Derivatized internal standard was added and the samples were evaporated to approximately half the volume, diluted in acetonitrile (see *Sample treatment*) and analysed in the scan mode. For each of the individual samples the area ratio between the molecular ion peak of MuAc and that of the internal standard was calculated.

To evaluate the chemical stability of the derivatives, two bacterial TFA preparations and one PG-PS TFA preparation were stored in a refrigerator (a) after removal of TFA by evaporation (as described under *Sample treatment*) and (b) in the presence of 10% TFA. The samples were analysed (scan mode) after 1, 3 and 7 days of storage, and the peak areas of the molecular ions of MuAc and the internal standard, selected from the total ion current profile, were integrated. The evaporated samples were compared with those of the corresponding samples stored in 10% TFA.

Linearity, precision, accuracy, quantification and limit of determination

To investigate the linearity and precision of the overall analytical procedure, six bacterial samples were heated in 4 M methanolic HCl, then extracted with hexane and evaporated to dryness (as described

under *Sample treatment*), and the resulting residues were dissolved in 2 ml of methanol. Volumes corresponding to 5, 12.5, 25, 50, 125 and 250 μg (dry mass) of bacterial cells were then taken from two of these solutions and placed in separate vials, and the methanol was subsequently evaporated. In addition, volumes corresponding to 50 and 250 μg of bacterial cells were transferred from the remaining four samples into separate vials. Internal standard (2.0 μg) was added to each of these vials and the samples were derivatized with TFA (see *Sample treatment*). After 5 min at room temperature, 100 μl of acetonitrile were added. A 100- μl portion was then transferred into a new test-tube, evaporated to approximately half the volume, diluted with 400 μl of acetonitrile and analysed in the SIM mode. A graph illustrating the area ratios between the molecular ion peak of MuAc and that of the internal standard *versus* the total amount of bacteria in the sample was constructed.

To investigate the limit of determination for bacterial MuAc in the GC–MS part of the method, bacterial samples were heated in 4 M methanolic HCl, extracted with hexane and evaporated (see *Sample treatment*). The residues were dissolved in 1 ml of methanol and then diluted tenfold. Portions (100 μl) of the diluted residues were transferred into

new tubes for evaporation and TFA derivatization (see *Sample treatment*). After 5 min at room temperature, 400 μl of acetonitrile were added, a 50- μl portion was evaporated to half the volume and diluted with 0.1–2.0 ml acetonitrile and finally analysed in the SIM mode. The limit of determination was defined as the amount of MuAc injected into the GC–MS system that gave a signal-to-noise ratio of about 6 (peak-to-peak noise).

For determination of the amount of MuAc in the bacteria, four samples of 1.2–1.5 mg of PG-PS and four bacterial samples were processed (see *Sample treatment*). The amount of MuAc in the PG-PS preparation (7.7% w/w, dry mass) had previously been determined by the alditol acetate method [17]. The GC–MS analyses were performed in the SIM mode. The amount of MuAc in the bacteria was determined by comparing the bacterial samples with the PG-PS samples with respect to the area ratio between the molecular ion peak of MuAc and that of the internal standard.

Detection of muramic acid in the presence of yeast

Bacterial and yeast samples were heated separately in 4 M methanolic HCl, extracted with hexane and evaporated. After this procedure, the yeast preparations were immediately derivatized with TFA and

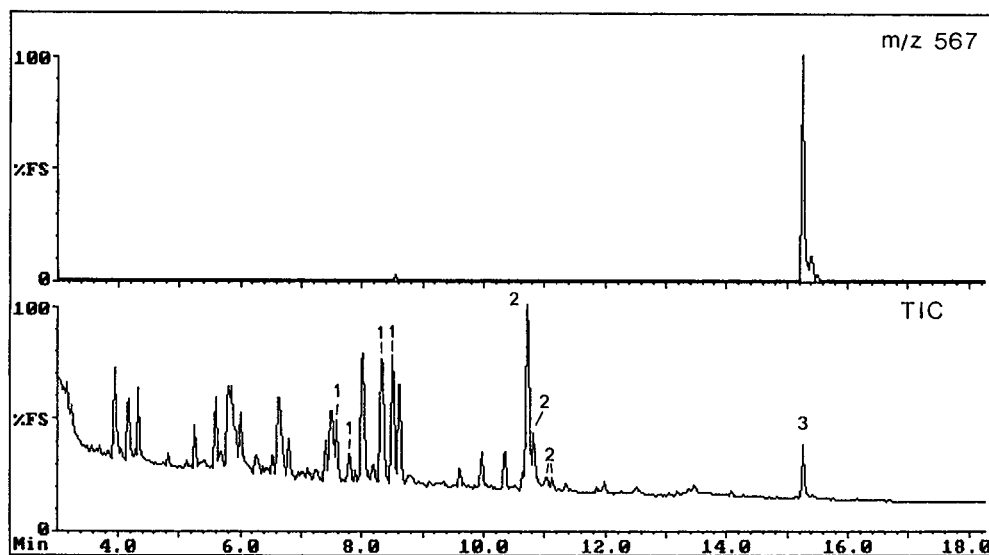


Fig. 1. Bottom trace: total ion current NICI profile of derivatized group G streptococcal carbohydrates analysed in the scan mode; glucose (1), glucosamine (2) and MuAc (3) are indicated. Top trace: ion current profile selected from the same analysis and showing the molecular ion of MuAc (m/z 567).

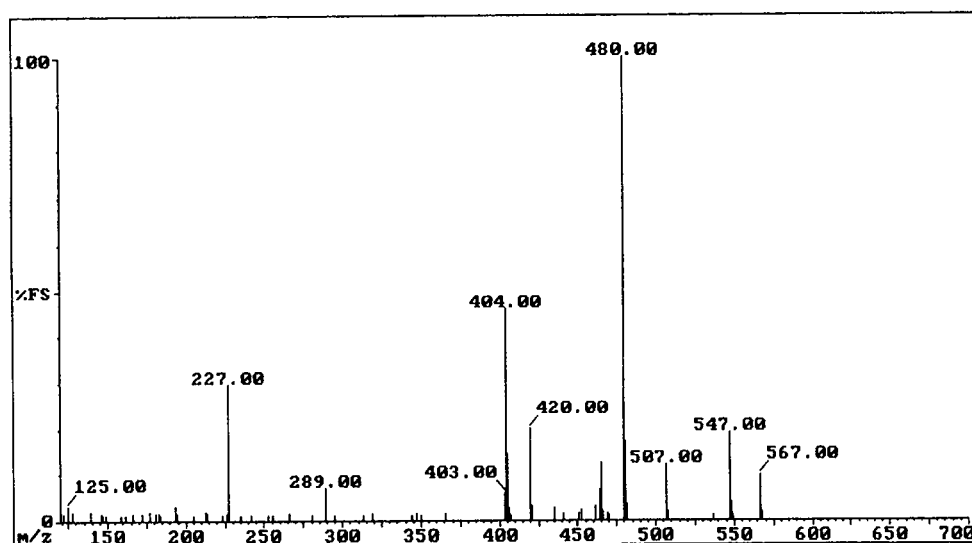
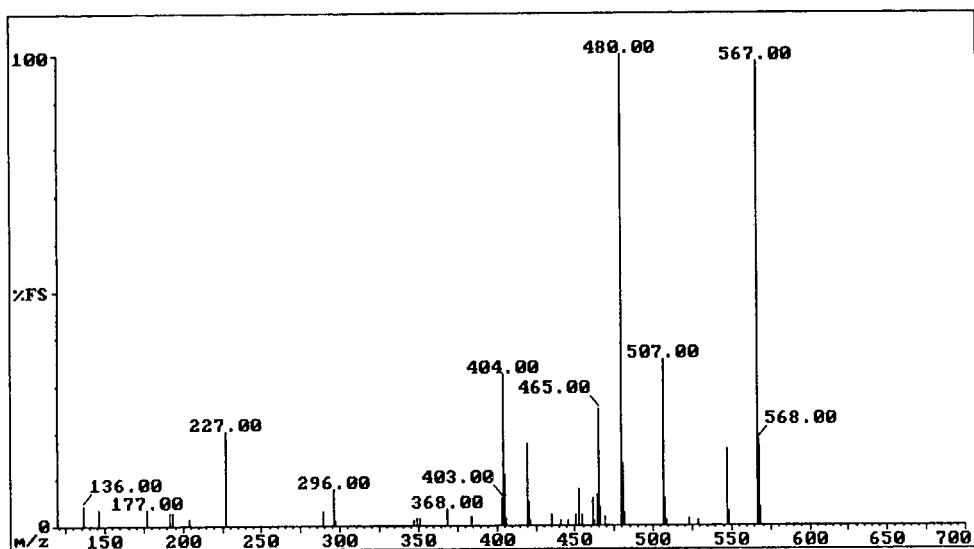


Fig. 2. NICI mass spectra of the MuAc TFA derivative at ion source temperatures of 80 (top) and 110°C (bottom).

then dissolved in 400 μ l of acetonitrile, whereas the bacterial preparations were dissolved in 1 ml of methanol, diluted tenfold, transferred (100- μ l aliquots) into new tubes and evaporated, and then derivatized with TFA and dissolved in 400 μ l of acetonitrile. Portions (25–50 μ l) of the derivatized bacteria samples were then mixed with portions (100 μ l) of the derivatized yeast, and these mixtures

were subsequently evaporated to half the volume, diluted with 1 ml of acetonitrile and subjected to GC-MS analysis in the SIM mode.

RESULTS

Gas chromatography-mass spectrometry

A total ion current (TIC) profile of the carbo-

hydrates in the group G streptococcal strain (analysed in the scan mode) is presented in Fig. 1 (bottom trace). The top trace shows an ion current profile that was selected from the TIC profile and focused on the molecular ion of the MuAc derivative (m/z 567). Glucosamine, galactosamine, glucose, galactose, ribose and rhamnose were identified by comparing their spectra and retention times with those of corresponding reference substances. The MuAc derivative eluted after 15.3 min, *i.e.*, about 5 min after the other amino sugars and 7 min after the internal standard derivative.

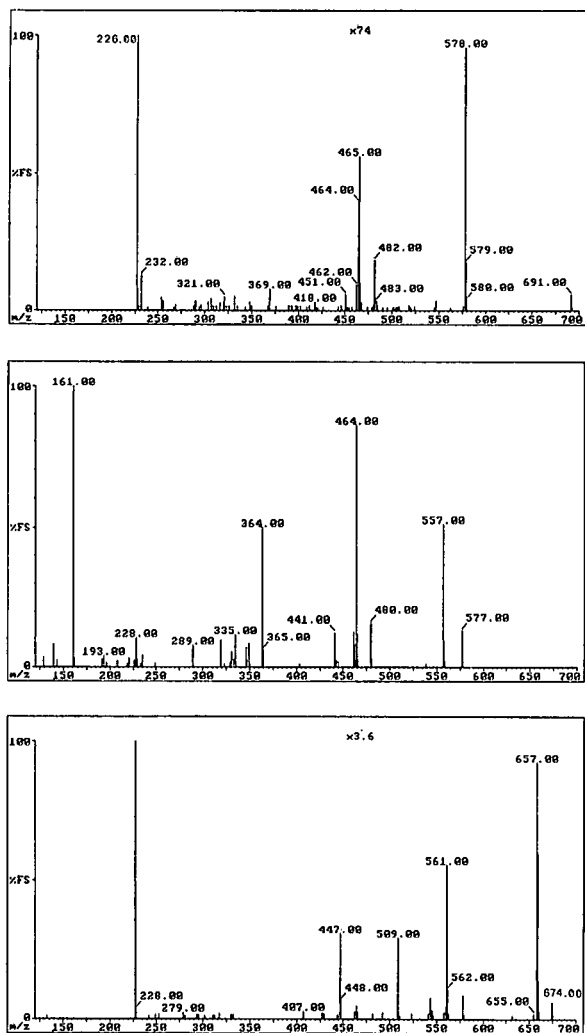


Fig. 3. NICI mass spectra of TFA-derivatized glucose (top), glucosamine (centre) and N-methyl-D-glucamine (internal standard) (bottom) at an ion source temperature of 110°C.

The relative abundance of the fragments in the mass spectrum of the MuAc derivative varied with the ion source temperature, and for the molecular ion of m/z 567, $[M]^-$, a significant decrease was seen at higher temperatures. Mass spectra produced at ion source temperatures of 80 and 110°C are shown in Fig. 2. The fragments found in the higher m/z range were interpreted as $[M - HF]^-$ (m/z 547), $[M - CH_3OCH = O]^-$ (m/z 507) and $[M - CH_3CHCOOCH_3]^-$ (m/z 480).

For comparison, mass spectra of the TFA derivatives of glucose, glucosamine (peaks marked 1 and 2 in Fig. 1) and N-methyl-D-glucamine are shown with the molecular ions of m/z 578, 577 and 674, respectively in Fig. 3. In the glucose spectrum additional prominent ions were found and interpreted as $[M + O = COCF_3]^-$ (m/z 691), $[M - O = CCF_3]^-$ (m/z 482); and $[M - O = COCF_3]^-$ (m/z 465); in the glucosamine spectrum the ions $[M - HF]^-$ (m/z 557) and $[M - O = COCF_3]^-$ (m/z 464) were found. Corresponding mass spectra were found for galactosamine, galactose, ribose and rhamnose.

Relative yield and chemical stability

The relative yield of MuAc achieved under different methanolysis conditions is illustrated in Fig. 4. When using 4 M methanolic HCl, the maximum

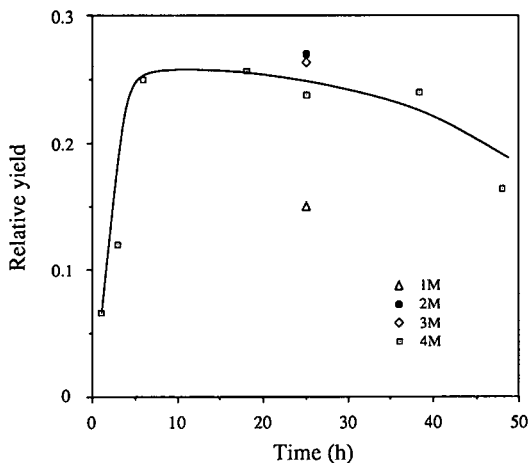


Fig. 4. Relative yield of MuAc obtained after heating streptococci in (□) 4 M methanolic HCl at 85°C for 1–48 h and in (Δ) 1, (●) 2 and (◇) 3 M methanolic HCl at 85°C for 25 h. Relative yields are expressed as bacterial response relative to the internal standard, *i.e.*, the area ratio between m/z 567 and m/z 674 ions. Values represent means for duplicate samples.

yield was reached after heating for 6 h. Yields obtained using 2, 3 and 4 M methanolic HCl were similar, whereas the yield using 1 M HCl was comparatively lower (methanolysis time 25 h).

The final TFA derivatization conditions chosen were heating for 5 min at 60°C. An increased temperature or derivatization time did not increase the yield.

The MuAc derivative was stable for 7 days, even when TFA had been evaporated. After 1 day of storage, the TFA-derivatized internal standard (in the absence of TFA) was not degraded, whereas after 3 days only 78% remained and after 1 week 44% (mean of three values).

Linearity, precision, accuracy, quantification and limit of determination

The relative response, *i.e.*, the area ratio between the molecular ion peak of MuAc (m/z 567) and the internal standard (m/z 674), *versus* the total amount of bacteria in the prepared samples is shown in Fig. 5. The straight line, fitted to the individual data using the method of least squares, followed the equation $y = 3.0 \cdot 10^{-3}x - 4.4 \cdot 10^{-3}$, where y is

the relative response and x is amount of bacteria. The relative standard deviation of the relative response was 10% for the six 50- μg samples (mean 0.143, $s_{n-1} = 0.016$) and 5.3% for the six 250- μg samples (mean 0.739, $s_{n-1} = 0.039$). The amount of MuAc in the bacteria was found to be 0.49% (dry mass). The limit of determination of the overall method, defined as the amount of MuAc which gave a relative standard deviation of 10%, was found to be 250 ng in the original sample, whereas the limit of determination of MuAc in the GC-MS part of the method was found to be 3 pg (injected amount).

Detection of muramic acid in the presence of yeast

SIM chromatograms focused on the ion of m/z 567 (MuAc) in the analysis of a preparation of 0.6 ng of bacterial cells (corresponding to 3 pg of MuAc) and 120 ng of yeast cells (injected amounts) and a corresponding chromatogram for 120 ng pure yeast are shown in Fig. 6. The noise was of equal magnitude to that when pure bacterial samples were analysed and no interfering responses from pure yeast were detected.

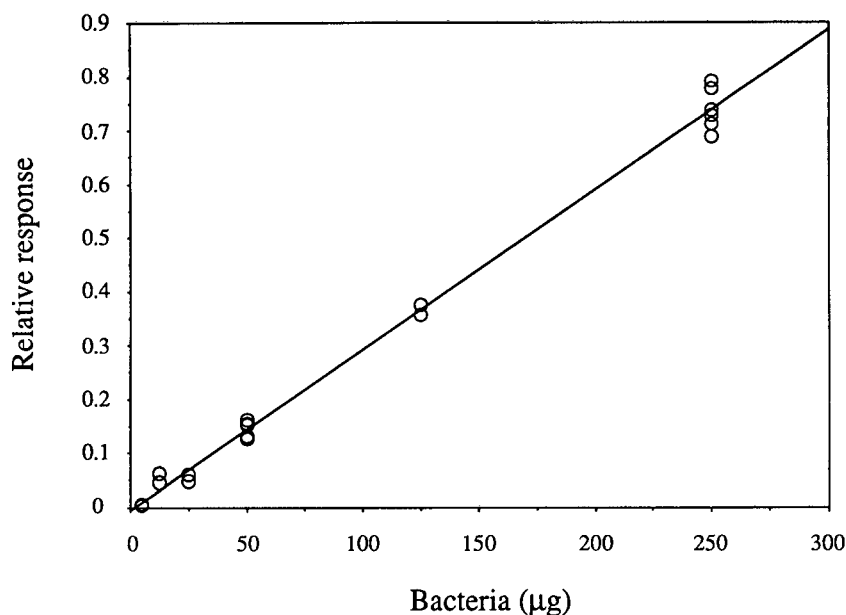


Fig. 5. Test of linearity, precision and accuracy. Relative response, *i.e.*, the area ratio between the molecular ion peak area of MuAc (m/z 567) and that of the internal standard (m/z 674), *versus* the total amount of bacteria in the samples, are shown. The method of least squares was used to fit a straight line to the individual data.

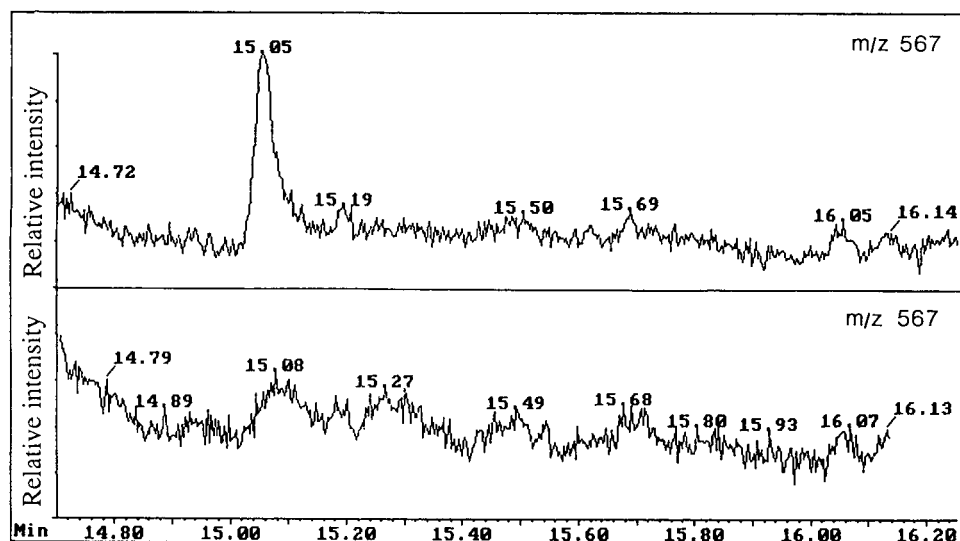


Fig. 6. Selected ion monitoring chromatograms (m/z 567) from analysis of MuAc. The top trace represents the injection of an amount corresponding to 0.6 ng of bacterial cells and 120 ng of yeast cells and the bottom trace the injection an amount corresponding to 120 ng of pure yeast. The higher noise apparent in the bottom trace is due to automatic normalization of the total ion current.

DISCUSSIONS

Chromatographic analysis of bacterial constituents is a useful method for the detection of bacteria or bacterial debris in biological samples and, in contrast to classical microbiological and biochemical procedures, culturing is not required. By coupling GC separation with MS detection, a high level of sensitivity is achieved that permits the determination of very small amounts of bacteria. The selectivity can be deliberately chosen by using analytes that are specific for particular species or genera or for bacteria in general. MuAc exemplifies the latter type of analyte, or chemical marker, as it is unique for bacteria. A highly sensitive and selective method for the determination of MuAc would allow the detection of trace amounts of peptidoglycan in, for example, environmental samples (*e.g.*, soil, ground water and air), foods, pharmacological products, biotechnical processes or body fluids (*e.g.*, samples for clinical diagnosis of infectious diseases).

Compared with GC–EI–MS analysis of the MuAc alditol acetate derivative, which provides a limit of detection of 2.5 ng (injected amount) [3], the NICI TFA method offers a considerable improvement in sensitivity, as MuAc can be determined at low pico-

gram levels. However, the alditol acetate method is more attractive for carbohydrate profiling than the NICI TFA method, as alditol acetates elute as single peaks, whereas multiple peaks appear upon TFA derivatization. The TFA derivative of MuAc eluted as one dominating and one minor peak (not baseline separated), with only the major peak being considered in the quantification.

Even under mild conditions TFA reacts with the hydroxyl groups of carbohydrates. As TFA derivatives are known to be unstable in the presence of moisture, it has been recommended that preparations should be stored at -20°C in a 10% excess of TFA [18]. We followed this recommendation and then evaporated the excess of TFA prior to analysis in order to prolong the life of the GC column. On storing the evaporated samples, the MuAc derivative was found to be stable for at least 1 week, whereas degradation of the N-methyl-D-glucamine derivative was observed after 3 days. We therefore recommend that samples devoid of an excess of TFA be analysed on the same day they are prepared to avoid problems in the quantification.

Compared with previously reported techniques, the NICI TFA method is simple, as it includes only one “clean-up” step. The hexane extraction of

methanolysates is effective in separating fatty acid methyl esters from methyl glycosides [19]. All water-soluble methanolysis products are present in the final sample, however. Despite this, the presence of a 200-fold excess of yeast did not interfere with analysis for trace amounts of MuAc derivative. To ascertain the identity of the MuAc and the internal standard derivative, we monitored four ions in the SIM analyses.

Methanolysis was the most time-consuming step in the TFA procedure. In addition to the production of methyl glycosides from the hydroxyl groups involved in linkage of monomeric units, the carboxyl group of muramic acid is methylated. The maximum yield was achieved after 6 h of heating.

The influence of the ion source temperature on the NICI mass spectra of halogenated derivatives has been described previously [20]. For the MuAc derivative, there was a major difference between the relative abundance of the fragments obtained at 80°C and those obtained at 110°C, whereas the mass spectrum at 150°C was almost identical with that at 110°C. To ensure optimum selectivity in the analysis, a high abundance of the molecular ion is desirable. A temperature of 110°C was used because it is the lowest stable ion source temperature permitted by our GC–MS system when using standard filaments. Previously reported data on fragmentation patterns of carbohydrate TFA derivatives [21] and N-heptafluorobutyl-2-butyl ester derivatives of (*R*)-alanine [22] were used in the interpretation of spectra.

Methanolysis of the free MuAc standard produced a mixture of compounds containing methyl and TFA groups (data not shown), whereas when bacteria were processed only the MuAc methyl glycoside was detected. A MuAc standard therefore cannot be used in the quantification. Instead, a peptidoglycan-containing specimen with a known amount of MuAc can be used; in our study, a PG-PS preparation with a MuAc content previously determined by the alditol acetate method was employed. In other investigations, N-methyl-D-glucamine has been used as an internal standard in determinations of bacterial carbohydrates [3,8]. The amount of bacterial MuAc found (0.49% of the dry mass) corresponded well with the amount found in *S. pyogenes* (0.53%) when using the alditol acetate method [5], and the complete carbohydrate compo-

sition of the group G streptococci analysed agreed well with previously reported results [10].

So far, the alditol acetate method has been used most often when determining MuAc. The NICI TFA method described here is superior in sensitivity, but its selectivity for different sample matrices remains to be evaluated. In addition, it should be investigated whether the use of a different internal standard would improve the precision in the overall method. Experiments are now being planned to assess the technique with regard to its applicability for the determination of peptidoglycan in organic dust and different kinds of clinical samples and for the detection of bacterial contamination of biotechnical processes.

ACKNOWLEDGEMENTS

We thank the Biotechnology Research Foundation (Sweden), the Swedish Board for Technical Development and the Center for Indoor Air Research (USA) for financially supporting our work.

REFERENCES

- 1 S. L. Morgan, A. Fox and J. Gilbert, *J. Microbiol. Methods*, 9 (1989) 57.
- 2 B. Christensson, J. Gilbert, A. Fox and S. L. Morgan, *Arthritis Rheum.*, 32 (1989) 1268.
- 3 J. Gilbert, A. Fox, R. S. Whiton and S. L. Morgan, *J. Microbiol. Methods*, 5 (1986) 271.
- 4 R. H. Findlay, D. J. W. Moriarty and D. C. White, *Geomicrobiology*, 3 (1983) 135.
- 5 W. L. Eudy, M. D. Walla, S. L. Morgan and A. Fox, *Analyst (London)*, 110 (1985) 381.
- 6 D. G. Pritchard, R. L. Settine and J. C. Bennett, *Arthritis Rheum.*, 23 (1980) 608.
- 7 A. Tunlid and G. Odham, *J. Microbiol. Methods*, 1 (1983) 63.
- 8 I. Elmroth, L. Larsson, G. Westerdahl and G. Odham, *J. Chromatogr.*, 598 (1992) 43.
- 9 A. Fox, S. L. Morgan and J. Gilbert, in J. Bierman and G. McGinnis (Editors), *Analysis of Carbohydrates by GLC and MS*, CRC Press, Boca Raton, FL, 1989, pp. 87–117.
- 10 D. G. Pritchard, J. E. Coligan, S. E. Speed and B. M. Gray *J. Clin. Microbiol.*, 13 (1981) 89.
- 11 L. Larsson, G. Odham, G. Westerdahl and B. Olsson, *J. Clin. Microbiol.*, 25 (1987) 893.
- 12 A. Sonesson, L. Larsson, A. Fox, G. Westerdahl and G. Odham, *J. Chromatogr.*, 431 (1988) 1.
- 13 K. Ueda, S. L. Morgan, A. Fox, J. Gilbert, A. Sonesson, L. Larsson and G. Odham, *Anal. Chem.*, 61 (1989) 265.
- 14 G. Odham, A. Tunlid, G. Westerdahl, L. Larsson, J. B. Guckert and D. C. White, *J. Microbiol. Methods*, 3 (1985) 331.

- 15 I. Elmroth, A. Valeur, G. Odham and L. Larsson, *Biotechnol. Bioeng.*, 35 (1990) 787.
- 16 L. Axelsson, T. C. Chung, W. J. Dobrogosz and S. E. Lindgren, *Microbiol. Ecol. Health Dis.*, 2 (1989) 131.
- 17 J. Gilbert, J. Harrison, C. Parks and A. Fox, *J. Chromatogr.*, 441 (1988) 323.
- 18 K. Bryn and E. Jantzen, *J. Chromatogr.*, 240 (1982) 405.
- 19 E. Jantzen and K. Bryn, in M. Goodfellow and D. Minnikin (Editors), *Chemical Methods in Bacterial Systematics* (Society for Applied Bacteriology Series, No. 20), Academic Press, London, 1985, pp. 145–171.
- 20 D. V. Crabtree, A. J. Adler and G. J. Handelman, *J. Chromatogr.*, 466 (1989) 251.
- 21 W. A. König, H. Bauer, W. Voelter and E. Bayer, *Chem. Ber.*, 106 (1973) 1905.
- 22 A. Tunlid and G. Odham, *Biomed. Mass Spectrom.*, 11 (1984) 428.

Thin-layer chromatography of the positional isomers of some 1,2,3,4-tetrahydro-2-naphthol and 3-amino-1,2,3,4-tetrahydro-2-naphthol derivatives

Konstantin Drandarov and Ivo M. Hais

Department of Biochemical Sciences, Faculty of Pharmacy, Charles University, Heyrovského 1203, 501 65 Hradec Králové (Czechoslovakia)

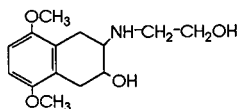
(First received June 19th, 1992; revised manuscript received September 7th, 1992)

ABSTRACT

The separation of 29 isomer pairs, namely three pairs of 5- and/or 8-substituted 1,2,3,4-tetrahydronaphthols, one pair of naphthalene derivatives (naphthalene-1,7-diol and naphthalene-1,6-diol) and 25 pairs of N-substituted 3-amino-1,2,3,4-tetrahydro-2-naphthols (including their lactone derivatives, tetrahydro-4H-naphth[2,3-b][1,4]oxazin-2-ones) in TLC systems on silica or alumina was studied. The possibility of two-point contact with the adsorbent in the case of more strongly retained isomers and their edgewise orientation against its surface is discussed. Attention is also paid to the influence of substituents in position 3 of the 1,2,3,4-tetrahydro-2-naphthol ring system on the retention sequence of the respective isomers.

INTRODUCTION

trans-3-[(2-Hydroxyethyl)amino]-5,8-dimethoxy-1,2,3,4-tetrahydro-2-naphthol* (tetraminol, **1**) is a



Tetraminol (**1**)

drug exhibiting α -adrenomimetic, vasoconstrictory and pressoric effects [1–3]. In the course of a study of its biotransformation *in vitro* involving the eluci-

dation of the structure of the isomeric products of mono-O-demethylation (**12** and **13**), three isomeric pairs of 1,2,3,4-tetrahydro-2-naphthols substituted in the aromatic nucleus (**2–7**) and nine pairs of isomeric derivatives of 3-amino-1,2,3,4-tetrahydro-2-naphthols 5,8-disubstituted in the aromatic nucleus as well as on the N-atom (**12–15**, **20/21**, **40/41**, **44–47**, **54–59**) [4,5] were prepared (Table I).

This paper is devoted to the interpretation of the retention sequence of isomers. In order to check some conclusions, N-acetyl (**18/19**) and N-benzoyl (**36/37**) derivatives of compounds **12** and **13** were prepared. For the sake of comparison, five isomeric pairs devoid of a methoxy group in the aromatic nucleus (**10/11**, **16/17**, **34/35**, **38/39**, **42/43**) were also prepared [6]. It has been found that during chromatography in basic systems S3 and S4, lactones **54–59** react with the components of the mobile phases (methanol, ethanol, ammonia). Chromatographic retention of the resulting esters **22–25**, **28–31** and **48–51** and the amides **26–27**, **32/33** and **52/53**, most of which were prepared synthetically [6], has been shown to be important for the correct interpretation

Correspondence to: Professor Ivo M. Hais, Department of Biochemical Sciences, Faculty of Pharmacy, Charles University, Heyrovského 1203, 501 65 Hradec Králové, Czechoslovakia.

* In agreement with standard chemical nomenclature, position of the alcohol group is indicated here as 2- and that of the amino group as 3- (cf., C.A. code No. 64381-81-8), although the name 2-hydroxyethylamino-3-hydroxy-5,8-dimethoxy-1,2,3,4-tetrahydronaphthalene has been used in the chemical and pharmacological literature [1–3].

TABLE I
STRUCTURES OF THE COMPOUNDS

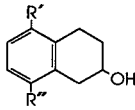
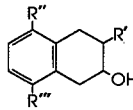
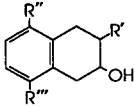
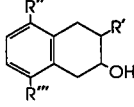
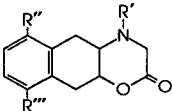
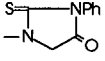
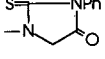
Compound No.				Compound No.			
	R' (5)	R'' (8)			R' (3)	R'' (5)	R''' (8)
2	OH	H			O=CCH ₃		
3	H	OH					
4	OCH ₃	H		20	-NCH ₂ COOH	OH	OCH ₃
5	H	OCH ₃			O=CCH ₃		
6	OH	OCH ₃		21		OCH ₃	OH
7	OCH ₃	OH			-NCH ₂ COOH		
					O=CCH ₃		
				22		OH	OCH ₃
					-NCH ₂ COOCH ₃		
					O=CCH ₃		
				23		OCH ₃	OH
					-NCH ₂ COOCH ₃		
					O=CCH ₃		
8 (1,6-diol)	OH	H		24		OH	OCH ₃
9 (1,7-diol)	H	OH			-NCH ₂ COOC ₂ H ₅		
					O=CCH ₃		
				25		OCH ₃	OH
					-NCH ₂ COOC ₂ H ₅		
					O=CCH ₃		
				26		OH	OCH ₃
					-NCH ₂ CONH ₂		
					O=CCH ₃		
				27		OCH ₃	OH
					-NCH ₂ CONH ₂		
					O=CCH ₃		
10	-NHCH ₂ CH ₂ OH	OH	H	28		-OCOCH ₃	OCH ₃
11	-NHCH ₂ CH ₂ OH	H	OH		-NCH ₂ COOCH ₃		
12	-NHCH ₂ CH ₂ OH	OH	OCH ₃		O=CCH ₃		
13	-NHCH ₂ CH ₂ OH	OCH ₃	OH	29		OCH ₃	-OCOCH ₃
14	-NHCH ₂ COOH	OH	OCH ₃		-NCH ₂ COOCH ₃		
15	-NHCH ₂ COOH	OCH ₃	OH		O=CCH ₃		
				30		-OCOCH ₃	OCH ₃
16	O=CCH ₃				-NCH ₂ COOC ₂ H ₅		
		OH	H		O=CCH ₃		
	-NCH ₂ CH ₂ OH			31		OCH ₃	-OCOCH ₃
	O=CCH ₃				-NCH ₂ COOC ₂ H ₅		
17		H	OH		O=CCH ₃		
	-NCH ₂ CH ₂ OH			32		-OCOCH ₃	OCH ₃
	O=CCH ₃				-NCH ₂ CONH ₂		
18		OH	OCH ₃		O=CCH ₃		
	-NCH ₂ CH ₂ OH			33		OCH ₃	-OCOCH ₃
	O=CCH ₃				-NCH ₂ CONH ₂		
19		OCH ₃	OH				
	-NCH ₂ CH ₂ OH						

TABLE I (continued)

Compound No.		Compound No.				
	R' (3)	R'' (5)	R''' (8)	R' (3)	R'' (5)	R''' (8)
34	O=CPh -NCH ₂ CH ₂ OH	OH	H	48	O=COCH ₂ Ph -NCH ₂ COOCH ₃	OH OCH ₃
35	O=CPh -NCH ₂ CH ₂ OH	H	OH	49	O=COCH ₂ Ph -NCH ₂ COOCH ₃	OCH ₃ OH
36	O=CPh -NCH ₂ CH ₂ OH	OH	OCH ₃	50	O=COCH ₂ Ph -NCH ₂ COOC ₂ H ₅	OH OCH ₃
37	O=CPh -NCH ₂ CH ₂ OH	OCH ₃	OH	51	O=COCH ₂ Ph -NCH ₂ COOC ₂ H ₅	OCH ₃ OH
38	CH ₂ Ph -NCH ₂ CH ₂ OH	OH	H	52	O=COCH ₂ Ph -NCH ₂ CONH ₂	OH OCH ₃
39	CH ₂ Ph -NCH ₂ CH ₂ OH	H	OH	53	O=COCH ₂ Ph -NCH ₂ CONH ₂	OCH ₃ OH
40	CH ₂ Ph -NCH ₂ CH ₂ OH	OH	OCH ₃			
41	CH ₂ Ph -NCH ₂ CH ₂ OH	OCH ₃	OH			
42	S=CNHPh -NCH ₂ CH ₂ OH	OH	H		(2,3,4a,5,10,10a-hexahydro-4H-naphth[2,3-b][1,4]oxazin-2-one derivatives)	
43	S=CNHPh -NCH ₂ CH ₂ OH	H	OH		R' (4)	R'' (6) R''' (9)
44	 -NCH ₂ CH ₂ OH	OH	OCH ₃	54	-COCH ₃	OH OCH ₃
				55	-COCH ₃	OCH ₃ OH
				56	-COCH ₃	-OCOCH ₃ OCH ₃
				57	-COCH ₃	OCH ₃ -OCOCH ₃
45	S=CNHPh -NCH ₂ CH ₂ OH	OCH ₃	OH	58	-COOCH ₂ Ph	OH OCH ₃
				59	-COOCH ₂ Ph	OCH ₃ OH
46		OH	OCH ₃			
47		OCH ₃	OH			

of some of the effects noted in the chromatography of compounds **54–59**.

EXPERIMENTAL

Materials

Kieselgel 60 F₂₅₄ and Aluminiumoxid 60 F₂₅₄ glass plates were obtained from Merck (Darmstadt, Germany).

Analytical-reagent grade chemicals were used unless indicated otherwise. Chloroform [stabilized with 1% ethanol (Merck), not redistilled], absolute methanol (Merck, not redistilled), 96% ethanol (chemically pure, distilled), butanol (Merck), acetic acid (Merck), 4-nitrobenzenediazonium fluoroborate (Reanal, Budapest, Hungary) and 1,7-naphthalenediol (**9**) [95% (pract.) (Fluka, Buchs, Switzerland)] were commercial products.

1,6-Naphthalenediol (**8**) was prepared by heating 5-amino-2-naphthol at 180°C in 10% sulphuric acid for 4.5 h in a sealed ampoule as recommended by Dr. J. Latinák (VChZ, Pardubice-Semtín, Czechoslovakia), who also supplied the starting substance.

Compounds **2–7**, **12–15**, **20/21**, **40/41**, **44–47** and **54–59** were prepared by procedures described elsewhere [4,5].

Compounds **10** and **11** were prepared by aminolysis of 2,3-epoxy-5-acetoxy-1,2,3,4-tetrahydronaphthalene with 2-hydroxyethylamine, using a method analogous to that for the production of **12** and **13** [4,5,7].

Compounds **16–19** were prepared by N-acetylation and **34–37** by N-benzoylation of **10–13**. Compounds **38** and **39** were prepared by the reduction of **34** and **35** with lithium aluminium hydride. Compounds **42** and **43** were prepared from **10** and **11** by means of phenyl isothiocyanate [5]. Compounds **26** and **27** were prepared by heating the lactones **54** and **55** with 25% ammonia.

Compounds **22/23** and **48/49** were prepared by briefly heating methanolic solutions of the lactones **54/55** and **58/59**, respectively. Compounds **24/25** and **50/51** were similarly prepared by heating of ethanolic solutions of the respective lactones.

Methyl esters **28/29** and ethyl esters **30/31** were prepared by adding catalytic amounts of triethylamine to the solutions of the lactones **56/57** in chloroform–methanol (1:1, v/v) or chloroform–ethanol (1:1, v/v), respectively.

The amides **32/33** and **42/43** resulted during chromatography of the lactones **56/57** and **58/59**, respectively, on silica in systems S3 and S4, which contain ammonia. Chromatographic spots corresponding to the amides were identified according to their chromatographic retention and the colours of the detection reactions.

Compounds **2–7** are racemates; **10–53** are 2,3-*trans* racemates; the 2,3,4a,5,10,10a-hexahydro-4*H*-naphth[2,3-*b*] [1,4]oxazin-2-one derivatives **54–59** are 4a,10a-*trans* racemates.

Chromatographic technique

A Camag (Muttens, Switzerland) Model 20/20 chromatographic tank was used. Equilibration was applied for 30 min before chromatography.

TLC solvent systems. The following systems were used: S1 = chloroform; S2 = chloroform–methanol (95:5, v/v); S3 = chloroform–methanol–25% (w/v) aqueous ammonia (80:10:1, v/v/v); S4 = chloroform–96% (v/v) ethanol–25% (w/v) aqueous ammonia (80:10:1, v/v/v) (turbidity is removed by filtration through cotton-wool); S5 = chloroform–methanol–acetic acid (15:5:1, v/v/v); and S6 = butanol–acetic acid–water (40:10:50, v/v/v) (the organic phase is used).

Solutions for spotting. These were freshly prepared, as some of the compounds are not stable. Volumes of 2–3 µl of 1% solutions of the compounds tested were spotted in the following solvents: chloroform, **4/5**, **28/31**, **42–45**, **56/57**; chloroform–ethanol (4:1, v/v), **2/3**, **6–9**, **22–25**, **48–51**, **54/55**, **58/59**; chloroform–ethanol (1:1, v/v), **38–41**, **46/47**; ethyl acetate, **16–19**, **34–37**; methanol, **20/21**, **26/27**; and methanol–25% (w/v) aqueous ammonia (8:2), **10–15**.

Detection. Method D1 was as follows: 5 ml of an aqueous solution of 2-nitrobenzene diazonium fluoroborate (0.2%, w/v) was mixed with 3 ml of aqueous NaHCO₃ (1%, w/v). This mixture was immediately used for spraying of the chromatogram. Detection limits were ca. 0.1 µg/cm² on silica and 0.5 µg/cm² on alumina (Table II). For alternative detection of the compounds, see ref. 8.

Compounds **4/5** are detected by quenching of fluorescence excited at 254 nm.

RESULTS AND DISCUSSION

The results for all the compounds under study are given in Table III.

It should be realized that when lactones **54–59** are chromatographed in S3 or S4, which contain ammonia and methanol or ethanol, they undergo alcoholysis to give esters as indicated in Table III. In addition to the esters indicated in Table III, certain amounts of amides are produced from the lactones **54–59** in system S3 or S4 on silica.

Systems S5 and S6 usually did not resolve the isomer pairs, with the exception of **12** which is more strongly retained than **13** in S5.

With respect to the resolution of the isomer pairs, the compounds under study can be grouped into three classes: in (a) and (b) the retention sequence can be predicted on simple assumptions, whereas in (c) the prediction is difficult.

(a) In the case of isomeric 1,2,3,4-tetrahydronaphthalenediols **2/3** and **6/7**, a stronger retention corresponds to a shorter distance between the OH groups. This also applies to the pair of isomeric naphthalenediols **8/9**.

The stronger retention of **8** and **9** in the basic system S3, especially on alumina, is probably due to their biphenolic nature compared with **2/3** and **6/7**.

The stronger retention of isomers with a shorter distance between the OH groups could be explained by their capacity to form two-point contacts with the adsorbents in the case of edgewise orientation

with respect to the adsorbent surface. This hypothesis is also applicable to the methoxyhydroxy isomers **4** and **5** in system S1. A weaker interaction of the methoxy groups with the adsorbent in **4** and **5**, when compared with phenolic OH groups in the remaining isomer pairs (**2/3**, **6–9**), may explain the loss of separation of **4** and **5** in the more polar systems S2 and S3.

With all the other compounds, nitrogen occurs in position 3 of the tetrahydronaphthalene or in the oxazine ring.

(b) In all instances in which a bulky substituent is bound to this nitrogen (compounds **34–53** and **58/59**), compounds with OH or OCOCH₃ in position 8 of the tetrahydronaphthalene or in position 9 of the hexahydronaphthoxazinone are more strongly retained. Here again, one would postulate the formation of two-point contacts of the analyte with the adsorbent in the case of edgewise orientation with respect to the adsorbent surface. Such an orientation involving OH (or OCOCH₃) in position 5 (or 6) would be prevented by the bulky substituent on the nitrogen.

(c) With the remaining compounds (**10–33** and **54–57**), it is difficult to establish whether the nitrogen- or the oxygen-containing grouping is more polar and to predict whether the isomer with OH (or OCOCH₃) in position 5 or 8 of the tetrahydronaphthalene (or 6 or 9 of the hexahydronaphthoxazinone) would be more strongly retained.

Primary alcohols **16/17** and **18/19** and the esters **22/23** and **24/25** resemble the groups discussed under (a) and (b) by their stronger retention of the 8-OH isomers.

With the **10/11** and **12/13** [9] pairs, the 8-isomer is distinctly more strongly retained in S3 on alumina; electrostatic attraction might increase the adsorption of the –NHCH₂CH₂OH group on silica, but not on alumina.

Of the N-acetylated compounds **16–33**, amides **26** (with 5-OH) and **32** (with 5-OCOCH₃) and the O-acetylated esters **28** and **30** (with 5-OCOCH₃) show stronger retentions than their isomers. Similarly, in the **54/55** and **56/57** pairs, those with 6-OH (**54**) or 6-OCOCH₃ (**56**) are more strongly retained.

Amino acids **14/15** and **20/21** are not resolved; in both instances, system S6 gave the best shape of the spots.

TABLE II

DETECTION OF THE COMPOUNDS ON SILICA WITH 4-NITROBENZENEDIAZONIUM FLUOROBORATE

For alternative detection of the compounds, see ref. 8.

Compounds	D1
2/3 , 10/11 , 16/17 , 34/35 , 38/39 , 42/43	Yellow-orange
6/7 , 12–15 , 18–27 , 28–33^a , 36/37 , 40/41 , 44/45 , 48–55 , 56/57^a , 58/59	Red-purple
8	Ochre
9	Crimson
46/47	Brownish red

^a The chromatogram is first enclosed in an atmosphere of ammonia in order to liberate the phenolic group by ammonolysis.

TABLE III
 TLC RETENTION DATA

Compound	$R_F \times 100$						
	Silica						Alumina
	S1	S2	S3	S4	S5	S6	S3
2	6	20	38				46
3	5	16	32				40
4	19	47	66				71
5	17	47	66				71
6	6	19	38				49
7	5	14	32				42
8	7	22	32				28
9	5	17	26				18
10	0	0	7 (26) ^a		32	51	15
11	0	0	7 (27) ^a		32	51	8
12	0	0	7 (28) ^a		33	51	15
13	0	0	7 (30) ^a		36	51	10
14	0	0	0		14 ^b	44	0
15	0	0	0		14 ^b	44	0
16	0	8	25		94		36
17	0	6	20		94		26
18	0	7	24		94		38
19	0	6	21		94		31
20	0	0	0		42 ^b	48	0
21	0	0	0		42 ^b	48	0
22	7	29	53	49			62
23	5	27	49	43			55
24	7	33	58	53			65
25	5	29	52	46			57
26	0	3	14	6			14
27	0	4	16	8			14
28	8	55	74	73			81
29	10	59	76	75			81
30	11	58	76	75			81
31	12	61	78	77			81
32	—	—	33	25			—
33	—	—	36	29			—
34	0	14	35				42
35	0	12	29				34
36	0	14	35				46
37	0	12	32				39
38	0	19	52				63
39	0	14	39				50
40	0	18	51				63
41	0	14	40				53
42	0	19	40				56
43	0	13	29				42
44	0	19	42				56
45	0	13	30				44
46	0	33	56				65
47	0	20	41				53

TABLE III (continued)

Compound	$R_f \times 100$						
	Silica						Alumina
	S1	S2	S3	S4	S5	S6	S3
48	10	44	65	61			70
49	7	37	57	51			63
50	13	51	66	63			70
51	12	46	58	53			63
52	–	–	30	21			–
53	–	–	27	18			–
54^c	6	26	53 (22)	53 (24)			62 (22)
55^c	8	33	49 (23)	45 (25)			55 (23)
56^c	13	59	74 (28)	75 (30)			81 (28)
57^c	15	62	76 (29)	77 (31)			81 (29)
58^c	12	48	65 (48)	63 (50)			70 (48)
59^c	11	44	57 (49)	53 (51)			63 (49)

^a Fivefold elution.

^b Diffuse spots.

^c Numbers in parentheses refer to esters into which the lactones have been converted in the respective solvent systems.

REFERENCES

- 1 D. Dantchev, K. Christova, D. Staneva, L. Rainova and L. Tschakarova, *Arch. Pharm. (Weinheim, Ger.)*, 310 (1977) 369.
- 2 L. Rainova, D. Staneva and L. Chakurova, *Eksp. Med. Morfol.*, 21, No. 4 (1982) 183.
- 3 D. Staneva, L. Chakurova and L. Rainova, *Eksp. Med. Morfol.*, 22, No. 4 (1983) 42.
- 4 K. Drandarov and I. M. Hais, *Česk. Farm.*, 40 (1991) 240.
- 5 K. Drandarov, *Collect. Czech. Chem. Commun.*, 57 (1992) 1111.
- 6 K. Drandarov, unpublished results.
- 7 F. P. Hauk, Ch. M. Cimarusti and J. E. Sundeen, *US Pat.*, 3 930 022 (1975); *C.A.*, 84 (1976) 135367e.
- 8 K. Drandarov and I. M. Hais, *J. Chromatogr.*, 285 (1984) 373.
- 9 K. Drandarov, E. Kvasničková and I. M. Hais, *Arch. Pharm. (Weinheim, Ger.)*, 325 (1992) 589.

Structural characterization of polypeptides and proteins by combination of capillary electrophoresis and ^{252}Cf plasma desorption mass spectrometry

Wolfgang Weinmann, Kerstin Baumeister, Ingrid Kaufmann and Michael Przybylski

Fakultät für Chemie, Universität Konstanz, Postfach 5560, W-7750 Konstanz (Germany)

(First received June 9th, 1992; revised manuscript received September 1st, 1992)

ABSTRACT

An efficient and sensitive method for the isolation and transfer of peptides and proteins from capillary zone electrophoresis separation for subsequent analysis by ^{252}Cf plasma desorption mass spectrometry was developed. Sample isolation on to nitrocellulose-coated targets for mass spectrometric analysis is performed by using a stainless-steel microtube pre-filled with aqueous buffer solution, to which the capillary end is connected, and the peptide is collected by applying a suitable transfer voltage according to the separation voltage. Low- and sub-picomolar sample amounts were isolated with high transfer efficiency and reproducibility, without the necessity for independent determination of electroosmotic flow-rates. Plasma desorption mass spectra of several peptides and proteins showed predominantly intact molecular ions; however, for several peptides partial oxidative modification was found which can be accounted for by the electrophoretic separation and/or transfer conditions. First applications to peptides and proteins show the feasibility of this off-line combination for primary structure characterization, such as by *in situ* chemical modification and enzymatic proteolysis reactions on the sample target prior to mass spectrometric analysis.

INTRODUCTION

Capillary electrophoresis (CE) has been developed in recent years as a powerful, high-resolution microanalytical separation method [1], which is currently finding growing attraction and application to the characterization of drug metabolites and biomacromolecules, such as peptides and proteins [2,3]. One of the key analytical features of CE is the high detection sensitivity in the pico- to femtomolar range, at high separation efficiency, obtained at very low flow-rates and small sample volumes of microcell UV or fluorescence detectors [4]. In contrast, the identification and structural characterization of separated compounds is at present a major problem with the CE method, particularly in the analysis of multi-component mixtures [5].

The successful development of desorption-ionization methods of mass spectrometry (MS) in recent years such as fast atom bombardment (FAB-MS), ^{252}Cf plasma desorption (PD-MS) and, more recently, electrospray (ES-MS) and laser desorption (LD-MS) has permitted molecular mass determinations and structural analyses of biopolymers, particularly polypeptides and proteins up to and beyond M_r 100 000 [6–9]. Direct mass spectrometric methods have been successfully integrated in primary structure studies of proteins by combination with selective chemical and enzymatic modification, sequential degradation reactions and with proteolytic digestion procedures (peptide mapping) [10–12]. For example, the combination of PD-MS with Edman degradation has been successfully applied to primary structure studies of polypeptides and peptide mixtures [13]. A particular advantage of the PD-MS method has been the possibility of directly carrying out and analysing “*in situ*” chemical reac-

Correspondence to: M. Przybylski, Fakultät für Chemie, Universität Konstanz, Postfach 5560, W-7750 Konstanz, Germany.

tions on the nitrocellulose (NC) sample target, which has been developed as an efficient approach in structural studies, *e.g.*, by peptide mapping [14,15].

In this paper an isolation and transfer method for CE-separated polypeptides is described, which is feasible for direct subsequent analysis by PD-MS or other desorption–ionization mass spectrometric methods. Suitable “on-line” interfaces for the direct coupling of CE with ES-MS [16] and FAB-MS [17] have recently been reported, using either a coaxial sheath flow or a liquid-junction interface [18]. However, an efficient and practical “off-line” isolation and microtransfer procedure appeared to be advantageous in structural studies of polypeptides by providing the possibility for microsequencing and alternative analytical methods such as *in situ* reactions, thus complementing the mass spectral analysis [19]. An isolation procedure using a porous glass joint at the end of the CE capillary has been reported previously by Takigiku and co-workers [20,21], but this is technically demanding and requires independent determinations of electroosmotic flow-rates. In this study an isolation procedure similar to the fraction collector described by Rose and Jorgenson [5] was developed by using suitable micro-sample tubes for direct injection on to the PD-MS sample target. PD-MS studies of a variety of model peptides and small proteins revealed high transfer efficiencies. The straightforward feasibility of this approach is demonstrated by first application examples of structural analysis, in combination with sequential and proteolytic degradation. Further, PD-MS analyses of several peptides are described, showing the occurrence of structural (oxidative) modification, and degradation of phenylthiocarbonyl–peptide adducts which have not been observed previously [20].

EXPERIMENTAL

Polypeptides

The following commercially available peptides and proteins were used: bradykinin (acetate salt), luteinizing hormone-releasing hormone (LHRH) (acetate), human angiotensin I (acetate), melittin and hen egg white lysozyme (HEL) from Sigma (St. Louis, MO, USA) and neurotensin (research grade) and bovine insulin from Serva (Heidelberg, Germa-

ny). The homogeneity and purity of all polypeptides were assessed by HPLC and mass spectral analysis, and was found to be $\geq 95\%$ except for melittin (*cf.*, Fig. 2).

Capillary electrophoresis

A CE-100 instrument (Grom, Herrenberg, Germany) equipped with an uncoated 50 μm I.D. fused-silica capillary was used. All separations were performed with 20 mM citric acid–15 mM ammonium chloride (pH 2.2) buffer solutions in deionized water obtained from a Milli-Q system (Waters–Millipore), filtered through a 0.45- μm membrane filter and degassed by ultrasonication prior to use. The total length L of the capillary varied from 62 to 73.5 cm, while the length l from the beginning of the capillary to the UV detector cell was kept constant at 48.5 cm (Fig. 1). All CE separations were carried out at approximately 20°C at a potential difference of 20–25 kV and a current of 25–31 μA ; electropherograms were obtained with a Linear UVIS-100 multiple-wavelength detector and recorded with a Shimadzu C6a integrator.

CE isolation and transfer for PD-MS analysis

For the isolation of peptides, the end of the capillary from the UV detector was plugged into a 5- μl stainless-steel sample tube or, alternatively, connected to a microbore stainless-steel block containing 2 μl of solvent; in both instances sample tubes were at ground potential (Fig. 1). CE migration times were determined with the integrator and subsequent sample isolation or transfer performed under identical voltage (20–25 kV) conditions but with a slightly reduced current. The isolation start time ($t_{i,s}$) and isolation time (t_i) were calculated from the beginning (t_1) and end (t_2) of the UV-detected peak (1% baseline) according to

$$t_{i,s} = t_1 L/l \quad (1)$$

$$t_i = (t_2 - t_1)(L/l)C \quad (2)$$

where L/l = ratio of total capillary length to capillary length to UV detector and C (1.05) = correction factor for the decreased current.

For subsequent PD-MS analysis the isolated sample solutions were transferred on to nitrocellulose-coated surfaces by means of a microlitre syringe.

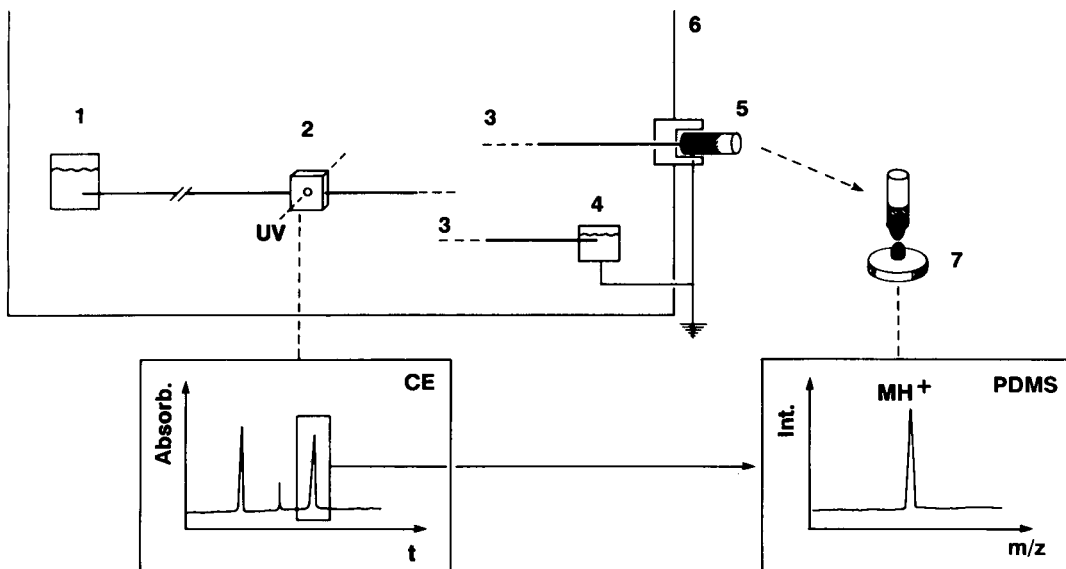


Fig. 1. Scheme of the CE isolation and transfer procedure for PD-MS analysis. Following the CE separation the capillary end is removed from the buffer reservoir (4) and connected to a stainless-steel tube or metal block (5) as described under Experimental. The isolation times for separated components are calculated from the migration times of the UV-detected peak. The collected sample solution is transferred on to the NC target with a microsyringe. 1 = Sample loading reservoir; 2 = UV detector cell; 3 = CE capillary; 4 = buffer reservoir; 5 = transfer capillary; 6 = insulated CE instrument housing; 7 = PD-MS sample target.

Mass spectrometry

Nitrocellulose (NC) targets for sample adsorption were prepared by electrospraying from an acetone solution as previously described [22]. Peptides isolated from CE into 2–5 μl of 0.1% trifluoroacetic acid (TFA) were allowed to adsorb for 3 min on the NC target, followed by twofold washing with 50 μl of 0.1% TFA and spin drying [23] for removal of salt contamination. PD-MS analyses were performed with a Bio-Ion/Applied Biosystems 20 K (Uppsala, Sweden) time-of-flight spectrometer as described [24], using an accelerating voltage of 16 kV.

In situ tryptic peptide mapping analysis

Experimental details of the *in situ* PD-MS peptide mapping analysis of proteins on the NC target surface have been described [12,25]. Disulphide linkages of lysozyme adsorbed on NC after CE isolation were cleaved by addition of 2 μl of a 80 mM dithiothreitol (DTT) solution in 50 mM NH_4HCO_3 (pH 8.3), and reduction was carried out for 30 min at 20°C under a microscope cover-slip. After removal of excess of DTT by washing with 50 mM

NH_4HCO_3 , proteolytic digestion was carried out for 30 min at 37°C under a microscope cover-slip by addition of 2 μl of TPCK-treated trypsin (Sigma) (0.1 mg/ml) in 50 mM NH_4HCO_3 , and sample targets were prepared by spin drying for PD-MS analysis.

Edman-PD-MS analysis

Combined Edman-PD-MS analysis cycles of CE-separated polypeptides were performed by manual Edman degradation as described [13]. Edman coupling of angiotensin I was carried out by adding a solution (20 μg in 20 μl of water) to 20 μl of a 5% (v/v) solution of phenyl isothiocyanate (PITC) (sequencing grade; Pierce, Rockford, IL, USA) in pyridine, and the reaction was allowed to proceed for 45 min at 25°C with gentle shaking. After lyophilization to dryness the cleavage step was carried out with 20 μl of anhydrous TFA for 15 min at 20°C. The lyophilized cleavage product was dissolved in 40 μl of 50 mM NH_4HCO_3 , an approximately 10% aliquot was withdrawn for CE and PD-MS analysis and the remaining solution was subjected to subsequent Edman degradation cycles.

RESULTS AND DISCUSSION

Capillary electrophoresis isolation and transfer method for ^{252}Cf plasma desorption mass spectrometry

The instrumental scheme used for isolation and transfer of CE-separated polypeptides to subsequent PD mass spectrometric analysis is shown in Fig. 1. An essential precondition for PD-MS analysis with high sensitivity is the application and adsorption of homogeneous peptide solutions of typically 1–10 μl on to the nitrocellulose-coated target surface [18,22], where final sample preparation can be carried out by spin drying [23] or additional washing steps for removal of buffer or residual salt contaminants [22]. Owing to the minimal liquid flow in CE separation [26], sample isolation was performed by connecting a stainless-steel microtube or metal block to the CE instrument housing, pre-filled with a suitable solvent (typically 2–5 μl of 0.1% TFA), into which the end of the fused-silica CE capillary is fed (*cf.*, Fig. 1). Isolation times for CE-separated components were calculated from the ratio of total capillary length to the capillary length to the UV detector (see Experimental), and the migration times of the UV-detected peak. This procedure enables the reproducible isolation of peptides without independent determination of electroosmotic flow-rates and with a free choice of CE buffers and pH, in contrast to isolation by means of a porous glass joint [20].

An example for the isolation conditions thus ob-

tained is shown in Fig. 2 by comparison of PD mass spectra of the polypeptide melittin before and after CE separation. The PD spectrum of melittin (Fig. 2A) yielded the most abundant protonated molecular ion $[\text{M} + \text{H}]^+$ at m/z 2849 together with the doubly charged $[\text{M} + 2\text{H}]^{2+}$ ion, which is associated by a by-product ion at m/z 2878. The electropherogram (Fig. 2B) revealed the most intense peak at an average migration time of 8.6 min, accompanied by two minor UV-detectable impurities. Isolation of the major peak was carried out at a migration time of approximately 13.7 min, which yielded $[\text{M} + \text{H}]^+$ and $[\text{M} + 2\text{H}]^{2+}$ as the only major ions in the PD mass spectrum (Fig. 2C). Assuming a nearly quantitative efficiency of the hydrostatic sample loading procedure used (see below), a sample amount of approximately 0.02 μg was estimated for the spectrum in Fig. 2C, which is close to the detection limit of PDMS for this polypeptide.

The straightforward applicability of the present CE isolation method, using eqns. 1 and 2 (see Experimental) for determination of transfer times, was demonstrated by PD-MS analyses yielding unequivocal molecular mass identification of several oligo- and polypeptides up to small proteins (see Table I). Relatively large sample amounts (*ca.* 0.1 μg), required to obtain sufficient molecular ion abundances for higher molecular mass polypeptides, can be partly accounted for by using increased hydrostatic loading times. However, even CE separations carried out under capillary overloading conditions did not impede the determina-

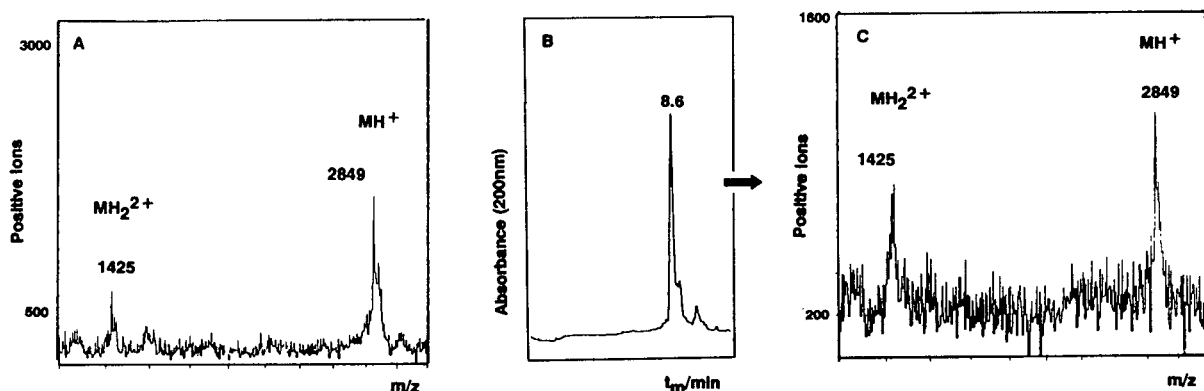


Fig. 2. PD-MS analysis of melittin after CE isolation. (A) PD spectrum (approximately 0.5 μg); (B and C) CE separation and PD spectrum of isolated polypeptide. The estimated sample amount loaded and transferred on to the NC target was 0.2 μg .

tion of suitable isolation conditions for PD-MS analysis.

Transfer efficiency, sensitivity and stability of polypeptides by combined CE–PD–MS analysis

Estimations of the overall sample transfer efficiency and sensitivity of the combined CE–PD–MS analysis were carried out by comparison of molecular ion abundances of model polypeptides under identical PD-MS conditions before and after CE separation, using standard conditions and previously reported yields for hydrostatic sample loading in CE [27]. As structural modification was observed for some polypeptides (see below), the mass spectrometric comparison was considered necessary to obtain reliable quantitative results. PD-MS analyses of 5- and 20-pmol samples of the polypeptides bradykinin and bovine insulin and the corresponding mass spectra after CE isolation and transfer are shown in Fig. 3. Using identical conditions of spectra acquisition (10^7 fission events) for PD-MS [23], comparable intensities of the $[M+H]^+$ ion (m/z 1061) of bradykinin were obtained after hydrostatic loading (60 s) of a 1 nmol/ μ l sample on to the CE capillary. The PD-MS analysis of insulin gave similar results with molecular ion intensities of good reproducibility in repeated experiments (see legend to Fig. 3). As the loading yields (approximately 5 nl) under these conditions are in good agreement with previously reported values for hydrostatic sample loading in CE [27], this indicates a high efficiency ($\geq 80\%$) of the sample isolation and transfer procedure employed. Notable in the PD mass spectra of both polypeptides after CE separation is the observation of an increased mass of molecular ions by 16 u, corresponding to the incorporation of an oxygen atom (see below). In the spectrum of bradykinin an additional molecular ion (m/z 1077) of minor abundance was found; the broad (unresolved) molecular ion peak of insulin with a centroid mass of m/z 5748 also suggests some oxidative modification.

PD-MS data and migration times for a series of isolated polypeptides and proteins are summarized in Table I. Unequivocal molecular mass determinations by protonated molecular ions were consistently obtained with sample amounts of approximately 1–10 pmol for smaller peptides, and could be increased to approximately 100 pmol of isolated sam-

ple if required for the characterization of proteins. Although these figures are significantly beyond typical CE sample amounts for the CE of polypeptides, the high transfer efficiency of the present isolation procedure offers the possibility of applying several microanalytical techniques for structural analysis in combination with mass spectrometry, as shown below.

Further, the advantage of using alternative analytical methods, compared with structural analysis by mass spectrometry only, was clearly suggested from PD-MS analyses showing oxidative structural modification of some of the polypeptides investigated (Table I). Molecular ions due to single and/or multiple oxidation were observed for smaller peptides such as LHRH and angiotensin. A larger molecular mass increase was found with increasing molecular mass of proteins such as lysozyme (M_r 14 306). The formation of molecular ions in addition to $[M+H]^+$ by possible cationization with alkali metal ions from buffer constituents or salt contamination was excluded, as the present sample isolation procedure with a large excess of TFA solution strongly favours protonation and appeared to be tolerant towards salt impurities. Oxidation was observed particularly in peptides containing tryptophan residues and thiourea substituents; however, no detailed structural identification was undertaken in this study. Although electrochemical oxidation of peptides appears possible from the CE separation and/or isolation conditions, no structural identification of such products has yet been reported. Systematic studies to identify oxidation sites in peptides, using different buffers for CE separation and conditions of sample isolation, are in progress.

Applications of combined CE–PD–MS in structural studies of polypeptides

The efficiency of the combined CE isolation–PD–MS method was clearly demonstrated by its integration within primary structure studies of polypeptides and proteins, using chemical and enzymatic modification and degradation reactions. An application example to sequence determination is shown in Fig. 4 by the Edman degradation of angiotensin I, in conjunction with PD-MS analysis. A combined Edman–PD–MS sequencing method has recently been developed [13], in which the stepwise phenyl-

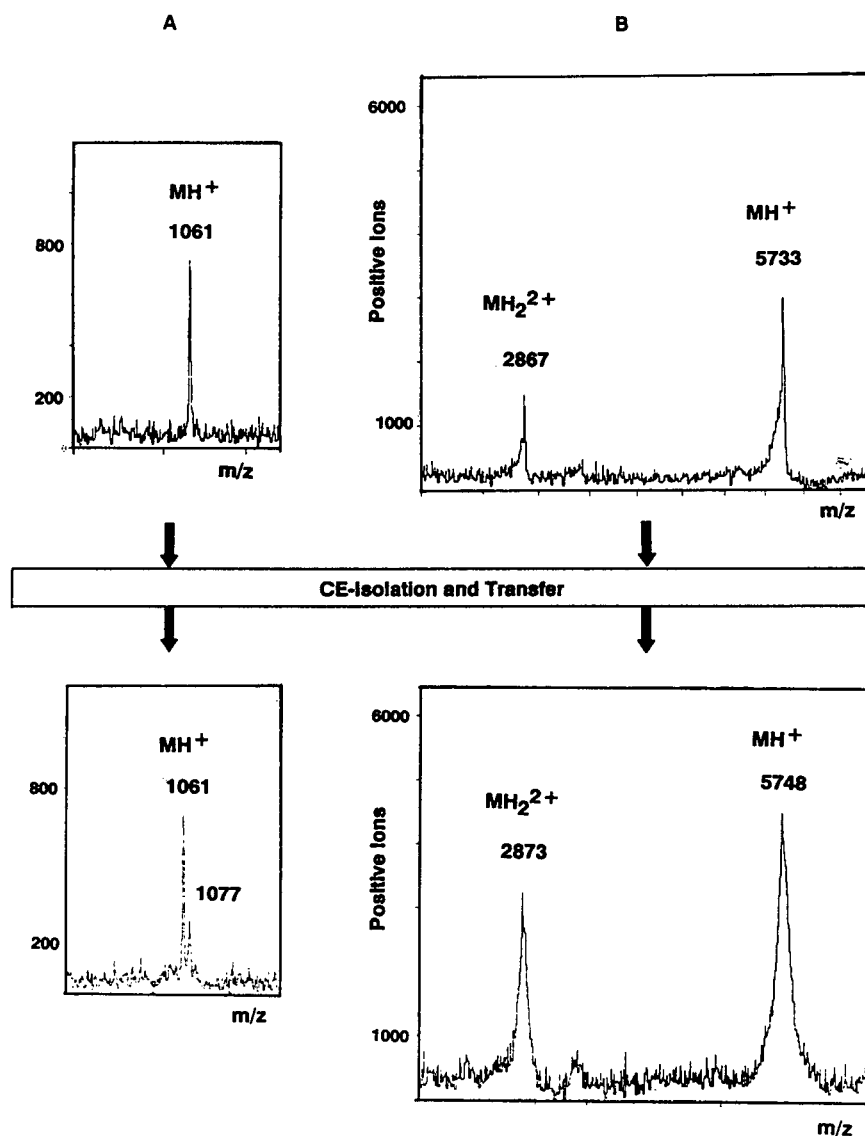


Fig. 3. Determination of sample loading and transfer efficiencies in PD-MS analyses of CE-isolated bradykinin and bovine insulin. (A) PD mass spectrum (molecular ion region) of 5 pmol of bradykinin before CE analysis (upper panel); lower panel, spectrum of CE-isolated peptide obtained from a 1 nmol/ μ l sample solution by hydrostatic loading for 60 s on to the capillary. (B) PD mass spectra of bovine insulin (0.2 pmol; upper panel) and CE-isolated insulin (lower panel) after loading a solution of 40 pmol/ μ l.

thiocarbamoyl (PTC) coupling and cleavage products of polypeptides from manual Edman degradation are subjected to PD-MS analysis. The "reverse" sequencing approach by identification of the molecular mass differences of the truncated polypeptide rather than the phenylthiohydantoin

(PTH)-amino acid released, has been successfully employed in structural studies, particularly in the simultaneous sequence determination of polypeptide mixtures and modified primary structures [13,28,29].

The PD spectrum of the third phenyl isothiocya-

TABLE I
CHARACTERIZATION OF MODEL PEPTIDES AND PROTEINS BY PD-MS AND CE ISOLATION-PD-MS

Polypeptide Sequence	M_r	PD-MS		CE isolation-PD-MS			
		Sample amount (μg)	$[\text{M} + \text{H}]^+$ (m/z)	Sample ^a loaded	t_m^b (min)	$[\text{M} + \text{H}]^+$	
						m/z	Int. ^c (%)
Bradykinin							
H-RPPGFSPFR-OH	1060	0.005	1061	0.005	6.6	1061	100
LHRH							
pEHWSYGLEPG-NH ₂ ^d	1181	1	1191	– ^e	12.4	1182	60
						1196	40
						1212	100
						1227	20
Neurotensin/pE-LY							
ENKPRRPYIL-OH ^d	1673	1	1674	– ^e	9.4	1673	100
Mellitin/H-GIGAV							
VKVLTTGLPA-							
LISWKRKRQQ-OH	2848	0.5	2849/2878	– ^e	8.6	2849	100
Bovine insulin	5733	0.1	5734	0.1 ^a	6.4	5748	100
Hen egg white lysozyme	14 305	1	14 306	– ^e	7.3	14 391 ^f	< 10
Angiotensin I							
H-DRVYIHPFHL-OH	1297	0.5	1298	0.01	6.0	1298	100
PTC-DRVYIHPFHL-OH ^g	1431	0.5	1432	0.01	6.8	1417	100
						1432	70
						1449	70
PTC-VYIHPFHL-OH ^h	1161	0.5	1162	0.01	10.2	1130	100
						1146	65
						1161	20
H-VYIHPFHL-OH ⁱ	926	1	927	0.01	6.2	927	100

^a Sample amount estimated by comparison of $[\text{M} + \text{H}]^+$ ion abundances in PD-MS and PD-MS after CE separation and isolation.

^b Migrations time determined by UV detection (*cf.*, Fig. 1).

^c Relative intensity.

^d pE, pyroglutamyl.

^e Not determined.

^f Molecular mass determined from doubly charged $[\text{M} + 2\text{H}]^{2+}$ ion (*cf.*, Fig. 5).

^g PTC, phenylthiocarbonyl; Edman coupling product of angiotensin I.

^h Coupling product of third Edman degradation cycle of angiotensin I.

ⁱ Cleavage product of third Edman degradation cycle of angiotensin I.

nate (PITC) coupling step in the Edman degradation of angiotensin I (Fig. 4A) yielded a most abundant $[\text{M} + \text{H}]^+$ ion at m/z 1161 of the PTC-peptide adduct, PTC-VYIHPFHL, together with a molecular ion resulting from the incomplete preceding cleavage step (m/z 1317; PTC-RVYIHPFHL). The separation of the coupling product mixture by CE afforded a homogeneous major component at a migration time of 10.4 min (Fig. 4B), which was isolated and subjected to PD-MS (Fig. 4C). However, the PD-MS analysis of this peak revealed only a minor $[\text{M} + \text{H}]^+$ ion due to the intact PTC-peptide. Pre-

dominant ions were observed due to molecular mass decreases by 16 and 32 u, respectively, corresponding to oxidative formation of the phenylcarbamoyl-peptide adduct (m/z 1146) and probably further oxidative degradation. Evidence for the oxidative desulphurization of the phenylthiocarbonyl residue, a well recognized side-reaction of the Edman degradation, was obtained by (i) the finding that the CE-isolated peptide was not amenable to subsequent Edman cleavage; while (ii) direct Edman cleavage of the PTC-peptide afforded molecular ions of the expected product, YIHPFHL, at

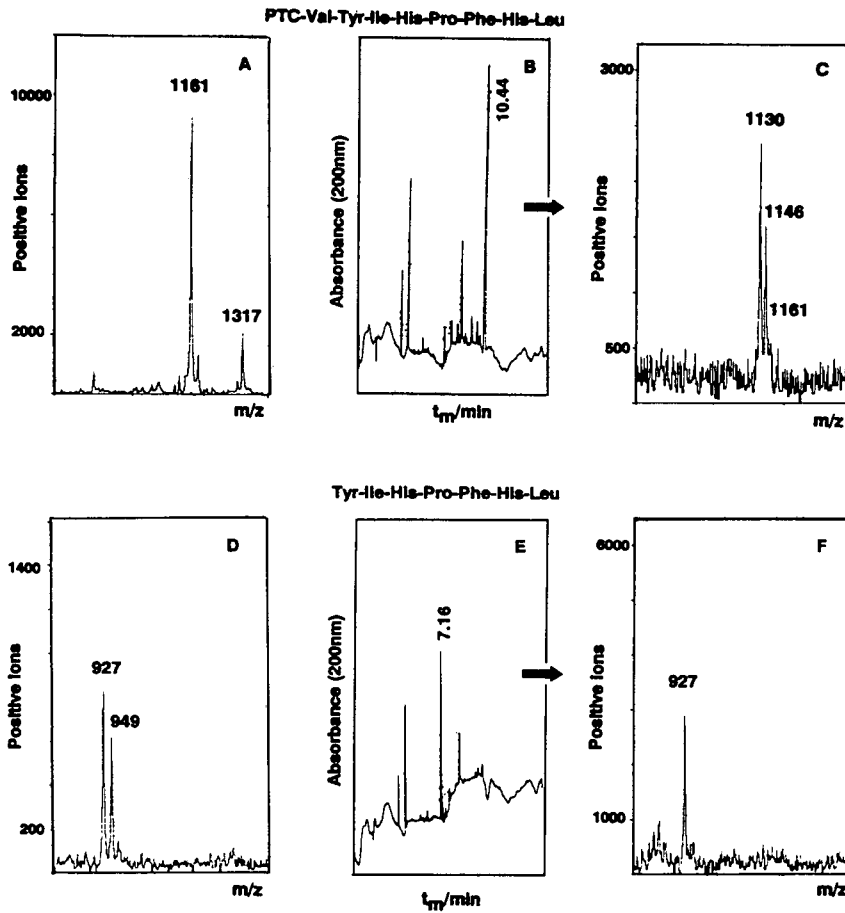


Fig. 4. Identification of PTC coupling and cleavage products from the third Edman degradation cycle of human angiotensin I by PD-MS and CE isolation-PD-MS. (A) $[M + H]^+$ ion of m/z 1161 in PD-MS analysis of PTC-Val-Tyr-Ile-His-Pro-Phe-His-Leu coupling product, showing an additional molecular ion (m/z 1317) from the incomplete preceding degradation step; (B) electropherogram of reaction product mixture from PTC coupling step (A); (C) PD mass spectrum of CE-isolated coupling product with $t_m = 10.4$ min; (D) PD mass spectrum of TFA cleavage product from the PTC coupling product (A); (E) CE separation of Edman cleavage in (D); (F) PD mass spectrum of CE-isolated peptide from (E) ($t_m = 7.16$ min).

m/z 927 ($[M + H]^+$) and m/z 949 due to partial formation of the $[M + NA]^+$ ion (Fig. 4G). CE analysis of the TFA cleavage product yielded a major peak at 7.16 min, which showed a homogeneous $[M + H]^+$ ion in the PD mass spectrum (Fig. 4E and F).

Oxidation of PTC-peptides after CE separation and isolation was consistently found in Edman-PD-MS sequence analyses by corresponding molecular ions decreased in mass by 16 u (see Table I). As the formation of the phenylcarbamoyl derivative

blocks further Edman degradation, this would preclude purification of PTC coupling products by CE in microsequencing protocols. A procedure obviating this problem is the direct cleavage of PTC adducts and CE isolation of the corresponding cleavage product.

An example of the structural characterization of a protein after CE isolation by direct proteolytic degradation and PD-MS peptide mapping is shown in Fig. 5. Hen egg white lysozyme (HEL) (ca. 100 ng), isolated from CE and transferred to PD-MS,

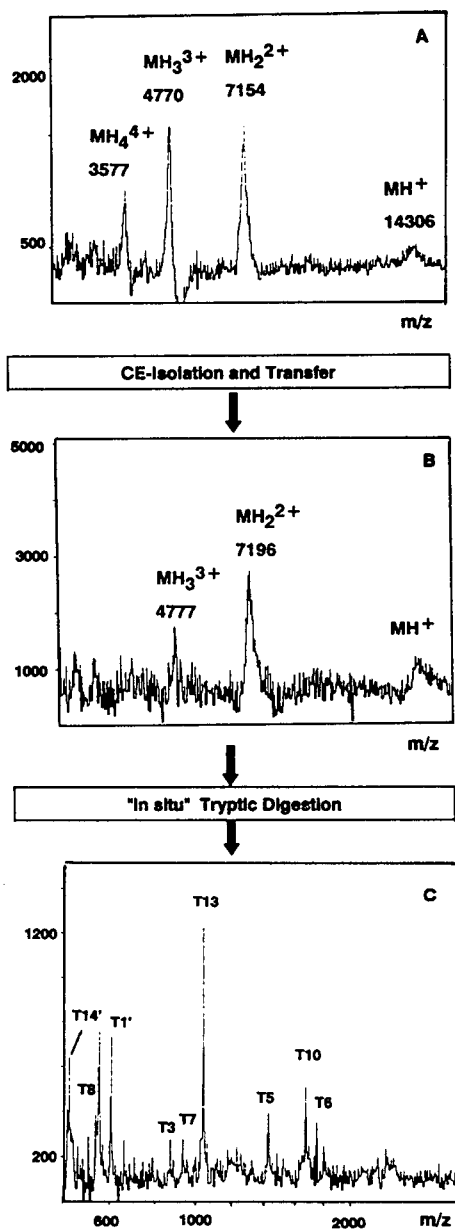


Fig. 5. PD-MS and peptide mapping analysis by *in situ* trypsin digestion of hen egg white lysozyme. (A) PD mass spectrum of HEL (1 μ g); (B) PD mass spectrum of HEL after CE isolation and transfer on to the NC target; (C) PD-MS peptide mapping analysis of the HEL sample from (B), after *in situ* DTT reduction and trypsin digestion (see Experimental).

yielded a pattern of singly, doubly and triply charged molecular ions similar to that of the direct PD mass spectrum. However, a significant molecular mass increase by approximately 80 u indicated

partial oxidation. The remaining sample from the PD-MS analysis shown in Fig. 5B was subjected to *in situ* DTT reduction and subsequent trypsin digestion on the NC target. In the resulting peptide mapping analysis (Fig. 5C), a series of tryptic peptides were directly identified by their molecular masses expected from the sequence, yielding structural characterization of a substantial part of the protein. The tryptic fragments and partial sequences identified for the CE-isolated protein are compared in Table II with peptide fragments found by direct PD-MS peptide mapping of HEL [12,15]. Notably, no peptides were found for partial sequences (22–33) and (74–96), in which several tryptophan and cysteine residues as possible sites of oxidative modification are located. The present results, however, did not provide a definite identification of modified structures upon CE separation and isolation, which will be the subject of further studies with the combination of CE and PD-MS.

CONCLUSIONS

An efficient approach for peptide and protein isolation by CE has been combined with PD-MS analysis. Model studies and first applications to polypeptides have shown high efficiency and reproducibility of the CE isolation and transfer procedure and sensitivity of the PD-MS analysis; further, the present approach can be used, in principle, in combination with any CE separation conditions. The combination with PD-MS provides the possibility of applying further analytical methods for the structural characterization of polypeptides, before or subsequent to the mass spectrometric molecular mass determination, *e.g.*, employing *in situ* enzymatic degradation or chemical derivatization reactions [15,29]. Moreover, its application in combination with Edman microsequencing [13] has been demonstrated. In contrast to “on-line” CE-ES-MS methods [30], the off-line CE-PD-MS combination is highly tolerant to buffer salts and different pH conditions, and allows the efficient removal of contaminants from the NC sample target. Therefore, the present approach should prove to be a useful complementary method to “on-line” CE-MS combinations. Also, its evaluation in combination with other desorption-ionization methods such as electrospray and laser desorption [21] should be worthwhile.

TABLE II

COMPARISON OF PD-MS PEPTIDE MAPPING ANALYSIS OF HEL BY DIRECT *IN SITU* TRYPSIN DIGESTION AND HEL AFTER CE ISOLATION

Tryptic peptide fragment	Partial sequence	Calculated M_r	[M + H] ⁺ ions found, m/z	
			Direct PD-MS ^a	PD-MS after CE isolation ^b
T1'	(1–5)	606	607	607
T1	(2–5)	478	478	478
T2	(6–13)	837	– ^c	– ^c
T3	(15–21)	875	875	875
T4	(22–33)	1269	1269	– ^d
T5	(34–45)	1429	1430	1430
T6	(46–61)	1754	1755	1756
T7	(62–68)	937	937	938
T8	(69–73)	517	517	517
T9	(74–96)	2338	2339	– ^e
T10	(98–112)	1676	1677	1677
T11	(113–114)	289	– ^f	– ^f
T12	(115–116)	250	– ^f	– ^f
T13	(117–125)	1046	1046	1047
T14	(126–128)	335	– ^f	– ^f
T14'	(126–129)	448	448	448

^a Direct *in situ* peptide mapping analysis of HEL [12,15].^b *In situ* peptide mapping analysis of CE-isolated HEL.^c Not detected owing to molecular ion suppression [12,15].^d Peptide containing Trp²⁸ and Cys³⁰ residues.^e Peptide containing Cys⁷⁶, Cys⁸⁰ and Cys⁹⁶ residues.^f Not detected because of background interferences in the low-mass range.

ACKNOWLEDGEMENTS

We thank the German Academic Exchange Service (DAAD, Bonn, Germany) for providing a stipend to one of us (I.K.). This work was supported by the Deutsche Forschungsgemeinschaft, Bonn, Germany, and the Fonds der chemischen Industrie.

REFERENCES

- J. W. Jorgenson and K. D. Lukacs, *Science (Washington, D.C.)*, 222 (1983) 266.
- S. Fujiwara and S. Honda, *Anal. Chem.*, 58 (1986) 1811.
- H. H. Lauer and D. McManigill, *Anal. Chem.*, 58 (1986) 166.
- D. J. Rose and J. W. Jorgenson, *J. Chromatogr.*, 447 (1988) 117.
- D. J. Rose and J. W. Jorgenson, *J. Chromatogr.*, 438 (1988) 23.
- R. J. Cotter, *Anal. Chem.*, 60 (1988) 781A.
- J. B. Fenn, M. Mann, C. K. Meng, S. F. Wong and C. M. Whitehouse, *Science (Washington, D.C.)*, 246 (1989) 64.
- A. L. Burlingame and J. A. McCloskey (Editors), *Biological Mass Spectrometry*, Elsevier, Amsterdam, 1991.
- M. Karas and F. Hillenkamp, *Anal. Chem.*, 60 (1988) 2299.
- K. Biemann and S. A. Martin, *Mass Spectrom. Rev.*, 6 (1987) 1.
- H. R. Morris and F. M. Grier, *Trends Biotechnol.*, 6 (1988) 140.
- P. F. Nielsen, K. Schneider, D. Suckau, B. Landis and M. Przybylski, in E. Hilf and A. Tuczynski (Editors), *Mass Spectrometry of Large Non-Volatile Molecules*, World Scientific, Singapore, 1990, p. 194.
- P. F. Nielsen, B. Landis, M. Svoboda, K. Schneider and M. Przybylski, *Anal. Biochem.*, 191 (1990) 302.
- B. T. Chait and F. H. Field, *Biochem. Biophys. Res. Commun.*, 134 (1986) 420.
- D. Suckau, M. Mak and M. Przybylski, *Proc. Natl. Acad. Sci. U.S.A.*, 89 (1992) 5630.
- J. A. Olivares, N. T. Nguyen, C. R. Yonker and R. D. Smith, *Anal. Chem.*, 59 (1987) 1230.
- M. A. Moseley, L. J. Deterding, K. B. Tomer and J. W. Jorgenson, *Anal. Chem.*, 63 (1991) 109.
- E. D. Lee, W. Mück, J. D. Henion and T. R. Covey, *Biomed. Environ. Mass Spectrom.*, 18 (1989) 844.
- P. Roepstorff, G. Talbo, K. Klarskov and P. Horjup, in A. L. Burlingame and J. A. McCloskey (Editors), *Biological Mass Spectrometry*, Elsevier, Amsterdam, 1990, p. 25.

- 20 R. Takigiku, T. Keough, H. P. Lacey and R. E. Schneider, *Rapid Commun. Mass Spectrom.*, 4 (1990) 24.
- 21 M. P. Lacey, T. Keough, R. Takigiku, R. E. Schneider, T. N. Asquith, M. P. Purdon, R. A. Sanders, J. D. Pinkston and R. T. Hentschel, *Proceedings of 39th Conference ASMS, Nashville, 1991*, American Society for Mass Spectrometry, 1991, p. 358.
- 22 G. P. Jonsson, A. B. Hedin, A. B. Hakansson, B. R. Sundquist, G. S. Save, P. F. Nielsen, P. Roepstorff, K. E. Johansson, I. Kamensky and M. S. L. Lindberg, *Anal. Chem.*, 58 (1986) 1084.
- 23 P. F. Nielsen, K. Klarskov, P. Hojrup and P. Roepstorff, *Biomed. Environ Mass Spectrom.*, 17 (1988) 355.
- 24 P. Roepstorff, P. F. Nielsen and P. Hojrup, *Biochem. Soc. Trans.*, 15 (1987) 155.
- 25 K. Schneider, P. F. Nielsen, D. Suckau and M. Przybylski, in E. Hilf and A. Tucziynski (Editors), *Mass Spectrometry of Large Non-Volatile Molecules*, World Scientific, Singapore, 1990, p. 176.
- 26 A. van de Goor, B. J. Wanders and F. M. Everaerts, *J. Chromatogr.*, 470 (1989) 95.
- 27 S. E. Moring, J. C. Colburn, P. D. Grossman and H. L. Lauer, *LC-GC Int.*, 3 (1989) 46.
- 28 C. Gauss, J. Klein, K. Post, D. Suckau, K. Schneider, H. Thomas, F. Oesch and M. Przybylski, *Environ. Health Perspect.*, 88 (1990) 57.
- 29 T. Voss, K. P. Schäfer, P. F. Nielsen, A. Schäfer, C. Maier, E. Hannappel, J. Maassen, B. Landis, K. Klemm and M. Przybylski, *Biochem. Biophys. Acta*, 1138 (1992) 261.
- 30 M. A. Moseley, J. W. Jorgenson, J. Shabanowitz, D. F. Hunt and K. B. Tomer, *J. Am. Soc. Mass Spectrom.*, 3 (1992) 289.

Short Communication

Determination of kinetin in callus of *Panax ginseng* by liquid chromatography

Kayoko Takagi, Masatake Toyoda and Yukio Saito

National Institute of Hygienic Sciences, 1-18-1, Kamiyoga, Setagaya-ku, Tokyo, 158 (Japan)

Keiko Mizuno and Megumi Shimizu

Kitasato University, 1-15-1, Kitasato, Sagami-hara-shi, Kanagawa, 228 (Japan)

Susumu Satoh

Nitto Denko Corporation, 1-1-2, Shimohozumi, Ibaraki, Osaka, 567 (Japan)

(First received July 2nd, 1992; revised manuscript received October 19th, 1992)

ABSTRACT

A high-performance liquid chromatographic (HPLC) method was developed for the determination of kinetin levels in *Panax ginseng* dried callus, fresh callus and culture media. Ground dried callus was suspended in borate buffer and extracted with ethyl acetate. The extract was eluted through a cation-exchange column (Amberlite CG-50), then re-extracted with ethyl acetate. This extract was subjected to HPLC. Kinetin levels were determined by gradient elution on an Inertsil ODS-2 column and UV detection at 280 nm. The ion-exchange column chromatographic purification step could be eliminated with kinetin extracts from fresh callus and culture media. The recovery of kinetin from dried callus spiked at $5 \mu\text{g g}^{-1}$ was 72.0% and those from fresh callus and media spiked at 1.0 and $0.5 \mu\text{g g}^{-1}$ were 72.8 and 84.2%, respectively. Kinetin was not detected in dried callus of *P. ginseng*.

INTRODUCTION

Large numbers of useful substances such as food additives and medicinal drugs can be produced by plant tissue culture. It has been reported that *Panax ginseng* callus, coded Pg-1, produces almost the same pharmacologically active saponins and ginsenosides as cultivated ginseng root [1–4].

Recently interest has been increasing in the con-

centrations of residual plant growth regulators from callus, including that in growth medium. Analyses of plant hormones from cultures have generally been carried out by gas chromatography (GC) [5–7], GC-mass spectrometry (MS) [8,9] and high-performance liquid chromatography (HPLC) [10,11].

Kinetin has been determined after permethylation, using GC with nitrogen-phosphorus [6] or MS detection (single-ion monitoring) [9], or after trifluoroacetylation [7] or trimethylsilylation [5] using GC with electron-capture detection. These methods

Correspondence to: K. Takagi, National Institute of Hygienic Sciences 1-18-1 Kamiyoga, Setagaya-ku, Tokyo, 158, Japan.

suffer several problems related to clean baseline separation of chromatograms, conciseness and reproducibility, owing to the similarity of the structures of kinetin and of nucleic acids originally contained in the callus, and the low kinetin concentration. Various HPLC procedures have been applied to the determination of kinetin in recent years [10,11], but only model systems and not real samples were assayed.

The purpose of this investigation was to develop a sensitive method for the determination of kinetin in *Panax ginseng* callus to establish whether kinetin is taken up by fresh and dried callus from the medium.

EXPERIMENTAL

Materials

Panax ginseng C. A. Mayer callus was cultivated by Furuya *et al.*'s method [12]. Selected Pg-1 callus was transplanted on to modified Murashige and Skoog's medium containing $2 \mu\text{g g}^{-1}$ of indole-3-butyric acid and $0.1 \mu\text{g g}^{-1}$ of kinetin. The callus was maintained at 25°C in the dark, then subcultured and harvested at 4-week intervals. The harvested callus was dried under a stream of warm air at $40\text{--}50^\circ\text{C}$ until the water content was reduced to 3%.

Reagents

Kinetin of biochemical grade was obtained from Wako (Osaka, Japan) and Amberlite CG-50 Type I from Orugano (Tokyo, Japan). Other reagents were of special grade, except acetonitrile, which was of analytical-reagent grade, from Wako.

Apparatus

A Model 880-PU pump, Model 7125 injector, Model 870 UV detector (Japan Spectroscopic, Tokyo, Japan) and Chromatopac C-R5A integrator (Shimadzu, Kyoto, Japan) were used, and identifications were made using HP1090A HPLC systems with UV photodiode-array detection (DAD) (Yokogawa Electric, Tokyo, Japan).

The analytical HPLC gradient flowed at 1.0 ml min^{-1} on an Inertsil ODS-2 HPLC column ($250 \times 4.6 \text{ mm I.D.}$; $5\text{-}\mu\text{m}$ diameter particles) (GL Science, Tokyo, Japan) at 30°C . A mixture of water and 95% acetonitrile containing 0.1% of trifluoroacetic acid was programmed from 97:3 to 65:35 (v/v) over

20 min, monitoring the wavelength at 280 nm. The injection volume was $20 \mu\text{l}$. DAD was used for kinetin identification. The wavelength ranged from 210 to 350 nm.

Extraction and purification of kinetin from *P. ginseng* dried callus

A 1-g amount of dried callus was homogenized in 20 ml of 1 M borate buffer (pH 8.5), to which 5 g of sodium chloride were added. The homogenate was mixed well, then extracted with 50 ml of ethyl acetate three times.

The extracts were combined and concentrated to dryness, then the residue was dissolved in 20 ml of 0.01 M hydrochloric acid (sonicated for 15 min). A 20-ml volume of acetate buffer (pH 5.6) was added and the solution was purified on an ion-exchange column. The Amberlite CG-50 cation-exchange resin was washed with five column volumes of 1 M ammonia solution until the water layer became clear, then with water until the resin became neutral. The column was washed with five volumes of 1 M hydrochloric acid. Finally, it was washed with water until the pH stabilized between 5 and 6. The treated resin was suspended in 0.1 M acetate buffer (pH 5.6), then packed into a glass column of 1.6 cm I.D. to a height of 4 cm. The packed column was prewashed with 20 ml of 0.1 M acetate buffer (pH 5.6). The sample was applied to the column and drained at a flow-rate of about $2\text{--}3 \text{ ml min}^{-1}$ until the surface of the resin was just covered, then the column was washed with 25 ml of 0.025 M acetate buffer (pH 5.6) followed by 1 M ammonia solution. The first 20 ml of ammonia eluate was drained and kinetin was eluted in the second 20 ml. This eluate was neutralized with 6 M hydrochloric acid, mixed with 1 M borate buffer (pH 8.5), then kinetin was re-extracted with 50 ml of ethyl acetate three times. The extract was concentrated to dryness and the residue was dissolved in 2 ml of 0.1% trifluoroacetic acid and analysed by HPLC.

Extraction of kinetin from *P. ginseng* fresh callus

Fresh callus (2.5 g) was chopped into small pieces and added to 5 ml of 0.1 M hydrochloric acid and homogenized. The homogenized sample was clarified by vacuum filtration and the residue was re-extracted as above. The filtrates were pooled and 5 ml of 1 M borate buffer (pH 8.5) and 5 g of NaCl

were added. Kinetin was extracted with 50 ml of ethyl acetate three times, the extracts were pooled and evaporated to dryness, then the residue was dissolved in 2 ml of 0.1% trifluoroacetic acid.

The ion-exchange column chromatographic purification step could be eliminated when analysing fresh callus.

Extraction of kinetin from the culture medium

A 5-ml volume of 1 M borate buffer (pH 8.5) and 5 g of sodium chloride were added to 10 g of medium and kinetin was extracted with ethyl acetate using the same method as described for fresh callus.

RESULTS AND DISCUSSION

Extraction of kinetin from aqueous solution

When 2 g of standard kinetin were added to 20 ml of 1 M borate buffer with 5 g of sodium chloride, then extracted with 50 ml of ethyl acetate three times, the recovery was 98%.

Purification by cation-exchange chromatography

The ethyl acetate extract of *Panax ginseng* callus contained numerous interfering compounds when determined by HPLC, and purification was necessary. A C₁₈ cartridge and liquid–liquid extraction columns (Extrelut) were unsuitable for this process (data not shown). This was ascribed to the high concentration of pyrimidines and purines, which have similar structure and polarity to the kinetin in *Panax ginseng* cells.

Kinetin was isolated from autoclaved DNA by cation-exchange chromatography according to the method of Miller *et al.* [13]. First, we investigated the elution profile of kinetin from the Amberlite CG-50 column (2 × 1 cm I.D.) with hydrochloric acid. The column was prewashed with 1 M hydrochloric acid and water, then the applied kinetin was washed with 5 ml of 0.025 M acetate buffer (pH 5.6) and eluted with 25 ml of 1 and 2 M hydrochloric acid. However, when the resin was prewashed with 1 M ammonia solution, 1 M hydrochloric acid and water, in that order, the elution volume decreased. The capacity of the resin also decreased on pretreatment with ammonia solution. Therefore, the treated resin was packed into a column of 1.6 cm I.D. to a height of 4 cm to avoid a decreased elution rate. The elution profile of kinetin with 1 M ammonia solu-

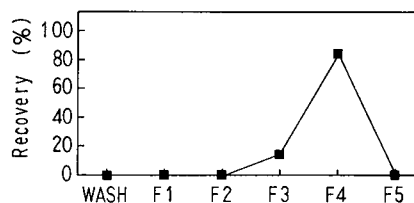


Fig. 1. Stepwise elution of kinetin from ion-exchange column. Resin treated with 1 M ammonia solution and 1 M hydrochloric acid was packed into a glass column of 1.6 cm I.D. to a height of 4 cm. The packed column was prewashed with 15 ml of buffer, then kinetin (20 µg) was applied. The column was washed with 25 ml of buffer and kinetin was eluted with 1 M ammonia solution (■). Each fraction (F1–F5) was 10 ml.

tion became a sharp peak (Fig. 1), yielding a 99% recovery.

HPLC conditions

Determination of kinetin was attempted using an ODS column. Ernstsén and Jensen [10] have investigated all binary systems of methanol or acetonitrile and water, and controlled the pH using an aqueous phase of either 20 mM ammonium acetate (pH 7.0) or 20 mM acetic acid (pH 3.5). On the other hand, Hardin and Stutte [11] used a 15-min linear gradient from 25% (in 0.67% acetic acid) to 32% methanol. Some of the major plant hormones were isolated by these methods. However, the separation of kinetin from *P. ginseng* callus extract was unsatisfactory. Adding trifluoroacetic acid to the solvent system of acetonitrile–water allowed a high resolution of kinetin and a linear calibration graph within the range 0.1–5 µg g⁻¹ was obtained.

Recovery of kinetin

Table I shows recoveries of kinetin from dried callus, fresh callus and medium, spiked at 5, 1 and 0.5 µg g⁻¹, respectively. The recoveries were 72.0, 72.8 and 84.2%, respectively. The detection limit was 0.02 µg g⁻¹. Fig. 2 shows chromatograms of dried callus and spiked extracts.

Kinetin content in dried callus

The chromatogram of dried callus extracts is shown in Fig. 2(1). A peak corresponding to kinetin was not detected. The same extract was then analysed by HPLC with the DAD system (Fig. 3). A

TABLE I
RECOVERY OF KINETIN FROM DRIED CALLUS,
FRESH CALLUS AND CULTURE MEDIA

Sample	Added ($\mu\text{g g}^{-1}$)	Recovery (%)	Mean \pm S.D. (%)
Dried callus			
No. 1	5.0	73.7	72.0 \pm 3.7
No. 2	5.0	74.5	
No. 3	5.0	67.8	
Fresh callus	1.0	72.8	
Medium	0.5	84.2	

small peak (a) was observed that corresponded to kinetin on magnification of the chromatogram [Fig. 3(1)]. Although peak a had a different spectrum to kinetin, peak b was identical [Fig. 3(2)]. The level of kinetin residues in dried callus was lower than the detection limit.

Uptake of kinetin from medium to callus

Pg-1 callus of *P. ginseng* was transplanted to fresh medium containing $0.1 \mu\text{g g}^{-1}$ of kinetin and cultured as above. The callus and the medium were withdrawn after 0, 1, 2, 4 and 28 days and analysed for kinetin. As shown in Fig. 4, within 1 day the kinetin content in the callus reached a maximum, then decreased and after 28 days no kinetin was detected. The kinetin concentration in the medium

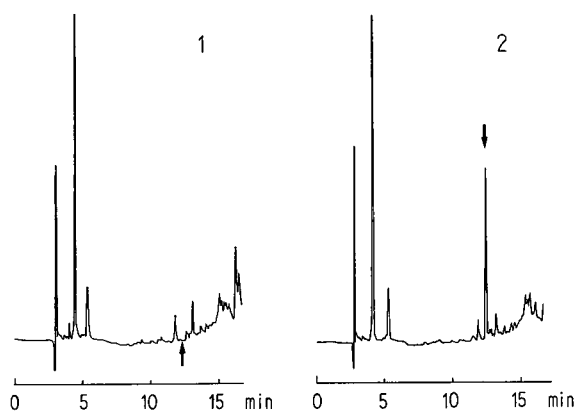


Fig. 2. Chromatograms of the extracts from (1) dried and (2) spiked callus of *P. ginseng*. Arrows indicate the spot corresponding to the kinetin peak.

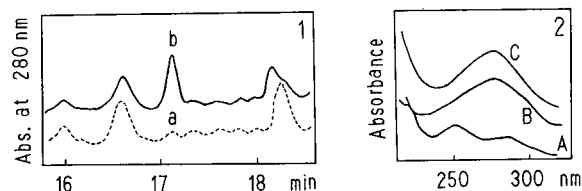


Fig. 3. (1) Magnified chromatograms of the extract from dried and spiked callus detected by DAD and (2) UV spectra. (1) The dashed line indicates chromatogram of the extract and the solid line indicates that of the spiked extract. The retention times of peaks a and b correspond to that of kinetin. (2) Lines A and B indicate the UV spectra of peaks a and b, respectively, and line C is that of a standard solution of kinetin detected by DAD.

decreased by 50% after 4 days, and it could not be detected after the 28th day. We found that ginseng callus absorbs kinetin from the medium rapidly and that the kinetin is metabolized it. Hence, kinetin was not detected in both callus and medium after the 28th day.

When *P. ginseng* was cultured by Furuya *et al.*'s method [12], it appeared that concentration of kinetin residue was below the detection limit. However, some products from tissue cultured plants may contain kinetin, depending on the concentration of kinetin in the growth medium.

Until recently, the toxicity of kinetin has been the subject of only a limited number of studies. Kajimoto *et al.* [14] showed that long-term administration of a small amount of kinetin resulted in weight in-

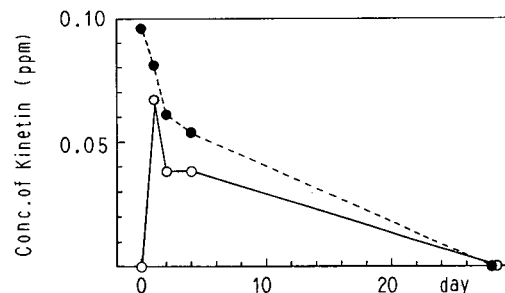


Fig. 4. Time course of uptake of kinetin from the medium by *P. ginseng* callus. Callus was transplanted to fresh medium supplemented with $0.1 \mu\text{g g}^{-1}$ of kinetin and cultured for 28 days. Callus samples were withdrawn after 1, 2, 4 and 28 days and medium samples after 0, 1, 2, 4 and 28 days. O = Kinetin concentration in the callus and ● = that in the medium.

creases in dogs and mice, and that its LD₅₀ value following intraperitoneal administration in the mouse was 450 mg kg⁻¹. Farrow *et al.* [15] examined the effect of kinetin on the incorporation of uridine and thymidine into the nucleic acids of human leukocytes. Apparently the effects of kinetin on the treated animals were not serious, but the intake levels for humans need to be confirmed, since kinetin inhibits or stimulates nucleic acid synthesis in plant systems as well as in human leukocytes [15]. The method presented here will be applicable to the analysis of kinetin from other products of plant biotechnology.

ACKNOWLEDGEMENT

This research was supported by a grant from Japan Health Sciences Foundation.

REFERENCES

- 1 T. Furuya, T. Yoshikawa, Y. Orihara and H. Oda, *Planta Med.*, 48 (1983) 83.
- 2 T. Furuya, T. Yoshikawa, T. Ishii and K. Kajii, *Planta Med.*, 47 (1983) 183.
- 3 T. Furuya, T. Yoshikawa, T. Ishii and K. Kajii, *Planta Med.*, 47 (1983) 200.
- 4 T. Furuya, H. Kojima, K. Syono, T. Ishii, K. Uotani and M. Nishio, *Chem. Pharm. Bull.*, 21 (1973) 98.
- 5 B. H. Most, J. C. Williams and K. J. Parker, *J. Chromatogr.*, 38 (1968) 136.
- 6 A. Zelleke, G. C. Martin and J. M. Labavitch, *J. Am. Soc. Hort. Sci.*, 105 (1980) 50.
- 7 M. Ludewig, K. Dorffling and W. A. König, *J. Chromatogr.*, 243 (1982) 93.
- 8 M. Nishio, S. Zushi, T. Ishii, T. Furuya and K. Syono, *Chem. Pharm. Bull.*, 24 (1976) 2036.
- 9 M. Claeys, E. Messens, M. Van Montagu and J. Schell, *Fresenius' Z. Anal. Chem.*, 290 (1978) 125.
- 10 A. Ernsten and E. Jensen, *J. Liq. Chromatogr.*, 8 (1985) 369.
- 11 J. M. Hardin and C. A. Stutte, *J. Chromatogr.*, 208 (1981) 124.
- 12 T. Furuya, T. Yoshikawa, Y. Orihara and H. Oda, *J. Nat. Prod.*, 47 (1984) 70.
- 13 C. O. Miller, F. Skoog, S. Okumura, M. H. Von Saltza and F. M. Strong, *J. Am. Chem. Soc.*, 78 (1956) 1375.
- 14 Y. Kajimoto, H. Matsuura, A. Kuramoto, S. Osumi, I. Imaoka, K. Ichiji, T. Isono, S. Okumura and K. Nishimada, *Nippon Yakurigaku Zasshi*, 61 (1965) 43s.
- 15 M. G. Farrow, D. F. Blaydes and K. van Dyke, *Experientia*, 32 (1976) 29.

Short Communication

Optimization of the separation of technical aldicarb by semi-preparative reversed-phase high-performance liquid chromatography

Qin-Sun Wang, Ru-Yu Gao and Bing-Wen Yan

National Laboratory of Elemento-Organic Chemistry, Nankai University, Tianjin 300071 (China)

(First received July 22nd, 1992; revised manuscript received September 22nd, 1992)

ABSTRACT

A computer-assisted method is presented for optimization of separation of technical aldicarb pesticide by semi-preparative reversed-phase HPLC. The optimization of the expected separation is based on a polynomial estimation from five preliminary experiments. A statistical scanning technique was used for optimization and the designated resolution was established for chromatographic performance measurement in this method. Excellent agreement was obtained between the predicted and experimental results.

INTRODUCTION

In recent years, various procedures have been described for the selection of the optimum mobile phase composition in HPLC and there are several reviews on this subject [1–5]. The sequential simplex method [6,7], window diagrams [8,9], overlapping resolution maps [10,11], the Prisma model method [12,13] and iterative mixture design [14,15] have been suggested as optimization methods for mobile phase composition in HPLC. Recently we described a computer-assisted optimization of binary mobile phase composition, pH and ion concentration selectivity using a scanning technique [16] and a simplex optimization of the experimental parameters in pre-

parative liquid chromatography has been also described [17].

In this paper, a computer-assisted method is presented for the optimization of the selection of the composition of the mobile phase in semi-preparative reversed-phase HPLC. The successful separation of technical aldicarb (a synthetic pesticide) is presented as an example. Excellent agreement was obtained between the predicted and experimental results. For the optimization the computer program OS-PLC (Optimization System for Preparative Liquid Chromatography) was developed.

EXPERIMENTAL

Materials

Technical aldicarb and its impurities were prepared in our Organic Synthesis Laboratory. Solutions with a concentration of 2.3 mg/ml in the mobile phase solvent were used for injection. Before

Correspondence to: Q.-S. Wang, National Laboratory of Elemento-Organic Chemistry, Nankai University, Tianjin 300071, China.

TABLE I

k' VALUES OF ALDICARB AND IMPURITIES MEASURED BY SEMI-PREPARATIVE HPLC WITH DIFFERENT MOBILE PHASE COMPOSITIONS

Mobile phase: methanol-water with volume fractions (X_s) of methanol from 0.3 to 0.7.

No.	Compound	X_s				
		0.30	0.40	0.50	0.60	0.70
1	Aldicarb sulphoxide	1.279	1.161	1.148	1.085	1.050
2	Aldicarb sulphone	1.534	1.237	1.211	1.089	1.050
3	Unknown A	2.508	1.832	1.754	1.475	1.240
4	Unknown B	3.168	1.989	1.869	1.475	1.240
5	Propionaldoxime	4.473	2.756	2.540	1.869	1.416
6	Aldicarb	5.752	3.004	2.734	1.893	1.429

use, all solvents were redistilled, filtered through a 0.45- μ m filter and vacuum degassed.

Apparatus

All computer studies were carried out on a Model HP-220 computer (Hewlett-Packard) with an HP-9133A disk drive, HP-2225A printer and HP-7470A graphics plotter. The OS-PLC program was written in HP basic 4 language. Alternatively, an IBM-XT personal computer with True BASIC language was used.

The reversed-phase HPLC system was composed of Series 4 liquid chromatograph (Perkin-Elmer) with a Perkin-Elmer LC-75 UV detector and C-R1B data system (Shimadzu). A Spherisorb C₁₈ column (300 mm \times 8 mm I.D.) (Dalian Institute of Chemical Physics, Dalian, China) was used.

Chromatography

Methanol-water in different proportions (Table I) was used as the mobile phase. The injection volume was 200 μ l. Experiments were run at 20°C with a flow-rate of 2.5 ml/min. The UV detector was used at 240 nm.

RESULTS AND DISCUSSION

The principle of the method is based on the relationship between the capacity factor, k' , of each solute and the mobile phase composition. In a binary solvent system, the capacity factor of a solute is related to the volume fraction, X_s , in the following manner:

$$k' = A_0 + A_1 X_s + A_{11} X_s^2 \quad (1)$$

where A_0 , A_1 and A_{11} are constants of the given solute. It is necessary to determine experimentally the constants for each solute in the binary solvent system. Five preliminary experiments were used for solving eqn. 1 to yield A_0 , A_1 and A_{11} .

Minimum resolution ($R_{s \min}$) was used as the criterion for separation. The predicted k' values of the solutes were used to calculate the R_s values for adjacent pairs. If n is the peak number, only $n-1$ pairs were calculated at each solvent composition and the minimum resolution, *i.e.*, the least separated pair of peaks, was selected. Then a diagram of $R_{s \min}$ versus solvent composition (X_s) was obtained. The maximum $R_{s \min}$ was selected and this shows that the solvent composition will give a better separation for the least separated pair, so all other peak pairs will have higher R_s values. The result of chromatographic selectivity optimization is the separation of the solutes of interest from all the other (unimportant) components of the sample mixture.

Obviously, sometimes the separation of the least

TABLE II

COEFFICIENTS A_0 , A_1 AND A_{11} FOR ALDICARB AND IMPURITIES

No. ^a	A_0	A_1	A_{11}	r
1	1.6022	-1.3626	0.8286	0.9775
2	2.4722	-4.1160	3.0000	0.9727
3	4.3271	-7.7573	4.8643	0.9744
4	6.7848	-15.8986	11.5286	0.9713
5	9.5170	-21.8082	14.8071	0.9756
6	14.4074	-38.3070	28.5500	0.9700

^a See Table I.

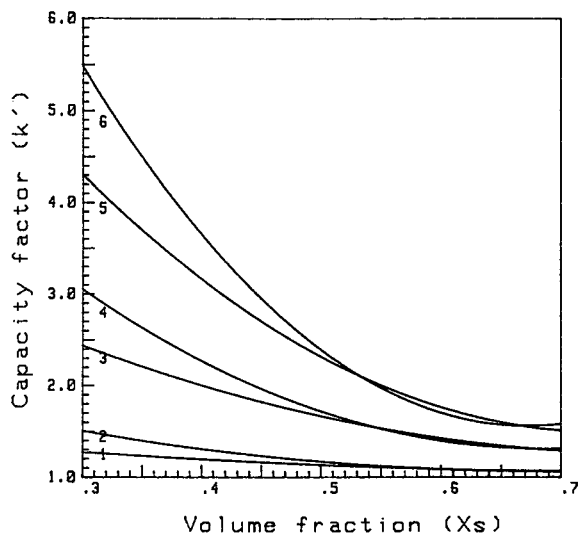


Fig. 1. Capacity factor, k' , versus mobile phase composition for aldicarb and impurities. For compounds (1-6), see Table I.

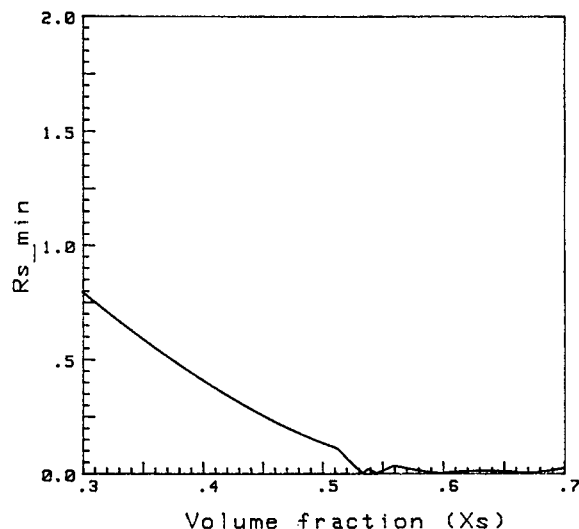


Fig. 2. Relative resolution map for aldicarb and impurities.

the general resolution criterion that only the least separated pair of peaks is considered is a disadvantage. A direct approach is to calculate the resolution only between the peaks of interest and their nearest neighbours, and set the minimum resolution criterion (R_{s_min}) equal to the lowest value. This is the designated resolution that was used in this study. The results concern only the required separation. The maximum R_{s_min} is then selected, and this shows that the solvent compositions will give a better separation for the peaks of interest. The entire procedure described above is performed by the software (OS-PLC). The mobile phase optimization procedure was evaluated with the separation of technical aldicarb.

The k' values of five preliminary experiments are given in Table I and the values of A_0 , A_1 , A_{11} in Table II. Fig. 1 shows the plots of k' for each composition as a function of the volume fraction of methanol. The computer scanning technique was used for optimizing the binary solvent composition (X_s from 0.3 to 0.7). Fig. 2 gives the corresponding diagrams. The maximum R_{s_min} is 0.79, and the optimum X_s is 0.30. Obviously an X_s of less than 0.30 will give a resolution of more than 0.79, but the analysis time is then too long. Note that in Fig. 1 the least separated pair is compounds 1 and 2, if we consider the peak of interest (compound 6, aldi-

carb) and their nearest neighbours for separation. The results are shown in Fig. 3. The resolution for aldicarb separation is 1.57. The experimental result under optimum conditions is shown in Fig. 4. There is good agreement between the predicted and experimental results.

Obviously, in practical application the method

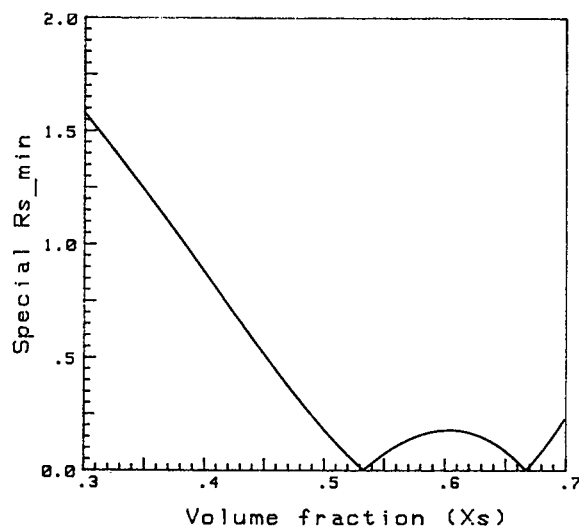


Fig. 3. Relative designated resolution map for aldicarb and impurities.

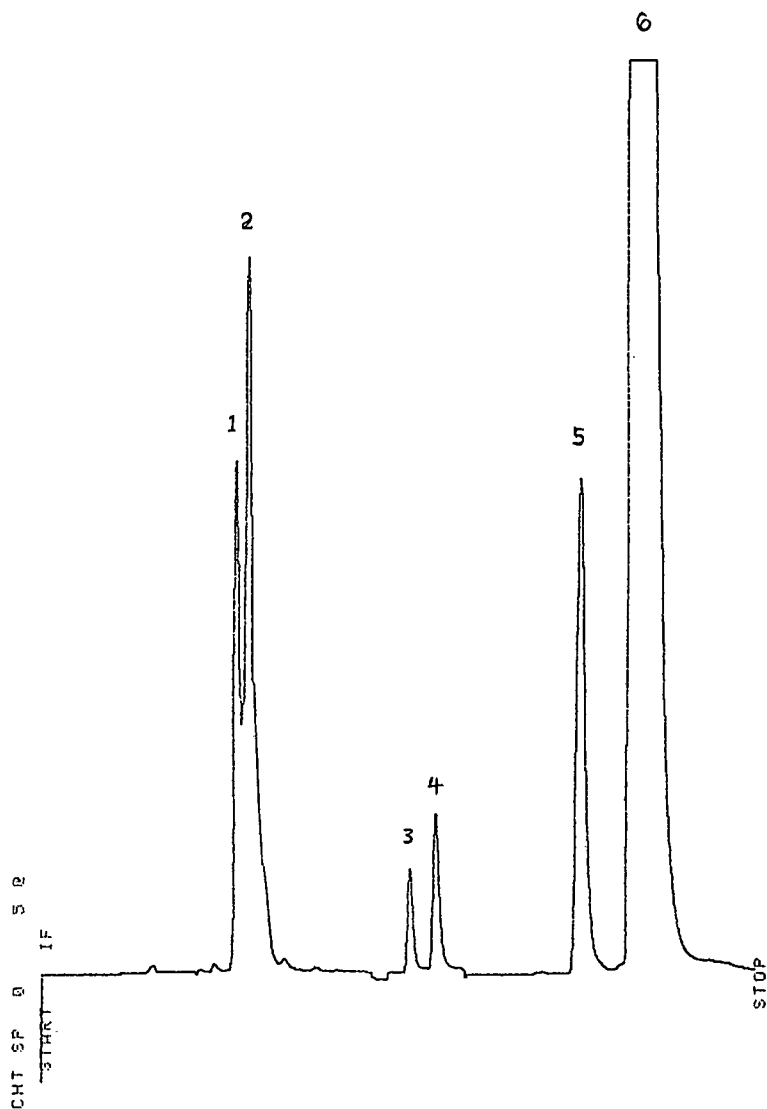


Fig. 4. Experimental chromatogram at optimum condition $X_s = 0.30$ (200 μ l, 2.3 mg/ml).

can be used to increase the injection volume for aldicarb for preparations under overload conditions, for which Snyder *et al.* [18] combined certain features of the Knox-Pyper model with their own model of preparative HPLC so as to allow convenient and reliable computer simulations to be carried out under conditions of mass overload. The use of the program PREPSIMX in conjunction with the Knox-Pyper model made it possible to draw a

number of general conclusions relating to optimum conditions for preparative HPLC. Here 200- μ l solutions with a concentration of 43.8 mg/ml in the mobile phase solvent were used for injection. The results are shown in Fig. 5. The maximum amount of sample that can be injected on to the column is much smaller than when there is higher resolution. A yield of aldicarb of 87.1% was achieved in 30 min. The amount of sample required is not obtained

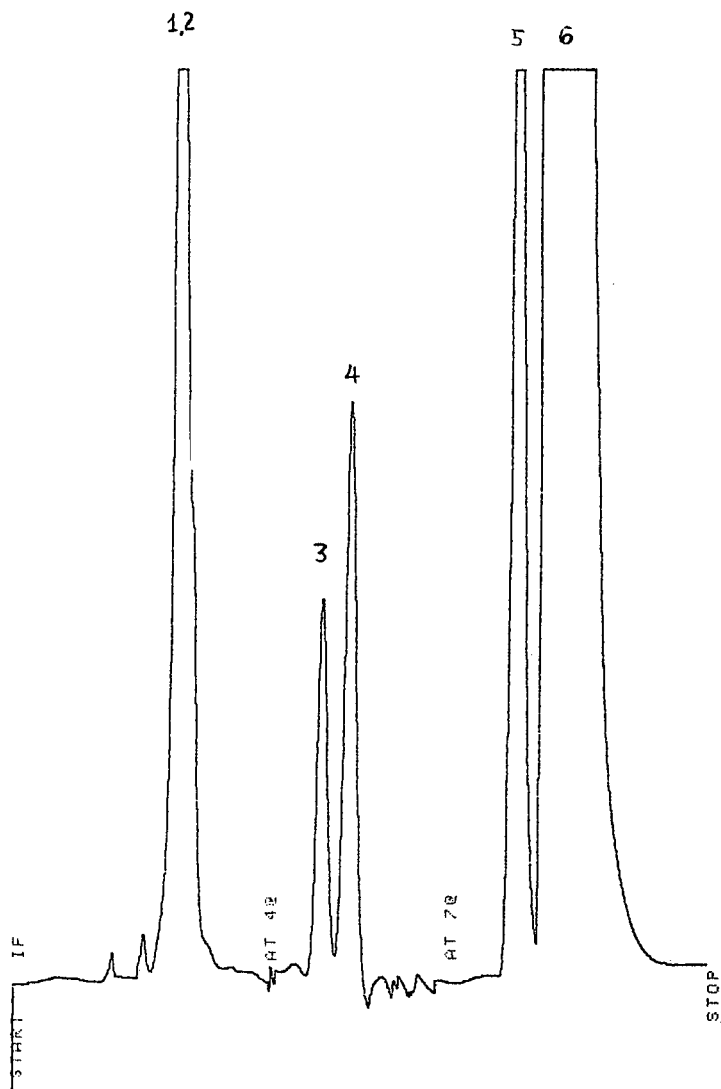


Fig. 5. Experimental preparative chromatogram at optimum condition $X_s = 0.30$ (200 μ l, 43.8 mg/ml).

in one injection, hence repetitive injections must be made and the eluate fractions collected and combined.

CONCLUSIONS

We have shown that it is possible to apply optimum conditions for the separation of technical aldicarb in semi-preparative reversed-phase HPLC using the computer scanning technique. The designat-

ed resolution was used as the criterion. Excellent agreement was obtained between the predicted data and the experimental results.

ACKNOWLEDGEMENTS

This work was supported by the National Education Commission of China. We thank Mrs. Bao-Ying Qu for technical assistance.

REFERENCES

- 1 J. C. Berridge, *Techniques for the Automated Optimization of HPLC Separation*, Wiley, New York, 1985.
- 2 P. J. Schoenmakers, *Optimization of Chromatographic Selectivity*, Elsevier, Amsterdam, 1986.
- 3 Sz. Nyiredy (Editor), *J. Liq. Chromatogr.*, 12, Nos. 1 and 2 (1989).
- 4 J. L. Glajch and L. R. Snyder (Editors), *J. Chromatogr.*, 484 (1989).
- 5 Sz. Nyiredy (Editor), *J. Liq. Chromatogr.*, 14, Nos. 16 and 17 (1991).
- 6 J. C. Berridge, *J. Chromatogr.*, 244 (1982) 1.
- 7 J. C. Berridge, *Analyst (London)*, 109 (1984) 291.
- 8 H. J. Issaq, G. M. Muschik and G. M. Janini, *J. Liq. Chromatogr.*, 6 (1983) 259.
- 9 Q. S. Wang, R. Y. Gao and H. Y. Wang, *Chromatographia*, 28 (1989) 285.
- 10 J. L. Glajch, J. J. Kirkland, K. M. Squire and J. M. Minor, *J. Chromatogr.*, 199 (1980) 57.
- 11 J. L. Glajch, J. C. Gluckman, J. G. Charikofsky, J. M. Minor and J. J. Kirkland, *J. Chromatogr.*, 318 (1985) 23.
- 12 Sz. Nyiredy, K. Dallenbach-Toelke, O. Sticher, *J. Liq. Chromatogr.*, 12 (1989) 95.
- 13 S. J. Ziegler, O. Sticher, *J. Liq. Chromatogr.*, 12 (1989) 199.
- 14 A. C. J. H. Drouen, H. A. H. Billiet, P. J. Schoenmakers and L. de Galan, *Chromatographia*, 16 (1982) 48.
- 15 P. R. Haddad, A. C. J. H. Drouen, H. A. H. Billiet and L. de Galan, *J. Chromatogr.*, 282 (1983) 71.
- 16 Q. S. Wang, R. Y. Gao and H. Y. Wang, *J. High Resolut. Chromatogr.*, 13 (1990) 173.
- 17 S. Ghodbane and G. Guiochon, *Chromatographia*, 26, (1988) 53.
- 18 L. R. Snyder, G. B. Cox and P. E. Antle, *Chromatographia*, 24 (1987) 82.

Short Communication

High-performance liquid chromatography of inorganic mercury and organomercury with 2-mercaptobenzothiazole

Yao-Chin Wang and Chen-Wen Whang

Department of Chemistry, Tunghai University, Taichung 40704 (Taiwan)

(First received July 14th, 1992; revised manuscript received September 28th, 1992)

ABSTRACT

A reversed-phase liquid chromatographic method is described for the determination of inorganic mercury and organomercury in aqueous solution. Using an eluent of methanol–10 mM sodium acetate buffer (80:20, pH 6.2) containing 0.1 mM 2-mercaptobenzothiazole (MBT), methylmercury, ethylmercury, phenylmercury and inorganic mercury can be separated on a C₁₈ column in less than 9 min. UV detection was carried out at 285 nm. Calibration graphs were linear ($r \geq 0.997$) over three orders of magnitude of concentration for the three organomercury species. The linear range of inorganic mercury was smaller. Detection limits (3σ) ranged from 0.3 ng of Hg for methylmercury to 0.5 ng of Hg for inorganic mercury. Interference due to metal ions can be eliminated by inclusion of a low concentration (*ca.* 50 μ M) of EDTA in the eluent.

INTRODUCTION

Conventionally, speciation and determination of mercury in biological and environmental samples have been performed by gas chromatographic (GC) methods (usually based on that developed by West-ö [1,2]) and cold-vapour atomic absorption spectrometry (CVAAS, originally developed by Poluektov and co-workers [3,4]). In GC analysis, it is essential to form strong, thermally stable derivatives, whereas in CVAAS, complete reduction and quantitative collection of mercury are necessary.

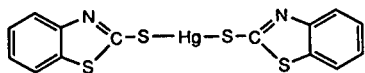
In the past decade, several high-performance liquid chromatography (HPLC) procedures for the determination of inorganic and organomercury

have also been developed. In comparison with GC and CVAAS methods, the use of HPLC for mercury speciation generally has the advantage of simplified sample preparation. However, the detection of mercury(II) compounds is problematic because of their lack of chromophores, which precludes the direct use of simple ultraviolet (UV)–visible detection. Several methods have been employed to overcome this problem, such as on-column derivatization with 2-mercaptoethanol followed by electrochemical [5–7], AAS [8,9], inductively coupled plasma atomic emission spectrometric (ICP-AES) [10] and ICP mass spectrometric (ICP-MS) detection [11]. Most of these methods require the use of expensive and specialized detectors. An alternative approach to the use of simple UV–visible detection in HPLC of mercury(II) compounds is to incorporate an on- or off-column derivatization procedure with organ-

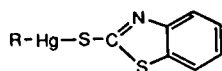
Correspondence to: C.-W. Whang, Department of Chemistry, Tunghai University, Taichung 40704, Taiwan.

ic complexing agents. The commonly used complexing agents include dithizone [12,13], 6-mercaptopurine [14] and various dithiocarbamates [15-18].

In this paper, we describe an HPLC procedure for the separation and determination of inorganic mercury and organomercury as their 2-mercaptobenzothiazole (MBT) complexes. MBT can form stable complexes with both inorganic mercury and organomercury ions. The structures of the mercury-MBT complexes have been determined by infrared spectrometry [19] and X-ray diffraction analysis [20], and can be represented as



and



where R = alkyl or phenyl. A preconcentration method for inorganic mercury and organomercury in sea water with MBT supported on silica gel also has been described [21], but to our knowledge there has been no previous report on the use of MBT in the HPLC of mercury(II) compounds. In this study, the mercury-MBT complexes were formed on-column by direct injection of the analyte into a mobile phase containing the complexing agent and detection was performed with a UV detector operated at 285 nm.

EXPERIMENTAL

Apparatus

The HPLC system consisted of an Eldex 9600 solvent-delivery system, a Rheodyne Model 7125 injector with a 100- μ l sample loop, a Brownlee Labs. RP-18 column (220 \times 4.6 mm I.D., 5 μ m), a Soma S-3702 variable-wavelength UV detector operated at 285 nm and a Pantos U-228 strip-chart recorder. A 15 \times 3.2 mm I.D. guard column packed with 7- μ m RP-18 particles was placed in front of the analytical column.

Reagents

All chemicals were of analytical-reagent grade. Distilled deionized water was obtained using a Nanopure II system.

Inorganic mercury and organomercury chlorides were obtained from Merck. Stock standard solutions (1000 μ g ml⁻¹ of mercury) were prepared in HPLC-grade methanol and stored in glass bottles below 4°C. Working standard solutions of lower concentration were freshly prepared by appropriate dilution with methanol before use.

The chromatographic eluent consisted of methanol-10 mM sodium acetate buffer (80:20) (pH 6.2) containing 0.1 mM MBT. This solution was filtered through a 0.45- μ m membrane filter and degassed ultrasonically before use.

RESULTS AND DISCUSSION

HPLC of mercury-MBT complexes

MBT can form stable complexes with inorganic mercury and organomercury. The neutral compounds formed can be separated by reversed-phase liquid chromatography using a Brownlee Labs. C₁₈ column. Fig. 1 shows a typical chromatogram for

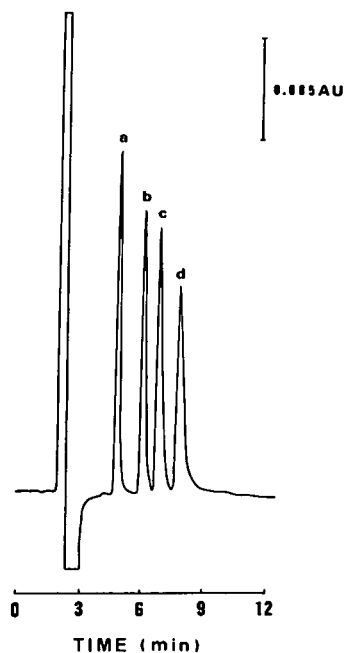


Fig. 1. Chromatogram of (a) methylmercury(I), (b) ethylmercury(I), (c) phenylmercury(I) and (d) inorganic mercury(II) complexes of MBT. Conditions: Brownlee Labs. RP-18 column; eluent, methanol-10 mM sodium acetate buffer (80:20) (pH 6.2) containing 0.1 mM MBT; flow-rate, 1.0 ml min⁻¹; UV detection, 285 nm; sample amount, 45 ng of Hg for each species.

TABLE I

CALIBRATION DATA FOR DETERMINATION OF INORGANIC MERCURY AND ORGANOMERCURY BY HPLC

Injection volume, 100 μ l; other conditions as in Fig. 1.

Compound	Linear range ^a (μ g Hg)	r^b	D.L. ^c (ng Hg)	R.S.D. (%)
Methylmercury	0.001–3.0	0.9989	0.3	2.1
Ethylmercury	0.002–2.5	0.9986	0.4	2.6
Phenylmercury	0.002–2.5	0.9995	0.4	3.4
Inorganic mercury	0.002–0.5	0.9969	0.5	3.1

^a Range between the limit of quantification (LOQ) and the limit of linearity (LOL) [22].^b Correlation coefficient.^c Detection limit.

methylmercury, ethylmercury, phenylmercury and inorganic mercury. Complete separation of all four mercury–MBT complexes was obtained in less than 9 min. The elution order was the same as observed for dithizonate complexes [13] and diethyldithiocarbamate chelates [15].

Calibration

A series of spiked, distilled water samples containing known amounts of the four mercury species were used for construction of calibration graphs. The results are summarized in Table I. A linear correlation between the peak height and the amount injected was obtained for each species. The correlation coefficients of the calibration graphs were ≥ 0.997 in all instances. For inorganic mercury, linearity was observed only up to about 0.5 μ g, above which the calibration graph gradually approached a plateau. This phenomenon may be explained by the fact that each Hg(II) needs two MBT molecules to form a neutral complex whereas other organomercury ions just only one [Hg(MBT)₂ versus RHg(MBT)]. At a certain concentration of MBT in the eluent, *e.g.*, 0.1 mM in the present instance, the linear range of the calibration graph for inorganic mercury will be smaller than that for organomercury, assuming all inorganic mercury– and organomercury–MBT complexes have similar stability constants. Increasing the MBT concentration in the eluent may extend the linear range of the calibration graph for inorganic mercury. However, a higher MBT concentration and accompanying higher

background noise levels were found to deteriorate both the resolution and detection of the four mercury species.

The detection limits listed in Table I were calculated from peak heights corresponding to three times the average standard deviation of the baseline noise [23]. The baseline noise was calculated from the height of the largest noise fluctuation measured in a preselected chart interval. The detection limits range from 0.3 ng of Hg for methylmercury to 0.5 ng of Hg for inorganic mercury.

The reproducibility of the method was tested with seven replicate injections of 5 ng of each mercury species. The relative standard deviations ranged from 2.1% for methylmercury to 3.4% for phenylmercury.

Interferences

Possible interferences of Ca(II), Mg(II), Cu(II), Cd(II), Pb(II), Zn(II), Co(II), Ni(II), Mn(II), Fe(III), Al(III) and Cr(III) in the HPLC of mercury were studied. The results indicated that, except for Ca(II), Mg(II), Co(II), Ni(II), Fe(III) and Al(III), the metals tested at a level of five times the amount of mercury species also showed detectable signals. Under the optimum HPLC conditions for mercury, most of these interfering ions were eluted at *ca.* 4 min, which is close to the elution time of methylmercury (4.9 min). This interference can be effectively eliminated by inclusion of a low concentration (*e.g.*, 50 μ M) of EDTA in the eluent. The EDTA apparently forms stronger complexes with the

metals than does the MBT, but organomercury does not. In addition, the peak size of inorganic mercury was not affected by the presence of EDTA in the eluent. The complex formed between Hg(II) and MBT is obviously much stronger than the Hg(II)–EDTA complex.

Applications

In order to validate the method, mercury was determined in the standard reference material NIST SRM 1641b (mercury in water). The sample was diluted 5:1 with distilled, deionized water before injection. The value obtained for inorganic mercury was $1.43 \pm 0.07 \mu\text{g ml}^{-1}$, based on six replicate injections, which compares favourably with the certified mercury content of $1.52 \mu\text{g ml}^{-1}$. No organomercury species could be found in this sample.

A commercial contact lens cleaning solution containing thimerosal [ethyl (sodium *o*-mercaptobenzoato)mercury(I)] was analysed. Thimerosal was known to degrade rapidly in aqueous solution, forming an ethylmercury salt and thiosalicylic acid [24]. The sample analysed had been stored at ambient temperature for about 1 month after purchase. The solution was diluted 2:1 with water before in-

jection. Fig. 2 shows a typical chromatogram obtained for this sample. The presence of free ethylmercury is evident. Results of quantitative measurement indicated that the ethylmercury content in this particular sample corresponds to 15% of the original concentration of thimerosal (10 mg l^{-1}) marked on the sample container. However, it had been reported that by forming a more stable complex, a thiol-containing complexing agent (*e.g.*, dithiocarbamate) can easily displace the bound ethylmercury group from the undecomposed thimerosal [25]. Therefore, in the present instance, the measured ethylmercury content may not represent the true degree of degradation of thimerosal in the original sample. Further study in this respect is needed.

CONCLUSIONS

A simple HPLC procedure for the determination of inorganic mercury and organomercury in aqueous solution has been developed. On-column complexation between mercury species and MBT permits the use of a UV detector for rapid and sensitive detection. Interferences from metal ions can be avoided by the inclusion of a low concentration of EDTA in the eluent. This method is applicable to the determination of mercury species in aqueous samples of a relatively simple matrix, such as pharmaceutical formulations. On the other hand, the detection limits of the method are probably insufficient for the direct determination of trace mercury in natural waters. In combination with a suitable means of sample pretreatment, *e.g.*, solvent extraction or preconcentration, this method should be useful for environmental and/or biological applications. An on-line preconcentration procedure for trace mercury using a short enrichment column and a switching valve directly connected to the HPLC column [26] is under study.

REFERENCES

- 1 G. Westöö, *Acta Chem. Scand.*, 20 (1966) 2131.
- 2 G. Westöö, *Acta Chem. Scand.*, 22 (1968) 2277.
- 3 N. S. Poluektov and R. A. Vitkun, *Zh. Anal. Khim.*, 18 (1963) 33.
- 4 N. S. Poluektov, R. A. Vitkun and Y. V. Zelyukova, *Zh. Anal. Khim.*, 19 (1964) 873.
- 5 W. A. MacCrehan, R. A. Durst and J. M. Bellama, *Anal. Lett.*, 10 (1977) 1175.
- 6 O. Evans and G. D. McKee, *Analyst*, 112 (1987) 983.

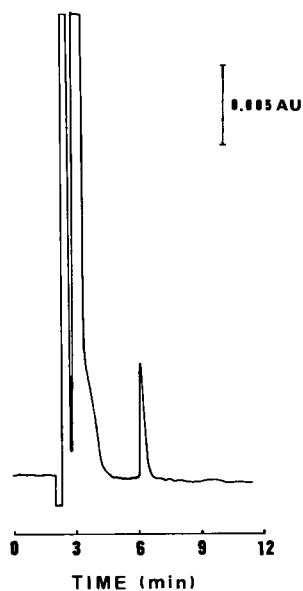


Fig. 2. Chromatogram of a contact lens cleaning solution. Conditions as in Fig. 1, except that the eluent also contained 0.1 mM EDTA.

- 7 O. Evans and G. D. McKee, *Analyst*, 113 (1988) 243.
- 8 W. Holak, *J. Liq. Chromatogr.*, 8 (1985) 563.
- 9 W. Holak, *Analyst*, 107 (1982) 1457.
- 10 I. S. Krull, D. S. Bushee, R. G. Schleicher and S. B. Smith, Jr., *Analyst*, 111 (1986) 345.
- 11 D. S. Bushee, *Analyst*, 113 (1988) 1167.
- 12 C. H. Gast and J. C. Kraak, *Int. J. Environ. Anal. Chem.*, 6 (1979) 297.
- 13 W. Langseth, *Anal. Chim. Acta*, 185 (1986) 249.
- 14 J. E. Parkin, *J. Chromatogr.*, 370 (1986) 210.
- 15 S. Inoue, S. Hoshi and M. Mathubara, *Talanta*, 32 (1985) 44.
- 16 J. E. Parkin, *J. Chromatogr.*, 407 (1987) 389.
- 17 J. E. Parkin, *J. Chromatogr.*, 472 (1989) 401.
- 18 W. Langseth, *J. Chromatogr.*, 438 (1988) 414.
- 19 N. V. Mel'nikova, *Russ. J. Inorg. Chem.*, 33 (1988) 1785.
- 20 J. Bravo, J. S. Casas, M. V. Castano, M. Gayoso, Y. P. Mascarenhas, A. Sanchez, C. Santos and J. Sordo, *Inorg. Chem.*, 24 (1985) 3435.
- 21 K. Terada, K. Morimoto and T. Kiba, *Bull. Chem. Soc. Jpn.*, 53 (1980) 1605.
- 22 L. H. Keith, R. A. Libby, W. Crummett, J. K. Taylor, J. Deegan, Jr. and G. Wentler, *Anal. Chem.*, 55 (1983) 2210.
- 23 J. E. Knoll, *J. Chromatogr. Sci.*, 23 (1985) 422.
- 24 H. J. Readers and C. B. Lines, *J. Pharm. Sci.*, 72 (1983) 1406.
- 25 J. E. Parkin, *J. Chromatogr.*, 542 (1991) 137.
- 26 C. W. Whang and L. L. Yang, *J. Chin. Chem. Soc.*, 35 (1988) 109.

Short Communication

Two-solute method for indicating polarity changes of conventional and novel gas chromatographic stationary phases with temperature increase

T. J. Betts

School of Pharmacy, Curtin University of Technology, GPO Box U 1987, Perth, W. Australia (Australia)

(First received August 19th, 1992; revised manuscript received October 22nd, 1992)

ABSTRACT

This author's previous work suggested that a ratio of corrected retention times for cuminal (cu) against caryophyllene (cy) pragmatically indicated the polarity of a gas chromatographic stationary phase. A c ratio of $3c_{cu}/4c_{cy}$ below 0.8 corresponded to low-polarity phases, and above 1.2 to high-polarity ones. Changes in the c ratio for liquid crystal, toroid molecular and conventional phases were observed with increases in temperature, particularly for Carbowax 20M, which appeared to decline considerably in polarity. Some high-polarity liquid crystals were reduced to intermediate polarity c ratios (0.8–1.2). Previous anomalous observations by this author can now be explained.

INTRODUCTION

Since 1981 [1,2] this author has been interested in finding a simple method for determining the polarity of stationary phases used for gas chromatography. It became more urgent during recent studies of novel phases [3,4]. Kollie and Poole [5] recently remarked that "the general concept of polarity is a measure of the capacity of a stationary phase to enter into all intermolecular interactions. No exact method has emerged for calculating or determining this term". The general concept has been reviewed since 1989 [6,7].

McReynolds values [8] are often used as indicators of phase polarity—usually by placing them in

sequence of the sum of the values for say five (of the full ten) solute probes. However, all McReynolds values have a non-polar bias, as they are the retention index of each probe rated against non-polar normal alkanes on the phase, minus the index of the same probe on non-polar squalane phase. Logically, a "polar" phase should retain the polar solute *n*-butanol much more than low-polarity benzene. However, various phases all have McReynolds values for benzene which form a consistent about 40% of the sum of their butanol and benzene values. The respective values, for example are 158 and 119 (43%) on the phenyl,methylpolysiloxane OV-17; 536 and 322 (38%) on polyethyleneglycol 20M; and 751 and 499 (40%) on diethyleneglycol succinate (DEGS). These diverse phases, and others, appear to show hardly any difference in their relative affinity for these two distinct solutes. A further limitation of the McReynolds system is that determina-

Correspondence to: T. J. Betts, School of Pharmacy, Curtin University of Technology, GPO Box U 1987, Perth, W. Australia, Australia.

tions should be made at the low temperature of 120°C. Other deficiencies have been observed [5].

We proposed in 1981 a system [1], subsequently [3] named “LEC”, using the retention indices on the test phase of three typical volatile oil constituents; linalol, estragole and carvone (two terpenoids and an aromatic) at the more generally used temperature of 160°C. These indices were determined against polar normal alcohols as well as alkanes, and compared to values from a “standard” phenyl, methylpolysiloxane phase. The test phase was then numerically more or less polar than the standard [1]. Castello *et al.* [9,10] later devised a system in 1988 which also used both normal alcohols and alkanes; taking the difference in apparent carbon number between an alkane and an alcohol with the same retention time on a capillary phase.

Our “LEC” method was later modified [3] by the replacement of the carvone by cineole (both terpenoids), and by omission of the alcohol-based indices. It then indicated three liquid crystal phases in packed columns as being of low polarity, although by another lower-temperature method used in these laboratories, they confusingly rated much higher. This [2] utilises three McReynolds probe solutes, including the uncommon low-polarity 2-octyne (O). *n*-Butanol (B) always emerged before pyridine (P), but the sequence O–B–P was given by high-polarity phases, B–P–O by low-polarity ones, and B–O–P by intermediate polarities. These same solute sequences were later hidden in Kollie and Poole’s Table II [11] amongst the values of partial molal Gibbs free energy of solution for 18 solutes on 23 phases. Here, the sequences of values show 20M and DEGS to be highly polar, whilst the “problem” phases OV-225 (cyanopropyl, phenyl, dimethylpolysiloxane) and QF-1 (trifluoropropyl, methylpolysiloxane) are appropriately indicated by B–O–P to be of intermediate polarity. Principal component analysis extracting eigenvectors confirmed these solutes to be in three different groups, but gave five classes of phases, with some behaving “independently”. Cluster analysis reduced these to four classes, but grouped squalane with OV-225 and 20M! Their later paper [5], using the same procedures on a new free energy of solution parameter, did put 20M with DEGS, with a separate group of various polysiloxanes, and could thus “provide a logical and intuitive(!) classification of phases”. A complex mathematical way

of achieving something quite evident to chromatographers who use these phases!

The need was apparent for a simple procedure which could be applied over a range of temperatures, unlike McReynolds’, and other methods. Consideration of my recent work on volatile oil constituents [4] suggested that this could be provided by the pair of solutes polar aromatic cuminal [$\text{CHO}-\text{C}_6\text{H}_4-\text{CH}(\text{CH}_3)_2$], and non-polar bicyclic non-aromatic diene sesquiterpene caryophyllene [$\text{CH}_2=\text{C}_{11}\text{H}_{13}(\text{CH}_3)_3$] with a nine-carbon ring system. Having made previous records of their relative retention times on novel phases [4,12,13], it only needed some new observations on traditional phases. The use of just two solute probes to evaluate stationary phases goes back to 1959, when Rohrschneider [14] used butane and butadiene. Abraham *et al.* [15] currently claim that a “single parametercannot possibly reflect the various solute–(phase) interactions”. They feel the need for a complex equation of five terms with six constants, although they previously acknowledged [16] that three of their constants were “not very useful”, “minor” or “not significant”. Their tables listing calculations for various phases of the surviving three terms (ref. 15, Table IV; ref. 16, Table XII) reveal they cannot discriminate five different probe solutes. All phases show lowest value of one term along with highest values for the other two terms, and the same pattern of values for each solute. Their equation, deduced from a hypothetical model involving the creation of cavities in the phase to receive solute molecules [16], seems unable to reflect phase polarity differences. A later paper [17] uses, for two low polarity phases, a “truncated” equation involving just two terms for molar refraction and a partition coefficient in hexadecane at the impractical temperature of 25°C; seemingly distant from actual gas chromatography! It seems sense to use two appropriate probe solutes, as is done in the present pragmatic work.

EXPERIMENTAL

Apparatus

A Hewlett-Packard 5790A gas chromatograph was used, fitted with a capillary control unit, and a splitter injection port and flame ionisation detector both set at 235°C. A Hewlett-Packard 3380A recorder/integrator was attached.

Materials and methods

Details of the capillaries used have been recorded previously [18]. Helium was used as mobile phase at about 1 ml min^{-1} except for the “ChiralDEX-A-DA” toroid phase, where double this flow-rate was needed. Injections were made of trace residues from an “emptied” microsyringe. Holdup times were obtained by extrapolating to methane the retention times of *n*-heptane and *n*-hexane plotted on semi-logarithmic graph paper.

Details of the packed columns have been given previously. The liquid crystal phases, (all 3%, w/w) [13] were bis(methoxybenzylideneanilchloroaniline) [(MBCA)₂], bis(methoxybenzylideneanilbitoluidine) [(MBT)₂] and azoxydiphenetol (ADP), all from T.C.I. (Tokyo, Japan). The toroid molecular phases (both 3%, w/w) [4] dicyclohexano- and dibenzo-24-crown-8 ethers were from Aldrich. Cholesteryl acetate (10%, w/w), was from Sigma, and although a liquid crystal at about 115°C, had been found to function best as a normal isotropic liquid above this temperature [19]. The linalol used was from Sigma, the cuminal (*p*-isopropylbenzaldehyde) from Eastman, and the (impure) caryophyllene from Koch-Light.

RESULTS AND DISCUSSION

Average results, newly obtained for this work, and from my previous studies [4,12,13] are given in Table I as relative retention times to linalol, after deducting holdup times. The ratio of these values for cuminal (cu) against caryophyllene (cy) presented best if reduced by three-quarters, and this is included in Table I as an indicator of phase polarity. If its “*c* ratio” of $3\text{cu}/4\text{cy}$ was about unity (say 0.80–1.20) a phase had intermediate polarity like the cyanopropyl,phenyl,dimethylpolysiloxane OV-225 [2]. A bigger *c* ratio (up to almost 1.60 was observed) indicated a strongly polar phase; whilst a lower ratio (down to near 0.25 was observed), with caryophyllene emerging after cuminal, indicated a low-polarity phase. Of course, simple corrected retention times gave the same *c* ratios, but relative times are quoted in Table I as these are what have been published before.

Fully methylpolysiloxane is a classic very low-polarity phase, and gave very low *c* ratios around 0.30, which went from 0.27 to 0.33 as the oven temper-

ature increased from 140 to 200°C. This phase thus behaved in a slightly less non-polar fashion with temperature rise. Isotropic (normal liquid) cholesteryl acetate (not functioning as a liquid crystal) showed less low-polar *c* ratios, around 0.40, which also rose slightly with temperature increase. Two toroid (ring) molecular phases showed very consistent values around 0.65, and so were not as low-polar as those above, but still could not be considered to be up to intermediate polarity. These phases all gave the B–P–O (see Introduction) low polarity sequence [2,4,19] except the dicyclohexane crown ether, which probably did not behave “normally” at the low 120°C used for this method. Its *c* ratios indicated that it was very similar to the ChiralDEX phase, and at 140°C this latter yielded the same sequence of eight chemically different solutes as the crown ether at 170°C [4].

OV-225 gave *c* ratios around 1.00, which decreased from 1.03 to 0.94 with oven temperature increase from 140°C to 200°C. The liquid crystal (MBCA)₂ showed similar ratios, also decreasing from 1.07 to 1.00 as the temperature went from 145 to 175°C—the reverse of the small rises in polarity shown by the low-polarity phases. Another liquid crystal, mesogenic polymeric methyl siloxane “MPMS” showed constant ratios, when melted, of 1.19 (more polar than OV-225 or (MBCA)₂ and almost falling into the high-polarity category), with a similar ratio when unmelted. OV-225 and “MPMS” showed the intermediate solute sequence of B–O–P [2,18] but not (MBCA)₂ [3]. However, the 120°C used with these three solutes was well below the melting point of (MBCA)₂, so it was probably not behaving typically then.

Carbowax 20M is a typical high-polarity phase and gave higher *c* ratios which decreased from almost 1.6 at 120°C to 1.4 at 160°C, indicating a rapid decrease in polarity with oven temperature increases. This had been used for some years, and was possibly partly oxidized. ADP also suffered a big fall in *c* ratios from 140 to 165°C, due particularly to increase in caryophyllene relative retention times, taking it down to an intermediate polarity phase at the higher temperature. At 140°C it rates as more polar than Carbowax 20M and, like the other liquid crystal “MPMS”, this polarity is mostly maintained in the unmelted condition—in contrast to (MBT)₂.

The melted liquid crystal (MBT)₂ also showed

TABLE I

AVERAGE RELATIVE RETENTION TIMES (LINALOL = 1.00) FOR THREE GROUPS OF STATIONARY PHASES IN PACKED COLUMNS OR CAPILLARIES AT TEMPERATURES (°C) INDICATED

Phase	Temperature (°C)	Cuminal (cu)	Caryophyllene (cy)	c ratio (3cu/4cy)	
<i>Low polarity</i>					
Methylpolysiloxane capillary	200	1.89	4.10 ^a	0.33	
	160	2.01	4.97	0.30	
	140	2.10	5.75	0.27	
Cholesteryl acetate packed column [15]	isotropic	155	2.69	5.08 ^a	0.40
	isotropic	140	2.69	5.26	0.38
"Chiraldex-A-DA" ring capillary [4]	140	3.22	3.61 ^a	0.67	
	125	3.28	3.75	0.66	
	110	3.25	3.77	0.65	
Dicyclohexano-24-crown-8 ether ring packed column [4]	170	2.68	3.04 ^a	0.66	
	155	2.69	3.12	0.65	
<i>Intermediate polarity</i>					
Cyanopropyl (25%)–phenyl (25%)–methyl (50%) polysiloxane OV-225 packed column	200	3.44	2.75	0.94	
	160	3.60	2.72	0.99	
	140	3.78	2.75	1.03	
(MBCA) ₂ liquid crystal packed column [11]	175	3.25	2.43	1.00	
	160	3.48	2.51	1.04	
	supercool	145	3.61	2.53	1.07
"MPMS" polysiloxane liquid crystal capillary [11]	160	4.97	3.12	1.19	
	140	5.50	3.47	1.19	
	unmelted	120	5.91	3.82	1.16
<i>High polarity</i>					
Carbowax 20 M polyethylene glycol capillary	160	2.97	1.60	1.39	
	140	2.90	1.45	1.50	
	120	3.03	1.44	1.58	
(MBT) ₂ liquid crystal packed column [10,11]	200	4.38	2.22	1.48	
	175	4.62	2.41	1.44	
	unmelted	160	3.35	2.80	0.90 ^b
	unmelted	150	3.30	2.87	0.86 ^b
Dibenzo-24-crown-8 ether ring packed column [4]	170	4.21	2.52	1.25	
	155	4.30	2.43	1.33	
ADP liquid crystal packed column [11]	165	4.20	3.00	1.05 ^b	
	140	4.64	2.22	1.57	
	unmelted	130	2.81	1.47	1.43

^a Caryophyllene emerges after cuminal on this phase.^b The phase has only intermediate polarity at this temperature.

high values until cooled to near or below its melting point, whereupon its *c* ratios became only those of an intermediate polarity phase (about 0.9). This was confirmed by its 120°C B–O–P sequence [3] that was unlike Carbowax 20M, liquid crystal ADP and the toroid dibenzo crown ether which all gave the typ-

ical high polarity sequence of O–B–P [2–4]. This crown ether again showed a decline in *c* ratios with temperature increase, like Carbowax 20M. It was clearly different to the other two toroid phases, Chiraldex and dicyclohexane crown, and gave a different solute retention sequence to them [4].

The observations above explain some of the anomalies in polarity determination that I have noted previously [3] for liquid crystal phases. It is not surprising that such substances change in polarity with temperature changes, but it is alarming that a conventional phase like Carbowax 20M appears to suffer a considerable fall in polarity with temperature increase. The c ratios for this capillary were confirmed with a packed column. Chromatographers should be warned that this polarity change is a hazard for temperature-programmed work, even with methylpolysiloxane. The latter exhibits a slight rise in polarity as the temperature rises (although it remains “low”), so these two conventional phases both approach intermediate polarity from opposite directions at higher temperatures. Abraham *et al.* [16] claim that “the effect of temperature is very important (but) it has generally been overlooked as regards characterisation of stationary phases. In general (our) main characteristic constants all decrease, often quite markedly, with temperature”. The classic concept of gas-liquid chromatography is that separations are achieved by partition phenomena in the phase. However, adsorption by the polar phases is likely to contribute significantly to the retention of caryophyllene. Adsorption effects should decrease with increasing temperature, and may explain, in part, the observations here.

The O–B–P result [3] correctly indicated the high polarity of ADP, but was wrong for (MBCA)₂, which is only of intermediate polarity here. In contrast, B–O–P under-rated the polarity of (MBT)₂ as “intermediate” [3] because it was done at 120°C, well below its melting-point. The modified LEC method at 160°C greatly underestimated the polarity of all three liquid crystals, and cannot be relied on for such phases. However B–P–O correctly designated isotropic cholesteryl acetate as low polarity [19], confirmed by the LEC method. The liquid crystal “MPMS” was also properly rated as intermediate by B–O–P [18].

The toroid phases had “ChiralDEX-A-DA” correctly placed as low polarity by B–P–O [4], and the dibenzo crown ether as high-intermediate by O/B (together)–P. The dicyclohexane crown was over-rated by B–O–P, however, although octyne was only “just ahead of pyridine” [4]. If octyne had been last, it would have agreed with the c ratio here.

The simple two-solute determination used here (it can be done without linalol) immediately shows low polarity phases by caryophyllene emerging before cuminal; and their retention time ratio then resolves the more polar phases into high- and intermediate-polarity groups. This polarity determination can be made at various temperatures, to observe any changes in polarity with heating.

REFERENCES

- 1 T. J. Betts, G. J. Finucane and H. A. Tweedie, *J. Chromatogr.*, 213 (1981) 317.
- 2 T. J. Betts, *J. Chromatogr.*, 354 (1986) 1.
- 3 T. J. Betts, *J. Chromatogr.*, 605 (1992) 276.
- 4 T. J. Betts, *J. Chromatogr.*, 606 (1992) 281.
- 5 T. O. Kollie and C. F. Poole, *J. Chromatogr.*, 556 (1991) 457.
- 6 C. F. Poole and S. K. Poole, *Chem. Rev.*, 89 (1989) 337.
- 7 R. V. Golovnya and B. M. Polanuer, *J. Chromatogr.*, 517 (1990) 51.
- 8 W. O. McReynolds, *J. Chromatogr. Sci.*, 8 (1970) 685.
- 9 G. Castello, A. Timossi and T. C. Gerbino, *J. Chromatogr.*, 454 (1988) 129.
- 10 G. Castello, A. Timossi and T. C. Gerbino, *J. Chromatogr.*, 522 (1990) 329.
- 11 T. O. Kollie and C. F. Poole, *J. Chromatogr.*, 550 (1990) 213.
- 12 T. J. Betts, C. M. Moir and A. I. Tassone, *J. Chromatogr.*, 547 (1991) 335.
- 13 T. J. Betts, *J. Chromatogr.*, 588 (1991) 231.
- 14 L. Rohrschneider, *Z. Anal. Chem.*, 170 (1959) 256.
- 15 M. H. Abraham, G. S. Whiting, R. M. Doherty and W. J. Shuely, *J. Chromatogr.*, 587 (1991) 229.
- 16 M. H. Abraham, G. S. Whiting, R. M. Doherty and W. J. Shuely, *J. Chromatogr.*, 518 (1990) 329.
- 17 M. H. Abraham and G. S. Whiting, *J. Chromatogr.*, 594 (1992) 229.
- 18 T. J. Betts, *J. Chromatogr.*, 626 (1993) 294.
- 19 T. J. Betts, *J. Chromatogr.*, 600 (1992) 337.

Short Communication

Gas chromatographic method for the determination of chlorobenzophenone isomers[☆]

Amruta S. Tambe, Thomas Daniel, Sujata Biswas and Nagraj R. Ayyangar

Division of Organic Chemistry: Technology, National Chemical Laboratory, Pune 411008 (India)

(First received April 15th, 1992; revised manuscript received October 1st, 1992)

ABSTRACT

A simple, rapid and an efficient gas chromatographic method for the determination of chlorobenzophenone isomers is described. This was necessary in order to determine the amounts of *o*- and *m*-chlorobenzophenone isomers in *p*-chlorobenzophenone, which is a starting material in the manufacture of Systral, an anti-Parkinsonism agent. Complete separation of chlorobenzophenone isomers was achieved using Apiezon L as stationary phase. The determination of *o*-chlorobenzophenone in *p*-chlorobenzophenone was carried out by using benzophenone as an internal standard. The minimum detectable amount of *m*-chlorobenzophenone in *p*-chlorobenzophenone was established.

INTRODUCTION

Recently, the existence of a remarkably stable phenyldichlorocarbenium tetrachloroaluminate complex derived from benzotrichloride under Friedel–Crafts acylation conditions has been reported [1]. We have also reported that (trichloromethyl) benzene is a more reactive benzoylating agent for the preparation of substituted benzophenones under milder reaction conditions [2]. As chlorphenoxamine (Systral), which is used as an anti-Parkinsonism agent, can be manufactured from *p*-chlorobenzophenone, we wished to establish a synthetic method in which *p*-chlorobenzophenone is produced in quantitative yields. Therefore, it was necessary to

develop a method to determine the amounts of *ortho* and *meta* isomers in *p*-chlorobenzophenone.

The separation of dichlorobenzophenone isomers and of substituted benzils and benzophenones has been reported [3,4]. Bishara and Smith [5] reported the separation of dichloro- and chlorobenzophenone isomers by high-performance liquid chromatography (HPLC). Recently, a collection of analytical data for benzodiazepines and benzophenones has been published which includes GC, HPLC and TLC methods [6,7]. Analyses for chlorophenylphenols, chlorinated products of ketones and alcohols and methyl ethers of chlorinated *o*-phenoxyphenols have been reported [8–10]. However, no reference to the separation of *ortho*, *meta* and *para* isomers of chlorobenzophenone could be found. In this paper, we describe a rapid and an efficient GC method for the determination of *p*-chlorobenzophenone.

Correspondence to: A. S. Tambe, Division of Organic Chemistry: Technology, National Chemical Laboratory, Pune 411008, India.

[☆] NCL Communication Number 5383.

EXPERIMENTAL

Analyses were performed on a Hewlett-Packard Model 5880A gas chromatograph equipped with a level 4 integrator, computing system, and flame ionization detector. A cross-linked methylsilicone gum (25 m × 0.2 mm I.D., 0.33 μm film thickness) fused-silica column from Hewlett-Packard and 10% Carbowax 20M, 3% OV-210 and 5% OV-17 columns were procured from Chromato-Pak Enterprises. In addition, columns from Alltech were used, as follows: 10% OV-351, 3% Dexil 300 and KG-02 on Uniport HP [10 ft. × 2 mm I.D. (1 ft. = 30.48 cm), glass-lined stainless steel (GLT)], 10% Alltech CS-10 [6 ft. × 2 mm I.D., (GLT)], 0.3% Carbowax 20M + 0.1% H₃PO₄ on Graphpac GC and 10% Apiezon L + 2% KOH on Chromosorb W AW (80–100 mesh (GLT) (1.8 m × 1.7 mm I.D.) (column A).

Apiezon L was coated on Chromosorb W AW (80–100 mesh at a concentration of 2% and packed in a 3 m × 2 mm I.D. stainless-steel SS column (column B). SE-30 (5% and 10%) columns and tri[4-(2'-phenylisopropyl)phenyl] phosphate (TPIPP) [11] columns were packed in the laboratory.

Complete separation of all the isomers of chlorobenzophenone was achieved on column B at 160°C. The determination and establishment of the minimum detectable amount of the *meta* isomer in *p*-chlorobenzophenone were achieved on column B at 200°C. The determination of the *ortho* isomer in *p*-chlorobenzophenone was achieved at 200°C on column A by an internal standard method with benzophenone as the internal standard.

The chemicals used were obtained from Aldrich and Merck and their purity was checked by GC. Nitrogen was used as the carrier gas at a flow-rate of 30 ml min⁻¹.

Preparation of the standard and unknown mixtures

Solutions of OCBP (0.1–5.0 mg/ml) were prepared in acetone containing benzophenone [internal standard (ISTD)] (2 mg/ml).

After stabilization of the instrument, 2.0 μl of each standard solution were injected three times. Areas of the individual peaks were obtained from the integrator. The ratios of peak areas of OCBP to ISTD were plotted against concentration (mg ml⁻¹). Separate graphs were plotted for two different concentration ranges, 1–5 and 0.1–0.3 mg ml⁻¹.

Samples (P-1, P-2, P-1 crude, P-4 and P-5) were

TABLE I
RETENTION TIMES (MIN) OF CHLOROBENZOPHENONE ISOMERS ON VARIOUS STATIONARY PHASES

Stationary phase	Temperature (°C)	Retention times (min)		
		OCBP	MCBP	PCBP
10% Carbowax 20M	210	13.65	13.14	14.29
3% OV 210	150	5.84	6.37	6.74
5% OV 17	160	19.72	19.50	21.00
10% OV 351 ^a	170	25.79	—	23.28
3% Dexil 300	150	8.95	11.6	11.95
KG-02	175	23.06	22.62	20.66
10% Alltech CS-10	190	8.0	7.46	8.10
0.3% Carbowax 20M + 0.1% H ₃ PO ₄ ^b	220	51.4	42.32	59.33
10% Apiezon L, stainless-steel column	180	14.58	18.83	20.35
2% Apiezon L, 1.8-m column	170	6.39	9.49	9.24
5% SE 30	150	2.17	2.32	2.51
10% SE 30	200	6.87	7.19	7.53
5% TPIPP ^a	180	16.60	17.60	18.90

^a These columns do not give reproducible retention times.

^b The peaks are very broad and tailing is observed.

weighed accurately and 2 ml of ISTD stock solution was added to each product before dilution to 10 ml with acetone.

Solutions of MCBP (0.01–0.1%) in PCBP were prepared using acetone as solvent.

After stabilization of the instrument, 1 μ l of each standard solution was injected three times on to column B at 200°C. Solutions of the products were also injected at the same temperature.

RESULTS AND DISCUSSION

Separation of chlorobenzophenone isomers was tried on the various liquid stationary phases coated on Chromosorb W AW or HP DMCS (80–100 mesh) at various loadings packed in stainless-steel or glass-lined stainless-steel columns (1.8 m \times 1.7 mm I.D.). Table I gives the corresponding retention data. Most of the stationary phases separate either *ortho* and *para* or *meta* and *para* isomers. Dexil 300 shows a good separation between the *ortho* and *para*, but the *meta* and *para* isomers do not separate, whereas KG-02 separates the *para* isomer but the

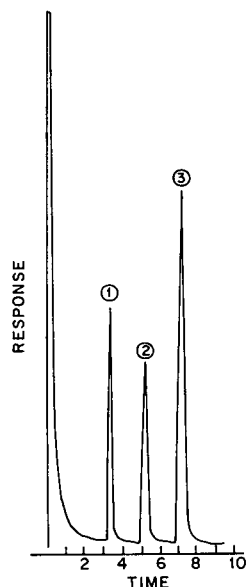


Fig. 1. Separation of benzophenone (ISTD), *o*-chlorobenzophenone and *p*-chlorobenzophenone on column A. Oven temperature, 200°C; carrier gas, nitrogen; flow-rate, 30 ml min⁻¹; injector temperature, 240°C; detector temperature, 300°C. Peaks: 1 = benzophenone; 2 = *o*-chlorobenzophenone; 3 = *p*-chlorobenzophenone.

meta and *ortho* isomers show overlapping peaks or a single peak. Graphitized carbon modified with Carbowax 20M or SP1000 retains all the isomers for a long time and the peaks are very broad. On TPIPP, all three isomers are partially resolved. Analysis was also tried on cross-linked methylsilicone gum (25 m \times 0.2 mm I.D., 0.33 μ m film thickness) at 200°C. The carrier gas was nitrogen at a flow-rate of 1.5 ml min⁻¹ and the splitting ratio was 1:135. A good separation between the *ortho* and *para* isomers was obtained but the *meta* and *para* isomers were only partially resolved. The separation did not improve further even at lower temperatures. We were able to obtain a very good separation of all three isomers on one of the packed columns which are comparatively cheaper (10% Apiezon L). Additionally, as most users employ packed columns, it was felt unnecessary to try the separations on different capillary columns.

Apiezon L (10%) coated on 2% KOH-treated Chromosorb W AW in a glass-lined stainless-steel column gave a good separation of all the three benzophenone isomers at 160°C and benzophenone (ISTD), OCBP and PCBP at 200°C (Fig. 1). Hence this column was used for the ISTD method. The calibration graphs for two concentrations ranges, 1–5 and 0.1–0.3 mg ml⁻¹, are linear and the slopes, determined from the equation $y = mx + c$ (here $c = 0$) are 0.48 and 0.7, respectively. Statistical evaluation of the method shows that the reproducibility of quantitative measurements is fairly good, as indicated by the standard deviations, ranging from $4.13 \cdot 10^{-3}$ to $1.27 \cdot 10^{-2}$. Table II gives the

TABLE II
RESULTS OBTAINED FROM CALIBRATION GRAPH FOR TECHNICAL SAMPLES

Sample	Concentration OCBP (mg ml ⁻¹)	Composition (%)	Standard deviation ^b
P-1 ^a	0.08	0.76	$1.27 \cdot 10^{-2}$
P-1 (crude)	0.1	0.95	$2.14 \cdot 10^{-3}$
P-2	0.85	7.94	$8.15 \cdot 10^{-3}$
P-4	1.125	10.96	$1.23 \cdot 10^{-2}$
P-5	0.475	4.75	$4.134 \cdot 10^{-3}$

^a Recrystallized from hexane.

^b For area ratio.

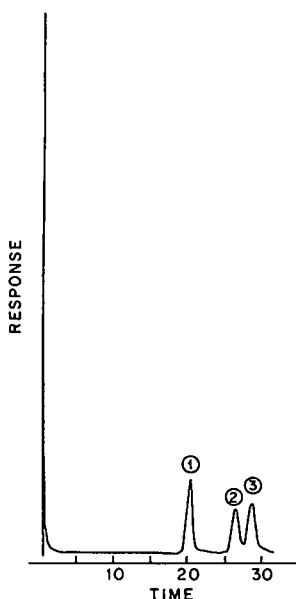


Fig. 2. Separation of chlorobenzophenone isomers on column B. Oven temperature 160°C; carrier gas, nitrogen; flow-rate, 30 ml min⁻¹; injector temperature, 200°C; detector temperature, 250°C. Peaks: 1 = OCBP; 2 = MCBP; 3 = PCBP.

results obtained for our products. In order to find the minimum detectable amount of MCBP in PCBP, a standard solution of 0.1% MCBP in PCBP was injected on to column A. As MCBP was not detected on this column, a longer column with a lower loading was prepared (column B). This gave a complete separation of all the three isomers (Fig. 2) and can detect MCBP at levels up to 0.04% in PCBP even at 200°C. When 1 μ l of 0.1 and 0.05% solutions of MCBP in BCPB was injected, the MCBP peak could be detected whereas detection of the MCBP peak was not possible for 1 μ l of 0.02%

solution. Therefore, 0.03 and 0.04% solutions were prepared and it was confirmed that the minimum detectable amount of MCBP in PCBP is 0.04%. The minimum detectable amount (MDA) of the *meta* isomer was found because the peaks of the *meta* and *para* isomers are very close and injecting a larger volume decreases the resolution. Our products contain the *meta* isomer in trace amounts whereas the *ortho* isomer is present in a significant amount. Preparing more concentrated solutions is difficult because of solubility problems. Determination of the MDA of the *ortho* isomer was not carried out as the *ortho* isomer is separated very well from the *meta* and *para* isomers. Therefore, the separation is not affected by the injection of larger volumes or more concentrated solutions.

Table III gives the retention times of the chlorobenzophenone isomers and ISTD on columns A and B. When our products were injected onto column B, the presence of MCBP in the range 0.04–0.16% was determined. An important point to be noted is that PCBP synthesized by our method contains 0.04% of the *meta* isomer at the crude stage. It disappears completely after recrystallization of PCBP from hexane. The recrystallized PCBP does not show presence of the *meta* isomer as an impurity. This suggests that, if present, it must be at a negligible concentration (less than the detection limit, *i.e.*, <0.04%).

CONCLUSION

We have described an efficient and rapid GC method for the determination of *o*-chlorobenzophenone in *p*-chlorobenzophenone using Apiezon L as stationary phase and benzophenone as an internal standard. The total analysis time is only 8 min and

TABLE III

RETENTION TIMES (MIN) OF CHLOROBENZOPHENONE ISOMERS AND BENZOPHENONE (ISTD)

Column	Temperature (°C)	Retention time (min)			
		Benzophenone	OCBP	MCBP	PCBP
A	200	3.46	5.29	6.34	7.34
B	160	12.43	20.61	26.75	28.95
B	200	5.39	8.00	9.94	10.92

the standard deviation ranges from $4.13 \cdot 10^{-3}$ to $1.27 \cdot 10^{-2}$. Complete separation of the *ortho*, *meta* and *para* isomers of chlorobenzophenone was achieved using 2% Apiezon L coated on Chromosorb W AW DMCS (80–100 mesh) packed in a $3 \text{ m} \times 2 \text{ mm}$ I.D. stainless-steel column. The minimum detectable amount of the *meta* isomer in the *para* isomer is 0.04%.

REFERENCES

- 1 U. S. Racherla, T. Daniel, P. R. Rajmohan and N. R. Ayyangar, *J. Am. Chem. Soc.*, 111 (1989) 7659.
- 2 N. R. Ayyangar, R. J. Lahoti, K. V. Srinivasan and T. Daniel, *Synthesis*, (1991) 322.
- 3 M. H. Abraham, D. Huq, R. U. Koenigsberger and J. B. Rose, *J. Chromatogr.*, 206 (1981) 147.
- 4 W. F. Brubakar and M. A. Ogliaruso, *J. Chromatogr.*, 324 (1985) 450.
- 5 R. H. Bishara and S. L. Smith, *J. Chromatogr.*, 234 (1982) 261.
- 6 M. Japp, K. Garthwaite, A. V. Geeson and M. D. Osselton, *J. Chromatogr.*, 439 (1988) 317.
- 7 S. I. Weston, M. Japp, J. Partridge and M. D. Osselton, *J. Chromatogr.*, 538 (1991) 277.
- 8 B. J. Gudzinowicz, *Anal. Chem.*, 34 (1962) 1032.
- 9 C. Walling and A. Padwa, *J. Am. Chem. Soc.*, 85 (1963) 1593.
- 10 C. A. Nilsson and K. Andersson, *Chemosphere*, 6 (1977) 263.
- 11 N. R. Ayyangar, A. S. Tambe, and S. S. Biswas, *J. Chromatogr.*, 483 (1989) 33.

Short Communication

Thin-layer chromatography on silica gel of a homologous series of bis(alkylxanthato)nickel(II) complexes

Ž. Lj. Tešić, T. J. Janjić and M. B. Čelap

Faculty of Chemistry, University of Belgrade, P.O. Box 550, 11001 Belgrade (Yugoslavia)

(First received July 16th, 1992; revised manuscript received September 30th, 1992)

ABSTRACT

The direct synthesis of bis(alkylxanthato)nickel(II) complexes is described, consisting in the addition of nickel(II) chloride to a previously heated solution of sodium hydroxide and carbon disulphide in the corresponding alcohol. It was established that the R_F values of complexes obtained with non-aqueous solvent systems increased with increasing number of carbon atoms in the xanthato ligands used, but the opposite order was found using an aqueous solvent system. There is a linear dependence between the R_M values of complexes and the number of carbon atoms in the hydrophobic part of the ligands. In the former instance the proposed separation mechanism involves the formation of hydrogen bonds between strongly electronegative atoms of the ligands (O and S) and silanol groups of silica gel and in the latter a hydrophobic interaction mechanism was assumed. In this manner it was established that the previously found regularities for octahedral alkylxanthatocobalt(III) complexes can be applied also to the investigated square-planar alkylxanthatonickel(II) complexes.

INTRODUCTION

In previous papers, the chromatographic behaviour of octahedral tris(alkylxanthato)cobalt(III) complexes was investigated [1,2]. It was established that under conditions of normal-phase chromatography, the R_F values of these complexes obtained on thin layers of silica gel [1] and polyacrylonitrile (PANS) [2] increase with increasing number of carbon atoms in the alkyl substituents, and that there is a negative linear dependence between the number of carbon atoms and their R_M values. However, under the conditions of reversed-phase chromatography on thin layers of PANS [2], a reversed order of the complexes and a positive linear dependence be-

tween their R_M values and the number of carbon atoms in the alkyl substituents were obtained.

Continuing these investigations on thin layers of silica gel, in this work we wanted to establish whether the aforementioned regularities are applicable also to square-planar nickel(II) complexes.

EXPERIMENTAL

Syntheses

In a 250-cm³ erlenmeyer flask, equipped with a stirrer, 100 cm³ of the corresponding alcohol and 2.0 g (0.05 mol) of ground sodium hydroxide was heated to 50°C, then 2.0 cm³ of carbon disulphide were added, whereby a yellow solution was obtained. To this solution, a solution of 6.1 g (0.025 mol) of nickel(II) chloride hexahydrate in 10 cm³ of water was added in small portions with constant

Correspondence to: Ž. Lj. Tešić, Faculty of Chemistry, University of Belgrade, P.O. Box 550, 11001 Belgrade, Yugoslavia.

TABLE I

YIELDS AND ELEMENTAL ANALYSES OF THE COMPLEXES $[Ni(S_2COR)_2]$, AND INDUCTIVE EFFECTS OF THE ALKYL GROUPS [2]

No.	R	Yield (%)	Analyses (%)				Inductive effect
			C		H		
			Calc.	Found	Calc.	Found	
1	Methyl	66	17.59	17.65	2.21	2.18	0.00
2	Ethyl	86	23.93	23.74	3.35	3.33	-0.10
3	<i>n</i> -Propyl	72	29.19	29.25	4.29	4.20	-0.115
4	<i>n</i> -Butyl	38	33.63	33.55	5.08	5.05	-0.130
5	<i>sec.</i> -Butyl	45	33.63	33.98	5.08	5.35	-0.210
6	Isobutyl	78	33.63	33.82	5.08	4.96	-0.125

stirring of the reaction mixture, which was prolonged for a further 30 min. The reaction mixture was left overnight in a refrigerator, then the precipitated yellow-brown crystals of the crude complex were separated by filtration under reduced pressure and recrystallized from warm acetone. The yields obtained and the corresponding results of elemental microanalyses are given in Table I.

Chromatography

Chromatographic investigation of the complexes obtained was carried out by ascending chromatography on thin layers of silica gel 60G (Merck, Darmstadt, Germany), on 5 × 5 cm plates. Freshly

prepared solutions of complexes in acetone (0.2 μl), having a concentration of 2 mg/cm³, were applied to the plates. Before development, the plates with starting spots were kept for 15 min in a 4 × 6 × 10 cm chromatographic chamber where development was performed. All solvents used were of analytical-reagent grade. The experiments were carried out at 20 ± 2°C. After development the coloured spots of the complexes were readily visible.

RESULTS AND DISCUSSION

As can be seen from Table I, the earlier described [3–5] series of six bis(alkylxanthato)nickel(II) com-

TABLE II

SOLVENT SYSTEMS USED

No.	Composition	Proportions (v/v)
1	<i>n</i> -Hexane	
2	Cyclohexane	
3	Carbon tetrachloride	
4	Benzene	
5	Toluene	
6	<i>n</i> -Hexane-toluene	80:20
7	<i>n</i> -Hexane-benzene	80:20
8	<i>n</i> -Hexane-chloroform	80:20
9	<i>n</i> -Hexane-carbon disulphide	80:20
10	<i>n</i> -Hexane-dioxane	80:20
11	<i>n</i> -Hexane-tetrahydrofuran	80:20
12	Cyclohexane-chloroform	85:15
13	Cyclohexane-carbon tetrachloride	80:20
14	Cyclohexane-toluene	80:20
15	Tetrahydrofuran-water-NiCl ₂ ·6H ₂ O	50:50:1 (v/v/w)

TABLE III
 R_F VALUES OF BIS(ALKYLXANTHATO)NICKEL(II) COMPLEXES $[\text{Ni}(\text{S}_2\text{COR})_2]$ OBTAINED BY TLC

No.	R	$R_F \times 100^a$														
		1	2	3	4	5	6	7	8	9	10	11	12	13	14	15
1	Methyl	8	13	45	71	82	26	30	43	19	46	36	29	21	34	77
2	Ethyl	11	17	50	78	88	34	42	53	25	53	47	43	29	43	66
3	<i>n</i> -Propyl	15	22	57	81	90	41	50	60	28	57	55	50	36	54	57
4	<i>n</i> -Butyl	19	28	62	84	93	47	59	67	32	61	64	57	42	63	50
5	<i>sec.</i> -Butyl	21	23	58	78	89	41	53	64	32	61	55	53	39	57	58
6	Isobutyl	23	28	62	78	93	50	60	69	38	61	61	56	44	64	51

^a The compositions of the solvent systems are given in Table II.

plexes were obtained for first time by direct synthesis in yields ranging from 38 to 86%, with respect to the crude reaction product.

The chromatographic investigation of these complexes was performed with fourteen non-aqueous solvent systems (five one-component and nine two-component) and with a three-component aqueous solvent system (Table II).

From the results obtained (Table III), it is seen that in chromatographic separations of the aforementioned square-planar complexes with non-aqueous solvent systems their R_F values increase with increasing number of carbon atoms in the side-chain of the *n*-alkylxanthato ligands. This behaviour is in agreement with results obtained previously in chromatographic separations of a homologous series of octahedral alkylxanthatocobalt(III) complexes on thin layers of silica gel [1] and PANS [2].

From Table III it is also seen that with the investigated square-planar isomeric butylxanthato complexes using non-aqueous solvent systems, the complex containing a secondary butylxanthato ligand, as a rule, exhibits the lowest R_F value, whereas the values for the other two isomers are most often very close or identical with one another, which is in accordance with their inductive effects (Table I). This is also in accordance with results obtained for octahedral tris(alkylxanthato)cobalt(III) complexes in their chromatographic separations on silica gel [1] and PANS [2].

As regards the explanation for the first-mentioned regularity, it was assumed that the dominant mechanism of complex separation is the generally

accepted mechanism of hydrogen bond formation between strongly electronegative atoms of the ligand (O, S) and silanol groups of the silica gel [6]. However, it is known that with increasing side-chain length the positive inductive effect of an alkyl group is also increased (Table I), which causes an increase in the electron density on the electronegative oxygen and sulphur atoms, and this would lead to a strengthening of hydrogen bonds between these atoms and hydrogens of the silanol groups of silica gel. The latter would, however, give rise to a reversed order of complexes relative to that which is obtained (Table III). Therefore, in considering the dependence of the complex mobility on the type of the substituent in the alkylxanthato ligand, attention should be also devoted to their steric effects. These effects, with increasing side-chain length, are manifested in a more difficult approach of strongly electronegative atoms of complexes to silanol groups of silica gel, with which hydrogen bonds might be formed. This would cause a decrease in the strength of complex adsorption with increasing side-chain length, which in fact was experimentally established for the investigated *n*-alkylxanthato complexes (Table III). This phenomenon was already noticed earlier in chromatographic separations of homologous series of transition metal complexes containing the same [1,2] or related [7–14] ligands.

The order of the investigated square-planar complexes described is reversed when an aqueous solvent system is applied (Table III, No. 15). This phenomenon might be explained by a change in the separation mechanism, *i.e.*, by non-specific hydro-

phobic interactions [15], as had been shown in previous work [16] for the octahedral transition metal tris(β -diketonato) complexes. These interactions are the greater the larger is the hydrocarbonaceous surface area [17], on account of which it is expected that the R_F values of complexes will decrease with increasing side-chain length of the alkylxanthato ligand, as was experimentally obtained.

In all instances investigated a linear dependence between the R_M values of the investigated square-planar complexes and the number of carbon atoms in the n -alkylxanthato ligands was established (Fig. 1), which is in accordance with the results obtained in previous work in which we investigated the corresponding octahedral cobalt(III) complexes using a non-aqueous solvent system in thin layer chromatographic separations on silica gel [1] and aqueous and non-aqueous solvent systems in separations on polyacrylonitrile [2].

In order to show quantitatively the difference in the selectivity [16,18] among the solvent systems used in this work, Fig. 2 shows the dependence between the R_M values of the investigated nickel(II) complexes, obtained by means of fourteen solvent systems, and their R_M values obtained by using n -hexane–dioxane (80:20, v/v), which gives the smallest difference in R_M values between the outermost members of the homologous series. From these data it might be concluded that in normal-phase chromatography high selectivity is achieved using solvent systems 5, 7, 11, 12 and 14, the selectivities of which do not differ much.

Finally, it might be concluded that the earlier es-

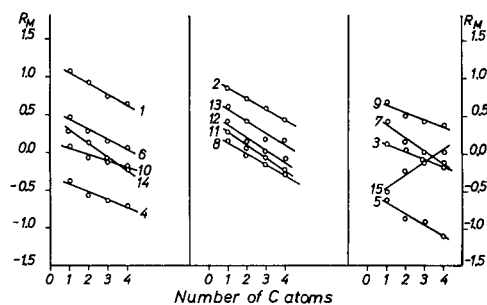


Fig. 1. Dependence of the R_M values on the number of carbon atoms in the n -alkyl group of the $[\text{Ni}(\text{S}_2\text{COR})_2]$ complexes. The numbers against the lines refer to the solvent system used (see Table II).

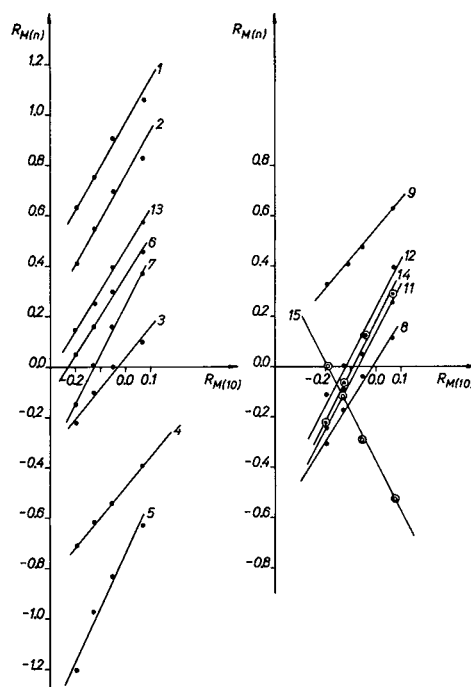


Fig. 2. Correlation between the R_M values of the investigated Ni(II) chelates obtained on a thin layer of silica gel with a given solvent system and solvent system 10. $R_{M(n)}$ = R_M values obtained with the solvent system by the number against the lines (see Table II); $R_{M(10)}$ = the same for solvent system 10.

tablished regularities for octahedral alkylxanthato-cobalt(III) complexes are also valid for square-planar alkylxanthatonickel(II) complexes.

ACKNOWLEDGEMENTS

The authors are grateful to the Serbian Republic Research Fund for financial support and to Dr. Ružica Tasovac and Mrs. Zorica Lukanić for elemental analyses.

REFERENCES

- 1 G. Vučković, N. Juranić and M. B. Čelap, *J. Chromatogr.*, 361 (1986) 217.
- 2 T. J. Janjić, D. M. Milojković, G. N. Vučković and M. B. Čelap, *J. Chromatogr.*, 596 (1992) 91.
- 3 *Gmelin's Handbuch der Anorganischen Chemie, Nickel*, Teil C, Lieferung 2, Achte Auflage, Springer, Berlin, 1969, p.982.
- 4 D. Coucouvanis, *Prog. Inorg. Chem.*, 11 (1970) 233.
- 5 D. Coucouvanis, *Prog. Inorg. Chem.*, 26 (1979) 301.
- 6 A. R. Timerbaev and O. M. Petrukhin, *Zhidkostnaya Ad-*

- sorbtsionnaya Khromatografiya Khelatov*, Nauka, Moscow, 1989, p.26.
- 7 K. Koenig, J. Becker, W. Henke, J. Stenshorn, H. Werner and K. Ballschmiter, *Fresenius' Z. Anal. Chem.*, 259 (1972) 11.
 - 8 O. Liška, J. Lehotay, E. Branšteterova and G. Guiochon, *J. Chromatogr.*, 171 (1979) 153.
 - 9 F. I. Onuska, *Anal. Lett.*, 7 (1974) 327.
 - 10 G. Soundararajan and M. Subbaiyan, *Sep. Sci. Technol.*, 18 (1983) 645.
 - 11 G. Soundararajan and M. Subbaiyan., *Indian. J. Chem., Sect. A*, 22 (1983) 402.
 - 12 G. Soundararajan and M. Subbaiyan, *Indian J. Chem. Sect. A*, 22 (1983) 1058.
 - 13 G. Soundararajan and M. Subbaiyan, *J. Indian. Chem. Soc.*, 60 (1983) 1182.
 - 14 A. R. Timerbaev, V. V. Salov and O. M. Petrukhin, *Zh. Anal. Khim.*, 40 (1985) 237.
 - 15 Cs. Horvath, W. Melander and I. Molnar, *J. Chromatogr.*, 125 (1976) 129.
 - 16 Ž. Lj. Tešić, T. J. Janjić and M. B. Čelap, *J. Chromatogr.*, 585 (1991) 359.
 - 17 M. T. Gilbert, *High Performance Liquid Chromatography*, Wright, Bristol, 1987, p. 165.
 - 18 K. Saitoh, M. Kobayashi and N. Suzuki, *Anal. Chem.*, 53 (1981) 2309.

Short Communication

Borate complexation of flavonoid-O-glycosides in capillary electrophoresis

I. Separation of flavonoid-7-O-glycosides differing in their flavonoid aglycone

Ph. Morin, F. Villard and M. Dreux

Laboratoire de Chimie Bioorganique et Analytique (LCBA), Université d'Orléans, B.P. 6759, Orléans Cédex 2 (France)

(First received April 22nd, 1992; revised manuscript received September 1st, 1992)

ABSTRACT

Capillary electrophoresis was found to give significantly greater efficiency, selectivity and speed compared with high-performance liquid chromatography for the separation of mixtures of flavonoid-O-glycosides. The migration behaviour of selected flavonoid-O-glycosides and their flavonoid aglycones in free solution capillary electrophoresis and micellar electrokinetic capillary chromatography (MECC) was investigated. A mixture of flavonoid-7-O-glycosides and their flavonoid aglycones was resolved by MECC. A 70 cm × 50 μm I.D. fused-silica capillary column and a 50 mM sodium dodecyl sulphate–20 mM Tris–HCl running buffer (pH 7.1) were used for these electrophoretic separations. Under these neutral conditions, the retention mechanism is based on hydrophobic interactions between flavonoids and the hydrophobic core of the micelles. Free zone capillary electrophoresis of borate complexes was more appropriate for the separation of a mixture of flavonoid-O-glycosides. In that case, the migration behaviour of these selected flavonoid-O-glycosides was explained by ionization of some hydroxyl groups and mainly by borate complexation of the sugar moiety. The identity of each flavonoid-O-glycoside was determined by using a fast-scanning multiple-wavelength UV detector and by recording its on-column UV spectrum in the range 190–360 nm.

INTRODUCTION

Flavonoids constitute one of the largest groups of naturally occurring phenols and are widespread components in all parts of plants. These compounds have structures based on 2-phenylbenzopyrone and differ in the pattern of hydroxylation, de-

gree of unsaturation and type and position of sugar links [1].

In micellar electrokinetic capillary chromatography (MECC), a surfactant is added to a buffer at a concentration above its critical micelle concentration. Micelles provide both ionic and hydrophobic sites of interaction, so this technique is suitable for the separation of ionic and uncharged solutes. Since the first description of MECC by Terabe and co-workers [2,3], many applications have been reported, such as to drug substances [4], acidic solutes [5],

Correspondence to: Ph. Morin, Laboratoire de Chimie Bioorganique et Analytique (LCBA), Université d'Orléans, B.P. 6759, Orléans Cédex 2, France.

ionic and non-ionic catechols [6–8], cationic solutes [9] and glucosinolates and desulphoglucosinolates [10].

The existing method used for the analysis of flavonoid-O-glycosides in very complex matrices is generally high-performance liquid chromatography [11–13]. Nevertheless, Seitz *et al.* [14] used capillary isotachopheresis for the rapid analysis of flavonoids and phenolcarboxylic acids in phytopharmaceutical industry. In addition, MECC has recently been investigated for the determination of flavonoid drugs, such as quercetin-, kaempferol- and isorhamnetin-3-O-glycosides [1]. In this paper, the separation of a mixture of flavonoids and flavonoid-7-O-glycosides was studied using capillary electrophoresis (CE) and MECC techniques; the migration behaviour and solubilization mechanism of these neutral and ionizable solutes were explained.

EXPERIMENTAL

Instrumental

All open-tube electrokinetic capillary chromatographic separations were performed on a Spectra-Physics (San Jose, CA, USA) Spectraphoresis 1000 instrument using a silica capillary tube (70 cm \times 50 μ m I.D. \times 375 μ m O.D.). Data were processed on an IBM PS/2 Model 70 386 computer. Software operating under IBM OS/2 was supplied by Spectra-Physics. The instrument contains a programmable, high-speed scanning, multiple-wavelength UV detector. Using the fast scanning mode, we were able to record on-column spectra of the compounds. The scanning mode ranged from 200 to 360 nm in 5-nm increments. Electrokinetic separations were performed at 60°C at 25 kV (electrical field strength 350 V/cm), a run average current of 45 μ A and a capillary resistance of 0.18 G Ω . Analytes were injected in the hydrodynamic mode using a 0.75 p.s.i. (1 p.s.i. = 6894.76 Pa) vacuum for 1–5 s.

All free solution capillary electrophoretic separations were performed on a Europhor (Toulouse, France) Prime Vision instrument using a 65 cm \times 50 μ m I.D. silica capillary tube. A small section (1-cm length) of the polyimide coating of the capillary column was removed prior to filling to obtain an optical window for UV detection. Analyses were carried out at ambient temperature with the Europhor instrument. All electropherograms were re-

corded on a Shimadzu (Kyoto, Japan) C-R 5A integrator. The on-column detector was operated at 270 nm at an absorbance range of 2.0 a.u.f.s. and a rise time of 0.1 s.

The capillaries were conditioned daily by washing first with 1 M sodium hydroxide solution (10 min) at 60°C (at ambient temperature for the Europhor instrument), then 0.1 M sodium hydroxide (10 min) at 40°C, water at 60°C (10 min) and the electrophoretic buffer (15 min) at 40°C. Between two analyses, the capillary tubes were flushed with water (2 min), 0.1 M sodium hydroxide solution (2 min), water (3 min) and finally with the electrophoretic buffer (10 min) in order to improve reproducibility of the migration time.

Reagents

All chemicals were of analytical-reagent grade. Tris(hydroxymethyl)aminomethane (Sigma, St. Louis, MO, USA), hydrochloric acid (Sigma), boric acid (Fluka, Buchs, Switzerland), sodium dihydrogenphosphate (Fluka) and the surfactant sodium dodecyl sulphate (SDS) (Fluka) were used without further purification. Water used for dilutions or as buffer solution was of HPLC grade (Carlo Erba, Milan, Italy).

For free solution capillary electrophoresis under alkaline conditions, the electrophoretic medium composition was either 0.03 M NaH₂PO₄ (adjusted to pH 10.5 by addition of 0.1 M NaOH) or 0.2 M H₃BO₃ buffer (adjusted to pH 10.5 by addition of 0.1 M NaOH).

For MECC separations under neutral conditions, the electrophoretic medium consisted of SDS micelles in Tris-HCl buffer. Stock solutions to prepare pH buffer were 0.1 M Tris and 0.1 M HCl. The buffer (pH 7.1) was prepared by mixing these two stock solutions in the proportions 50:45.7 (v/v) and diluting to 100 ml and adjusting the pH to 7.1 with hydrochloric acid. The aqueous buffer composition was 0.050 M Tris–0.046 M HCl with a 0.050 M surfactant concentration. Methanol was used to determine the retention time of a neutral unretained solute and anthracene the migration time of the micelles.

Authentic samples of diosmin, hesperidin, isorhoifolin, hesperitin, linarin and diosmetin were obtained from Extrasynthese (Genay, France). A standard solution of each flavonoid or flavonoid-7-

O-glycoside was prepared in dimethyl sulphoxide–methanol (80:20, v/v) at a concentration of *ca.* 100 ppm for each of these solutes. Finally, this solution was filtered through a Whatman (Maidstone, UK) polypropylene filter (0.2 μm pore size, 25 mm diameter) prior injection.

RESULTS AND DISCUSSION

Flavonoids commonly occur as flavonoid-O-glycosides in which one flavonoid hydroxyl groups is bound to a sugar by an acid-labile hemiacetal bond [15]. For our solutes, an identical disaccharide, rutinose (6-O- α -rhamnopyranosyl-D-glucose), is found in association with flavonoids (Fig. 1).

Free solution capillary electrophoresis under no complexing conditions

The separation mechanism in free solution capil-

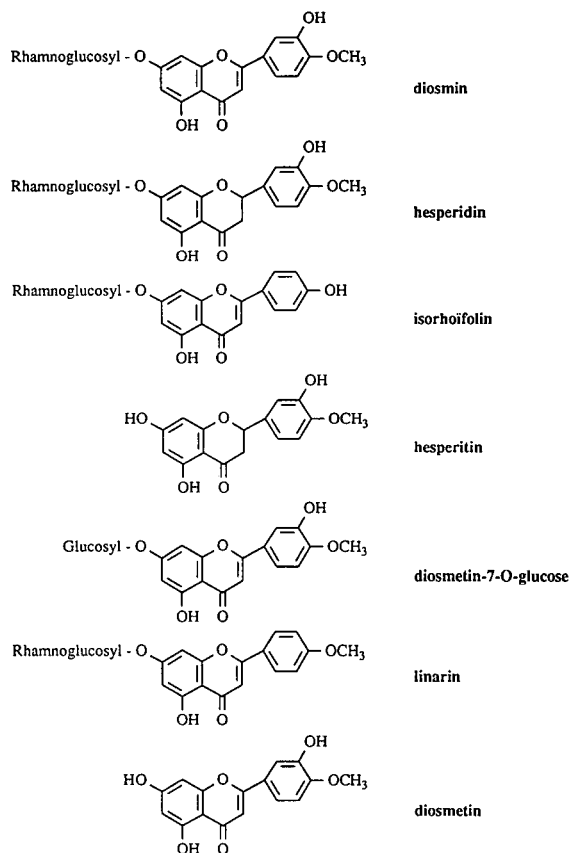


Fig. 1. Structures of flavonoids and flavonoid-7-O-glycosides.

lary CE is based on differences in the electrophoretic mobilities of species. Flavonoid compounds are weak acids with ionization constants in the pH range 10–12; their apparent charge depends on their pK_a values and on the pH of the running buffer. At neutral pH, these flavonoid-O-glycosides could not be resolved by CE. Because of their phenolic nature, an alkaline buffer system was chosen in order to ensure an adequate degree of dissociation of the flavonoids. A 30 mM phosphate running buffer (pH 10.5) was used for this electrophoretic separation (Fig. 2). Under these conditions, anionic species moved toward the cathode with the velocity of electrophoretic migration minus that of electroosmotic flow.

Linarin with one free hydroxyl group has a smaller mobility than the other three flavone-O-glycosides with two free hydroxyl groups; this almost undissociated analyte migrates only with electroosmotic flow. Linarin and diosmin give sharp and symmetrical peaks well resolved from each other. Diosmin and hesperidin differ only in a carbon–carbon double bond; their effective mobilities are too close for them to be resolved.

Hence, the resolution of this separation cannot

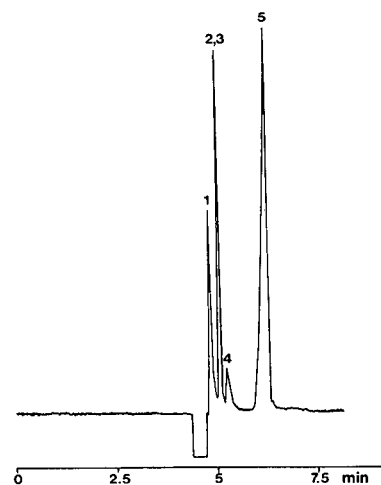


Fig. 2. Separation of a mixture of two flavonoids and four flavonoid-7-O-glycosides by free zone CE. Applied voltage, + 25 kV; capillary, 65 cm \times 50 μm I.D., running electrolyte, 30 mM NaH_2PO_4 (pH 10.5); current, 43 μA ; detection wavelength, 270 nm. Solutes: 1 = linarin; 2 = diosmin; 3 = hesperidin; 4 = impurity; 5 = isorhoifolin.

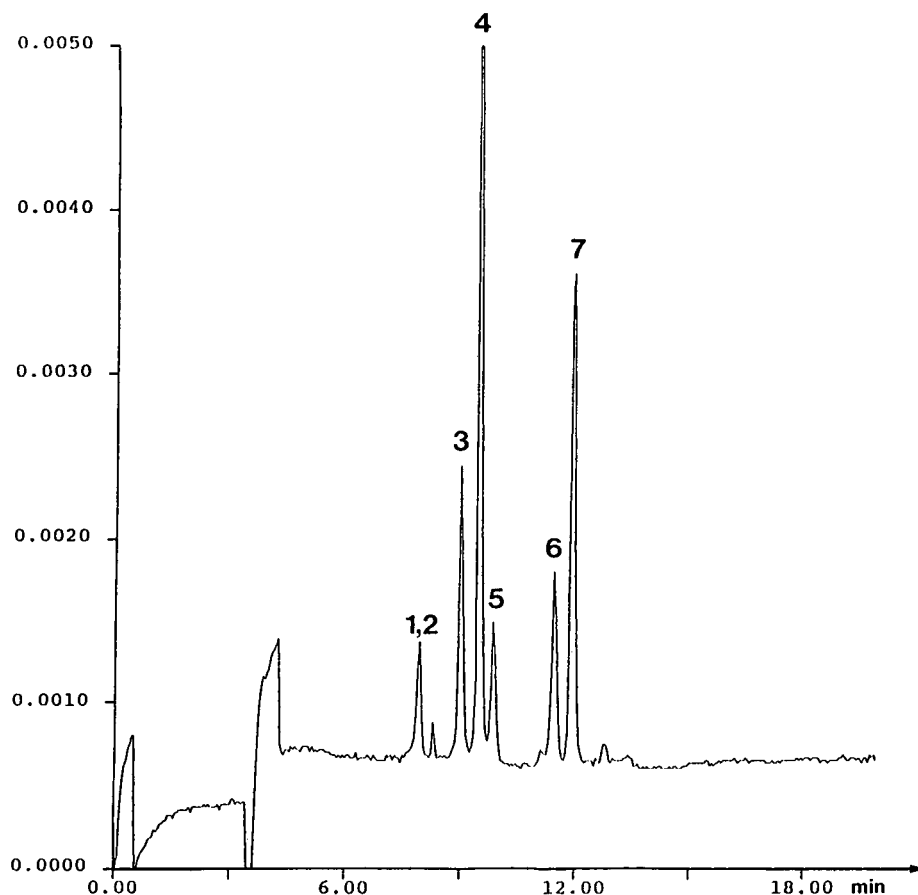


Fig. 3. Separation of a mixture of flavonoids and their flavonoid-7-O-glycosides by MECC. Applied voltage, 25 kV; capillary, 70 cm \times 50 μ m I.D.; buffer, Tris-HCl-50 mM SDS (pH 7.1); detection wavelength, 280 nm; current, 45 μ A. Solutes: 1 = diosmin; 2 = hesperidin; 3 = isorhoifolin; 4 = hesperitin; 5 = diosmetin-7-O-glycoside; 6 = linarin; 7 = diosmetin.

be improved in CE simply by controlling the pH of the alkaline buffer.

Micellar electrokinetic capillary electrophoresis

A 50 mM SDS solution with a neutral running buffer (pH 7.1) was used for the electrophoretic experiments. Under such neutral conditions, only hydrophobic interactions between these flavonoid compounds, which have weak acids properties, and SDS micelles explain the migration order in MECC. For instance, the less hydrophobic flavonol-3-O-glycoside (rutin) migrates faster than its flavonoid aglycone (quercetin).

A mixture consisting of one flavone (hesperitin), one flavanone (diosmetin) and five flavonoid-7-O-

glycosides (diosmin, hesperidin, isorhoifolin, linarin, diosmetin-7-O-glycoside) migrated to the cathode within 12 min (Fig. 3). The selectivity obtained by MECC is great enough to resolve these solutes, except for diosmin and hesperidin. This method offers the opportunity of the separation of both flavonoids and flavonoid-7-O-glycosides in a single run, without a gradient approach such as in reversed-phase HPLC.

The more hydrophilic flavonoid-7-O glycosides (diosmin and hesperidin) migrate faster than their hydrophobic flavonoid aglycones (diosmetin and hesperitin, respectively). Indeed, the effect of glycosylation is to render these flavonoids more hydrophilic and water soluble (see the migration order of

diosmin, diosmetin-7-O-glycoside and diosmetin). Two flavonoid 7-O-glycosides with a slight structure difference (methoxy or hydroxyl group in the 4' position) have different migration times: a methoxy group (see the 4'-OCH₃ group in linarin) clearly enhances the hydrophobicity compared with a hydroxyl group (see the 4'-OH group in isorhoifolin). Nevertheless, when a hydroxyl group is close to a methoxy group, the total hydrophobicity of the molecule decreases (compare the migration times of diosmin with those of linarin and isorhoifolin) [16].

However, a difficult problem concerns the resolution of two compounds that differ in the occurrence of a carbon–carbon double bond. For example, diosmin and hesperidin, which differ only in a carbon–carbon double bond, are not resolved with this MECC system, whereas their flavonoid aglycones, diosmetin and hesperitin, respectively, have very different migration times. This specific behaviour, strongly dependent on surfactant type, is the unsaturation contribution, which distinguishes flavones from flavanones. In fact, there were differences in molecular structure, the flavones being planar and the flavanones partially planar.

The retention mechanism in MECC with a neutral running buffer is mainly based on hydrophobic interactions between flavonoids and the hydrophobic core of micelles. In contrast, working under alkaline conditions in MECC should induce hydrophobic interactions with the micelles and also electrophoretic mobility of ionized flavonoid aglycone. In that event, some interactions should occur between anionic solutes and SDS micelles.

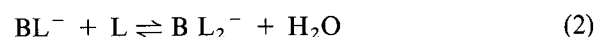
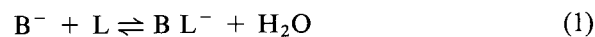
Complexation of flavonoid-7-O-glycosides with boric acid

By adding boric acid to the background electrolyte, the retention time of each flavonoid-O-glycoside is increased as they react with boric acid to form borate complexes with negative charge. It is well known that certain neutral polyhydroxy compounds or sugars react with borate ions to form borate complexes which are negatively charged ions [14,17,18].

The influence of different borate buffers as background electrolytes on the electrophoretic mobilities of underivatized mono- and oligosaccharides has recently been studied [19]. The very low UV absorbance of carbohydrates makes photometric

detection very difficult without a derivatization step. However, by adding borate to the running buffer, absorbance in the low UV range (195 nm) becomes slightly increased (for hexose, pentose and the main common disaccharides, the increase factor is *ca.* 5–15). Hence, the enhanced UV absorption of sugars in the presence of borate allows a more sensitive UV detection than that in pure water and consequently their electrophoretic separation in a capillary electrophoretic system using a borate complexing buffer.

The complex formation can be described by the following equations [19]:



where L is the polyol ligand and B⁻ represents tetrahydroxyborate, B(OH)₄⁻. Further, alkaline borate anion solutions (pH 8–12) contain not only B(OH)₄⁻ or (B₃O₃(OH)₅)²⁻ but also (B₄O₅(OH)₄)²⁻. Hoffstetter-Kuhn *et al.* [19] mentioned some very interesting structural characteristics of polyol–borate and sugar–borate complexes: polyols can form 1:1 and 1:2 complexes with borate; hydroxyl groups on adjacent carbon atoms but also those on alternate carbon atoms occurred in a complexation mechanism; the complex is stabilized by a

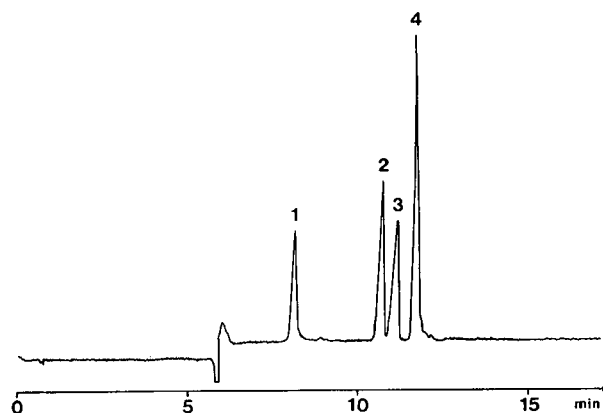


Fig. 4. Separation of a mixture of four flavonoid-7-O-glycosides by free zone CE with borate complexing buffer. Applied voltage, + 25 kV; capillary, 65 cm × 50 μm I.D.; current, 62 μA; running buffer, 200 mM boric acid (pH 10.5); detection wavelength: 270 nm. Solute: 1 = linarin; 2 = diosmin; 3 = isorhoifolin; 4 = hesperidin.

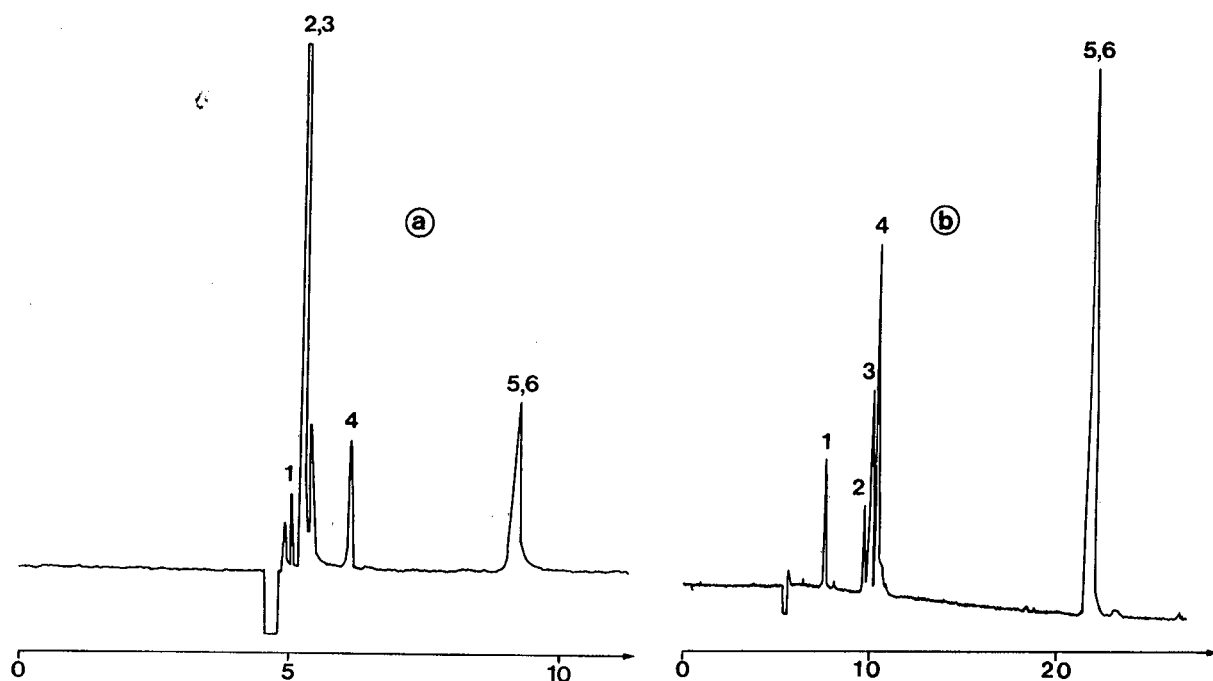


Fig. 5. Separation of a mixture of flavonoids and their flavonoid-7-O-glycosides by free zone CE. Applied voltage, + 25 kV; capillary, 65 cm \times 50 μ m I.D.; detection wavelength: 270 nm; current, 62 μ A. Solutes: 1 = linarin; 2 = diosmin; 3 = isorhoifolin; 4 = hesperidin; 5 = diosmetin; 6 = hesperetin. (a) With no complexing buffer (30 mM NaH_2PO_4 , pH 10.5). (b) With complexing buffer (200 mM boric acid, pH 10.5).

large number of hydroxyl groups; and *cis*-1,2-diols are preferred in complexation over *trans*-1,2-diols.

Hence the possibilities for borate complexation of a sugar are numerous, including α - and β -pyranose forms, α - and β -furanose forms, hydrated open-chair form and carbonyl open-chain form. By adding borate to running buffer, saccharides are complexed in different ways according to their different forms.

The separation of flavonoid-O-glycosides can be performed in CE with a borate running buffer at pH 10.5 (Fig. 4). The ionization constants of the main mono- or disaccharides are in the range 11.9–12.5, according to Lee and Bunker [17]. Hence we may assume that the sugar moiety of the flavonoid-7-O-glycoside is not ionized at the pH value of the running buffer. Well resolved peaks were obtained and identified by comparison with authentic specimens.

The mixture of flavonoids and their glycoside derivatives has also been resolved by CE at the same pH value with a non-complexing buffer (Fig. 5a) or

a complexing buffer (Fig. 5b); in both instances, the chromatogram was divided into two parts on the basis of retention times: the first part consisted of the heterosides (compounds 1–4) and the second part contained the flavone diosmetin and the flavanone hesperetin. Under these both conditions, flavonoid-O-glycosides migrate faster than flavones. Indeed, diosmetin, which contains three free hydroxyl groups, has a greater electrophoretic mobility than diosmin at this alkaline pH. Nevertheless, no separation occurred between the two flavonoids diosmetin and hesperetin, even with complexing running buffers.

Spectral identification

The instrument contains a programmable, high-speed, scanning, multiple-wavelength UV detector. Using the fast scanning mode we were able to record on-column spectra of the compounds; the scanning mode ranged from 200 to 360 nm in 5-nm increments. It is well known that UV spectra of fla-

vonoid glycosides include important structural information concerning the aglycones. The precise position and relative intensities of these maxima give valuable information on the nature of the fla-

vonoid aglycone and its oxygenated pattern [15]. Table I reports the UV absorption maximum wavelengths for these solutes resolved by MECC and by using a multiple-wavelength UV detector.

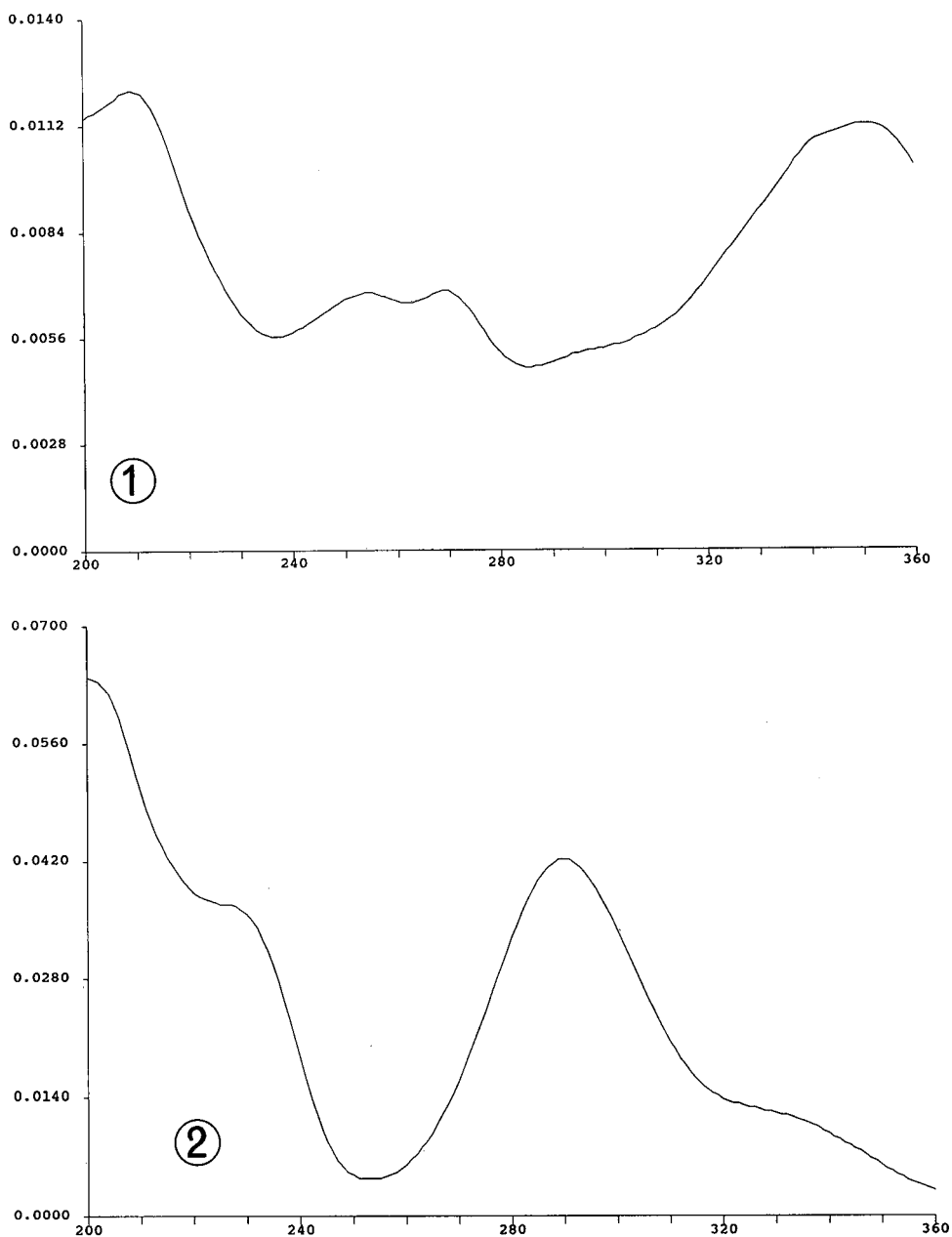


Fig. 6. Full on-line UV spectra of selected flavonoids and their glycoside derivatives in the 190–360 nm range. Resolution, 5 nm; bandpass, 1 nm. Solutes: 1 = diosmetin; 2 = hesperitin.

TABLE I
UV ABSORPTION MAXIMA FOR FLAVONOID-7-O-
GLYCOSIDES AND FLAVONOID AGLYCONES

Compound	λ_{\max} (nm)
<i>Flavonones</i>	
Hesperitin	290, 228 (shoulder), 200
Hesperidin	285, 225 (shoulder), 200
<i>Flavones</i>	
Diosmetin	351, 269, 255, 209
Diosmetin-7-O-glucose	350, 269, 208
Diosmin	348, 270, 207
Linarin	333, 273, 209
Isorhoifolin	336, 269, 200

Fig. 6 shows that the UV spectrum of a flavone (diosmetin) typically consists of two absorption maxima near 250–280 nm (band I) and 310–350 nm (band II); for a flavanone (hesperetin), two absorption maxima appear in the range 275–295 nm (band I) and a shoulder near 300–330 nm (band II). These two flavonoids, which differ only in the presence of a carbon-carbon double bond, have very different features in their UV spectra. Glycosylation of the 7-hydroxyl group appears generally to cause small band shifts to shorter wavelength (Table I). The nature of the sugar in the glycoside has no effect on the position of bands but induces different relative intensities of these maxima.

CONCLUSIONS

Capillary electrophoresis is a useful technique for investigating the composition of flavonoids and flavonoid-O-glycoside mixtures. Micellar electrokinetic capillary chromatography has been used for the separation of both flavonoid-O-glycosides and their flavonoid aglycones. Under neutral pH conditions, the retention mechanism involves mainly hydrophobic interactions with the micelles. This determination of flavonoid-O-glycosides is rapid and reproducible, and may serve as a valuable means for as-

sessing quality in the pharmaceutical industry. The identity of each flavonoid O-glycoside was determined by recording its on-column UV spectrum using a high-speed, scanning, multiple-wavelength detector.

Further investigations are in progress for a better understanding of the mechanism of insertion of a flavonoid-O-glycoside into the interior of micelles in MECC, and of borate complexation of flavonoids and flavonoid-O-glycosides in CE.

REFERENCES

- 1 P. Pietta, P. Mauri, A. Rava and G. Sabbatini, *J. Chromatogr.*, 549 (1991) 367.
- 2 S. Terabe, K. Otsuda, K. Tsuchiya and T. Ando, *Anal. Chem.*, 56 (1984) 111.
- 3 S. Terabe, K. Otsuda and T. Ando, *Anal. Chem.*, 57 (1985) 834.
- 4 R. Weinberger and I. S. Lurie, *Anal. Chem.*, 63 (1991) 823.
- 5 M. G. Khaledi, S. C. Smith and J. K. Strasters, *Anal. Chem.*, 63 (1991) 1820.
- 6 R. A. Wallingford and A. G. Ewing, *J. Chromatogr.*, 441 (1988) 299.
- 7 R. A. Wallingford, P. D. Curry and A. G. Ewing, *J. Microcol. Sep.*, 1 (1989) 23.
- 8 C. Ong, S. Pang, S. Low, H. Lee and S. Li, *J. Chromatogr.*, 559 (1991) 529.
- 9 J. K. Strasters and M. G. Khaledi, *Anal. Chem.*, 63 (1991) 2503.
- 10 Ph. Morin, F. Villard, A. Quinsac and M. Dreux, *J. High. Resolut. Chromatogr.*, 15 (1992) 302.
- 11 P. Pietta, P. Mauri, A. Bruno, A. Rava, E. Manera and P. Ceva, *J. Chromatogr.*, 553 (1991) 223.
- 12 K. Hostettmann and A. Marston, *Prog. Clin. Biol. Res.*, 213 (1986) 43.
- 13 E. Revilla, E. Alonso and M. Estrella, in G. Charalambous (Editor), *Frontiers of Flavor*, Elsevier, Amsterdam, 1988 p. 711.
- 14 V. Seitz, G. Bonn, P. Oefner and M. Popp, *J. Chromatogr.*, (1991) 499.
- 15 K. R. Markham, *Techniques of Flavonoid Identification*, Academic Press, London, 1982.
- 16 F. Dondi and Y. Kahie, *J. Chromatogr.*, 461 (1989) 281.
- 17 D. Lee and M. Bunker, *J. Chromatogr. Sci.*, 27 (1989) 496.
- 18 T. Kaneta, S. Tanaka and H. Yoshida, *J. Chromatogr.*, 538 (1991) 385.
- 19 S. Hoffstetter-Kuhn, A. Paulus, E. Gassmann and H. Widmer, *Anal. Chem.*, 63 (1991) 1541.

Short Communication

Borate complexation of flavonoid-O-glycosides in capillary electrophoresis

II. Separation of flavonoid-3-O-glycosides differing in their sugar moiety

Ph. Morin, F. Villard and M. Dreux

Laboratoire de Chimie Bioorganique et Analytique, Université d'Orléans, B.P. 6759, 45 067 Orléans Cédex 2 (France)

P. André

Laboratoire des Substances Naturelles, Parfums Christian Dior SA, 45 804 St Jean-de-Braye (France)

(First received June 10th, 1992; revised manuscript received September 16th, 1992)

ABSTRACT

Capillary electrophoresis was found to give significantly higher efficiency, selectivity and speed than high-performance liquid chromatography for the separation of a mixture of flavonoid-3-O-glycosides differing in their sugar moiety. Boric acid running buffer (0.2 M, pH 10.5) was used for this electrophoretic separation. The migration order in free solution capillary electrophoresis (CE) and the selectivity of these flavonoid-3-O-glycosides can be mainly explained by *in situ* borate complexation of both the sugar moiety and the *cis*-1,2-hydroxyl groups on the flavonoid skeleton and, to a lesser extent, by the ionization of hydroxyl groups on the flavonoid skeleton due to alkaline pH conditions. The correlation of the electrophoretic mobilities with the configuration and conformation of the compounds is discussed.

INTRODUCTION

Flavonoids constitute one of the largest groups of naturally occurring phenols and are widespread components in all parts of plants. These compounds have structures based on 2-phenylbenzopy-

rone and differ in the pattern of hydroxylation, degree of unsaturation and type and position of sugar links [1].

Recent improvements in capillary zone electrophoresis (CZE) are attractive for studies of natural products because of the high-resolution separations achievable with on-column UV detection [1,2]. Existing methods for the analysis of flavonoid-O-glycosides generally involve high-performance liquid chromatography (HPLC) [3–5]. However, this tech-

Correspondence to: Ph. Morin, Laboratoire de Chimie Bioorganique et Analytique, Université d'Orléans, B.P. 6759, 45 067 Orléans Cédex 2, France.

nique requires gradient elution which tends to be inconvenient, time consuming and laborious. Pietta *et al.* [1] have applied micellar electrokinetic capillary chromatography (MECC) to the determination of several flavonoid drugs (quercetin-, kaempferol- and isorhamnetin-3-O-glycosides). Seitz *et al.* [6] used capillary isotachopheresis for the rapid determinations of flavonoids and phenolcarboxylic acids. Optimum separations were achieved at pH 9.5 with a leading electrolyte containing 0.015 M hydrochloric acid, 30% methanol and 0.2% hydroxypropylmethylcellulose. In a recent study [7], the separation of several flavonoid-7-O-glycosides, differing in their flavonoid aglycone, was achieved by CE. However, a mixture of both flavonoid-7-O-glycosides and their flavonoid aglycones was better resolved in MECC using sodium dodecyl sulphate as anionic surfactant.

In this work, a mixture of quercetin-3-O-glycosides, differing in their sugar moiety, was resolved by CE using a borate complexing running buffer. The migration order in CE and the borate complexation mechanism of these solutes were elucidated.

EXPERIMENTAL

Instrumental

Free solution capillary electrophoretic (FSCE) separations were mainly performed on a Europhor (Toulouse, France) Prime Vision instrument using a silica capillary column. A small section (1 cm length) of the polyimide coating of the capillary column was removed prior to filling to give an optical window for UV detection. Analyses were carried out at ambient temperature (Europhor). All electropherograms were recorded on a Shimadzu (Kyoto, Japan) C-R 5A integrator. A 65 cm \times 50 μ m I.D. silica capillary column filled with phosphate–borate buffer or boric acid–sodium hydroxide buffer served as the separation column operated at high voltages. On-column detection was effected at 270 nm at 2.0 AUFS with a rise time of 1s.

Some of the separations were performed on a Spectra-Physics (San Jose, CA, USA) Spectrophoresis 1000 instrument using a 70 cm \times 375 μ m O.D. \times 50 μ m I.D. silica capillary column. Separations were performed at 40°C at a voltage of 24.4 kV (electrical field strength 385 V/cm) and a run average current of 80 μ A. For this instrument, analytes

for each run were injected in the hydrodynamic mode for 1.0–3.0 s. Data were processed on an IBM PS/2 Model 70 386 computer. Software operating under IBM OS/2 was supplied by Spectra-Physics. The instrument contains a programmable, high-speed scanning, multiple-wavelength UV detector. Working in the fast scanning mode, we were able to record on-column spectra of the flavonoid-3-O-glycosides. The scanning mode was from 200 to 360 nm with a 5-nm wavelength increment.

The capillaries were conditioned daily by washing first with 1 M sodium hydroxide solution (10 min) at 60°C (at ambient temperature for the Europhor instrument), then with 0.1 M sodium hydroxide solution (10 min) at 40°C, with water at 60°C (10 min) and with finally the electrophoretic buffer (15 min) at 40°C. Between consecutive analyses, the capillaries were flushed with water (2 min), 0.1 M sodium hydroxide solution (2 min), water (3 min) and finally with the electrophoretic buffer (10 min) in order to improve the migration times and peak-shape reproducibility.

Reagents

All chemicals were of analytical-reagent grade. Boric acid, sodium dihydrogenphosphate and 0.1 M sodium hydroxide solution (all from Fluka, Buchs, Switzerland) were used as received. Water used for dilutions and in buffer solutions was of HPLC grade (Carlo Erba, Milan, Italy).

For free solution CE under alkaline conditions, the running buffer composition was either 0.006 M $\text{Na}_2\text{B}_4\text{O}_7$ –0.010 M NaH_2PO_4 (pH adjusted with 1 M NaOH) or 0.2 M H_3BO_3 (pH adjusted to 6, 7.8 or 10.5 with 1 M NaOH).

Authentic samples of quercitrin (quercetin-3-O-rhamnoside), peltatoside (quercetin-3-O-arabinoglucoside), isoquercitrin (quercetin-3-O-glucoside), hyperoside (quercetin-3-O-galactoside) and avicularin (quercetin-3-O-arabinoside) (Fig. 1) were obtained from Extrasynthese (Genay, France). A standard solution of ca. 100 ppm of each flavonoid-3-O-glycoside was prepared in dimethyl sulphoxide–methanol (80:20, v/v).

Each analyte and each solution (water, sodium hydroxide and electrophoretic buffer) were filtered prior to injection through a polypropylene filter (0.2 μ m pore size, 25 mm diameter) from Whatman (Maidstone, UK).

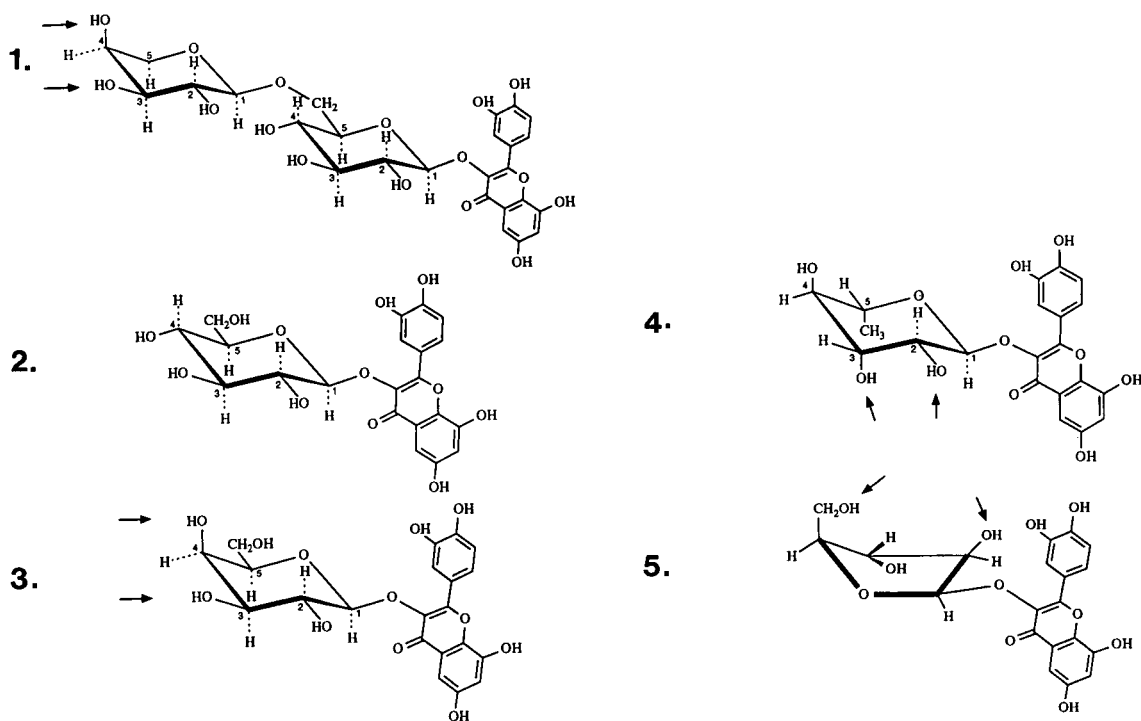


Fig. 1. Structures of quercetin-3-O-glycosides. 1 = Peltatoside [quercetin-3-O-arabinoglucoside; 3-[(6-O- α -L-arabinopyranosyl)- β -D-glucopyranosyl]oxy]-2-(3,4-dihydroxyphenyl)-5,7-dihydroxy-4H-1-benzopyran-4-one]; 2 = isoquercitrin {quercetin-3-O-glucoside; 3-[(β -D-glucofuranosyl]oxy]-2-(3,4-dihydroxyphenyl)-5,7-dihydroxy-4H-1-benzopyran-4-one}; 3 = hyperin {quercetin-3-O-galactoside; 3-[(β -D-galactopyranosyl]oxy)-2-(3,4-dihydroxyphenyl)-5,7-dihydroxy-4H-1-benzopyran-4-one}; 4 = quercitrin {quercetin-3-O-rhamnoside; 3-[(6-deoxy- α -L-mannopyranosyl]oxy)-2-(3,4-dihydroxyphenyl)-5,7-dihydroxy-4H-1-benzopyran-4-one}; 5 = avicularin {quercetin-3-O-arabinoside; 3-[(α -L-arabinofuranosyl]oxy)-2-(3,4-dihydroxyphenyl)-5,7-dihydroxy-4H-1-benzopyran-4-one}; Arrows indicate hydroxyl groups occurring as boration sites on the sugar molecule, but the same boration sites in the 3',4'-positions on the flavonoid skeleton are not shown.

RESULTS AND DISCUSSION

Flavonoids commonly occur in plants as the 3-O-glycosides in which one flavonoid hydroxyl group is bound to a sugar by an acid-labile hemiacetal bond [8]. Some quercetin-like-glycosides have a carbohydrate component represented either by a monosaccharide residue such as 3-O-D-galactosyl (hyperin) or by a disaccharide residue such as 3-O-rutinosyl (rutin). Further, several O-methylated derivatives of quercetin and their glycosides are also found in nature, and on hydrolysis yield molecules of saccharides and a molecule of flavonoid, such as tamarixetin (the 4-methyl ether of quercetin).

For the compounds shown in Fig. 1, the same flavonoid aglycone (quercetin) is found in associ-

ation with either a monosaccharide (β -D-glucose, β -D-galactose, α -L-rhamnose, α -L-arabinose) or a disaccharide (α -L-arabino- β -D-glucoside).

Influence of the nature of the running electrolyte

A standard mixture of the five quercetin-3-O-glycosides was resolved by free solution CE using running buffers having the constant pH (10.5) but differing in their chemical nature, either phosphate-borate buffer (Fig. 2a) or boric acid-NaOH buffer (Fig. 2b). In the alkaline and none-complexing phosphate-borate buffer, the electrophoretic mobility of each flavonoid-3-O-glycoside increases with ionization of the hydroxyl groups located on the flavonoid skeleton. However, the ionization of the flavonoid skeleton is not great enough to allow dif-

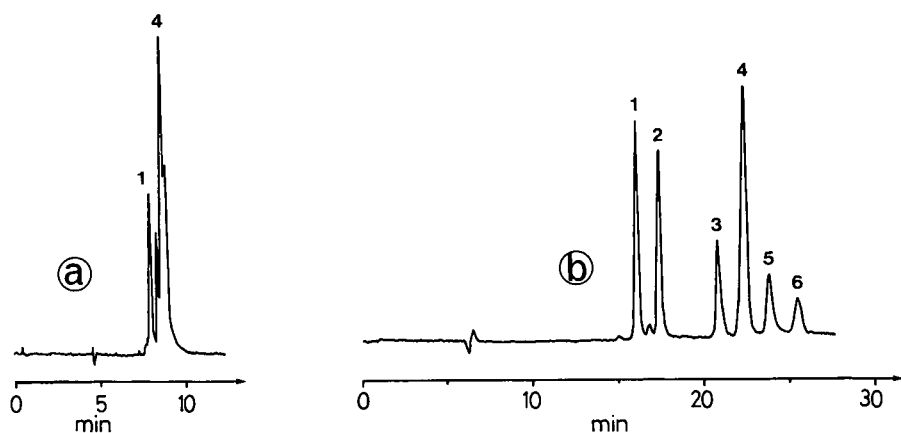


Fig. 2. Influence of the complexing nature of the running buffer in free solution CE on the separation of flavonoid-3-O-glycosides. Voltage, +24.4 kV; capillary, 65 cm \times 50 μ m I.D.; detection wavelength, 270 nm. Peaks 1–5, as in Fig. 1; 6 = impurity. Running buffer: (a) 0.006 M $\text{Na}_2\text{B}_4\text{O}_7$ –0.010 M NaH_2PO_4 (pH 10.8); (b) 0.2 M H_3BO_3 (pH 10.5).

ferentiation among the electrophoretic mobilities of the five compounds (Fig. 2a). The ionization constants of common monosaccharides or disaccharides are in the $\text{p}K_a$ range 11.9–12.5, according to

Lee and Bunker [9]. More alkaline conditions are required to induce hydroxyl group ionization and different electrophoretic mobilities of sugars.

Another analytical approach involves a complex

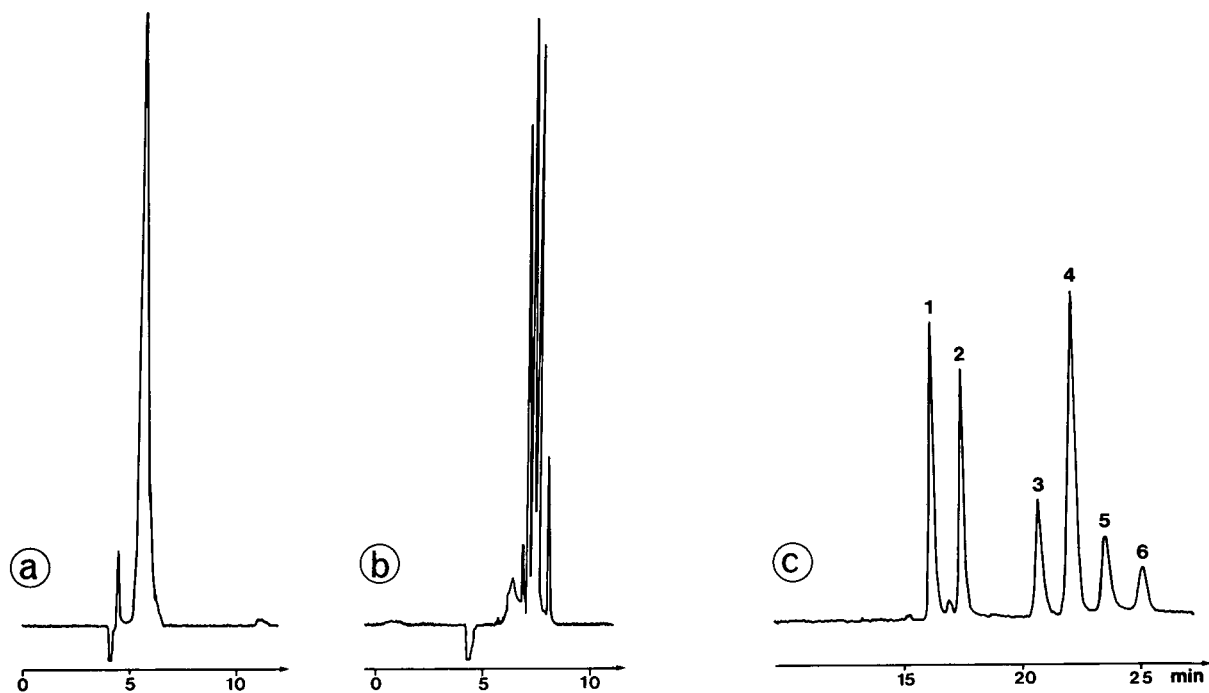


Fig. 3. Influence of the running buffer pH in free solution CE on the separation of flavonoid-3-O-glycosides. Conditions as in Fig. 2, except running buffer, 0.2 M H_3BO_3 . Peaks 1–5, as in Fig. 1; 6 = impurity. (a) pH 6.0; (b) pH 7.8; (c) pH 10.5.

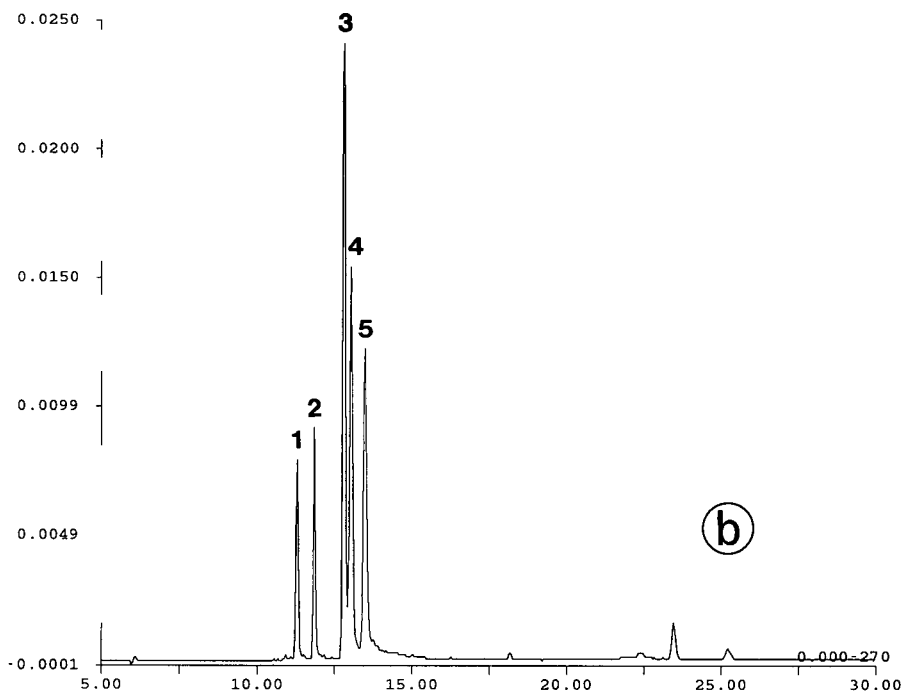
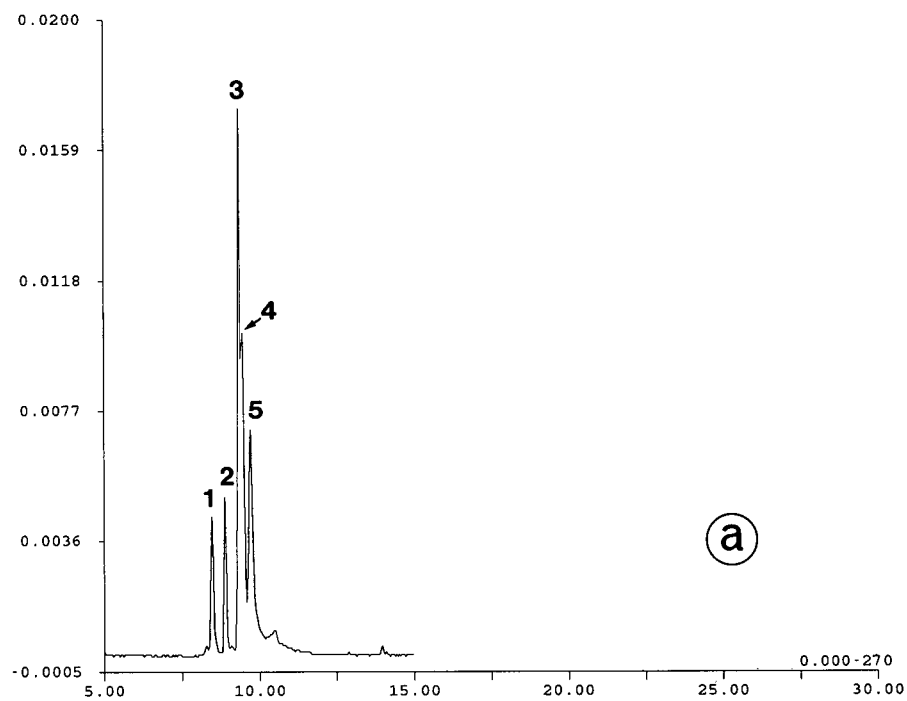


Fig. 4.

(Continued on p. 166)

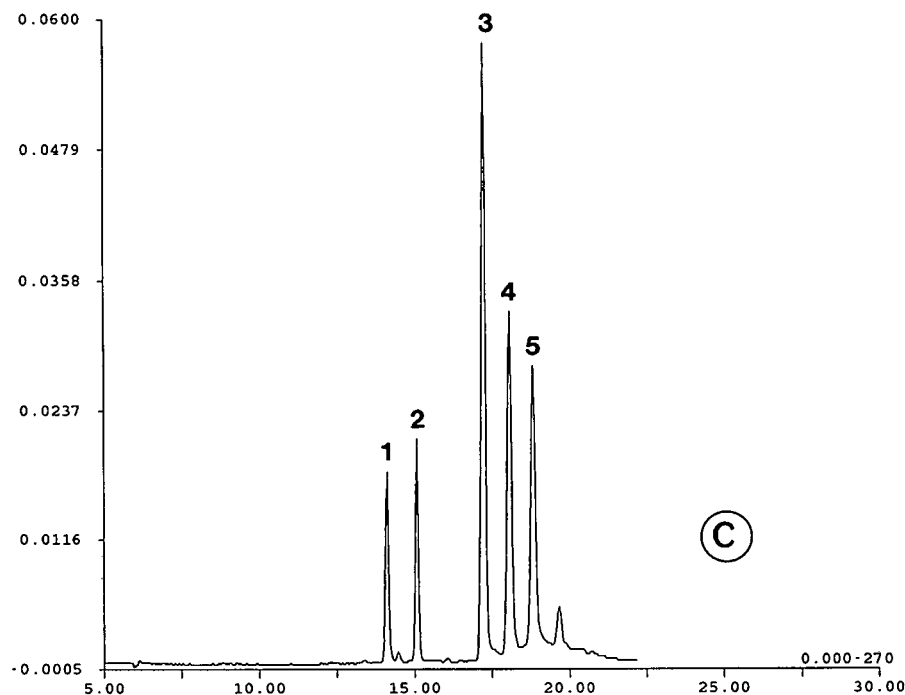


Fig. 4. Influence of boric acid concentration in free solution CE on the separation of flavonoid-3-O-glycosides. Voltage, +20 kV; capillary, 70 cm \times 50 μ m I.D.; running buffer, H_3BO_3 (pH 10.5); detection wavelength, 270 nm; temperature, 40°C. Peaks 1–5, as in Fig. 1. Boric acid concentration: (a) 0.05; (b) 0.10; (c) 0.20 *M*.

formation equilibrium by adding to the electrophoretic buffer a complexing agent of the saccharide or the flavonoid skeleton (Fig. 2b); the retention time of each solute is increased as they react with boric acid to form a borate anionic complex.

Influence of borate buffer pH

The different borate buffers tested in CE to resolve the flavonoid-3-O-glycosides had the same borate concentration (0.2 *M*) but different pH values (6–11). The complex formation reaction is a strongly pH-dependent equilibrium (Fig. 3). Displacement of equilibria 2 and 3 towards the complex formation becomes greater at higher pH values, inducing a greater electrophoretic mobility and resulting in retardation of migration.

Influence of borate concentration

The effect of borate concentration on the CE selectivity was studied at pH 10.5 using several electrolyte systems of different borate concentrations

(0.05–0.2 *M*). The migration time of each flavonoid-3-O-glycoside and the overall resolution increased with increasing concentration of boric acid (Fig. 4). Borate of higher concentration converts each flavonoid-O-glycoside into a charged complex form and provides separations due to the differences in the charge-to-mass ratio. The optimum buffer solution for the separation of these five quercetin-3-O-glycosides contained 0.2 *M* borate at an alkaline pH (10.5), which combines sufficient resolution with a moderate analysis time. Separation was complete and all peaks gave larger numbers of theoretical plates, as shown in Table I.

Flavonoid-O-glycoside complexation by borate anions

The 1,2-dihydroxy compounds form borates under alkaline conditions, as detailed in Fig. 5. Boric acid (B^0) is a Lewis acid and can bind a hydroxyl ion to form the borate anion (B^-). Both boric acid and borate can react with a suitable dihydroxy com-

TABLE I

ELECTROPHORETIC PARAMETERS OF FLAVONOID-3-O-GLYCOSIDES

Applied voltages, 21.5 kV; field strength, 307 V/cm; electroosmotic flow, $5.62 \cdot 10^{-4} \text{ cm}^2 \text{ V}^{-1} \text{ s}^{-1}$; electrolyte, 0.2 M H_3BO_3 (pH 10.5).

Quercetin-3-O-X X =	Efficiency ^a	Asymmetry factor	Electrophoretic mobility ($\times 10^4$) ($\text{cm}^2 \text{ V}^{-1} \text{ s}^{-1}$)
Arabinoglucoside	96 080	0.89	3.19
Glucoside	146 750	0.78	3.35
Galactoside	98 220	0.52	3.63
Rhamnoside	75 850	0.84	3.72
Arabinoside	80 630	0.95	3.80

^a Expressed as theoretical plate number.

pound (L), resulting in the boric acid ester (B^0L) and the borate monoester ($\text{B}^- \text{L}$), respectively. Subsequently, the two esters can react with another dihydroxy compound to give the borate diester ($\text{B}^- \text{L}_2$) [10,11].

The formation of complexes between borate and hydroxy compounds was first examined by Böeseken [12] by monitoring the changes in conductivity and pH that occur on adding compounds to boric acid or borax solutions, and by measuring the electrophoretic mobility of hydroxy compounds in borax solutions.

Spectroscopic methods offer physical means of examining chemical equilibria and measuring directly the concentrations of species in solution; Raman spectroscopy has been used to study borate complex formation [13]. Henderson *et al.* [14]

showed by ^{11}B NMR spectroscopic studies that the interconversion of boric acid and tetrahydroxyborate (borate) anions in aqueous solution is pH dependent. The interaction of 1,2-diols with borate anions at pH 12 induces the formation of 1:1 and 1:2 anionic complexes, as deduced from the existence of discrete ^{11}B resonances for these anions in the equilibrating systems. Increased substitution in 1,2-diols enhances their complexing ability.

The very stable borate complexes of ketoses and aldoses have been the subject of numerous studies. First, various aldoses have been derivatized to their 3-methyl-1-phenyl-2-pyrazolin-5-one derivatives or N-2-pyridylglycamines and then measured by free solution CE as their borate complexes [15,16]. In another instances, carbohydrates can be converted *in situ* into anionic borate complexes.

Chapelle and Verchère [17] showed that *cis*-1,2-diol groups complex borate more strongly than any other diol systems in polyhydroxy compounds. This study demonstrated also that in all 1:2 borate–sugar complexes, the borate anion was bound to two vicinal hydroxyl groups in a furanose ring, based on the fact that *cis*-1,2-cyclopentane-1,2-diol formed more stable complexes than its *cis*-1,2-cyclohexane-1,2-diol homologue. This effect is so large that the free sugars are forced into the furanose form by complexation, although they mainly adopt the pyranose structure when uncomplexed. For free sugars, the ability of a sugar to mutarotate creates a favourable situation for equilibration to a *cis*-1,2-glycol, which then forms a borate complex. Those sugars which can mutarotate and equilibrate to furanose forms will have the greatest potential to forming stable borate

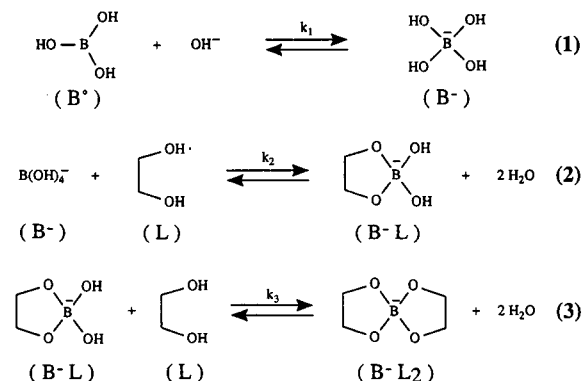


Fig. 5. Equilibria between boric acid, borate and a diol in alkaline aqueous medium [10,11].

complexes. Sterically, the most favourable configuration for complex formation is a *cis*-oriented pair of hydroxyl groups at C-2 and C-4. For instance, glucose does not have vicinal *cis*-OH groups in the pyranose form, so complex formation is assumed to take place mainly in the open-chain form [18].

The present quercetin-3-O-glycosides have one flavonoid hydroxyl group bound to a sugar by an acid-labile hemiacetal bond [8]. Consequently, the sugars maintained their unique natural form (furanose or pyranose) during borate complexation processes. Hence, complex formation cannot involve the open-chain form of the sugar. The magnitude of the borate complexation depends on the number of boration sites on sugar moiety and consequently on the sugar configuration.

In this borate complexation mode, flavonoid-3-O-glycosides migrated in the order quercetin-O-disaccharide (α -L-arabinoside- β -D-glucoside) and then quercetin-O-monosaccharides (β -D-glucoside, β -D-galactoside, β -L-rhamnoside and α -L-arabinoside). We tried to elucidate for this series of quercetin-3-O-glycosides the relationship between the migration order and the nature of the sugar moiety. The migration order depends on the structural preference for the formation of the borate complex and also on the relative molecular mass of the borate-solute complex (Fig. 1). Indeed, the electrophoretic mobility of an anionic borate-solute complex depends on its net charge and on its mass.

The α -L-arabinofuranoside unit has obviously no *cis*-1,2-diol system but can probably form a borate complex between the 2- and 5-hydroxyl groups [19]. *cis*-1,2-Glycols in a furanose system are known to form stronger borate complexes, whereas those in a pyranose system show little affinity to form borate complexes [20]. As indicated in Fig. 4c, quercetin-3-O-rhamnoside (4) migrates more slowly than quercetin-3-O-galactoside (3); this is probably due to the formation of a more stable complex at the 2- and 3-hydroxyl groups in quercetin-3-O-rhamnoside rather at the 3- and 4-hydroxyl groups in quercetin-3-O-galactoside [19] or a weaker charge density for compound 3. Quercetin-3-O-galactoside (3) migrates more slowly than quercetin-3-O-glucoside (2) because of the favourable structure of the galactopyranosyl unit for formation of a borate complex (presence of the 3,4-*cis*-diol system). The quercetin-3-O-disaccharide (1) has a lower electrophoretic

mobility than the quercetin-O-monosaccharides because of its lower charge density. However, this disaccharide has *cis*-3,4-hydroxyl groups which can form diol complexes with borate.

In order to determine the electrophoretic mobility of a solute by free solution CE, we must also consider the influence of electroosmosis on the mobility measurements. The electrophoretic mobility is defined as $u_{ep} = L_d L_t V (1/t_0 - 1/t_m)$, where L_d is the length of the capillary from the inlet to the detector, L_t the total length of the capillary, t_m the migration time, t_0 the migration time for a neutral marker (methanol) and V the applied voltage. The electrophoretic mobility of a borate-diol complex is affected by the complex stability constants [16], and consequently this parameter depends on the disposition of hydroxyl groups, as indicated in Fig. 1.

The number of theoretical plates was fairly high (from 147 000 for quercetin-3-O-glucoside to 76 000 for quercetin-3-O-rhamnoside), but the separation appears to be kinetically retarded owing to the complexation with the borate anion. As an indication of peak asymmetry, the B/A ratio taken at 10% of the peak maximum was determined for these compounds; the values were less than unity from 0.95 for quercetin-3-O-arabinoside to 0.52 for quercetin-3-O-galactoside).

CONCLUSIONS

The formation of sugar-borate complexes is of particular value in the CE of flavonoid-O-glycosides having the same flavonoid aglycone but differing in their sugar moiety. In this borate complexation mode, flavonoid-3-O-glycosides migrated in the order quercetin-O-disaccharide (α -L-arabinoside- β -D-glucoside) and then quercetin-O-monosaccharides (β -D-glucoside, β -D-galactoside, β -L-rhamnoside and α -L-arabinoside). The magnitude of the borate complexation depends on the number of boration sites on sugar moiety and also of their charge density. The formation of a borate complex from a flavonoid-O-glycoside is facilitated by an alkaline buffer and the resolution *versus* boric acid concentration is increased. The migration order, which depends on the nature of the sugar moiety, has been explained for this series of quercetin-3-O-glycosides.

REFERENCES

- 1 P. Pietta, P. Mauri, A. Rava and G. Sabbatini, *J. Chromatogr.*, 549 (1991) 367.
- 2 Ph. Morin, F. Villard, A. Quinsac and M. Dreux, *J. High Resolut. Chromatogr.*, 15 (1992) 271.
- 3 K. Hostettmann and A. Marston, *Prog. Clin. Biol. Res.*, 213 (1986) 43.
- 4 E. Revilla, E. Alonso and M. Estrella, in G. Charalambous (Editor), *Frontiers of Flavor*, Elsevier, Amsterdam, 1988, p. 711.
- 5 D. J. Daigle and E. J. Conkerton, *J. Liq. Chromatogr.*, 11 (1988) 309.
- 6 V. Seitz, G. Bonn, P. Oefner and M. Popp, *J. Chromatogr.*, (1991) 499.
- 7 Ph. Morin, F. Villard and M. Dreux, *J. Chromatogr.*, 628 (1993) 153.
- 8 K. R. Markham, *Techniques of Flavonoid Identification*, Academic Press London, 1982.
- 9 D. Lee and M. Bunker, *J. Chromatogr. Sci.*, 27 (1989) 486.
- 10 M. van Duin, J. A. Peters, A. P. G. Kieboom and H. van Bekkum, *Tetrahedron*, 41 (1985) 3411.
- 11 M. van Duin, J. A. Peters, A. P. G. Kieboom and H. van Bekkum, *Tetrahedron*, 40 (1984) 2901.
- 12 J. Böseken, *Adv. Carbohydr. Chem.*, 4 (1949) 189.
- 13 R. P. Oertel, *Inorg. Chem.*, 11 (1972) 544.
- 14 W. G. Henderson, M. J. How, G. R. Kennedy and E. F. Mooney, *Carbohydr. Res.*, 28 (1973) 1.
- 15 S. Honda, S. Iwase, A. Makino and S. Fujiwara, *Anal. Biochem.*, 176 (1989) 72.
- 16 S. Honda, S. Suzuki, A. Nose, K. Yamamoto and K. Kakehi, *Carbohydr. Res.*, 215 (1991) 193.
- 17 S. Chapelle and J. F. Verchère, *Tetrahedron*, 44 (1988) 4469.
- 18 S. Hoffstetter-Kuhn, A. Paulus, E. Gassmann and H. Widmer, *Anal. Chem.*, 63 (1991) 1541.
- 19 H. Yamaguchi, H. Matsuura, R. Kasai, K. Mizutani, H. Fujino, K. Ohtani, T. Fuwa and O. Tanaka, *Chem. Pharm. Bull.*, 34 (1986) 2859.
- 20 P. Shaw (Editor), *Handbook of Sugar Separations in Foods by HPLC*, CRC Press, Boca Raton, FL, 1988, p. 23.

Book Review

Analysis of substances in the gaseous phase (Comprehensive Analytical Chemistry, Vol. XXVIII), by E. Smolková-Keulemansová and L. Felzl, Elsevier, Amsterdam, Oxford, New York, 1991, XIV + 480 pp., price Dfl. 400.00, US\$ 205.00, subscription price Dfl 360.00, US\$ 184.50, ISBN 0-444-89122-6.

In modern analytical chemistry, many different methods are used for the analytical study of definite groups of samples. Therefore, the development of optimum strategies for the complex use of known methods is very important and various approaches to this problem are possible. The publication of books devoted to the analytical chemistry of a definite sample type is one of the ways of solving this problem.

This book by E. Smolková-Keulemansová and L. Felzl describes many analytical methods used for analysis of substances in the gaseous phase. Gaseous samples are very widely used in industry, air pollution studies, medicine, scientific research, etc.

In the Introduction the authors write, "This book is based on years of experience of lecturing to students in analytical chemistry and in specialized postgraduate courses. It will be useful for students and workers in scientific research laboratories and in fields dealing with the protection of the environment. It is hoped that it will provide the most useful information in its field and that, although it is of necessity far from exhaustive, it will give a comprehensive description of the state of the art and of future possibilities in the analysis of gaseous substances". In my opinion, the authors have successfully fulfilled these tasks. The book will be interesting for many readers whose work involves the analytical chemistry of the gaseous phase.

At the beginning of the book early periods of evolution of general and analytical chemistry are described. The first part (Chapters 3–9) is devoted to classical chemical and physico-chemical methods of gas analysis. In Chapter 5 the authors discuss sample storage and treatment. This is a particularly important problem in the analytical chemistry of

gaseous samples, but usually is discussed only very briefly in the literature. Methods of volumetric absorption analysis, combustion methods and hybrid methods (absorption and titration, absorption and optical methods, absorption and electrochemical methods) are described in Chapter 8. Physical methods of gas analysis, including thermal conductivity, interferometry, adsorption and emission spectrometry, mass spectrometry, viscosimetry, radiometry and some others, are discussed in Chapter 9. General methods for the preparation of mixtures of gases and vapours are also described in this chapter. It would have been desirable, in the reviewer's opinion, to have paid more attention to the role of sensors in gas analysis.

The second part of the book is devoted to gas chromatography. This is natural because gas chromatography is the most important method in gas analysis and also its application usually requires more creative efforts than other methods. This part includes a discussion of the theory, instrumentation, qualitative and quantitative analyses and applications. Unfortunately, the authors hardly discuss the role of adsorption phenomena in gas-liquid chromatography, although these phenomena are important for understanding sources of systematic errors in qualitative and quantitative analysis. Unfortunately, combinations of different independent methods, physical methods and gas chromatography are only briefly discussed.

In generally, the book reflects the state of the art in the analysis of substances in the gaseous phase and will undoubtedly be of value to many workers concerned with gas analysis.

Moscow (Russian Federation) V. G. Berezkin

PUBLICATION SCHEDULE FOR THE 1993 SUBSCRIPTION

Journal of Chromatography and *Journal of Chromatography, Biomedical Applications*

MONTH	O 1992	N 1992	D 1992	J	F	
Journal of Chromatography	623/1 623/2 624	625/1 625/2	626/1 626/2 627/1 + 2	628/1 628/2 629/1 629/2	630/1 + 2 631/1 + 2 632/1 + 2 633/1 + 2	The publication schedule for further issues will be published later.
Cumulative Indexes, Vols. 601–650						
Bibliography Section						
Biomedical Applications				612/1	612/2	

INFORMATION FOR AUTHORS

(Detailed *Instructions to Authors* were published in Vol. 609, pp. 439–445. A free reprint can be obtained by application to the publisher, Elsevier Science Publishers B.V., P.O. Box 330, 1000 AH Amsterdam, The Netherlands.)

Types of Contributions. The following types of papers are published in the *Journal of Chromatography* and the section on *Biomedical Applications*: Regular research papers (Full-length papers), Review articles, Short Communications and Discussions. Short Communications are usually descriptions of short investigations, or they can report minor technical improvements of previously published procedures; they reflect the same quality of research as Full-length papers, but should preferably not exceed five printed pages. Discussions (one or two pages) should explain, amplify, correct or otherwise comment substantively upon an article recently published in the journal. For Review articles, see inside front cover under Submission of Papers.

Submission. Every paper must be accompanied by a letter from the senior author, stating that he/she is submitting the paper for publication in the *Journal of Chromatography*.

Manuscripts. Manuscripts should be typed in **double spacing** on consecutively numbered pages of uniform size. The manuscript should be preceded by a sheet of manuscript paper carrying the title of the paper and the name and full postal address of the person to whom the proofs are to be sent. As a rule, papers should be divided into sections, headed by a caption (*e.g.*, Abstract, Introduction, Experimental, Results, Discussion, etc.). All illustrations, photographs, tables, etc., should be on separate sheets.

Abstract. All articles should have an abstract of 50–100 words which clearly and briefly indicates what is new, different and significant. No references should be given.

Introduction. Every paper must have a concise introduction mentioning what has been done before on the topic described, and stating clearly what is new in the paper now submitted.

Illustrations. The figures should be submitted in a form suitable for reproduction, drawn in Indian ink on drawing or tracing paper. Each illustration should have a legend, all the *legends* being typed (with double spacing) together on a *separate sheet*. If structures are given in the text, the original drawings should be supplied. Coloured illustrations are reproduced at the author's expense, the cost being determined by the number of pages and by the number of colours needed. The written permission of the author and publisher must be obtained for the use of any figure already published. Its source must be indicated in the legend.

References. References should be numbered in the order in which they are cited in the text, and listed in numerical sequence on a separate sheet at the end of the article. Please check a recent issue for the layout of the reference list. Abbreviations for the titles of journals should follow the system used by *Chemical Abstracts*. Articles not yet published should be given as "in press" (journal should be specified), "submitted for publication" (journal should be specified), "in preparation" or "personal communication".

Dispatch. Before sending the manuscript to the Editor please check that the envelope contains four copies of the paper complete with references, legends and figures. One of the sets of figures must be the originals suitable for direct reproduction. Please also ensure that permission to publish has been obtained from your institute.

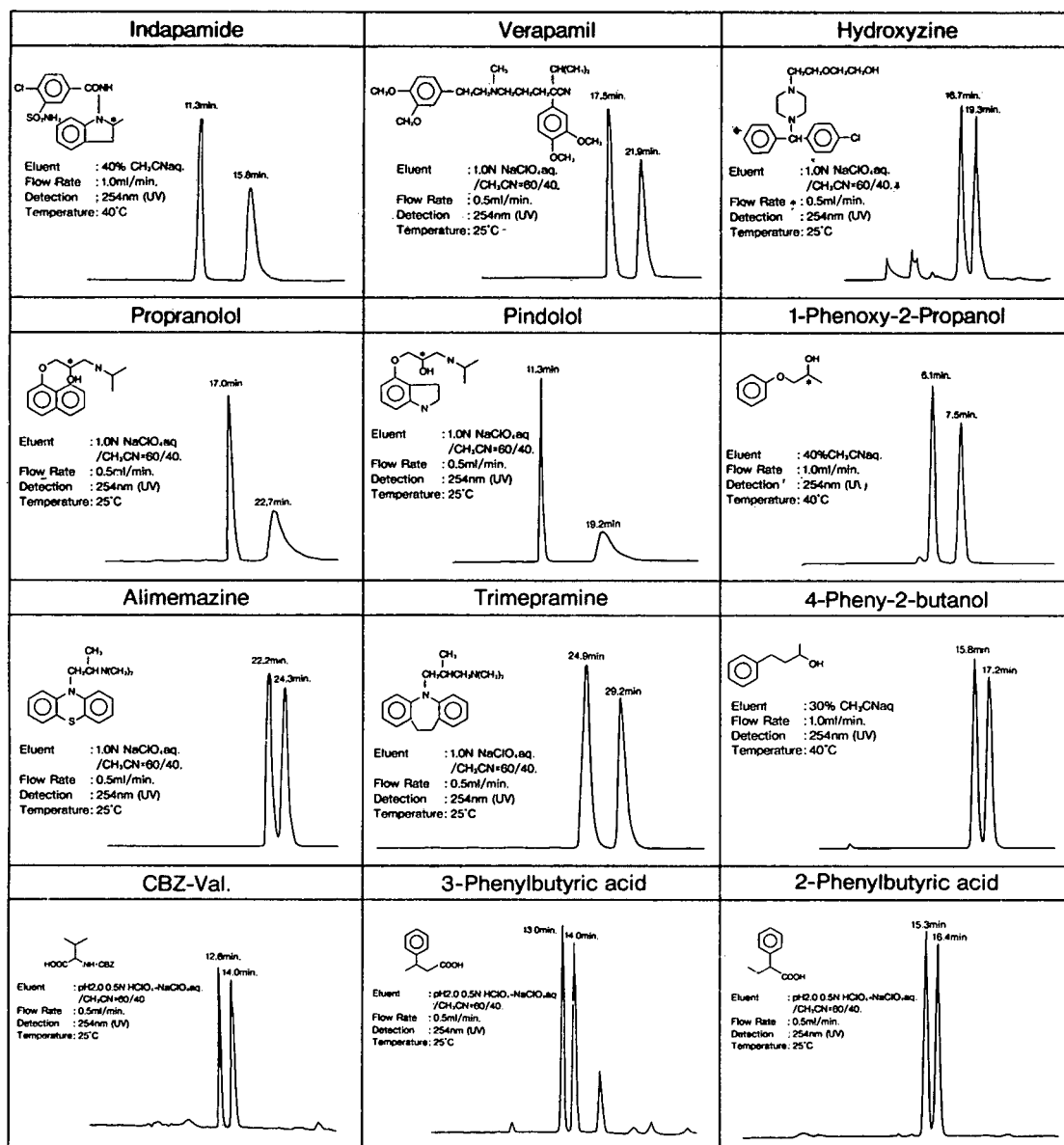
Proofs. One set of proofs will be sent to the author to be carefully checked for printer's errors. Corrections must be restricted to instances in which the proof is at variance with the manuscript. "Extra corrections" will be inserted at the author's expense.

Reprints. Fifty reprints will be supplied free of charge. Additional reprints can be ordered by the authors. An order form containing price quotations will be sent to the authors together with the proofs of their article.

Advertisements. The Editors of the journal accept no responsibility for the contents of the advertisements. Advertisement rates are available on request. Advertising orders and enquiries can be sent to the Advertising Manager, Elsevier Science Publishers B.V., Advertising Department, P.O. Box 211, 1000 AE Amsterdam, Netherlands; courier shipments to: Van de Sande Bakhuizenstraat 4, 1061 AG Amsterdam, Netherlands; Tel. (+31-20) 515 3220/515 3222, Telefax (+31-20) 6833 041, Telex 16479 els vi nl. UK: T. G. Scott & Son Ltd., Tim Blake, Portland House, 21 Narborough Road, Cosby, Leics. LE9 5TA, UK; Tel. (+44-533) 753 333, Telefax (+44-533) 750 522. USA and Canada: Weston Media Associates, Daniel S. Lipner, P.O. Box 1110, Greens Farms, CT 06436-1110, USA; Tel. (+1-203) 261 2500, Telefax (+1-203) 261 0101.

Reversed Phase CHIRAL HPLC Column

NEW CHIRALCEL® OD-R



For more information about CHIRALCEL OD-R column, please give us a call.



DAICEL CHEMICAL INDUSTRIES, LTD.

CHIRAL CHEMICALS DIVISION 8-1, Kasumigaseki 3-chome, Chiyoda-ku, Tokyo 100, JAPAN
Phone: +81-3-3507-3151 Facsimile: +81-3-3507-3193

AMERICA
CHIRAL TECHNOLOGIES, INC.
730 SPRINGDALE DRIVE
DRAWER I EXTON, PA 19341
Phone: 215-594-2100
Facsimile: 215-594-2325

EUROPE
DAICEL (EUROPA) GmbH
Ost Street 22
4000 Düsseldorf 1, Germany
Phone: +49-211-369848
Facsimile: +49-211-364429

ASIA/OCEANIA
DAICEL CHEMICAL (ASIA) PTE. LTD.
65 Chulia Street #40-07
OCBC Centre, Singapore 0104.
Phone: +65-5332511
Facsimile: +65-5326454